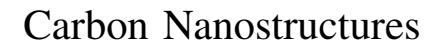
CARBON NANOSTRUCTURES

Rüdiger Klingeler Robert B. Sim *Editors*

Carbon Nanotubes for Biomedical Applications





For further volumes: http://www.springer.com/series/8633

Rüdiger Klingeler · Robert B. Sim Editors

Carbon Nanotubes for Biomedical Applications



Editors
Rüdiger Klingeler
Kirchhoff Institute for Physics
Heidelberg University
Im Neuenheimer Feld 227
69120 Heidelberg
Germany

e-mail: klingeler@kip.uni-heidelberg.de

Robert B. Sim
Department of Pharmacology
Oxford University
Mansfield Road
Oxford
OX1 3QT
UK

e-mail: bob.sim@bioch.ox.ac.uk

ISBN 978-3-642-14801-9

e-ISBN 978-3-642-14802-6

DOI 10.1007/978-3-642-14802-6

Springer Heidelberg Dordrecht London New York

Library of Congress Control Number: 2010936854

© Springer-Verlag Berlin Heidelberg 2011

This work is subject to copyright. All rights are reserved, whether the whole or part of the material is concerned, specifically the rights of translation, reprinting, reuse of illustrations, recitation, broadcasting, reproduction on microfilm or in any other way, and storage in data banks. Duplication of this publication or parts thereof is permitted only under the provisions of the German Copyright Law of September 9, 1965, in its current version, and permission for use must always be obtained from Springer. Violations are liable to prosecution under the German Copyright Law.

The use of general descriptive names, registered names, trademarks, etc. in this publication does not imply, even in the absence of a specific statement, that such names are exempt from the relevant protective laws and regulations and therefore free for general use.

Cover design: WMXDesign GmbH

Printed on acid-free paper

Springer is part of Springer Science+Business Media (www.springer.com)

Preface

Nanomaterials

New materials promise novel applications. This particularly holds for nanoscaled materials which can exhibit novel materials properties that appear upon reducing the dimensions of their bulk counterparts. Indeed, it is the fundamentally different physical and chemical properties of nano-sized materials which not only promise new nanotechnological applications but attract scientists' attention to their fundamental scientific importance. In particular, nano-sized materials have novel properties and applications in the fields of optics, magnetism, electricity, catalysis, and biomedicine. For biomedicine, besides the fundamentally novel properties, it is also the mere size reduction which opens a new field of applications: nanoparticles conform to the dimensions of living cells, and can be internalized. Therefore, control and sensing at the *cellular* level can be envisaged by applying intracellular probes by transferring nano-sized biocompatible devices into the cells. These devices (particles) must meet the demands of targeted investigation of relevant cell parameters as well as manipulation of the cells.

One of many possible examples of biomedical application of nanomaterials is cell killing by the use of magnetic nanoparticles exposed to external magnetic fields. Magnetic fields only very weakly interact with organic materials and do not cause known adverse effects. External magnetic fields can be used to "pull" or "push" magnetic nanoparticles into deep layers of (human) tissue (e.g. solid tumours). After being internalized, magnetic nanoparticles can hence be used for various purposes without need for surgery. External static magnetic fields fix ferromagnetic nanoparticles at a precise position; gradient fields move them and alternating (AC) fields lead to local heating. The latter effect can be utilized for so-called "hyperthermia", i.e. a therapeutic anti-cancer treatment which raises the temperature of tumor tissue in vivo [1]. This method applies the fact that a cancer cell-killing effect is caused when a temperature above 41–42°C is maintained in the target volume. One outstanding example of the use of ferromagnetic nanoparticles is "magnetic fluid hyperthermia" (MFH), i.e. the controlled heating of

vi Preface

tumour tissue, which is commercially used by one of the associated industrial partners of our Network [2]. In MFH therapy, magnetic nanoparticles are infiltrated deep into tumour tissue and inductively heated by applying AC magnetic fields.

Carbon Nanotubes

The use of nanoscaled functional materials requires that the materials are shielded within a protective coating until they reach their site of action. A promising way to provide such a shield appears to be the coating, e.g., of the magnetic iron with a carbon shell by insertion of the magnetic material inside carbon nanotubes and thereby protecting the biological environment and the filling material from each other. Degradation of filling materials is avoided and their potential toxicity and adverse effects are suppressed.

Carbon nanotubes (CNTs) are hollow carbon structures with one or more walls, a small diameter on the nanometer scale and a large length in comparison. They exhibit a well-ordered arrangement of carbon atoms linked via sp^2 bonds which renders them among the stiffest and strongest fibres known. In addition to mechanical properties, they exhibit superior electrical and thermal conductivity. Depending on the numbers of walls, the diameter is between 0.8-2 nm for single-walled CNTs and 2-100 nm for multi-walled ones. Their lengths range between hundreds of nanometers and up to tens of micrometers and even longer, yielding very high aspect ratios.

The mechanically and chemically stable carbon shells can be opened, filled and closed again without losing their stability. Experiences in filling CNTs range back to their discovery in 1991 [3]. Since then, extensive work has been performed to synthesise CNTs and to functionalise them both exohedrally, i.e. by attaching functional elements to the outer shell, and endohedrally by filling with various materials. CNTs can be filled with metals, semiconductors, salts, organic materials, fullerenes, etc., either during the synthesis process or through subsequent opening, filling, and closing of the CNT. The container feature of CNTs allows, in principle, simultaneous filling of CNTs with different materials thereby combining multiple functionalities in one kind of carrier. In this way, CNTs provide a smart carrier system on the nanometer scale which can be filled with tailored materials to address specific purposes.

Beyond the shielding effect against a biological environment, the carbon coating offers an interface for further exohedral functionalisation with suitable (bio-) molecules. A major task of such functionalisation is the stable dispersion of the nanoparticles in aqueous media which still is a major challenge. Both noncovalent and covalent modification strategies can be applied among which the former preserve the pristine CNT structure while covalent modification introduces partial damage of the outer wall but in general yields better dispersion. Dispersion becomes even more crucial if ferromagnetically filled CNTs are envisaged which

Preface vii

exhibit an increased tendency to agglomerate due to magnetic interactions. In addition, exohedral functionalisation is needed to make the highly symmetric carbon structures compatible with real biological environments. Nowadays, functionalisation is also aimed at performing dynamic tasks such as target recognition, target transformation, transport, or electrical conduction in the living cell. Some of these functions can be provided by biomolecules, such as DNA or proteins (enzymes, antibodies). Importantly for any therapeutic or biomedical usage, functionalised CNTs can effectively cross biological barriers such as the cell membrane and penetrate the individual cell. Recently, it was shown that DNAwrapped SWCNTs were enveloped by cancer cells and they were used to deliver a lethal dose of microwave radiation to the cancer cells [4]. In contrast to such noncovalent wrapping of CNTs with biomolecules, any covalent chemical exohedral functionalisation needed to improve the biocompatibility of CNTs will structurally perturb the external wall. This however in the case of multi-walled CNTs does not affect the overall carbon shielding. A variety of methods exist for exohedral functionalization of carbon nanotubes, some of which have been successfully applied for the conjugation of proteins, drugs and fluorescent dyes and active tumor targeting in vivo.

Although a very large number of toxicity studies has been published no clear picture evolves for CNTs in general. There are many conflicting reports mainly from in vitro studies. One reason for this ambiguity is the fact that—similar to other nanoparticles—a large number of specific factors govern the toxicity of CNTs such as their shape and size (diameter, length), the number of shells (single-or multi-walled CNTs), agglomeration state, homogeneity, and surface chemistry. In particular, the concentration of CNTs is not necessarily a main parameter. Ambiguity also results from a lack of standardisation and of thorough characterisation of, e.g., defects of the outer shell or potentially toxic contaminants. Such non-carbon material originating from the synthesis process of pristine empty CNTs can amount to several percent of the total mass. These factors may account for much of the reported differences so that details of synthesis, choice of catalyst particles, washing procedures and dispersion methods have to be considered thoroughly.

The successful application of CNTs for biomedical application faces a variety of severe problems to be solved. These include:

- Synthesis of CNTs with tailored functionalities and uniform morphology
- Modification of CNTs to become compatible to biological systems, in particular long-term stable dispersed in aqueous solution
- Detailed study of interaction with biological environments (immune response, toxicity, interaction with the single cell)
- In vivo testing for actual therapeutic and diagnostic purposes such as imaging (contrast agents, markers), sensing (nanoparticle-based diagnostics) and cancer treatment (hyperthermia, targeted drug delivery)

viii Preface

The Book

As described above, extraordinary physical and chemical properties render carbon nanotubes promising candidates as biomedical agents for diagnostic and therapeutic applications. Filling the nanotubes with tailored materials forms packages in which the active content is encapsulated by a protecting carbon shell. The nanoparticles are efficiently internalized by cells. Chemical alteration of the external surface confers biocompatibility and the potential to target specific cells or tissues. This book explores the potential of multi-functional carbon nanotubes for biomedical applications by combining diverse and detailed contributions from chemistry, physics, biology, engineering, and medicine. The overview of the current state-of-the-art addresses different synthesis and biofunctionalisation routes and shows the structural and magnetic properties of CNTs relevant to biomedical applications. Particular emphasis is given to the interaction of CNTs with biological environments, i.e. toxicity, biocompatibility, cellular uptake, intracellular distribution, interaction with the immune system and environmental impact. The insertion of NMR-active substances allows diagnostic usage as markers and sensors, e.g. for magnetic imaging and contactless local temperature sensing. The potential of CNTs for therapeutic applications is highlighted by studies on chemotherapeutic drug filling and release, targeting and magnetic hyperthermia studies for anti-cancer treatment at the cellular level.

The book is presented in four sections:

I Fundamentals: Synthesis of Multifunctional Nanomaterials and their Potential for Medical Application

Raffa et al. introduce the *Physical properties of carbon nanotubes for therapeutic applications*, emphasizing the unique, unprecedented combination of electrical, magnetic, optical and chemical properties which holds great promise for the development of a new class of CNT-based drugs and therapy. Raffa et al. provide a review of the physical properties of CNTs and discuss the current state of the art as well as future perspectives of applications of CNTs in the field of biotechnology.

The applications of *Carbon nanotubes in regenerative medicine* are reviewed by Paratala and Sitharaman. The focus of regenerative medicine is on developing methods that can be applied to create functional tissues, to repair or replace tissues/ organs lost due to trauma or disease. In this respect, the structural and mechanical properties of CNTs make them applicable for use as composites for tissue engineering. CNTs can act as delivery vehicles for drugs and gene therapy and thus are suitable for therapeutics in regenerative medicine. Further, as discussed in this chapter, they also show promise as contrast agents for non-invasive in vivo molecular imaging.

Preface ix

The production of uniform nanoparticles with controlled particle size and morphology is one of the main challenges in applied nanoscience. In this respect, remarkable progress in synthesis of carbon nanostructures has been made in the last two decades. Aspects of synthesis are addressed by Lukanov et al. who discuss various functionalisation routes of *Filling of Carbon Nanotubes with compounds in solution or melted*. The filling of CNTs with a particular functional material represents a remarkable example of matter manipulation at the nanometer scale aimed at designing a tailored nanosized device. These authors review different approaches to filling. The confinement of matter inside CNTs can lead to significant structural modifications, depending on both the bulk structure of the confined material and the CNT inner diameter, which likely causes modifications of the physical properties (electrical, optical, mechanical, thermal) of the composites.

The capacities and potential for nanofabrication of a tailored magnetic material relevant to magnetic imaging and magnetic hyperthermia applications is highlighted by the encapsulation of materials such as Fe, Co, Ni. Within this context, the synthesis of CNTs filled with magnetic materials has been widely investigated, especially with iron due to its excellent ferromagnetic characteristics. A detailed overview of diverse preparation routes of Fe-CNTs is given by Borowiak-Palen et al. Filling Carbon Nanotubes: containers for magnetic probes and drug delivery. Here, the effects of varying parameters in the chemical vapour deposition (CVD) synthesis method on the structure of the final material is shown, which varies in respect of the amount of iron encapsulated in the cavity, tube diameter and the number of graphitic walls forming the CNTs. The filling of hollow CNTs through wet chemistry reactions (as a post-synthesis route) and CVD process (filling during the synthesis of CNTs) is also addressed in this chapter, with the particular example of exploiting the potential of CNTs nanosized containers filled with therapeutic drugs, exemplified by the chemotherapeutic cisplatin.

II Magnetically Functionalised Carbon Nanotubes for Medical Diagnosis and Therapy

Sobik et al. describe, in the chapter *Magnetic nanoparticles for medical diagnosis and therapy*, the intrinsic properties of ferromagnetic CNTs and their potential to provide accurate medical imaging and medical therapy (magnetic hyperthermia, targeted drug delivery, etc...) at the cellular level. The unusual magnetic and magnetization properties of these "nanowires" (extremely thin, long assemblies of iron atoms within CNTs) are illustrated. These properties are compared in situations mimicking free suspension in body fluids, or immobilization in solid tissues.

In the chapter Feasibility of magnetically filled carbon nanotubes for biological applications: From fundamental properties of individual nanomagnets to

x Preface

nanoscaled heaters and temperature sensors, Lutz et al. present a detailed overview of fundamental magnetic properties and magnetisation reversal of individual nanostructures and of ensembles. In addition, heating effects in applied AC magnetic fields are highlighted. This effect is of great interest for thermoablation treatment, i.e. the killing of cells (for example within solid tumours) by direct local heating, The heat output and other relevant properties of various magnetic materials are compared, together with discussion of the control of heat output. NMR studies show that a non-invasive temperature control by virtue of a carbon-wrapped nanoscaled thermometer is feasible.

Anuganti and Velders (*Nuclear Magnetic Resonance Spectroscopy and Imaging of Carbon Nanotubes*) review the potential use of CNTs as contrast-enhancing agents for Magnetic Resonance Imaging, in vitro and in vivo with a detailed investigation of different types of CNT structures and properties by solution-state NMR, Solid State NMR and High-Resolution Magic-Angle-Spinning (HR MAS) NMR spectroscopy.

III Interaction with Biological Systems

Current developments in nanoparticle technology provide a vast variety of new particles, with different morphology and surface chemistry. If these are to be used in biology and medicine, constant and continued study of how they interact with biological materials, especially human tissues, must be carried out, to assess their benefit versus any potential risk. Despite various industrial applications of CNTs and their large scale synthesis relatively little is known in detail about the interaction of CNTs with biological environments. In the chapter *Exploring carbon nanotubes and their interaction with cells using atomic force microscopy*, Lamprecht et al. discuss how atomic force microscopy can be used to study some of the fine details of the interactions of functionalized CNTs with mammalian cells. This technique has the advantage that it does not require extensive processing or chemical treatment (fixing) of the sample before measurements are made, so that systems can be studied close to physiological conditions.

Neves et al. in the chapter entitled *Uptake, intracellular localization and biodistribution of carbon nanotubes* present a detailed, pharmacologically-oriented summary of in vivo studies of biodistribution and circulation of CNTs, together with extensive in vitro studies of uptake into cells and intracellular localisation. It is described how CNTs can be designed to form pharmaceutical complexes, which allow them to enter blood circulation, target cells, deliver payloads, be exocy-tosed and finally eliminated from the body. As nanoparticles for medical applications, CNTs shows promise in offering lower toxicity with enhanced efficacy.

CNTs and other nanomaterials when placed in contact with human (or other mammalian) body fluids and tissues are recognised by the immune system and

Preface xi

may also interact with other systems, such as coagulation proteins, other blood plasma components, and cell-surface proteins. Binding of immune system complement proteins activates the complement system and results in strong binding of several complement proteins to the CNT. Such complement activation may influence subsequent interaction of the CNT with cells and tissues and is a predictor of potential toxicity in animal models. Rybak-Smith et al. (*Recognition of Carbon Nanotubes by the Human Innate Immune System*) report on what is known of the molecular events, such as protein binding, that occur when CNTs are placed in contact with human blood or lung fluids, and the biological consequences of these interactions.

Industrial-scale synthesis of CNTs for a wide range of uses is now a reality, on the scale of hundreds of tons per year, and this brings into focus the need to study industrial and environmental toxicology of nanotubes. Flahaut, in the chapter *Toxicity and environmental impact of carbon nanotubes*, provides an overview of current knowledge of the life-cycle of CNTs, from manufacture to final destruction, covering aspects such as accidental uptake into living organisms, potential for toxicity, biopersistence, routes of elimination and degradation.

IV Towards Targeted Chemotherapy and Gene Delivery

More detailed considerations of the application of derivatised CNTs as drug carriers are developed in this section of the book. Heister et al. (*Carbon nanotubes loaded with anticancer drugs: a platform for multimodal cancer treatment*) present an overview of cancer, current treatments and the need for new developments. Strategies for design and targeting of drug carriers are described, followed by a detailed review of the experimental use of modified CNTs, in vitro and in vivo, in the killing of tumours or cancer cells. These authors conclude that "drug delivery is clearly one of the most promising bioapplications of carbon nanotubes and the coming years will reveal the suitability of this rather novel material in comparison to more established drug delivery systems, such as liposomes".

Haase et al. in the chapter Carbon Nanotubes filled with Carboplatin: Towards Carbon Nanotube supported delivery of the chemotherapeutic agent Carboplatin present a detailed experimental study of the development of a single system, CNTs filled with the anti-cancer drug carboplatin. The maintenance of the structure of the enclosed carboplatin was confirmed by spectroscopic techniques, and the cytotoxicity of the CNT-cisplatin composites explored using cell lines.

In the final chapter, Functionalized carbon nanotubes for gene biodelivery, Sanz-Beltrán et al. describe the design of CNTs derivatised for the delivery of DNA into cells (an approach to gene therapy or to therapeutic use of RNA). Noncovalent functionalization of CNTs with RNA and with amphiphilic polypeptides as model systems, the efficacy of these coatings in forming stable dispersions, and the capacity of the modified CNT to deliver functioning genes to cells is presented in detail.

xii Preface

The experimental work described in these chapters is very wide-ranging, diverse and multidisciplinary. Experimental techniques used range through those of several branches of physics, organic and inorganic chemistry, oncology, immunology, molecular biology, and the structures studied range from metal ions, through protein and DNA macromolecules, synthetic particles, up to animal cells, tissues and whole animal bodies. These illustrate the complexity of work and range of scientific disciplines required for the design of new modes of biomedical therapy.

The majority of the work presented has been done in the multi-disciplinary European Marie-Curie Research Training Network CARBIO (Multifunctional Carbon Nanotubes for Biomedical Applications) [5]. The Network provided collaborative training of young researchers in experimental biomedical nanoscience aiming at developing and optimizing multi-functionalised nanocontainers for human medical applications. The project has elucidated the usage of CNTs for previously known applications and has also shown their feasibility for novel applications not encountered before. A particularly high potential is found when multiple functionalities are combined, e.g., drug transport, imaging and local heat generation. The network's results which have been published in more than 100 papers allow better understanding and assessment of possible benefits and potential toxicological and environmental risks of a promising nanomaterial which is a prerequisite for responsible application of nanotechnology.

- 1. Pankhurst, Q.A., Conolly, J., Jones, S.K., Dobson, J.: Applications of magnetic nanoparticles in biomedicine. J. Phys. D Appl. Phys. **36**, R167–R181 (2003)
- Jordan, A., Scholz, R., Wust, P., Fahling, H., Felix, R.: Magnetic fluid hyperthermia (MFH): cancer treatment with AC magnetic field induced excitation of biocompatible superparamagnetic nanoparticles. J. Magn. Magn. Mat. 201, 413 (1999)
- 3. Iijima, S.: Helical microtubules of graphitic carbon, Nature **354**, 56 (1991)
- 4. Kam, N.W.S., O'Connell, M., Wisdom, J.A., Dai, H.: Carbon nanotubes as multi-functional biological transporters and near-infrared agents for selective cancer cell destruction. Proc. Natl. Acad. Sci. USA **102**, 11600 (2005)
- 5. http://www.carbio.eu

Acknowledgments

Substantial support by the European Community through the Marie Curie Research Training Network CARBIO (contract No. MRTN-CT-2006-035616) is gratefully acknowledged. It is our great pleasure to thank the CARBIO Advisory Board members Sabine Achten (Boehringer Ingelheim Fonds), François Rossi (European Commission Joint Research Centre Ispra), and Andreas Jordan (Mag-Force Nanotechnologies AG) for their valuable advice and ongoing support.

Preface xiii

Marion Malkoc greatly supported us during the course of writing this book. We also thank Anke Dürkoop. Our particular gratitude is recorded to all fellows and involved researchers of the CARBIO Network who have been responsible for making our project a success story.

Heidelberg September 2010

Rüdiger Klingeler Robert B. Sim

Contents

Part I Fundamentals: Synthesis of Multifunctional Nanomaterials and their Potential for Medical Application	
Physical Properties of Carbon Nanotubes for Therapeutic Applications	3
Carbon Nanotubes in Regenerative Medicine	27
Filling of Carbon Nanotubes with Compounds in Solution or Melted Phase	41
Filling of Carbon Nanotubes: Containers for Magnetic Probes and Drug Delivery	67
Part II Magnetically Functionalised Carbon Nanotubes for Medical Diagnosis and Therapy	
Magnetic Nanoparticles for Diagnosis and Medical Therapy Martin Sobik, Kirsten M. Pondman, Ben Erné, Bonny Kuipers, Bennie ten Haken and Horst Rogalla	85

xvi Contents

Feasibility of Magnetically Functionalised Carbon Nanotubes for Biological Applications: From Fundamental Properties of Individual Nanomagnets to Nanoscaled Heaters	
and Temperature Sensors	97
Nuclear Magnetic Resonance Spectroscopy and Imaging of Carbon Nanotubes	125
Part III Interaction with Biological Systems	
Exploring Carbon Nanotubes and Their Interaction with Cells Using Atomic Force Microscopy	153
Uptake, Intracellular Localization and Biodistribution of Carbon Nanotubes	169
Recognition of Carbon Nanotubes by the Human Innate	100
Immune System	183
Toxicity and Environmental Impact of Carbon Nanotubes	211
Part IV Towards Targeted Chemotherapy and Gene Delivery	
Carbon Nanotubes Loaded with Anticancer Drugs: A Platform for Multimodal Cancer Treatment	223

Contents xvii

Carbon Nanotubes Filled with Carboplatin: Towards Carbon Nanotube-Supported Delivery of Chemotherapeutic Agents	247
Functionalized Carbon Nanotubes for Gene Biodelivery	259
Index	275

Abbreviations

AC/DC Alternating/direct current

AFM Atomic force microscopy/atomic force microscope

AGM Alternating gradient magnetometer

CNT Carbon nanotube
CNTs Carbon nanotubes

CPPs Cell penetrating peptides
CVD Chemical vapour deposition
DNA Deoxyribonucleic acid

DWCNT/DWCNTs Double-walled carbn nanotubes
EPR Enhanced permeation and retention

HRTEM High-resolution transmission electron microscopy
MFM Magnetic force microscopy/magnetic force microscope

MRI Magnetic resonance imaging MTD Maximum tolerated dose MWCNT/MWCNTs Multi-walled carbon nanotubes

NBS Non-specific binding

NIR Near-infrared

NMR Nuclear magnetic resonance
PBS Phosphate buffer saline
PEG Polyethylene glycol
RBM Radial breathing mode
SAR Specific absorption rate

SQUID Superconducting quantum interference device

SWCNT/SWCNTs Single-walled carbon nanotubes

Part I Fundamentals: Synthesis of Multifunctional Nanomaterials and their Potential for Medical Application

Physical Properties of Carbon Nanotubes for Therapeutic Applications

Vittoria Raffa, Orazio Vittorio, Cristina Riggio, Gianni Ciofani and Alfred Cuschieri

Abstract Carbon nanotubes (CNTs) are molecular-scale tubes of graphitic carbon with outstanding properties. They are among the stiffest and strongest fibres known, and have remarkable electronic properties and many other unique characteristics. For these reasons they have attracted huge academic and industrial interest, with thousands of papers on nanotubes being published every year. Applications of CNTs in the field of biotechnology have emerged, raising great hopes. The discovery of carbon nanotubes has the potential of revolutionizing biomedical research as they can show superior performance over other nanoparticles. The advantage lies in a unique, unprecedented combination of electrical, magnetic, optical and chemical properties which is greatly promising for the development of a new class of CNT-based drugs and therapy. In the following discussion a brief summary of the CNT physical properties and how they can serve these purposes will be provided, followed by an overview of the current state of the art and the future perspectives.

1 Introduction

Carbon nanotubes are molecular-scale tubes of graphitic carbon with outstanding properties. They are among the stiffest and strongest fibers known, and have remarkable electronic properties and many other unique characteristics. For

V. Raffa (S), O. Vittorio, C. Riggio, G. Ciofani and

A. Cuschieri

Scuola Superiore Sant'Anna, Piazza Martiri della libertà 33,

^{56127,} Pisa, Italy

these reasons they have attracted huge academic and industrial interest, with thousands of papers on nanotubes being published every year. Applications of CNTs in the field of biotechnology have recently started to emerge, raising great hopes. CNTs have been proposed as components for DNA and protein biosensors, ion channel blockers and as bioseparators and biocatalysts [10]. Concerning the biomedical applications of CNTs, their use is becoming relevant in neuroscience research and tissue engineering. They have been developed as scaffolds for neuronal and ligamentous tissue growth for regenerative interventions of the central nervous system (e.g. brain, spinal cord) and orthopaedic sites. CNTs have also been used as new platforms to detect antibodies associated with human autoimmune diseases with high specificity. This finding paves the way to the development of CNT-based diagnostic devices for the discrimination and identification of different proteins from serum samples and in the fabrication of microarray devices for proteomic analyses. In a similar context, CNTs covalently modified at their open ends with DNA and PNA (peptide nucleic acid) have led to innovative systems for hybridization of complementary DNA strands allowing for ultrasensitive DNA detection. CNTs have also emerged as a new alternative and efficient tool for transporting and translocating therapeutic molecules. The development of new and efficient drug delivery systems is of fundamental importance to improve the pharmacological profiles of many classes of therapeutic molecules. CNTs can be functionalised with bioactive peptides, proteins, nucleic acids and drugs, and used to deliver their cargos to cells and organs.

With the prospect of gene therapy, cancer treatments, and innovative therapies, the science of nanomedicine has become an ever-growing field that has an incredible ability to bypass barriers previously thought unavoidable. The properties and characteristics of CNTs are still being researched heavily and scientists have barely begun to investigate the potential of these structures. CNTs have already proven to serve as safer and more effective alternatives to previous drug delivery methods. They can serve as ideal vehicles, carrying therapeutic drugs, vaccines, and nucleic acids deep into the cell to targets previously unreachable and responding to static and dynamic energetic fields.

The discovery of carbon nanotubes has the potential of revolutionizing biomedical research as they can show superior performance over other nanoparticles. The advantage lies in a unique, unprecedented combination of electrical, magnetic, optical and chemical properties which is greatly promising for the development of a new class of CNT-based drugs and therapy. The blue arrows of Fig. 1 connect CNT properties with their current exploitation in biomedicine and the near future holds the promise to discover and prove many new connections.

In the following discussion a brief summary of the CNT properties and how they can serve these purposes will be provided, followed by an overview of the current state of the art and the future perspectives. The discussion will be focused on CNTs as nanotransducers (a transducer is a system converting one type of energy to another) and nano-antennas, in a meaning larger than the familiar one (i.e. a detectors/transmitters of any wavelength, included optical and microwaves) related to biomedical applications.

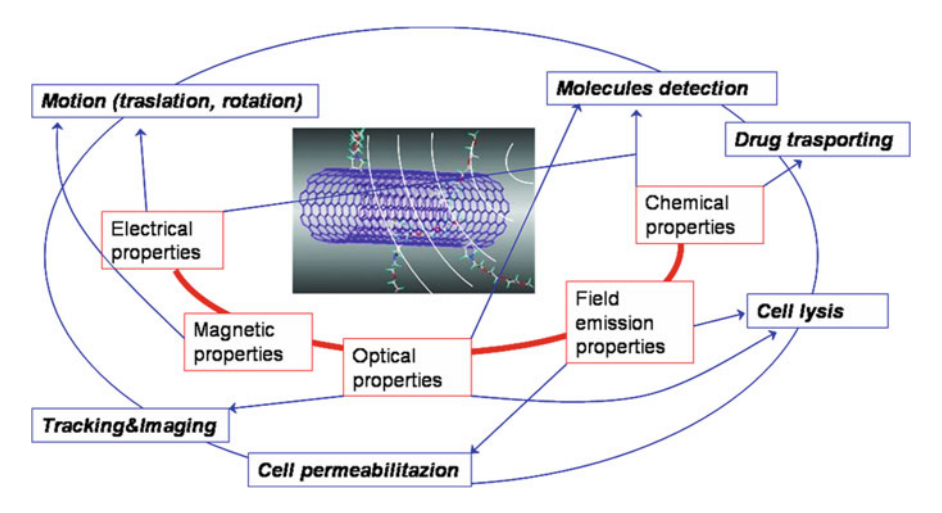


Fig. 1 CNT properties and their application in the biomedical field. Reproduced from [22] with the permission of Bentham Science Publishers Ltd

2 Electrical Properties

The nanometer dimensions of carbon nanotubes (CNTs), together with the unique electronic structure of a graphene sheet, make the electronic properties of this one-dimensional structure highly unusual [51]. A single wall CNT (SWCNT) is geometrically just a rolled up graphene sheet. Its structure can be specified or indexed by its circumferential periodicity. In this way, a SWCNT geometry is completely specified by a pair of integers (n, m) denoting the relative position c = na1 + ma2 of the pairs of atoms on a graphene sheet which, when rolled onto each other, form a tube.

Theoretical calculations and conductivity measurements demonstrated that isolated SWCNT exhibit unique electronic transport phenomena, which can lead to both metallic and semiconducting behaviour, depending on small variations in the chiral angle (n, m) of the hexagons or diameter [25, 28, 71]. If all wrapping vectors could occur with equal probability, 1/3 of the SWCNTs would be metallic and 2/3 semiconductor. The physical phenomena that lead to the electronic properties of carbon nanotubes can be understood with the band-folding theory. The general rules for the metallic behaviour of SWCNTs are as follows: (n, n) tubes are metals; (n, m) tubes with n - m = 3i, where j is a non-zero integer, are very tiny-gap semiconductors; and all others are large-gap semiconductors. Hence, we can find three kinds of carbon nanotubes: large-gap, tiny-gap, and zero-gap. As the tube radius R increases, the band gaps of the large-gap and tiny-gap varieties decreases with 1/R and $1/R^2$ dependence, respectively. This band-folding picture, first verified by tight-binding calculation, is expected to be valid for tube diameters larger than 4 Å. Experimental studies using scanning tunnelling and other techniques have basically confirmed this theoretical prediction.

Figure 2a is a schematization of typical three-terminal device geometry for transport measurement. The AFM image shows an individual SWCNT deposited on two electrodes (source and drain electrodes). Room transport characteristics fall into two distinct types: no or weak gate voltage dependence of the linear-response conductance (metallic type) and strong gate dependence (semiconducting type). Figure 1b shows typical room-temperature current–voltage (I–V) characteristic for semiconducting nanotubes [72]. It indicates that the nanotube is a hole-doped semiconductor and the device behaves as a p-type Field-Effect Transistor (FET).

Electronic properties of CNTs can be modified also by the presence of defects (e.g., additional pentagons and heptagons) within the predominantly hexagonal network [73, 74]. On-tube metal–semiconductor, semiconductor–semiconductor, and metal–metal junctions may be formed by introducing topological structural defects. For example, two half tubes jointed with a heptagon–pentagon defect pairs (Stone–Wales defect, 7–5–5–7) can form a metal–semiconductor Schottky barrier.

Multi wall CNTs (MWCNTs) consist of several coaxially arranged SWCNTs. It has been widely discussed whether MWCNTs properties are closer to graphite, or whether MWCNTs behave as a set of independent SWCNTs. A remarkable variety of physical phenomena have been observed in their electrical transport, presumably a consequence of the way in which nanotubes were contacted and the sample quality. Why the measured conductance is only one-half of the expected quantized conductance for an ideal metallic nanotube is not yet completely understood [29].

Tight-binding calculations for the static polarizabilities of both SWCNT and MWCNT have also found the dielectric response to be highly anisotropic [8, 45].

Both metallic and semiconducting nanotubes find application in biomedical fields [72]. The change in the electrical conductance, resulting from molecule adsorption on CNT surfaces, is largely exploited as a sensor signal [24, 43]. The adsorption of molecules on the nanotubes is associated with a partial charge transfer, which alters the charge-carrier concentration. For the detection of molecules that are only weakly adsorbed, CNT sidewalls can be modified with

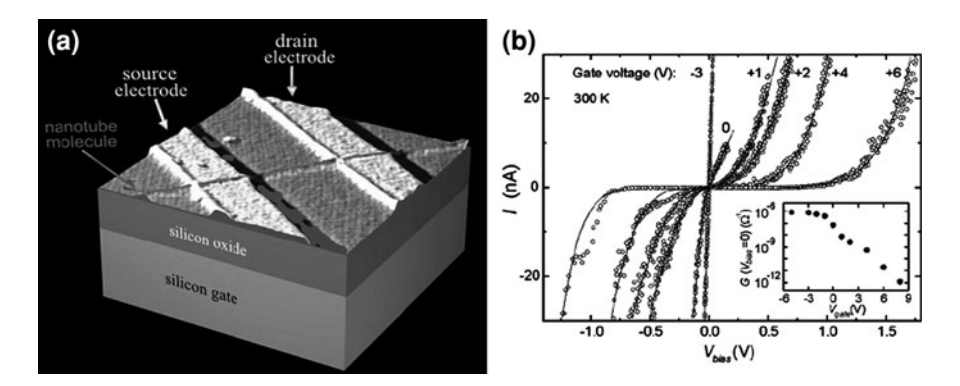


Fig. 2 a Three-dimensional AFM image of a SWCNT deposited on two electrodes (source and drain electrodes); **b** two-probe I-V bias curves for various values of the gate voltage ($V_{\rm gate}$). Reproduced from [72] with the permission of IOP Publishing Ltd

metallic nanoparticles which enhance the change in resistance. Similarly, graphitic sidewall functionalization leads to modifications of the nanotube delocalised π system, which offers a convenient and controllable means of tethering molecular species [4].

Besides raw semiconducting nanotubes not subjected to specific treatments which principally exhibit p-type semiconducting characteristics (holes are the majority carriers), also metallic nanotubes chemically modified e.g., by electrochemical methods, become insulating, and show semiconducting behaviour [6].

Sensors based upon CNT-FETs can be considered in two different modalities. One possibility is to monitor the conductance of an individual CNT or a network of CNTs during the introduction of the analyte solution (chemiresistor configuration). In this configuration, the resistance of the device is directly or inversely proportional to the concentration of the analyte. A second method is to measure the complete field-effect modulation of conductance after introduction of the test solution. This latter methodology is referred to as chem-FET, where the threshold voltage shift provides information about the analyte concentration.

CNTs exhibit also high electron transfer rates (comparable to those observed in other carbonaceous electrodes) for different redox couples in various media [5], which has stimulated an increasing research on CNT-based amperometric sensors for the detection of specific analytes in solution. Different mechanisms (e.g., oxidatively pretreated CNT surface, biofunctionalised surface) can be used in the preparation of CNT-based biosensing devices.

Because SWCNTs are only one molecular layer thick, every atom is at the surface. A consequence of every atom being on the surface is that the adsorption of any molecule onto the surface of a nanotube will change the electrical properties of an entire nanotube, which means that nanotube sensors are capable of extremely high sensitivity [23, 24], over a broad range of analytes in both gaseous and liquid environments. At the same time, carbon chemistry is robust, enabling reliable, long-lived sensors. Because nanotubes are so small, little power is required to operate the sensors. Semiconducting carbon nanotubes have been demonstrated to be promising nanoscale molecular sensors for detecting gas molecules with fast response time and high sensitivity at room temperature [43].

Biological macromolecules bound to the surface of a nanotube, and undergoing a binding event with change of charge state, can thus perturb the current flow in the nanotube [35]. The research groups of Dai [18], Dekker [9], Gruner [13] and Tao [30] have investigated the application of carbon nanotube devices as electrical biosensors, where biomolecules including enzymes, proteins and oligopeptides have been immobilized. Gruner and co-workers [70] used carbon nanotube transistor devices for detection of protein binding. A PEI/PEG polymer coating layer was used to avoid non-specific binding, with attachment of biotin to the layer for specific molecular recognition. Biotin–streptavidin binding was detected by changes in the device characteristic. Dai and co-workers [18] investigated a SWCNT transistor as a platform for investigating surface–protein and protein–protein binding and developing highly specific electronic biomolecule detectors. Non-specific binding of proteins on nanotubes, a phenomenon found with a wide

range of proteins, is again overcome by modifying the nanotubes with polyethylene oxide chains. A general approach is then advanced to enable the selective recognition and binding of target proteins by conjugation of their specific receptors to polyethylene oxide functionalized nanotubes. This approach, combined with the high sensitivity of nanotube electronic devices, enables highly specific electronic detection of clinically important biomolecules such as antibodies associated with human autoimmune diseases.

New nanomaterial approaches aimed at modifying surfaces have the potential to deliver a new generation of biosensors and bioelectronic devices for biomedical applications [75]. The integration of biomolecules with CNTs enables the use of such hybrid systems as electrochemical biosensors (enzyme electrodes, immunosensors or DNA sensors) and active field-effect transistors (Yang et al. 2007).

The specific advantage of CNTs for integrating biomolecules is their small size, allowing these nanoelectrodes to be plugged into locations where electrochemistry would otherwise be unable to be performed, such as inside protein complexes or on protein surfaces [57]. One of the opportunities CNTs will provide is a more efficient way in communicating to the outside world the activity of biological molecules used in biosensors [78]. Typically this communication is achieved via the transfer of electrons. The potential of carbon nanotubes to facilitate communication between enzymes and the outside world with efficient transfer of electrons is perhaps best demonstrated by the enzyme glucose oxidase (GOx), a oxidoreductase enzyme that oxidizes glucose to gluconolactone. Direct turnover of the enzyme at the underlying electrode will overcome problems associated with the shuttling of electron between the enzyme and the electrode by a diffusing species. A major advance in the direct electrical contacting of redox enzymes and electrodes using SWCNTs was recently accomplished attaching the enzyme microperoxidase MP-11 to the ends of SWCNTs, which were aligned normal to the electrode surface using self-assembly to give a nanoelectrode array [34]. An array of perpendicularly oriented SWCNTs on a gold electrode was fabricated by covalently attaching carboxylic acid functionalized SWCNTs, generated by the oxidative scission of the carbon nanotubes, to a cysteamine monolayer-functionalized gold electrode. Patolsky et al. [57] used the same approach to build an array of perpendicularly oriented SWCNTs on a gold electrode, and the amino-derivative of FAD cofactor (flavin adenine dinucleotide) was covalently coupled to the carboxylic groups at the free ends of the standing SWCNTs. Apoglucose oxidase (apo-GOx) was then reconstituted on the FAD units linked to the ends of the standing SWCNTs. The bioelectrocatalytic oxidation of glucose was observed at the reconstituted apo-GOx functionalized electrode surface, and the electrocatalytic anodic current increased as the concentration of glucose increased. Knowing the surface coverage of the GOx-SWCNT units, the turnover rate of electrons to the electrodes was estimated to be about 4,100 s⁻¹. This value is about six-fold higher than the turnover rate of electrons from the active site of native GOx to its natural oxygen (O_2) electron acceptor (700 s^{-1}) . Thus, the electron transfer barrier between the FAD centre and the electrode is lower for systems that include shorter SWCNTs as connectors.

Yu et al. [80] reported the combination of electrochemical immunosensors using SWCNT forest platforms with multilabel secondary antibody–nanotube bioconjugates for highly sensitive detection of a cancer biomarker in serum and tissue lysates. Greatly amplified sensitivity was attained by using bioconjugates featuring horseradish peroxidase (HRP) labels and secondary antibodies (Ab(2)) linked to carbon nanotubes at high HRP/Ab(2) ratio. This approach provided a detection limit of 4 pg/ml for prostate specific antigen (PSA) in 10 µl of undiluted calf serum, a mass detection limit of 40 fg. This immune sensor showed excellent promise for clinical screening of cancer biomarkers and point-of-care diagnostics.

Covalent attachment of DNA to chemically functionalized CNTs has been used in the development of DNA sensors [38] in which specific DNA sequences were covalently immobilized onto acid-oxidized and plasma-activated carbon nanotubes. Li et al. [48] used a nanoelectrode array based on vertically aligned MWCNTs embedded in SiO₂ for ultra-sensitive DNA detection. Oligonucleotide probes were selectively functionalized to the open ends of nanotubes. Interestingly, the detection sensitivity was dramatically improved by lowering the nanotube density. Similarly Cai et al. [14, 16] also demonstrated the detection of DNA hybridization at a DNA functionalized carbon nanotube array using daunomycin as a redox label that was intercalated into the double-stranded DNA–CNT assembly and detected by differential pulse voltammetry.

The interactions of various polypeptides with individual CNTs, both MWCNTs and SWCNTs, were investigated by atomic force microscopy by Li et al. (2006). It was demonstrated that polypeptides containing aromatic moieties, such as polytryptophan, showed a stronger adhesion force with oxidized MWCNTs than that of polylysine because of the additional π - π stacking interaction between the polytryptophan chains and CNTs.

The length scales of CNTs are similar to that of typical biological macromolecules, which gives to CNTs a considerable advantage over other materials in functioning as effective electrodes in biosensing; novel CNT-based interfaces between the neural tissues and solid-state electronics are particularly interesting for non-invasive sensing and/or stimulation of the cells and will be now briefly approached. CNTs have thus been applied in several areas of nerve tissue engineering to probe and augment cell behaviour, to label and track subcellular components, and to study the growth and organization of neural networks. Recent reports show that nanotubes can sustain and promote neuronal electrical activity in networks of cultured cells, but the ways in which they affect cellular function are still poorly understood. Cellot et al. show, using single-cell electrophysiology techniques, electron microscopy analysis and theoretical modelling, that nanotubes improve the responsiveness of neurons by forming tight contacts with the cell membranes [17]. Very interestingly, this report shows that nanotubes can sustain and promote neuronal electrical activity in networks of cultured cells, by favouring electrical shortcuts between the proximal and distal compartments of the neuron.

Intracellular compartments are electrically exposed to bundles of substrate nanotubes and such contacts might result in an electrical shortcut (summarized with an equivalent electric circuit model, Fig. 3a). The cell soma acts as a

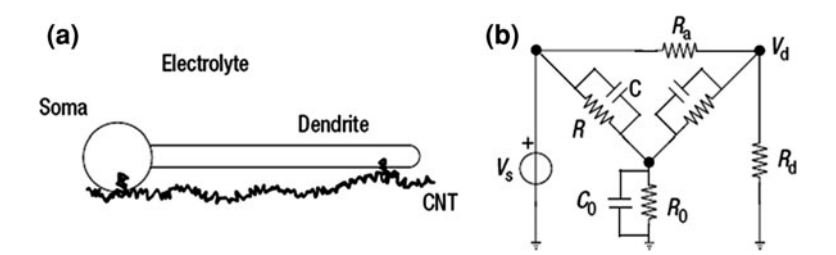


Fig. 3 Cell-CNT electrical interaction modelling. Reproduced from [17] with the permission of Nature Publishing Group

generator Vs during a spike, the somato-dendritic attenuation is modelled by a resistor Ra, and the shunting effect of the bulk electrolyte is represented by an R0–C0 parallel arrangement (Fig. 3b; [61]). The intracellular interface nanotube-electrolyte is also represented by an R–C parallel arrangement. This circuit model allows analysis of the physical conditions that might underlie the nanotube-mediated boosting effect of the somato-dendritic coupling.

Recent studies have suggested the great potential of high density, carbon nanotube (CNT) coated surfaces as an interfacing material with neural systems [7, 31, 32, 39, 50, 52, 53, 69, 81]. A study of Shein et al. [64] presents novel carbon nanotube-based electrode arrays composed of cell-alluring carbon nanotube (CNT) islands [64]. These play a double role of anchoring neurons directly and only onto the electrode sites (with no need for chemical treatments) and facilitating high fidelity electrical interfacing–recording and stimulation. This work presents a new and complete approach to engineer and interface with electrically viable neuronal systems. Each micro-electrode is coated by a layer of several microns of dense and entangled CNTs, synthesized by a CVD process thus forming a CNT island. The islands strongly attract and anchor cells to pre-defined locations, and enable the formation of stable sub-networks on electrically active recording sites (Fig. 4).

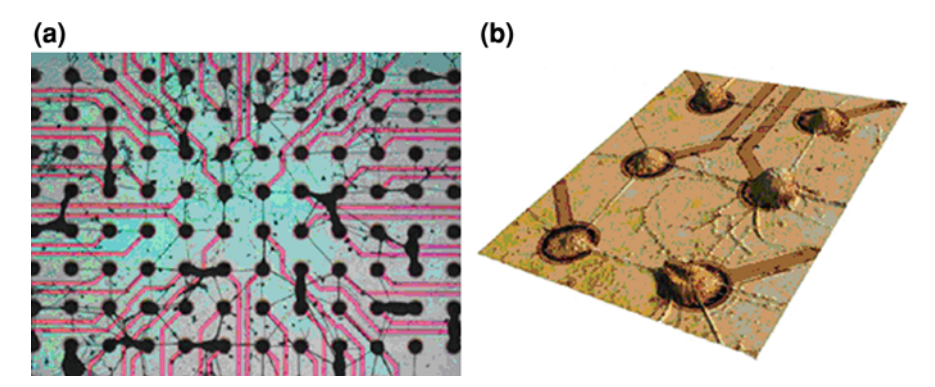


Fig. 4 Self-assembled neuronal patterned network on a CNT neurochip. After several days of plating, the cells on the CNT neuro-chip interconnect to form networks with cell aggregates at the CNT islands and cell-free connections in-between. Reproduced from [64] with the permission of Nature Publishing Group

Efficient cell patterning results with a stable neuronal network even though no adhesive agents were used. Low electrode impedance improves the electrochemical interface, and contributes to high quality recording and efficient stimulating signals. The electrical viability of the cell cultures on the CNT substrates, and their long term survivability (up to 2 months), substantiate the biocompatibility of these surfaces. Combined with their superior electrical performances, it was demonstrated that CNT coated electrodes are, in fact, well-suited to assist the interfacing between electrically active biological cells and conventional electronic systems.

A study of Keefer et al. [42] shows that conventional tungsten and stainless steel wire electrodes can be coated with carbon nanotubes using electrochemical techniques, and that this coating enhances both recording and electrical stimulation of neurons in culture, and in vivo, in rats and monkeys by decreasing the electrode impedance and increasing charge transfer. CNT-coated electrodes have improved electrochemical and functional properties in cultured neurons, rat motor cortex and monkey visual cortex. Controlled deposition of CNTs on flat multi-electrodes assay electrodes and sharpened wire electrodes demonstrated that the CNT coatings can be applied to a variety of substrates and geometries.

Figure 5a and b shows, for example, stereotrode recordings from the rat motor cortex, namely data recorded from a bare tungsten (red trace) and CNT/gold-coated (black trace) stereotrode tip over 150 ms: the CNT-coated electrode shows increased power when compared with the bare electrode (red trace) at all frequencies (1–1,000 Hz).

CNT-coated electrodes had increased sensitivity for recording neurons, decreased susceptibility to electrical noise, and functioned as broadband detectors of neural activity. It was possible to record local field potentials (LFPs), multiunit activity and neuronal spiking simultaneously with one electrode. The efficacy of electrical stimulation was also greatly increased by the CNT coatings.

Particularly interesting in CNTs, are also their field emission properties. When a high electric field in the order of 10^7 V/cm is applied on a solid surface with a negative electrical potential, electrons inside the solid are emitted into vacuum by the quantum mechanical tunnelling effect. This phenomenon is called field emission of electrons. In 1995, field emission (FE) from an isolated MWCNT was

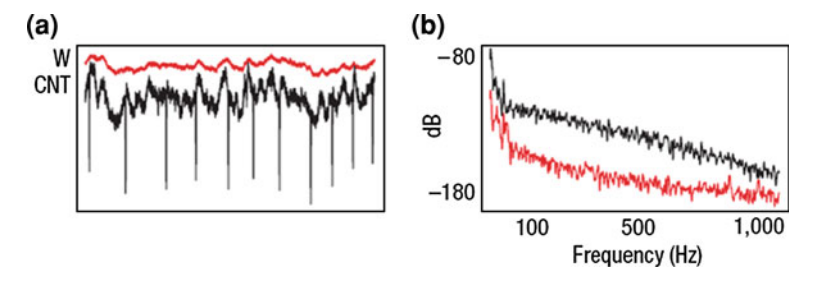


Fig. 5 Stereotrode recordings from the rat motor cortex. **a** Data recorded from a bare tungsten (*red trace*) and CNT/gold-coated (*black trace*) stereotrode tip over 150 ms; **b** power spectra calculated from 60 s of neural activity. Reproduced from [42] with the permission of Springer

first reported by Rinzler et al. [60]. The CNTs possess many properties favourable for field emitters [63]. In particular, when placed in an electric field, the CNTs strongly enhance the electric field at their ends and this effect is responsible for the lowest observed threshold of <10⁴ V/cm for the electron field emission from a CNT [19]. Saito et al. [63] performed systematic studies of field emission on carbon nanotubes of different types and confirm their excellent field emission performances. They observed significant differences in the emission characteristics between SWCNTs, closed and opened arc-discharge MWCNTs, and catalytically grown MWCNTs. Briefly, SWCNTs degrade substantially faster, as do MWCNTs with disordered structures. The tip structure is also important for field emission performances. To obtain low operating voltages as well as long emitter lifetimes, the nanotubes should be MWCNTs and have closed, well-ordered tips. The emission performances of MWCNT are in fact seriously degraded by opening their ends. This result indicates that nanotubes cannot be considered as ordinary metallic emitters. The large field amplification factor, arising from the small radius of curvature of the nanotube tips, is partly responsible for the good emission characteristics. On the other side, results suggest that electrons are not emitted from a metallic continuum as in usual metallic emitters, but rather from welldefined energy levels, corresponding to localized states at the tip.

Field emission properties of CNTs found application in irreversible electroporation for cell lysis. A study of Yantzi and Yeow [79] investigated the use of CNTs to reduce the voltage requirements for irreversible electroporation for portable lab-on-a-chip devices with strict power limitations. Experiments of cell lysis were carried out using DH5 α *E. coli* bacteria equipped with a kanamycin antibiotic resistance gene. The voltages required for 95% reduction in *E. coli* cultures was greatly reduced using electrodes covered with CNTs. Instead of using flat plates to achieve capacitance, CNTs can be patterned on the electrodes resulting in higher electric fields and power output at lower voltages. In addition to lowering the voltage requirements for pulsed electric field cell lysis, the concentrated field regions produced by the CNT represent an effective means of disrupting smaller sub cellular organelles, viruses and nuclei present in eukaryotic cells. The voltages required for >95% reduction in E. coli cultures was reduced from 135 V to around 35 V using electrodes covered with CNTs.

Another exploitation of CNTs as vectors for permeabilization of bacteria has been proposed by Chapana and colleagues with potential application in cell biology for in-vitro and ex-vivo molecule delivery [62]. The work describes a novel method to electroporate gram-negative bacteria (*Acidothiobacillus ferro-oxidans*) via MWCNTs. The authors demonstrated that addition of CNTs into a solution containing bacteria and gold nanoparticles (GNPs) and subsequent exposure to microwave radiation facilitates a rapid transport of GNPs across the cell wall (Fig. 6), without affecting the cell viability.

The activation of CNTs is due essentially to the "lightning rod" effect, and occurs when a metallic rod (e.g., a MWCNT) is inserted into a region of a uniform electric field E_0 . This causes a strong field enhancement at the CNT tip. A simple estimation of this enhancement for a single, straight CNT is given by:

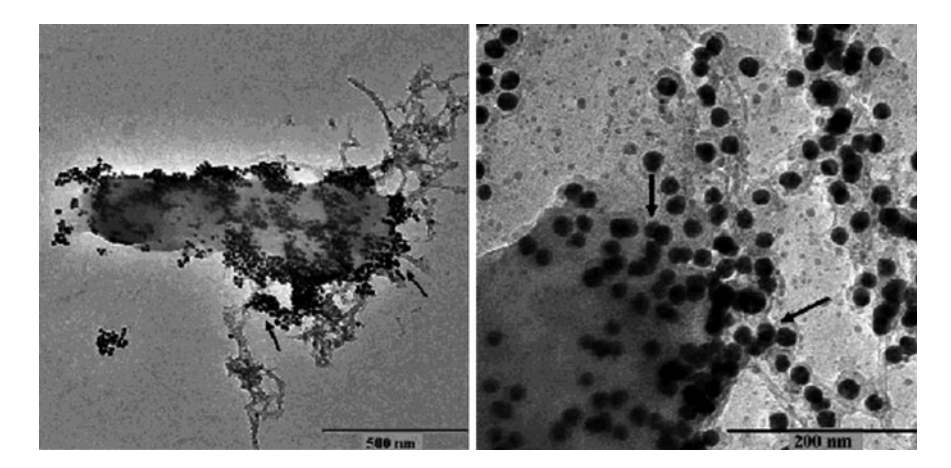


Fig. 6 Left TEM picture of the Acidothiobacillus ferrooxidans cell after the exposure to microwaves (5 s). Accumulation of CNTs on the cell wall is clearly visible. GNPs also accumulate on the cell wall, but mostly at the CNT-cell contact points (see arrows); right TEM picture of the area of contact of the cell with CNTs, and of massive GNP transfer into the cell. Reproduced from [62] with the permission of Nature Publishing Group

$$E/E_0 = \alpha \cdot L/D$$

where $\alpha \approx 3$ is a constant, E is the field at the tip, L is the CNT length, and D is its diameter.

The described process constitutes a novel reversible electroporation of gram negative bacteria. The mechanism proposed by the authors for pore generation and intracellular transport of GNPs via microwave-activated CNTs primarily consider an induced dipole along the CNTs, whose positive ends make contact with the negatively charged surface of gram-negative *A. ferrooxidans* bacteria. This initial electrostatic contact is enhanced by the microwave energy, which in turn determines the onset of CNT-sized pores across the cell membranes. GNPs attached onto the cell surface and having a size comparable to the pore openings take advantage of these transient membrane disruptions and diffuse inside the cells.

CNTs are usually considered as 1D conductive structures and this has been seen as the electric field enhancement at their tips was utilized for improving electroporation [62]. The field enhancement coefficient is a function of the distance to CNT tips (Fig. 7a, inset table). Provided that the CNT is 1 μ m long and 100 nm thick, the electric fields (E) nearly at the tips will be 33.5-fold of the applied electric field (E_0). However, at a 200 nm distance from the tips, the electric fields only have 0.6-fold enhancements. Thereafter, the efficiency of electroporation largely depends on the proximity of the cell membrane to the CNT tips. The close contact between CNTs and cell membranes guarantees therefore the poration of membranes with the highly enhanced field by CNTs.

A general indicator of electroporation is the transient time constant at the decaying phase when an electric pulse is used to generate the field. It is correlated

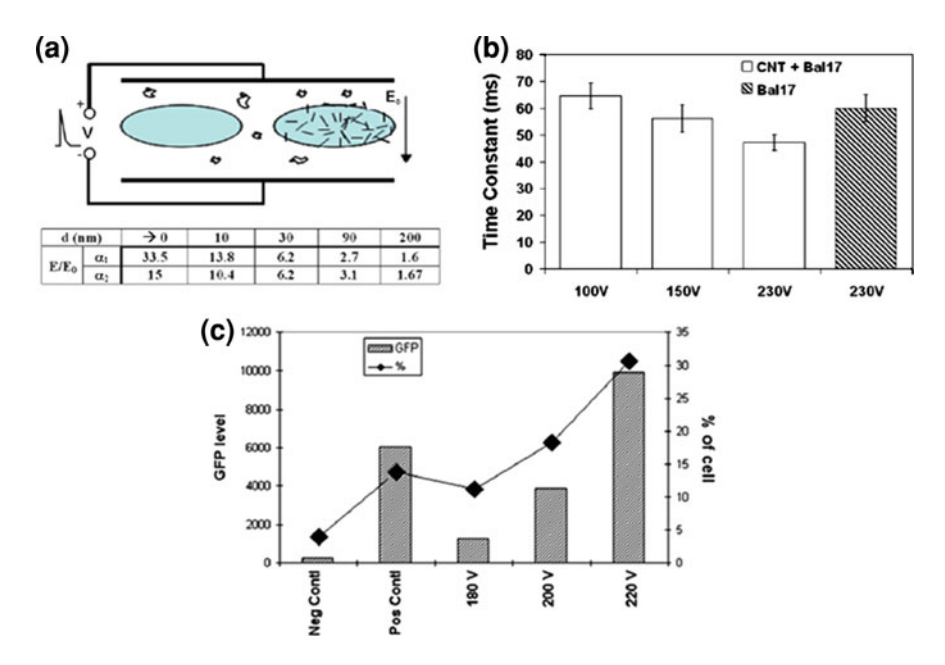


Fig. 7 Electric field enhancement by CNT in electroporation. **a** Sketch of electroporation with CNT-free (left) and CNT-associated cells (right). Table insert: theoretical electric field (E) enhancement over the applied field (E_0) by a nanotube of 1 μ m long. d denotes the distance to nanotube tip. a1 and a2 are the aspect ratios (i.e., diameter/length) of nanotubes, and equal to 0.1 and 0.5 respectively. **b** Electroporation time constants versus the voltages. **c** Improvement of EGFP transfection by CNT mediated electroporation in Bal17 cells. Reproduced from [15] with the permission of Springer

to the permeability of cell membrane as the result of electroporation. The extra and intracellular molecular (or ionic) exchange can lead to increase of the ionic strength and decrease of the dielectric constant. The corresponding reduction of resistance and capacitance result in a smaller time constant. Thus, the time constant is inversely proportional to the level of electroporation. Bal17 cells were used to test nanotube-facilitated electroporation [15]. The time constants corresponding to cells without CNTs and CNT-associated cells are plotted versus voltages in Fig. 7b. Clearly, the time constant decreased in CNT-associated cells compared to CNT-free Bal17 cells. The time constant of CNT-associated cells at 150 V was 58 ms. The value was comparable to the time constant obtained from CNT-free cells at 230 V, which was the voltage needed to obtain transfection in the CNT-free cells.

The transfection was carried out by adding pEGFP plasmid to the cell suspension in the cuvette. The transfection results 48 h after the electroporation were assessed by flow cytometry. As shown in Fig. 7c, CNT associated cells demonstrated improvement in the EGFP transfection in terms of the percentage of EGFP positive cells and the average amplitudes of EGFP signals in comparison to the control cells.

A new modality for cell electro-permeabilisation based on the use MWCNTs and external static electric fields was recently proposed by Raffa et al. [59]. The method is based on the exploitation of the dielectric response of MWCNTs. Cells are placed in contact with carbon nanotubes and then subjected to the action of two orthogonal pulsed electric fields according to a specific time sequence in such a way that, when one electric field is active, the other is deactivated and vice versa. The experimental data obtained indicate that this method of CNT-enhanced electro-permeabilisation provides an effective means of lowering the electric field voltage required for repairable cell electro-permeabilisation to below 50 V/cm and with an efficiency exceeding 80%.

The results of CNT facilitated electroporation suggest they may be used to improve electroporation allowing the consistency of CNT length and aspect ratio quantitative control and adjustment of the electroporation strength. Such advantages hold promise for the enhancement of electroporation upon optimization of the parameters, such as amount of CNTs, level of CNT association to cells, buffer contents, pulse waveform and cuvette size.

3 Magnetic Properties

Thanks to magnetic susceptibility, CNTs should be used as magnetically driven nanotools. Magnetic susceptibility can be intrinsic or induced by attached particles. For suspended CNTs, a motion can result from attractive or repulsive magnetic forces or alignment dynamics.

When a magnetic field is applied to a graphene sheet, the π -electrons are free to circulate along hexagonal carbon rings and are responsible for inducing a magnetic field that opposes the external one. This explanation, provided by Raman in 1929 [36], introduced the concept of molecular ring currents and still remains as the basis for our understanding of the magnetic susceptibility behaviour of carbon allotropes. By applying an external magnetic field along the CNT axis, independent ring currents perpendicular to the axis of the tube are formed; thus one should expect a paramagnetic response when the external field is applied along this direction [49].

An external magnetic field can alter the semiconducting or metallic nature of a CNT. This phenomenon corresponds to the Aharonov–Bohm effect of a CNT and is related to the oscillation of the electronic conductance of CNT at low temperature or with impurity and electronphonon scatterings [55].

Magnetic properties exhibited by CNTs can be also induced by metallic impurities entrapped during the fabrication process, enabling them to react to external magnetic fields. Carbon nanotubes usually grow through or from the surface of such metal catalyst particles. 3d metals (Fe, Co, Ni) or their combinations with other metals are very effective as catalysts. A combination of carbon nanotubes and the magnetic metal catalyst particles may allow use of carbon nanotubes for magnetically guided drug delivery purposes.

An application of magnetically-driven drug-carrying CNTs in cells was recently suggested by Cai et al. (2005) who have designed an alternative physical method of in-vitro and ex-vivo gene transfer, called nanotube "spearing": CNTs grown from plasma-enhanced chemical vapour deposition contain nickel particle catalysts entrapped into their tips, allowing them to respond to a magnetic field. The tubes were functionalized with DNA plasmids immobilized onto the CNTs and subsequently speared into target cells via external magnetic fields. They used a two step procedure for nanotube spearing: in the first step a rotating magnetic field drives nanotubes to spear the cells on a substratum (surface) and in the second step a static field pulls nanotubes into the cells.

Moreover, Cai and colleagues showed that CNT-cell complexes are formed in the presence of a magnetic field [15]. The complexes were analyzed by flow cytometry as a quantitative method for monitoring the physical interactions between CNTs and cells (Fig. 8). They observed an increase in side scattering signals, where the amplitude was proportional to the amount of CNTs that are associated with cells. Even after the formation of CNT-cell complexes, cell viability was not significantly decreased. The association between CNTs and cells was strong enough to be used for manipulating the complexes and thereby conducting cell separation with magnetic force. In addition, the CNT-cell complexes were also utilized to facilitate electroporation. They observed a time constant from CNT-cell complexes but not from cells alone, indicating a high level of pore

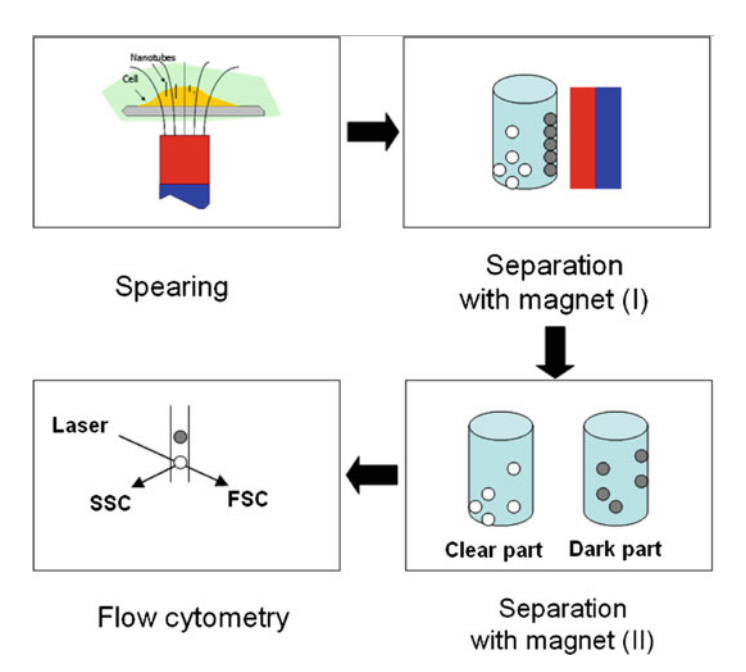


Fig. 8 Magnetic field-mediated CNT-cell association and characterization by flow cytometry. Reproduced from [15] with the permission of IOP Publishing Ltd

formation in cell membranes. Experimentally, they achieved the expression of enhanced green fluorescence protein by using a low electroporation voltage after the formation of CNT–cell complexes. These results suggest that higher transfection efficiency, lower electroporation voltage, and miniaturized setup dimension of electroporation may be accomplished through the CNT strategy outlined herein.

Pensabene et al. [58] demonstrated that, by combining the magnetic response with the ability to interact with cells, CNTs can also be used for cell manipulation. As shown in Fig. 9 the displacement effect has been observed in particular after 48 hours of incubation of cells with CNTs: the cell density increases close to the magnet (A2) and in the meantime on the opposite site (A1) the number of cells is stable or decreased. These data demonstrated that cells treated with nanotubes with 3% iron content are able to internalize this nanoparticle and to move towards a magnetic source.

This becomes potentially very useful in cancer therapy, especially to prevent cell migration in metastasis: CNTs could be functionalized in order to bind selectively cancer cells, and injected in the target site; f-CNT bound to cells could be constrained to the desired site by applying external magnetic field in order to prevent cancer cell migration. In addition, cancer cells could be treated by using CNTs also as intracellular transporters of chemotherapies or as heater probes.

The magnetic properties of the nanotubes can be used also to perform studies about in-vivo biodistribution by using magnetic resonance. Al Faraj et al. [3] performed a non-invasive follow-up study to evaluate the biodistribution of CNT and effect of nanotube deposition after exposure directly in vivo. They used Combined helium-3 and proton magnetic resonance (MRI) to evaluate the biodistribution and biological impact of raw single-wall CNTs (raw-SWCNTs) and superpurified SWCNTs (SP-SWCNTs) in a rat model. The susceptibility effects induced by metal impurities in the intrapulmonary-instilled raw-SWCNT samples were large enough to induce a significant drop in magnetic field homogeneity detected in 3He MR image acquired under spontaneous breathing conditions using a multiecho radial sequence. They demonstrated that superpurified SWCNTs cannot be visualized by MRI because of the low percentage of metal impurities. On the contrary, proton MRI allowed detection of intravenously injected raw-SWCNTs in spleen and kidneys using gradient echo sequences sensitive to

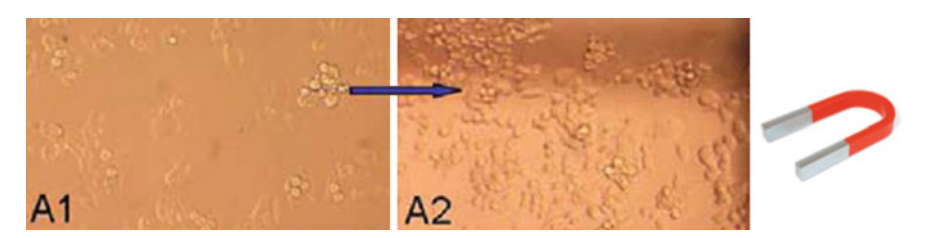


Fig. 9 Cell displacement after incubation in culture with MWCNT-modified medium. Cells move towards the magnet source. Reproduced from [58] with the permission of IEEE

changes of relaxation time values. Superpurified SWCNTs thanks to this low content of metal residuals, represent the best sample in terms of biocompatibility, but it is not possible with the MRI to fully understand their biodistribution in vivo. Instead nanotubes with a significant percentage of metal impurities are well detected. It is clear that we need to find the best level of purity of nanotubes in order to have both good biocompatibility and be able to visualize them by using common magnetic resonance or similar imaging techniques.

4 Optical Properties

Since biological tissues exhibit a deep penetrability with very low absorption of NIR photons in the wavelength range of 700–1100 nm the SWCNTs, with an absorption band in the NIR region, could have advantages in use in biomedical applications and in particular as diagnostic imaging contrast agents and in cancer photoablative therapy [44, 77].

The unique photostability of SWCNT photoluminescence allows for longer excitation time at higher laser flux than either organic fluorophores or quantum dots. Moreover, in contrast to alternative methods that track carbon nanotubes by linking them covalently or noncovalently to external fluorophores or chelated radioisotopes [65, 66, 68], the near-IR fluorescence technique provides a direct and unambiguous way to monitor chemically pristine SWCNTs with sensitivity high enough to detect even a single intracellular nanotube.

A method for observing pristine, hydrophobic SWCNTs in biological media through their unique near-infrared intrinsic fluorescence was presented by Cherukuri et al. [20]. In this in-vitro study, mouse macrophage cells were incubated in SWCNT suspension to actively ingest nanotubes. The long wavelengths of SWCNT emission allow high contrast detection with strong discrimination against endogenous fluorescence. Low concentrations of nanotubes in biological specimens were selectively detected. To obtain near-IR imaging a spectrofluorometer and a modified fluorescence microscope were used. It was demonstrated that macrophage can actively ingest significant quantities of single-walled carbon nanotubes without showing toxic effects. The ingested nanotubes remain fluorescent and can be imaged through near infrared fluorescence microscopy at wavelengths beyond 1100 nm. These findings are therefore relevant to the many envisioned biomedical applications that exploit properties of individualized SWCNTs.

In 2006 the same author investigated the use of the intrinsic near-IR fluorescence of individual SWCNTs, to measure their blood elimination kinetics. These experiments were performed in vivo: a suspension of SWCNTs in pluronic surfactant was injected into rabbits and after 24 h they were sacrificed to identify the organs in which the SWCNTs concentrate [21]. To quantify the kinetics of SWCNT elimination from the blood circulation, spectrally integrated SWCNT fluorescence intensities were measured from specimens representing different time

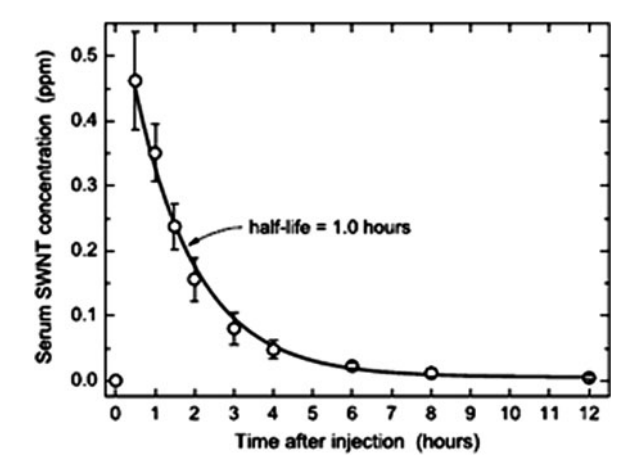


Fig. 10 Time dependence of blood serum SWCNT concentration after injection measured for four rabbits. Each data point is the averaged emission intensity spectrally integrated above a linear baseline connecting the minima at 1,100 and 1,250 nm. This baseline construction captures a major SWCNT fluorescence feature while avoiding systematic errors from an underlying background of weak autofluorescence. *Error bars* show standard errors of the mean. The *solid curve* is a first-order kinetic fit to the data. Reproduced from [21] with the permission of National Academy of Science, USA

points. The data are well modelled by first-order (exponential) decay with a half-life of 1 h (Fig. 10).

The absence of biexponential or multiexponential kinetic components indicates that there was no significant temporary accumulation of nanotubes in tissues that could act as reversible reservoirs.

The biodistribution of SWCNTs among organ systems after elimination from the systemic circulation was also examined by performing near-IR fluorescence microscopy on tissue specimens. Figure 11 shows representative micrographs of liver tissue taken from rabbits killed 24 h after SWCNT injection.

Figure 11a reveals numerous regions in the liver specimen with significant SWCNT concentrations. The more magnified image of Fig. 11b shows one or two green clusters in addition to 30 diffraction-limited green spots. Each of these spots is emission from a single semiconducting SWCNT. Similar analysis of tissue specimens from the kidneys, lungs, spleen, heart, brain, spinal cord, bone, muscle, pancreas, intestine, and skin revealed far fewer or no nanotubes, and the control specimens showed no emissive features identifiable as SWCNTs: at 24 h after i.v. injection, the only significant SWCNT concentration is in the liver.

During the 24-h period between exposure and termination of the experiment, the experimental animals displayed normal behaviour and showed no evidence of adverse effects from i.v. SWCNT administration at the 20 g/kg dosage used here. In addition, pathological examination during necropsy revealed no gross organ abnormalities, and histological evaluation of tissue sections found no pathological differences between the experimental and control animals. The absence of acute

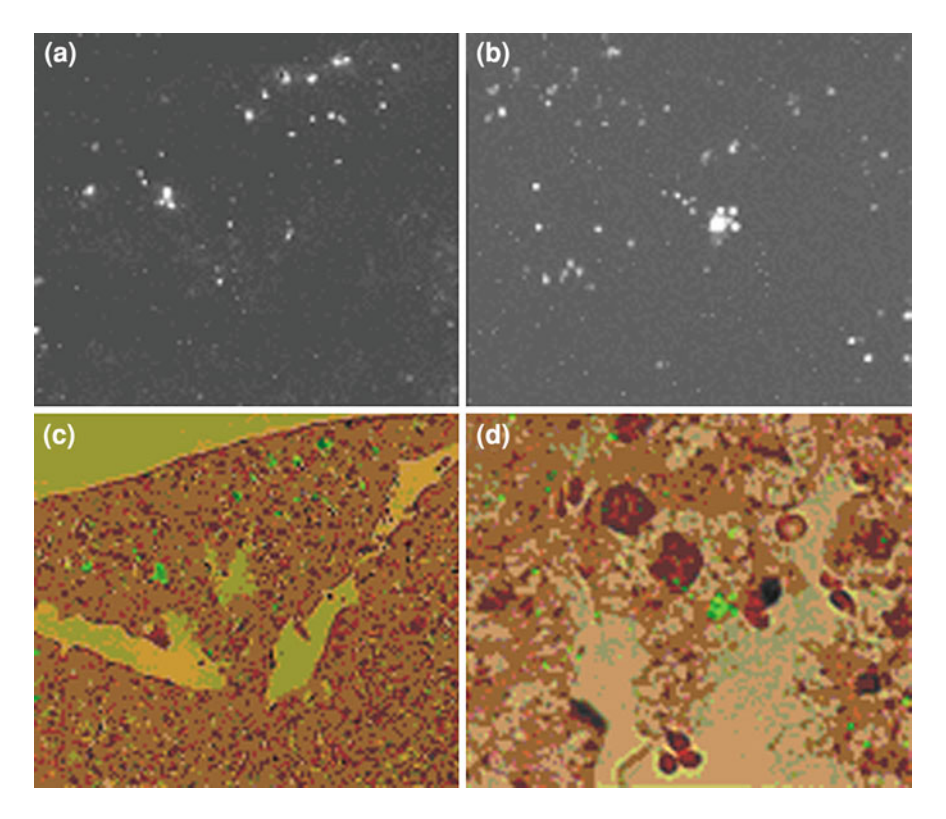


Fig. 11 Micrographs at two magnifications of liver tissue from rabbits killed 24 h after i.v. administration of suspended SWCNTs. **a**, **b** Near-IR SWCNT fluorescence images. Scattered isolated bright pixels are artefacts from defective sensor elements in the near-IR camera; all larger features represent emission from SWCNTs. In **c** and **d**, the SWCNT fluorescence from **a** and **b** is shown overlaid as false-colour green onto visible bright-field images from adjacent 3-μm-thick specimen slices that had been stained with haematoxylin and eosin. Reproduced from [21] with the permission of National Academy of Science, USA

toxicity (at a low dose level) and reasonably long blood circulation time found here suggest that SWCNTs may well prove useful in medicine.

From a clinical perspective, it is important that mammalian cancer cells generally are more sensitive to heat-induced damage and apoptosis than normal cells [41].

The intrinsic optical properties of carbon nanotubes with their suitable functionalization chemistry and transport capabilities were combined by Shi Kam et al., to synthesise new classes of nanomaterials for drug delivery in cancer therapy. In biological systems that are transparent to 700 to 1100 nm near-infrared light, the strong absorbance of SWCNT in this window can be used for optical stimulation of nanotubes to exploit their properties as NIR "heaters" or "antennas" inside living cells. Carbon nanotubes were used to transport across the cell membrane oligonucleotides that can translocate into the cell nucleus upon endosomal rupture triggered by NIR laser pulses. The use of continuous NIR radiation

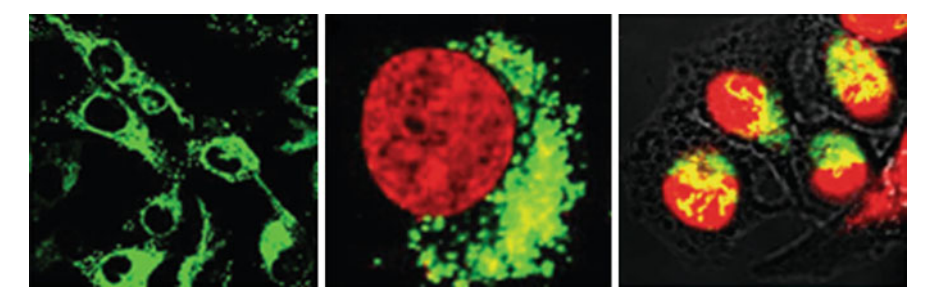


Fig. 12 Transporting DNA inside living cells by SWCNTs. **a** A confocal fluorescence image (excitation $\gamma=548$ nm; emission detected at $\gamma=560$ nm) showing the internalization and accumulation of Cy3-DNA-SWCNT around the nucleus of HeLa cells after incubation for 12 h at 37°C in a 2.5–5 mg/l Cy3-DNA-SWCNT solution. **b** Dual detection of Cy3-DNA-SWCNT (green) internalized into a HeLa cell with the nucleus stained by DRAQ5 (red), **c** confocal image of HeLa cells after 12-h incubation in a 2.5–5 mg/l Cy3-DNA-SWCNT solution for internalization and radiation by six NIR (808 nm) 10-s pulses (at 1.4 W/cm² power density). Colocalization (yellow colour) of Cy3-DNA (green) in cell nucleus (red) was detected, indicating translocation of Cy3-DNA to the nucleus of HeLa cells. Reproduced from [66] with the permission of National Academy of Science, USA

can induce cell death due to an excessive local heating of SWCNTs in vitro. The selectivity cell-SWCNTs was achieved by the functionalization of the nanotubes with folate [67].

In Fig. 12 confocal microscopy reveals that DNA molecules are transported across the cell membrane, into the cytoplasm by nanotubes and after NIR radiation (1.4 W/cm²) colocalization of DNA in the cell nucleus indicates release of DNA cargoes from SWCNT transporters and entry into the nucleus.

The same approach to use SWCNT for cancer photothermal therapy in the near-infrared region was applied by Zhou et al. [82]. In this study, the effects of irradiation by a 980-nm laser of antibody-conjugated $CoMoCAT^{\circledast}$ nanotubes, were explored.

The SWCNT were used efficiently to convert the 980-nm laser energy into heat and to selectively destroy target cells, increasing the surrounding temperature. The results of this work show that SWCNTs combined with suitable tumour markers can be used as novel nanomaterials for targeted cancer photothermal therapy.

5 Antenna Properties

Looking again at the scheme of Fig. 1, it appears clear that much progress has been made in understanding CNT chemical and physical behaviour during the last 10 years. However, the exploitation of these concepts is still weak, especially in biomedical fields, the most important efforts coming from Integrated Circuit (IC) industry.

It is well know that CNT electrical conductivity is modified by chemical functionalization and external electrical fields. It has been demonstrated that CNTs

V. Raffa et al.

can interact with different classes of compounds. f-CNTs are biological transporters able to cross cell membranes and deliver molecules. Coupling electrical properties with surface chemistry, an impressive number of CNT-based biosensors can be built and the usefulness of CNTs and CNT composites as scaffolds for tissue engineering has been proved. On the other side, when putting a CNT in an external electrical or electromagnetic fields many events can occur. Free CNTs can translate (driven by electrical and magnetic forces) or rotate (driven by alignment dynamics). CNT can be polarized by external electrical fields. Depending on the wavelengths of the external radiation, they can work as optical probes (e.g. NIR radiation), as field emitters (e.g. microwave), and in a larger meaning, as antennas [26]. The likely polarization and antenna properties of CNTs were recognized from a theoretical standpoint [2] soon after the first experimental synthesis of SWCNTs in 1993. Wang et al. [76] performed the first clear and direct demonstration of the antenna-length effect performing their experiments on random arrays of vertically aligned MWCNTs. All antennas have two major properties: their response varies with the polarization (electric field orientation) of the incoming radiation and with their length. Using visible light, they showed that maxima occur in the amount of reflected light when the average length of the nanotubes in an array is a half-integral multiple of the wavelength of the incident light. They also provided a vivid demonstration of the polarization effect: in contrast to a metal surface, for which light is maximally reflected when the electric-field vector is in the plane of the metal surface, reflection from the nanotube arrays is strongest when the electric-field vector of the polarized light falls along the CNT axis. These properties of CNTs are related to the special electromagnetic behaviour of layered graphite, which has a strongly anisotropic 'skin depth'. The skin depth is the characteristic distance of penetration of an electromagnetic wave into a material. If the incident radiation is polarized parallel to the plane of the graphite layers, the skin depth is short and the light is strongly absorbed. But if the polarization is normal to the plane of the layers, the penetration depth of the light is more than ten times larger and the absorption is very much weaker. Polarization effects are useful in fundamental studies of the optical absorption, reflection and emission of CNTs.

The work by Wang et al. [76] suggests a host of applications in optoelectronics of considerable commercial significance, following the trend of the decade-long history of CNTs that there has been substantial investment by the private sector in nanotube research and development.

It was proved that individual metallic SWCNTs are essentially ballistic conductors that support DC current densities approaching 10⁹ A/cm² [54]. As a consequence, metallic SWCNTs have a high axial dielectric constant [8] and rapidly polarize in response to externally applied electrical fields, with expected axial resonance in the THz region [37]. Therefore, metallic SWCNTs can be considered nanoscale antennas, and this polarization-based "antenna effect" has several interesting and useful manifestations. For example, radio frequency (RF) dielectrophoresis [47] can be employed to manipulate and type-separate suspension of individual SWCNTs [56], while SWCNT networks have been shown to

efficiently convert electromagnetic radiation into heat across radio frequency (RF) [33], microwave (MW) [40] and optical wavelengths [1]. Their high aspect ratio, $L/D \approx 1000$, provides a localised apparent field amplification factor (equal to the aspect ratio) at their tips, which enables substantial field emission currents in vacuo at nominal field strength around 10^6 V/m [11]. There are a few reports of similar effects in aqueous solutions using supported MWCNT electrodes in DC or quasi static fields, including production of solvated electrons [46], electrodeposition on the end of bundles [12] and electro-field-driven redox processes [27]. First attempts to apply these concepts to biological and biomedical fields have been made and the research in this exciting field has been in continuous evolution. Proof and development of f-CNTs capable of biosensing, controlled drug delivery, driven by external fields, transducing suitable external energetic stimuli and working as "energetic" probes for gene/vaccine therapy, cancer therapy, cellular regeneration, neural application and so on, seem to be not so far away.

References

- 1. Ajayan, P.M., Terrones, M., de la Guardi, A., et al.: Nanotubes in a flash–ignition and reconstruction. Science **296**, 705 (2002)
- Ajiki, H., Ando, T.: Aharonov–Bohm effect in carbon nanotubes. Physica B Cond Matt 201, 349–352 (1994)
- 3. Al Faraj, A., Cieslar, K., Lacroix, G., et al.: In vivo imaging of carbon nanotube biodistribution using magnetic resonance imaging. Nano Lett. 9(3), 1023–1027 (2009)
- 4. Azamian, B.R., Davis, J.J., Coleman, K.S., et al.: Bioelectrochemical single-walled carbon nanotubes. J. Am. Chem. Soc. **124**, 12664 (2002)
- Balasubramanian, K., Burghard, M., Kern, K.: In: Schwarz, J. A., Contescu, C.I., Putyera, K. (eds.) Dekker Encyclopedia of Nanoscience and Nanotechnology. Marcel Dekker, New York (2004)
- Balasubramanian, K., Burghard, M.: Chemically functionalized carbon nanotubes. Small 1, 180–192 (2005)
- 7. Bekyarova, E., Ni, Y., Malarkey, E.B., et al.: Applications of carbon nanotubes in biotechnology and biomedicine. J. Biomed. Nanotechol. 1, 3–17 (2005)
- 8. Benedict, L.X., Louie, S.G., Cohen, M.L.: Static polarizabilities of single-wall carbon nanotubes. Phys. Rev. B **52**, 8541 (1995)
- Besteman, K., Lee, J.O., Wiertz, F.G.M., et al.: Enzyme-coated carbon nanotubes as single-molecule biosensors. Nano Lett. 3, 727–730 (2003)
- 10. Bianco, A., Kostarelos, K., Partidos, C.D., et al.: Biomedical applications of functionalised carbon nanotubes. Chem. Commun. 7, 571–577 (2005)
- 11. Bonard, J.M., Salvetat, J.P., Stockli, T., et al.: Field emission from single wall carbon nanotube films. Appl. Phys. Lett. **73**, 918–920 (1998)
- Bradley, J.C., Babu, S., Ndungu, P.: Contactless tip-selective electrodeposition of palladium onto carbon nanotubes and nanofibers. Fullerenes Nanotubes Carbon Nanostruct. 13, 227–237 (2005)
- 13. Bradley, K., Briman, M., Star, A., et al.: Charge transfer from adsorbed proteins. Nano Lett. 4, 253–256 (2004)
- Cai, H., Cao, X.N., Jiang, Y., et al.: Carbon nanotube-enhanced electrochemical DNA biosensor for DNA hybridization detection. Anal. Bioanal. Chem. 375, 287–293 (2003)

V. Raffa et al.

 Cai, D., Blair, D., Dufort, F.J., et al.: Interaction between carbon nanotubes and mammalian cells: characterization by flow cytometry and application. Nanotechnology 19, 345102:10 (2008)

- 16. Cai, D., Mataraza, J.M., Quin, Z., et al.: Highly efficient molecular delivery into mammalian cells using carbon nanotube spearing. Nat. Methods **2**, 449–454 (2003)
- 17. Cellot, G., Cilia, E., Cipollone, S., et al.: Carbon nanotubes might improve neuronal performance by favouring electrical shortcuts. Nat. Nanotechnol. **4**, 126–133 (2009)
- Chen, R.J., Bangsaruntip, S., Drouvalakis, K.A., et al.: Noncovalent functionalization of carbon nanotubes for highly specific electronic biosensors. Proc. Natl. Acad. Sci. USA 100, 4984–4989 (2003)
- Chen, C.W., Lee, M.H., Clark: Field penetration induced charge redistribution effect on the field emission properties of carbon nanotubes—a first principles study. S J. Appl. Surf. Sci. 228, 143–150 (2004)
- Cherukuri, P., Sergei, M.: Near-infrared fluorescence microscopy of single-walled carbon nanotubes in phagocytic cells. JACS 126, 15638–15639 (2004)
- Cherukuri, P., Gannon, C.J., et al.: Mammalian pharmacokinetics of carbon nanotubes using intrinsic near-infrared fluorescence. Proc. Natl. Acad. Sci. USA 103, 18882–18886 (2006)
- 22. Ciofani, G., Raffa, V.: Chemically functionalized carbon nanotubes: emerging vectors for cell therapy. Mini-Rev Med. Chem. 9, 000 (2009)
- 23. Collins, P.G., Zettl, A., Bando, H., et al.: Nanotube nanodevice. Science 278, 100–103 (1997)
- 24. Collins, P.G., Bradley, K., Ishigami, M., et al.: Extreme oxygen sensitivity of electronic properties of carbon nanotubes. Science 287, 1801–1804 (2000)
- 25. Dai, H., Wong, E.W., Lieber, C.M.: Probing electrical transport in nanomaterials: conductivity of individual carbon nanotubes. Science **272**, 523–526 (1996)
- Dresselhaus, M., Dai, H.: MRS 2004 Carbon Nanotube Special Issue, vol. 29. Materials Research Society, Warrendale, PA (2004)
- Duque, J.G., Pasquali, M., Schmidt, H.K.: Antenna chemistry with metallic single-walled carbon nanotubes. JACS 130, 15340–15347 (2008)
- 28. Ebbesen, T.W., Lezec, H.J., Hiura, H., et al.: Electrical conductivity of individual carbon nanotubes. Nature **382**, 54–56 (1996)
- Forro, L., Schonenberger, C.: Physical properties of multi-wall nanotubes. In: Dresselhaus, M.S., Dresselhaus, G., Avouris, P. (eds.) Carbon Nanotubes: Synthesys, Structure, properties, and Application. Springer, Berlin (2001)
- 30. Forzani, E.S., Li, X.L., Zhang, P.M., et al.: Tuning the chemical selectivity of SWNT-FETs for detection of heavy-metal ions. Small 2, 1283–1291 (2006)
- 31. Gabay, T., Jakobs, E., Ben-Jacob, E., et al.: Engineered selforganization of neural networks using carbon nanotube clusters. Physica A **350**, 611–621 (2005)
- 32. Gabay, T., Ben-David, M., Kalifa, I., et al.: Electro-chemical and biological properties of carbon nanotube based multi-electrode arrays. Nanotechnology 18, 35201 (2007)
- Gannon, C.J., Cherekuri, P., Yakobson, B.I., et al.: Carbon nanotube-enhanced thermal destruction of cancer cells in a noninvasive radiofrequency field. Cancer 110, 2654–2665 (2007)
- 34. Gooding, J.J., Wibowo, R., Liu, J.Q., et al.: Protein electrochemistry using aligned carbon nanotube arrays. J. Am. Chem. Soc. **125**, 9006–9007 (2003)
- 35. Gruner, G.: Carbon nanotube transistors for biosensing applications. Anal. Bioanal. Chem. **384**, 322–335 (2006)
- 36. Haddon, R.C.: Magnetism of the carbon allotropes. Nature 378, 249 (1995)
- 37. Hao, J., Hanson, G.W.: Infrared and optical properties of carbon nanotube dipole antennas. IEEE Trans. Nanotechnol. **5**, 766–775 (2006)
- 38. He, P.G., Li, S.N., Dai, L.M.: DNA-modified carbon nanotubes for self-assembling and biosensing applications. Syn. Metals **154**, 17–20 (2005)
- 39. Hu, H., Ni, Y., Montana, V., et al.: Chemically functionalized carbon nanotubes as substrates for neuronal growth. Nano Lett. **4**, 507–511 (2004)

- 40. Imholt, T.J., Dyke, C.A., Hasslacher, B.: Nanotubes in microwave fields: light emission, intense heat, outgassing, and reconstruction. Chem. Mater. 15, 3969–3970 (2003)
- 41. Kampinga, H.H.: Cell biological effects of hyperthermia alone or combined with radiation or drugs: a short introduction to newcomers in the field. Int. J. Hyperthermia 22, 191–196 (2006)
- 42. Keefer, E.W., Botterman, B.R., Romero, M.I., et al.: Carbon nanotube coating improves neuronal recordings. Nat. Nanotechnol. 3, 434 (2008)
- 43. Kong, J., Franklin, N.R., Zhou, C.W., et al.: Nanotube molecular wires as chemical sensors. Science **287**, 622–625 (2000)
- 44. König, K.: Multiphoton microscopy in life sciences. J. Microsc. 200, 83–104 (2000)
- 45. Kozinsky, B., Marzari, N.: Static dielectric properties of carbon nanotubes from first principles. Phys. Rev. Lett. **96**, 166801 (2006)
- Krivenko, A.G., Komarova, N.S., Stenina, E.V., et al.: Electrochemical behavior of electrodes containing nanostructured carbon of various morphology in the cathodic region of potentials. Russ. J. Electrochem. 42, 1047–1054 (2006)
- 47. Krupke, R., Hennrich, F., von Löhneysen, H., et al.: Separation of metallic from semiconducting single-walled carbon nanotubes. Science **301**, 344–347 (2003)
- 48. Li, J., Ng, H.T., Cassell, A., et al.: Carbon nanotube nanoelectrode array for ultrasensitive DNA detection. Nano Lett. **3**, 597–602 (2003)
- Lopez-Urias, F., Rodriguez-Manzo, J.A., Munoz-Sandoval, E., et al.: Magnetic response in finite carbon graphene sheets and nanotubes. Opt. Mater. 29, 110–115 (2006)
- 50. Lovat, V., Pantarotto, D., Lagostena, L., et al.: Carbon nanotube substrates boost neuronal electrical signaling. Nano Lett. **5**, 1107–1110 (2005)
- 51. Louie, S.L.: Electronic properties, junctions, and defects of carbon nanotubes. In: Dresselhaus, M.S., Dresselhaus, G., Avouris, P. (eds.) Carbon Nanotubes: Synthesys, Structure, properties, and Application. Springer, Berlin (2001)
- 52. Mattson, M.P., Haddon, R.C., Rao, A.M.: Molecular functionalization of carbon nanotubes and use as substrates for neuronal growth. J. Mol. Neurosci. 14, 175–182 (2000)
- Mazzatenta, A., Giugliano, M., Campidelli, S., et al.: Interfacing neurons with carbon nanotubes: electrical signal transfer and synaptic stimulation in cultured brain circuits. J. Neurosci. 27, 6931–6936 (2007)
- 54. McEuen, P.L., Fuhrer, M., Park, H.: Single-walled carbon nanotube electronics. IEEE Trans. Nanotechnol. 1, 78 (2002)
- 55. Nakanishi, T., Ando, T.: Conductivity in carbon nanotubes with Aharonov–Bohm flux. J. Phys. Soc. Jpn. **74**, 3027 (2005)
- O'Connell, M.J., Bachilo, S.M., Huffman, C.B.: Band gap fluorescence from individual single-walled carbon nanotubes. Science 297, 593–596 (2002)
- 57. Patolsky, F., Weizmann, Y., Willner, I.: Long-range electrical contacting of redox enzymes by SWCNT connectors. Angew Chem. Int. Edn. 43, 2113–2117 (2004)
- 58. Pensabene, V., Vittorio, O., Raffa, V., et al.: Neuroblastoma cells displacement by magnetic carbon nanotubes. IEEE Trans. Nanobiosci. **7**(2), 105–110 (2008)
- 59. Raffa, V., Ciofani, G., Vittorio, O., et al.: Carbon nanotube-enhanced cell electropermeabilisation. Bioelectrochemistry. **79**, 136–141 (2010)
- Rinzler, A.G., Hafner, J.H., Nikolaev, P., et al.: Unraveling nanotubes—field-emission from an atomic wire. Science 269, 1550–1553 (1995)
- 61. Robinson, D.A.: The electrical properties of metal microelectrodes. Proc. IEEE 56, 1065–1071 (1968)
- 62. Rojas-Chapana, J.A., Correa-Duarte, M.A., Ren, Z., et al.: Enhanced introduction of gold nanoparticles into vital *Acidothiobacillus ferrooxidans* by carbon nanotube-based microwave electroporation. Nano Lett. **4**, 985–988 (2004)
- 63. Saito, Y., Uemura, S.: Field emission from carbon nanotubes and its application to electron sources. Carbon 38, 169–182 (2000)
- 64. Shein, M., Greenbaum, A., Gabay, T., et al.: Engineered neuronal circuits shaped and interfaced with carbon nanotube microelectrode arrays. Biomed. Microdev. 11, 495–501 (2009)

V. Raffa et al.

65. Shi Kam, N.W., Jessop, T.C., Wender, P.A., Dai, H.: Nanotube molecular transporters: internalization of carbon nanotube-protein conjugates into mammalian cells. J. Am. Chem. Soc. **126**, 6850–6851 (2004)

- 66. Shi Kam, N.W., O'Connell, M.J., Wisdom, J.A., Dai, H.: Carbon nanotubes as multifunctional biological transporters and near-infrared agents for selective cancer cell destruction. Proc. Natl. Acad. Sci. USA 102, 11600–11605 (2005)
- 67. Shi Kam, N.W., Dai, H.: Carbon nanotubes as intracellular protein transporters: generality and biological functionality. J. Am. Chem. Soc. 127, 6021–6026 (2005)
- 68. Singh, R., Pantarotto, D., et al.: Proc. Natl. Acad. Sci. USA 103, 3357-3362 (2006)
- 69. Sorkin, R., Greenbaum, A., David-Pur, M., et al.: Process entanglement as a neuronal anchorage mechanism to rough surfaces. Nanotechnology **20**, 015101 (2009)
- Star, A., Gabriel, J.C.P., Bradley, K., et al.: Electronic detection of specific protein binding using nanotube FET devices. Nano Lett. 3, 459–463 (2003)
- 71. Tans, S.J., Devoret, M.H., Dai, H.J., et al.: Individual single-wall carbon nanotubes as quantum wires. Nature **386**, 474–477 (1997)
- 72. Tans, S.J., Verschueren, A.R.M., Dekker, C.: Room-temperature transistor based on a single carbon nanotube. Nature **393**, 49 (1998)
- 73. Terrones, M., Hsu, W.K., Hare, J.P., et al.: Graphitic structures: from planar to spheres, toroids and helices. Phil. Trans. R. Soc. A **354**, 2025–2054 (1996)
- 74. Terrones, H., Terrones, M., Hernandez, E., et al.: New metallic allotropes of planar and tubular carbon. Rev. Lett. **84**, 1716–1719 (2000)
- 75. Thordarson, P., Atkin, R., Kalle, W.H.J., et al.: Developments in using scanning probe microscopy to study molecules on surfaces—from thin films and single-molecule conductivity to drug-living cell interactions. Aust. J. Chem. **59**, 359–375 (2006)
- Wang, Y., Kempa, K., Kimball, B., et al.: Receiving and transmitting light-like radio waves: antenna effect in arrays of aligned carbon nanotubes. Appl. Phys. Lett. 85, 2607–2609 (2004)
- 77. Weisslder, R.: A clearer vision for in vivo imaging. Nat. Biotechnol. 19, 316–317 (2001)
- 78. Willner, I.: Biomaterials for sensors, fuel cells, and circuitry. Science 298, 2407–2408 (2002)
- Yantzi, J.D., Yeow, J.T.W.: Carbon nanotube enhanced pulsed electric field electroporation for biomedical applications. In: Proceedings of the IEEE International Conference on Mechatronics & Automation, Niagara Falls, Canada, pp. 1872–1877 (2005)
- 80. Yu, X., Munge, Patel, V., et al.: Carbon nanotube amplification strategies for highly sensitive immunodetection of cancer biomarkers. J. Am. Chem. Soc. **128**, 11199–11205 (2006)
- 81. Zhang, X., Prasad, S., Niyogi, S., et al.: Guided neurite growth on patterned carbon nanotubes. Sens. Actuators B Chem. **106**, 843–850 (2005)
- 82. Zhou, F., Xing, D., et al.: Cancer photothermal therapy in the near-infrared region by using single-walled carbon nanotubes. J. Biomed. Opt. **142**, 021009 (2009)

Carbon Nanotubes in Regenerative Medicine

Bhavna S. Paratala and Balaji Sitharaman

Abstract This chapter focuses on the latest developments in applications of carbonnanotubes (CNTs) for regenerative medicine. Regenerative Medicine focuses on technologies to create functional tissues to repair or replace tissues or organs lost due to trauma or disease. Carbon nonotubes (CNTs) have been under investigation in the past decade for an array of applications due to their unique and versatile properties. In the field of regenerative medicine, they have shown great promise to improve the properties of tissue engineering scaffolds. Drug delivery and imaging of engineering tissues. The chapter will review these latest advances

1 Introduction

The focus of regenerative medicine is on developing methods that can be applied to create functional tissues, to repair or replace tissues/organs lost due to trauma or disease [4]. Nanomaterials show potential and promise in regenerative medicine due to their interesting physico-chemical properties [47]. Carbon nanotubes (CNTs) are widely researched as multi-functional nanomaterials due to their unique electronic, mechanical, optical and chemical properties [5]. A CNT can either be single-walled (SWCNT) (Fig. 1a) or multi-walled (MWCNT) (Fig. 1b). In case of SWCNTs, a graphene sheet rolls up to form seamless one dimensional

B. S. Paratala

BioEngineering Bldg, 1st floor, Room no. 111, Stony Brook University, Stony Brook, NY 11794-5281, USA

e-mail: bparatala@ic.sunysb.edu

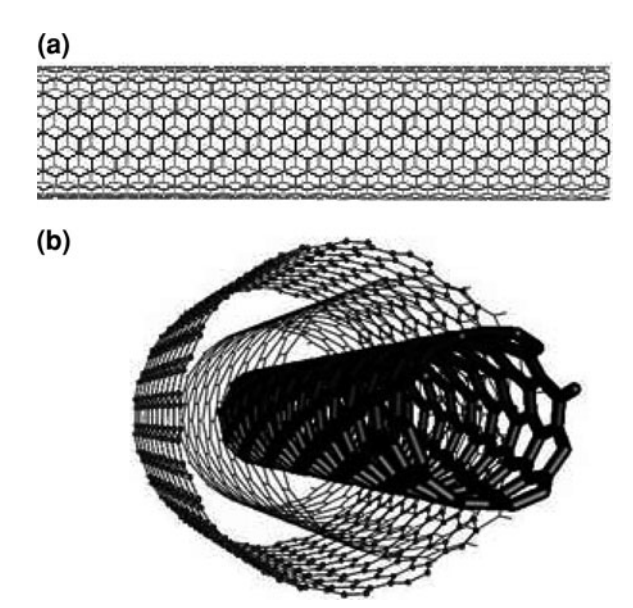
B. Sitharaman (⊠)

BioEngineering Bldg, 1st floor, Room no. 115, Stony Brook University,

Stony Brook, NY 11794-5281, USA

e-mail: balaji.sitharaman@stonybrook.edu

Fig. 1 Depiction of a SWCNT with armchair structure, and b MWCNT with multiple concentric tubes of graphene



cylindrical tube, and for MWCNTs, the cylinder can be conceptualized as concentric layers of graphene sheets. The well-ordered arrangement of carbon atoms linked via sp² bonds provides superior mechanical stiffness, electrical and thermal conductivity. CNTs have a high aspect ratio. The diameter is between 0.8 and 2 nm for SWCNTs and 2–100 for MWCNTs. The length ranges between hundreds of nanometers to tens of micrometers.

In regenerative medicine, the structural and mechanical properties of CNTs make them applicable for use as composites for tissue engineering. CNTs can act as delivery vehicles for drugs and gene therapy and thus are suitable for therapeutics in regenerative medicine. Further, they also show promise as contrast agents for non-invasive in vivo molecular imaging. The recent developments in the aspects mentioned above are the focus of this chapter.

2 Nanocomposites and Nanoscaffolds

Biomaterials with excellent mechanical properties are of importance in the development of implants used for tissue regeneration. For instance, total joint arthroplasty requires the type of implant materials and design that can support large functional loads. To date, these implants have been designed with ceramicor metal-based materials [31]. However, fatigue, corrosion, tissue infection, and poor implant-tissue interface create numerous problems in vivo. Polymers offer the flexibility to overcome these limitations. The mechanical properties of a polymer can be modified by composition, processing conditions and/or incorporating nanomaterials to create nanocomposites.

Carbon nanotubes (CNTs) have been characterized to possess excellent mechanical properties. Both SWCNTs and MWCNTs have high Young's modulus (~1TPa) due to the flexible hexagonal network of carbon atoms [21]. Thus, CNTs have been incorporated as reinforcing agents into natural or synthetic polymer matrices. In these nanocomposites, CNTs have been recognized to improve substantially the mechanical and structural properties of polymer composites. Poly (propylene fumarate) (PPF), a linear biodegradable polyester, is a promising polymeric biomaterial for tissue regeneration applications. SWCNTs incorporated into PPF polymer have been shown to substantially improve the mechanical properties of PPF [37–39]. The presence of very low concentrations of SWCNTs (less than 0.5 weight percent) in the PPF polymer matrix substantially enhances (up to two- to threefold increase) the compressive and flexural properties of the nanocomposite as against PPF alone [41].

Carbon nanotubes (CNTs) have also been incorporated into polymeric scaffolds for tissue engineering. Tissue engineering can be considered as a sub-field of regenerative medicine. This emerging field seeks to combine materials and engineering principles to improve the biological properties of a tissue. Scaffolds are porous biomaterials and play a pivotal role in the tissue engineering paradigm by providing temporary structural support, guiding cells to grow, assisting the transport of essential nutrients and waste products, and facilitating the formation of functional tissues and organs. However, porous scaffolds do not possess mechanical properties necessary for in vivo applications [31].

The previously mentioned SWCNT-PPF nanocomposites have also been investigated to fabricate porous scaffolds with better mechanical properties for bone tissue engineering (Fig. 2) [38]. The investigations showed a general trend of enhancement in compressive mechanical properties of SWCNT-PPF scaffolds over pure PPF scaffolds. However, there were large variations in the mechanical properties depending on the porosity of the scaffold. Scaffolds porosities have been shown to play a major role in determining the mechanical properties of the scaffolds in accordance with power-law relationships. At 80 volume%, the porous SWCNT-PPF nanoscaffolds showed up to 40% increase in the compressive modulus compared to porous PPF scaffolds. At 90 volume %, there was no difference in the compressive modulus between porous SWCNT-PPF and PPF scaffolds (Fig. 3). The enhancement in the mechanical properties due to the presence of the SWCNTs in nanoscaffolds is not as significant as in nanocomposites.

An important consideration in the development of implants for tissue regeneration is the interaction of tissue and synthetic material used in the fabrication of the implant for artificial replacement of a body part damaged by disease or trauma. There is now a large body of work investigating the interactions of CNT-based nanocomposites and scaffolds with cells and tissues.

The ability of SWCNT and MWCNT composites to enhance cellular adhesion and proliferation has been investigated. These nanomaterials have been incorporated into synthetic and natural materials to create nanocomposites. Aoki et al. [3] cultured osteoblast-like cells on a porous SWCNT-polycarbonate

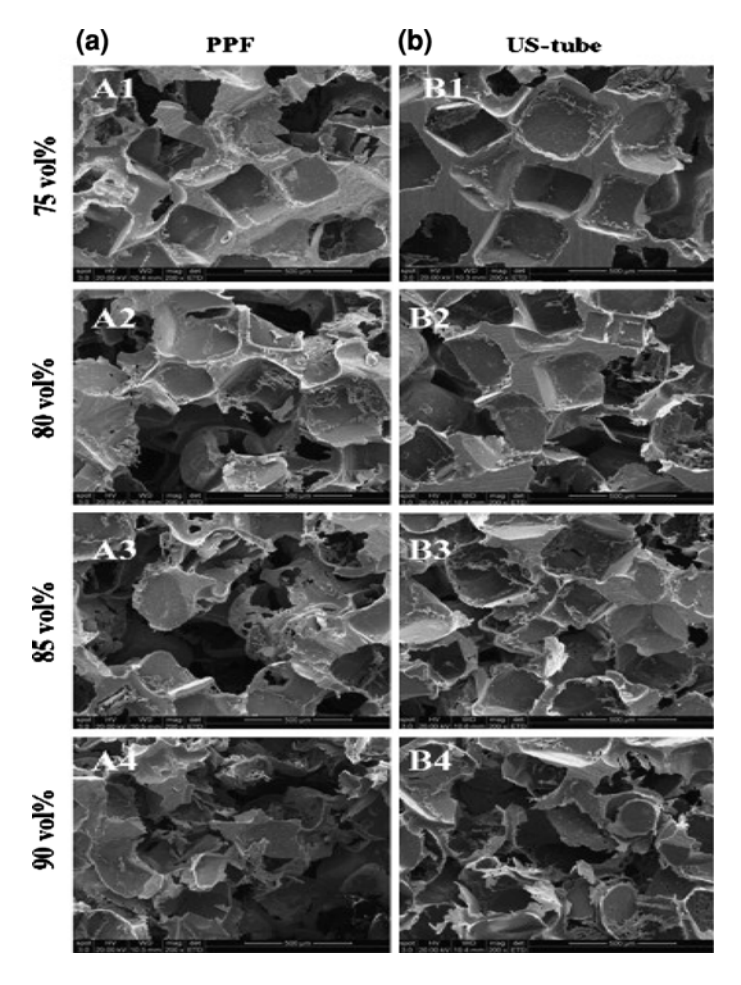
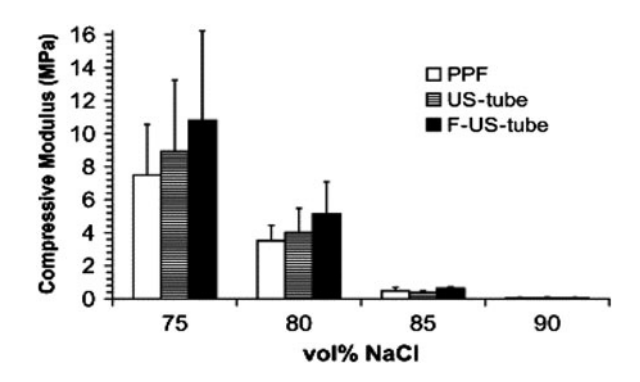


Fig. 2 SEM image of porous scaffolds made using varying percentages of porogen (NaCl); made of Poly propylene fumarate (PPF) (A1-A4), Ultra short SWCNT reinforced PPF (US-tube) (B1-B4). Adapted from [38]

Fig. 3 Compressive moduli of porous scaffolds made of polypropylene fumarate(PPF), ultra short SWCNT (US-tube) and functionalized ultra short SWCNT (F-US-tube) as a function of the porogen (NaCl) fraction used. Adapted from [38]



membrane to study cellular adhesion. When the cells were cultured on polycarbonate membranes without SWCNTs, fewer lamelipodia (cytoskeletal) extensions, and shorter lamelipodia extensions were apparent in comparison to the lamelipodia extensions of cells cultured on the polycarbonate membranes containing SWCNTs [3]. The filipodia were bound to the SWCNTs preventing the cells from lifting off of the polycarbonate CNT composite membrane [3]. Abarrategi et al. [1] created SWCNT-incorporated Chitosan scaffolds. They demonstrated the ability of these nanocomposites to support cell growth in vitro using C2Cl2 cells which are derived from the C2 myogenic cell line. Hirata et al. [19] studied cellular proliferation and adherence on a collagen sponge honeycomb scaffold, and compared the cellular proliferation and adhesion to a similar collagen sponge honeycomb containing a MWCNT film. They cultured MC3T3-E1 cells, a mouse osteoblast-like cell line, onto the honeycomb structures. Their results showed that the addition of the MWCNT onto the scaffold significantly increased cellular adhesion and proliferation [19]. Meng et al. [30] created polyurethane MWCNT nanocomposites, and cultured fibroblast cells onto these nanofibrous scaffolds. Their results show favorable interactions between the cells and the polyurethane surface. These fibroblasts were capable of proliferating and secreting proteins. Yildirium et al. [45] have created an alginate SWCNT composite scaffold which also showed greater cellular adhesion in comparison to the non-SWCNT alginate scaffold. In this case, the alginate scaffold was composed of 1% SWCNTs. The 1% addition of SWCNTs increased the mechanical strength and integrity of the scaffold. The SWCNTs also increased endothelial adhesion, and proliferation onto the alginate scaffold. The authors hypothesized that the increase in cellular adhesion and proliferation to the nanocomposite is due to factors that include the large aspect ratio of the SWCNTs, the increase in surface roughness of the scaffold, and the flexibility of the CNTs [45].

Carbon nanotubes can also effect the differentiation of cells. Chao et al. [8] cultured human embryonic stem cells onto poly(acrylic acid) grafted MWCNT substrates and their results indicate that this substrate increased cellular differentiation towards neurons in comparison to the embryonic stem cells cultured on poly(acrylic acid) acids without MWCNTs. The incorporation of MWCNTs into the substrate not only increased cellular differentiation to neurons, but also increased the level of neural adhesion [8].

In vitro studies with the SWCNT-PPF scaffold have shown it to support cell attachment, and proliferation [39]. In vivo studies of SWNT-PPF scaffolds implanted into rabbit tibia showed that after 12 weeks there was a change in the hard tissue response with increased levels of collagen in the extracellular matrix of these scaffolds [41]. Inflammatory cells appeared within the scaffold after 4 weeks, but this level decreased after 12 weeks. The results also suggested that these SWNT-PPF scaffolds were potentially bioactive and could promote osteogenesis.

3 Therapeutics

Controlled production and/or delivery of tissue-inducing macromolecules such as cytokines and growth factors is a widely used strategy in regenerative medicine. The physical and chemical properties of CNTs make them useful for a variety of therapeutic and drug-delivery applications in regenerative medicine. The external carbon sheath of the CNTs can be covalently or non-covalently functionalized with biological moieties that target specific cell or tissues types and/or pharmaceutical agents. Here, the CNTs target a specific cell or tissue type, and act as biological cargo vehicles to transport and deliver therapeutic agents via a biochemical or biophysical stimulus. Furthermore, the CNTs themselves can be used as a therapeutic agent by exploiting their unique physical properties. For example, the strong optical absorption properties of SWCNTs render them capable of generating acoustic waves upon irradiation. These waves have shown to induce differentiation of cells [17]. Other advantages of using SWCNTs for therapeutic purposes, and as delivery vehicles include their nanoscale dimensions, which enhance their retention and permeability in diseased tissues (e.g. tumors) [13]. Additionally, their large aspect ratio allows attachment of multiple functional groups for the targeted delivery of multiple therapeutic entities.

Carbon nanotubes can be functionalized using numerous methods of covalent interactions [12]. Carboxylic acid groups can be formed via oxidation by creating defects using acid treatments. The CNTs can undergo sidewall functionalization which includes fluorination, radical addition, nucleophilic addition, electrophillic addition, and cycloaddition. CNTs can also be functionalized using noncovalent interactions [20]. These include weak van der Waals interactions between the CNTs and the functional group; polymer (e.g. DNA) wrapping around the CNTs.

Post functionalization, the CNT conjugates can be used to translocate biological moieties into cells, and as transfection agents. SWCNT conjugates have been combined with proteins or oligonucleotides to transport these biological moieties into the cells via energy-dependent endocytosis [23]. SWCNT-based transfection agents have been reported to be superior to preexisting transfection agents due to their hydrophilic interaction with the cellular surface that allows them to bind to the cell surface, and subsequently translocate into cells. For example, Kam et al. [23] demonstrated that functionalized SWCNTs could deliver small interfering RNA (siRNA) against CXCR4 to T cells which could inhibit HIV entry into T cells. They compared this SWCNT-siRNA complex to multiple liposomes such as Lipofectamine2000TM-siRNA, and this liposome showed no effect on the T cells. A study by Zhang et al. [48] demonstrated that functionalized SWCNTs could carry siRNA and suppress the growth of tumor (HeLa) cells. Another method of cell transfection is "nanotube spearing," a process used to penetrate cellular membranes and the nucleus thereby delivering plasmid DNA. In this study, transfection was achieved by creating a magnetic field by placing a magnet below the cellular surfaces and rotating the magnet [6]. Due to the presence of

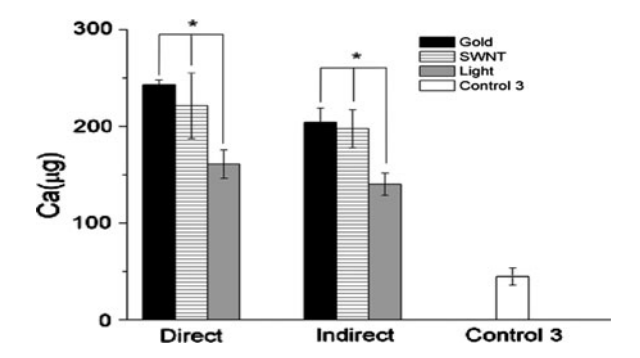


Fig. 4 Calcium content measured in the cells after 16 days in groups subjected to photoacoustic (PA) treatment and control. *Direct* samples indicate groups that were present in the path of the laser light during PA stimulation. *Indirect* samples include groups that were in wells adjacent to the direct laser light path. Mean \pm SD, n=4, P<0.05 between PA groups and *control*. Adapted from [17]

ferromagnetic catalyst nickel particles present in their tips, the CNTs responded to the magnet, allowing transfection of DNA plasmids across the cellular membrane. This study also suggested that the effect of spearing on cellular viability was minimal due to the small size of CNTs. This though may be dependent on the concentration of functionalized CNTs because increased concentration of CNTs implies greater levels of spearing. Adeli et al. [2] functionalized MWCNTs with polyglycerol to examine their potential as a drug delivery agent. They showed that MWCNT-polyglycerol conjugates are biocompatible, with promise as a versatile platform for drug delivery applications. Riggio et al. [36] have created an alginate-polymeric film embedded with SWCNT, and have studied the release of bovine serum albumin from this SWCNT-incorporated polymer. Their results indicate that the proteins released from the MWCNT polymer construct maintained their biological function, and that it shows potential for drug delivery applications.

Sitharaman et al. have recently reported that SWCNT-enhanced photoacoustic stimulation differentiates stem cells towards osteoblasts [17]. Photoacoustic stimulation refers to the generation of acoustic waves by the absorption of electromagnetic energy, such as optical or radiofrequency wave [44]. An electromagnetic source with a low fluence (number of particles intersecting a unit area) irradiates non-ionizing electromagnetic energy onto an absorbing surface giving rise to transient acoustic waves through a thermoelastic mechanism induced by a slight temperature rise (milli-Kelvin range). SWCNTs, which show strong intrinsic electromagnetic absorption at visible, near infrared wavelengths and in the radiofrequency domain, have been used as contrast agents for photoacoustic imaging. In their study, the authors demonstrated that a brief (10 min) daily exposure of stem cells to pulse laser-induced PA stimulation promotes differentiation of mesenchymal stem cells towards osteoblasts. This osteodifferentiation is substantially enhanced by SWCNTs present in the beam path, showing increased calcium deposition (Fig. 4) and osteopontin levels compared to the controls [17].

Their results suggest that PA stimulation of SWCNT-incorporated bone tissue engineering polymer scaffolds should assist the process of osteoinduction (differentiate osteoprogenitor cells towards osteoblasts). This approach is novel since it introduces a nanoparticle-based biophysical rather than biochemical cue to affect the osteodifferentiation of mesenchymal stem cells with potential implications for other bone tissue engineering strategies. For instance, mesenchymal stem cells could be labeled ex vivo with nanoparticles that enhance the PA effect, seeded onto a carrier scaffold, implanted into a bone defect, and stimulated towards osteoblasts. Further, this non-pharmacological strategy based on bone's sensitivity to mechanical/acoustic signals does not possess the limitations of pharmacological growth factor-based approaches for bone regeneration such as unstable biological activity, short half-life, minimal tissue penetration.

4 Bio-Imaging

The limitations of standard diagnostic tools and techniques for detecting, and monitoring the process of tissue regeneration in small animals are well known [16]. The most robust technique for the evaluation of de novo tissue formation, neo-vascularization or monitoring the fate of transplanted cells is histological analysis. Because histology is an endpoint evaluation, and large variation is observed, it is difficult to assess temporal results in a statistically significant manner. In search of alternatives, much progress has been made on new approaches for non invasive in vivo imaging using photoacoustic imaging, positron emission tomography (PET), magnetic resonance imaging (MRI) and X-ray computed tomography (CT). These imaging modalities offer scientists the spatial and temporal information in a faster and more convenient manner. For each imaging modality, substantial attention has been devoted to the development of contrast agents. Novel agents, such as CNT-based contrast agents, may enhance molecular imaging by improving detection sensitivity and selectivity. The strategies developed for design of CNT-based contrast agents for biomedical imaging include encapsulation of medically relevant metal ions within their carbon sheath, the functionalization of the carbon sheath with a variety of imaging agents, and exploiting the intrinsic physical properties of the CNTs.

Single-walled CNTs (SWCNTs) can be used in optical imaging as they exhibit a near-infrared photoluminescence in the 'biological spectral window' between 700 and 1,100 nm [32]. In this range, interference such as absorption, scattering, photobleaching and the autofluorescence effects in water, tissue and cells are minimized [18]. Cherukuri et al. [9] have utilized near infrared (NIR) fluorescence microscopy to image SWCNTs in phagocytic cells. They used SWCNTs at varying concentrations to track their ex vivo uptake in mouse peritoneal macrophage cells. NIR fluorescence imaging revealed that there was no difference in population growth, adhesion, morphology and confluence between the control and the cultures containing SWCNTs. Detectable emission was seen only in cells incubated with

SWCNTs. Based on the image taken for these cells, it was interpreted that the uptake of nanotubes was through phagocytosis. Weisman et al. [25] have used in vivo NIR imaging to assess the biocompatibility of SWCNTs in an intact organism, *Drosophila melanogaster*. This study suggests the effectiveness of SWCNTs as NIR probes for studying individual nanotubes in tissue specimens or inside living organisms during the course of tissue regeneration. Thus, fluorescence imaging may be a promising method for tracking SWCNTs in cells and small animals over long durations of time.

Raman spectroscopy is a technique that studies the vibrational and low frequency modes of CNTs based on inelastic scattering called Raman scattering. In both SWCNTs and MWCNTs, Raman modes also appear at 1,590–1,600 cm⁻¹, which is known as the G band, due to stretching along the C-C bond of graphene. Further, resonance-enhanced Raman bands for SWCNTs appear at 150–300 cm⁻¹ called the radial breathing modes, and can be related to the diameter of the SWCNTs [24]. Various features can be understood about SWCNTs by Raman spectroscopy, such as diameter and semiconducting or metallic properties [11]. Thus, Raman microscopy and imaging allows for the spatial and chemical imaging of SWCNTs in cells and small animals. Raman microscopy has been applied to monitor cells labeled with CNTs [18]. Raman scattering and fluorescence measurements of SWCNTs encapsulated by DNA oligonucleotide (DNA-SWNTs) in the stained, and live cells showed continuous emission, and spectral changes on uptake, respectively [18]. These nanotube aggregates remained in the cell, and displayed scattering even after several cycles of cell division. Thus, they show potential as markers in assessing the proliferation, and differentiation of cells in culture, long-term labeling of cell populations, and continuous monitoring of the cellular environments. In another study by Liu et al. [27] Raman microscopy was used to study biodistribution, and blood circulation of PEGylated SWCNTs in a mouse model. The results showed SWCNT accumulation in the intestine, feces, kidney, and bladder of mice, and suggested excretion and clearance of SWCNTs from mice via the biliary and renal pathways. Another study carried out by Zavaleta et al. [46] indicates the use of Raman imaging for real-time monitoring of SWCNTs for disease (tumor) targeting and localization. Specifically disease targeting SWCNTs (RGD-SWCNT, arginine-glycine-aspartic acid) were examined for localization in diseased (tumor) mice as against plain SWCNT. The images showed a higher accumulation of RGD-SWCNTs in the tumor compared to the non-functionalized SWCNT mouse group, and there was significantly less accumulation in the liver and spleen.

Carbon nanotubes have also been assessed for increasing contrast in photoacoustic (PA) imaging in vivo [10]. PA imaging is based on the photoacoustic effect (see last section), and occurs when non-ionizing laser pulses are absorbed by the tissue to generate acoustic/ultrasonic emissions that can be used to generate images. PA imaging allows for high spatial resolution and deep tissue imaging up to 700 µm resolution and 50 mm depth using 3.5 MHz ultrasound detectors [43, 44]. Pramanik et al. in recent in vivo studies in mice have shown that SWCNT-enhanced PA imaging of the lymph nodes and vasculature with a high contrast to

noise ratio (CNR) of \sim 79 and good resolution of \sim 500 µm [17, 34]. In most tissues, light-absorbing components such as hemoglobin of blood are the strongest endogenous PA generators. Under illumination by NIR laser light at a wavelength of 793 nm, the optical absorption of SWCNTs is much stronger than biological tissues. The absorption coefficient of SWCNTs at this wavelength is nearly 200 cm⁻¹ which is almost 10 times higher than that of epidermis and nearly 500 times higher than that of dermis, Therefore, SWCNTs generate strong PA signals, and manifest high image contrast, causing the vasculature in organs to stand out prominently in PA images. Functionalization of the SWCNTs with targeting groups has also been shown to allow molecular imaging of diseased (tumor) tissues. Zerda et al. [10] used RGD-SWCNTs to target tumors in mice, and demonstrated that an eight fold greater PA signal was seen in these compared to non-targeted SWCNTs. The results suggest that SWCNT-enhanced noninvasive deep tissue PA imaging at high spatial resolution can be obtained for imaging nanotherapeutics in the body. The PA techniques can also help understand several intrinsic factors of tissues and cells, for example vascularization and oxygen saturation in diseased tissues and tissue engineering constructs.

Carbon nanotubes have also been shown to amplify the contrast enhancement efficacy of metal ions such as Gadolinium; widely used in the development of clinical MRI contrast agents. MRI is a non-invasive imaging modality that provides anatomical details for diagnosis of various diseases, and physio-chemical states of tissue and blood flow [28, 33]. With an applied external magnetic field, and radio-frequency pulses, proton spin states are excited. The time required for the excited state spin to return to equilibrium is the relaxation time, which can be either longitudinal T_1 or transverse T_2 . This relaxation causes a change in the flux of the receiving coil of the MRI scanner, inducing a magnetic resonance signal. Therefore, the relaxation time affects the quality of the image, especially the contrast. Contrast agents can modulate the relaxation time to improve contrast. An important measure of an MRI contrast agent efficacy is a term called "relaxivity". Relaxivity is the change in the relaxation rate of the water protons per unit concentration of the contrast agent and has a unit of mM^{-1} s⁻¹.

Recently, Sitharaman et al. [40] reported a novel method of using SWCNTs as carriers of gadolinium (Gd). Until now, Gd has been used in a chelated form in order to sequester its toxic effects in vivo [7]. According to this study, the SWCNTs not only encapsulate the Gd³⁺ ions to sequester the toxic effect of Gd³⁺ ions, but also, amplify the contrast enhancing efficacy of Gd³⁺ ions. The SWCNT-based MRI contrast agent increases the proton relaxivities (T_1 weighted) by 40 at the standard MRI field strengths used for clinical imaging (20–60 MHz). With such a large contrast enhancing efficacy, SWCNT-based MRI contrast agents could be dispersed throughout an engineered tissue to monitor the process of the tissue regeneration [42].

The examples of CNT-based contrast agents discussed in this section have focused on studies that harness the intrinsic properties of SWCNTs. However, a number of studies have shown that "passive" functionalization of the external carbon sheath of CNTs (SWCNTs and MWCNTs) with suitable imaging agents

allows molecular imaging with MRI, PET, and nuclear imaging modalities [26, 29, 35]. Therefore, CNTs in a true sense show promise and potential as multi-modal contrast agents for molecular imaging.

5 Summary

Current research suggests that CNTs as biomaterials have immense potential for applications in regenerative medicine. CNTs have shown to improve the mechanical properties of implants. Implants containing scaffolds and composites that are incorporated with CNTs as reinforcing agents have superior mechanical properties and they have been tested for cytocompatibility (in vitro) and biocompatibility (in vivo). The external carbon sheath of the CNTs can be functionalized for targeting, drug delivery, and imaging agents. Further their intrinsic physical properties can be harnessed for therapeutics and imaging. However, significant challenges exist towards their eventual translation for clinical applications. A challenge is obtaining pure CNTs, free of metal catalysts (iron, nickel, cobalt, yttrium) or amorphous carbon [22]. Dispersion of CNTs in the polymer matrix remains a major challenge in spite of CNT-reinforced nanocomposites exhibiting enhanced mechanical properties compared to the polymer alone. CNTs usually exist as bundled ropes of many individual nanotubes, and also show a propensity to aggregate into micrometer-sized agglomerates. Further, while the CNT-based nanocomposites offer promising properties for tissue engineering scaffolds, little is known about their long-term biocompatibility, and biodistribution upon their release from the biodegradable polymers in vivo [14, 15]. In conclusion, even though the above challenges need to be overcome, CNTs show great promise as a single platform with multi-functional capabilities for regenerative medicine.

References

- Abarrategi, A., Gutiérrez, M.C., Moreno-Vicente, C., Hortigüela, M.J., Ramos, V., López-Lacomba, J.L., et al.: Multiwall carbon nanotube scaffolds for tissue engineering purposes. Biomaterials 29(1), 94–102 (2008)
- Adeli, M., Mirab, N., Alavidjeh, M.S., Sobhani, Z., Atyabi, F.: Carbon nanotubes-graft-polyglycerol: biocompatible hybrid materials for nanomedicine. Polymer 50(15), 3528–3536 (2009)
- 3. Aoki, N., Yokoyama, A., Nodasaka, Y., Akasaka, T., Uo, M., Sato, Y., et al.: Cell culture on a carbon nanotube scaffold. J Biomed Nanotechnol 1(4), 402–405 (2005)
- 4. Atala, A.: Tissue engineering and regenerative medicine: concepts for clinical application. Rejuvenation Res **7**(1), 15–31 (2004)
- Baughman, R., Zakhidov, A., De Heer, W.: Carbon nanotubes—the route toward applications. Science 297(5582), 787 (2002)

- Cai, D., Mataraza, J., Qin, Z., Huang, Z., Huang, J., Chiles, T., et al.: Highly efficient molecular delivery into mammalian cells using carbon nanotube spearing. Nat Methods 2(6), 449–454 (2005)
- 7. Caravan, P., Ellison, J., McMurry, T., Lauffer, R.: Gadolinium (III) chelates as MRI contrast agents: structure, dynamics, and applications. Chem Rev 99, 2293–2352 (1999)
- 8. Chao, T.-I., Xiang, S., Chen, C.-S., Chin, W.-C., Nelson, A.J., Wang, C., et al.: Carbon nanotubes promote neuron differentiation from human embryonic stem cells. Biochem. Biophys. Res. Commun. **384**(4), 426–430 (2009)
- Cherukuri, P., Bachilo, S., Litovsky, S., Weisman, R.: Near-infrared fluorescence microscopy of single-walled carbon nanotubes in phagocytic cells. J. Am. Chem. Soc. 126(48), 15638– 15639 (2004)
- De La Zerda, A., Zavaleta, C., Keren, S., Vaithilingam, S., Bodapati, S., Liu, Z., et al.: Carbon nanotubes as photoacoustic molecular imaging agents in living mice. Nat Nanotechnol 3(9), 557 (2008)
- Dresselhaus M., Dresselhaus G., Saito R., Jorio A.: Raman spectroscopy of carbon nanotubes.
 In: Carbon Nanotubes: Quantum Cylinders of Graphene, Elsevier Publishers 3, 83–108 (2008)
- Dyke, C., Tour, J.: Covalent functionalization of single-walled carbon nanotubes for materials applications. J Phys Chem A 108(51), 11151–11159 (2004)
- Gannon, C., Cherukuri, P., Yakobson, B., Cognet, L., Kanzius, J., Kittrell, C., et al.: Carbon nanotube-enhanced thermal destruction of cancer cells in a noninvasive radiofrequency field. Cancer 110(12), 2654–2665 (2007)
- 14. Gatti, A.: Biocompatibility of micro- and nano-particles in the colon. Part II. Biomaterials **25**(3), 385–392 (2004)
- 15. Gatti, A., Rivasi, F.: Biocompatibility of micro- and nanoparticles. Part I: in liver and kidney. Biomaterials 23(11), 2381–2387 (2002)
- Greco, G.N. (ed.): Tissue Engineering Research Trends. Nova Science Publishers, New York (2008)
- 17. Green, D., Longtin, J., Sitharaman, B.: The effect of nanoparticle-enhanced photoacoustic stimulation on multipotent marrow stromal cells. ACS Nano 3(8), 2065–2072 (2009)
- Heller, D., Baik, S., Eurell, T., Strano, M.: Single-walled carbon nanotube spectroscopy in live cells: towards long-term labels and optical sensors. Adv. Mater. 17(23), 2793–2798 (2005)
- Hirata, E., Uo, M., Takita, H., Akasaka, T., Watari, F., Yokoyama, A.: Development of a 3D collagen scaffold coated with multiwalled carbon nanotubes. J. Biomed. Mater. Res. Part B Appl. Biomater. 90B(2), 629–634 (2009)
- Hirsch, A., Vostrowsky, O.: Functionalization of carbon nanotubes. Top. Curr. Chem. 245, 193–238 (2005)
- Iijima, S., Brabec, C., Maiti, A., Bernholc, J.: Structural flexibility of carbon nanotubes. J. Chem. Phys. 104(5), 2089–2092 (1996)
- Kaiser, J., Wick, P., Manser, P., Spohn, P., Bruinink, A.: Single walled carbon nanotubes (SWCNT) affect cell physiology and cell architecture. J. Mater. Sci. Mater. Med. 19(4), 1523–1527 (2008)
- Kam, N., Liu, Z., Dai, H.: Carbon nanotubes as intracellular transporters for proteins and DNA: an investigation of the uptake mechanism and pathway. Angew. Chem. Int. Ed. 45(4), 577–580 (2006)
- 24. Kuzmany, H., Plank, W., Hulman, M., Kramberger, C., Grüneis, A., Pichler, T., et al.: Determination of SWCNT diameters from the Raman response of the radial breathing mode. Eur. Phys. J. B Condens. Matter Complex Syst. **22**(3), 307–320 (2001)
- 25. Leeuw, T., Reith, R., Simonette, R., Harden, M., Cherukuri, P., Tsyboulski, D., et al.: Single-walled carbon nanotubes in the intact organism: near-IR imaging and biocompatibility studies in Drosophila. Nano Lett. 7(9), 2650–2654 (2007)
- Liu, Z., Cai, W., He, L., Nakayama, N., Chen, K., Sun, X., et al.: In vivo biodistribution and highly efficient tumour targeting of carbon nanotubes in mice. Nat. Nanotechnol. 2(1), 47–52 (2007)

- Liu, Z., Davis, C., Cai, W., He, L., Chen, X., Dai, H.: Circulation and long-term fate of functionalized, biocompatible single-walled carbon nanotubes in mice probed by Raman spectroscopy. Proc. Nat. Acad. Sci. 105(5), 1410 (2008)
- Mansfield, P.: Snapshot Magnetic Resonance Imaging. Angew. Chem. Int. Ed. 43, 5456– 5464 (2004)
- McDevitt, M., Chattopadhyay, D., Kappel, B., Jaggi, J., Schiffman, S., Antczak, C., et al.: Tumor targeting with antibody-functionalized, radiolabeled carbon nanotubes. J. Nucl. Med. 48(7), 1180 (2007)
- 30. Meng, J., Kong, H., Han, Z., Wang, C., Zhu, G., Xie, S., et al.: Enhancement of nanofibrous scaffold of multiwalled carbon nanotubes/polyurethane composite to the fibroblasts growth and biosynthesis. J. Biomed. Mater. Res. Part A **88A**(1), 105–116 (2009)
- 31. Mistry, A., Mikos, A.: Tissue engineering strategies for bone regeneration. Adv. Biochem. Eng. Biotechnol. **94**, 1–22 (2005)
- 32. O'Connell, M., Bachilo, S., Huffman, C., Moore, V., Strano, M., Haroz, E., et al.: Band gap fluorescence from individual single-walled carbon nanotubes. Science **297**(5581), 593 (2002)
- 33. Ogawa, S., Lee, T., Kay, A., Tank, D.: Brain magnetic resonance imaging with contrast dependent on blood oxygenation. Proc. Nat. Acad. Sci. 87(24), 9868–9872 (1990)
- Pramanik, M., Swierczewska, M., Green, D., Sitharaman, B., Wang, L.: Single-walled carbon nanotubes as a multimodal-thermoacoustic and photoacoustic-contrast agent. J. Biomed. Opt. 14, 034018 (2009)
- 35. Richard, C., Doan, B., Beloeil, J., Bessodes, M., Toth, E., Scherman, D.: Noncovalent functionalization of carbon nanotubes with amphiphilic Gd3+ chelates: toward powerful T1 and T2 MRI contrast agents. Nano Lett. 8(1), 232–236 (2008)
- 36. Riggio, C., Ciofani, G., Raffa, V., Cuschieri, A., Micera, S.: Combination of polymer technology and carbon nanotube array for the development of an effective drug delivery system at cellular level. Nanoscale Res. Lett. 4(7), 668–673 (2009)
- Shi, X., Hudson, J.L., Spicer, P.P., Tour, J.M., Krishnamoorti, R., Mikos, A.G.: Rheological behaviour and mechanical characterization of injectable poly(propylene fumarate)/singlewalled carbon nanotube composites for bone tissue engineering. Nanotechnology 16, S531– S538 (2005)
- 38. Shi, X., Sitharaman, B., Pham, Q., Liang, F., Wu, K., Edward Billups, W., et al.: Fabrication of porous ultra-short single-walled carbon nanotube nanocomposite scaffolds for bone tissue engineering. Biomaterials **28**(28), 4078–4090 (2007)
- Shi, X., Sitharaman, B., Pham, Q.P., Spicer, P.P., Hudson, J.L., Wilson, L.J., et al.: In vitro cytotoxicity of single-walled carbon nanotube/biodegradable polymer nanocomposites. J. Biomed. Mater. Res. Part A 86(3), 813–823 (2008)
- Sitharaman, B., Kissell, K., Hartman, K., Tran, L., Baikalov, A., Rusakova, I., et al.: Superparamagnetic gadonanotubes are high-performance MRI contrast agents. Chem. Commun. 2005(31), 3915–3917 (2005)
- Sitharaman, B., Shi, X., Walboomers, X.F., Liao, H., Cuijpers, V., Wilson, L.J., et al.: In vivo biocompatibility of ultra-short single-walled carbon nanotube/biodegradable polymer nanocomposites for bone tissue engineering. Bone 43(2), 362–370 (2008)
- 42. Sitharaman, B., Van Der Zande, M., Ananta, J., Shi, X., Veltien, A., Walboomers, X., et al.: Magnetic resonance imaging studies on gadonanotube-reinforced biodegradable polymer nanocomposites. J. Biomed. Mater. Res. Part A 93, 1454–1462 (2009)
- 43. Wang, S., Humphreys, E., Chung, S., Delduco, D., Lustig, S., Wang, H., et al.: Peptides with selective affinity for carbon nanotubes. Nat. Mater. 2(3), 196–200 (2003)
- 44. Xu, M., Wang, L.: Photoacoustic imaging in biomedicine. Rev. Sci. Instrum. 77, 041101 (2006)
- Yildirim, E.D., Yin, X., Nair, K., Sun, W.: Fabrication, characterization, and biocompatibility
 of single-walled carbon nanotube-reinforced alginate composite scaffolds manufactured
 using freeform fabrication technique. J. Biomed. Mater. Res. Part B Appl. Biomater. 87B(2),
 406–414 (2008)

- 46. Zavaleta, C., de La Zerda, A., Liu, Z., Keren, S., Cheng, Z., Schipper, M., et al.: Noninvasive Raman spectroscopy in living mice for evaluation of tumor targeting with carbon nanotubes. Nano Lett. **8**(9), 2800–2805 (2008)
- 47. Zhang, L., Webster, T.: Nanotechnology and nanomaterials: promises for improved tissue regeneration. Nano Today 4(1), 66–80 (2009)
- 48. Zhang, Z., Yang, X., Zhang, Y., Zeng, B., Wang, S., Zhu, T., et al.: Delivery of telomerase reverse transcriptase small interfering RNA in complex with positively charged single-walled carbon nanotubes suppresses tumor growth. Clin. Cancer Res. 12(16), 4933 (2006)

Filling of Carbon Nanotubes with Compounds in Solution or Melted Phase

P. Lukanov, C.-M. Tîlmaciu, A. M. Galibert, B. Soula and E. Flahaut

Abstract Since their discovery, carbon nanotubes (CNT) have been found to exhibit remarkable structural, mechanical and electronic properties. One such property is the ability to encapsulate foreign materials inside their cylindrical cavity, for application in different fields. The procedures to fill CNT may be classified into two main groups: (a) filling in solution, using the wet chemistry route and (b) filling with a melted phase. In both cases, the filling is induced by the capillary forces. It is also possible to fill CNT in the vapour phase, although there are only few very specific examples available in the literature to date. After filling, oxides and metallic particles can be obtained by a subsequent thermal annealing in the required atmosphere. In the wet chemistry route, the nanotubes are usually treated by an oxidizing agent in order to open their tips. The filling is then performed by placing the opened tubes in a solution of the selected compound (or a precursor). When the compound is dissolved in an oxidizing acid such as nitric acid (HNO₃), it is possible to combine opening and filling in a single step. Although this method allows the introduction of heat-sensitive species inside carbon nanotubes, the yield varies strongly with the diameter of the carbon nanotubes and is generally rather low in the case of CNT with a small inner diameter. This filling route mainly leads to isolated nanoparticles or short nanowires. Filling with melted compounds is a solvent-free route. The CNT are directly immersed in the melted material and capillary forces drive the compound into the

e-mail: lukanov@chimie.ups-tlse.fr

C.-M. Tîlmaciu

e-mail: tilmaciu@chimie.ups-tlse.fr

P. Lukanov, C.-M. Tîlmaciu equally contributed to the work.

P. Lukanov (🖾), C.-M. Tîlmaciu, A. M. Galibert, B. Soula and E. Flahaut Institut Carnot Cirimat, Université de Toulouse, UPS, INP, 118 Route de Narbonne, 31062, Toulouse Cedex 9. France

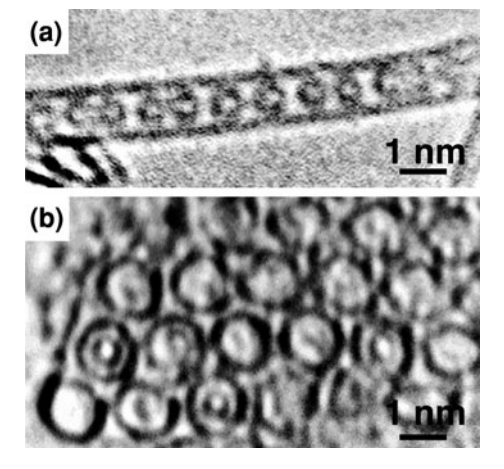
CNT. Although this route is more restrictive in terms of materials, it allows for the continuous filling of CNT with long nanocrystals (up to a few micrometers), with a higher filling yield in the available CNT (up to ca. 70%). This chapter will describe these two different methods for filling CNT and illustrate them with a few selected examples.

1 General Introduction

Why Fill Carbon Nanotubes? What is the Chemistry of CNT?

Following the discovery of these striking materials, numerous attempts to fill the nanoscale cavities of carbon nanotubes have been made. The story of X@CNT [hybrid nanotubes in which the inner cavity has been filled with foreign atoms, molecules or compounds and where X is the chemical symbol of the filling material and CNT is the nanotube type: single-walled (SWCNT), double-walled (DWCNT) or multi-walled (MWCNT)] started 2 years after it became possible easily to synthesize nearly defect-free MWCNT via a catalyst-free process (i.e., the same electric arc procedure used to produce fullerenes, reported by Iijima in 1991) [1]. The filling is generally attempted in order to achieve one of the two following goals: first, being a kind of template synthesis, filling allows the preparation of nanostructured materials with controlled size and shape. Secondly, filling can be seen as a kind of doping, which may also modify the electronic properties of the CNT. The very small inner cavity of CNT is an amazing tool to prepare and study the properties of confined nanostructures, such as salts, metals, oxides, gases or even discrete molecules like C_{60} . It actually took 5 years for the

Fig. 1 Pioneering high resolution transmission electron microscopy (HRTEM) images in the field of hybrid SWCNT published in 1998 [2]. a The first example of C₆₀@SWCNT (peapods). b Cross-sectional view of an ordered bundle of SWCNT among which some are filled by fullerenes



first definite example of X@SWCNT to be reported: the incidental discovery of the ability of fullerenes to enter SWCNT, thereby forming the so-called "peapods" (Fig. 1) [2].

Because of the almost 1D structure of CNT—this is especially true for SWCNT and DWCNT—one can expect different physical and chemical properties for the confined foreign materials and even for the composite formed by the filler and the CNT. Indeed, when the volume available inside a CNT is small enough, the foreign material can be made mainly (if not only) of "surface atoms" of reduced coordination. The question of the stability of such structures (once the surrounding CNT are removed) is complex and will probably depend both on their chemical nature and on the proportion of surface atoms. Applications of filled-CNT may range from superconducting materials (this effect has already been observed in the case of metallofullerenes) to biosensors, catalytic supports and even vectors for therapeutic biomolecules.

How to Fill Carbon Nanotubes?

Filling nanotubes while they grow (in situ filling) [3–8] was one of the pioneering methods. In most cases, however, the filling step is separated from the synthesis of the nanotubes. Three methods can then be distinguished: (a) wet chemistry procedures and physical procedures, involving capillarity filling by (b) a molten material or (c) a sublimated material [9, 10]. Within the pages of this chapter, we will focus our attention on the two-first methods of post-synthesis filling: filling of carbon nanotubes from solutions and from melted phases.

What About the Role of Wetting and Capillarity?

Soon after the discovery of CNT, on the basis of computer simulations, Pederson and Broughton [11] predicted that liquids may fill open CNT by capillary effect. Ajayan and Iijima [12] were the first to report that lead could be trapped inside MWCNT. Wetting a carbon surface by a foreign liquid is required for capillary filling [13]. Generally speaking, the mechanism of filling via liquid routes is not very well understood. The work of Dujardin et al. [14] stressed the surface tension of the liquid as a key parameter for the successful filling of CNT [15]. It was found that the cut-off value of 200 mN/m is at the border between wetting and non wetting (Table 1). Liquids as water (72 mN/m), nitric acid (43 mN/m) or organic solvents (from 26 up to 47 mN/m) should wet nanotubes and could thus be used as low surface tension media for different soluble precursors.

Water, ethanol, some oxides with low surface tension (PbO, V₂O₅) and some solids with low melting points (S, Cs, Rb, Se) were found to easily fill the inner cavities of CNT with large diameters. There is a rough relation between the inner diameters of CNT and capillarity behavior. For example, V, Co and Pb inorganic

Liquid	Melting point (°C)	Surface tension γ (mN/m)	Wetting		
			Raw	Oxidized	Annealed
HNO ₃ 70%		43	Yes	Yes	Yes
S	112	61	Yes	Yes	Yes
Cs	29	67	Yes	Yes	Yes
V_2O_5	690	80	Yes	Yes	Yes
Se	217	97	Yes	Yes	Yes
PbO	886	132	Yes	Yes	Yes
Te	450	190	No	No	No
Bi_2O_3	825	200	No	No	No
Pb	327	470	No	No	No
Hg	-39	490	No		
Ga	30	710	No		

Table 1 Melting point, surface tension at the melting point and wetting abilities of different elements or compounds [14]

salts with low surface tension can fill thin MWCNT with inner diameters of 1–2 nm, while AgNO₃ can fill MWCNT with inner diameter larger than 4 nm [16].

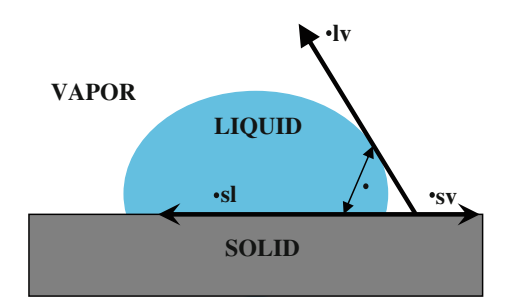
Pure metals or metal compounds with high surface tension can fill the CNT only in oxidizing atmosphere possibly due to the fact that low surface tension oxides are formed [17]. Filling CNT with materials that could not have been introduced directly was also proved to be possible. This can be accomplished by first filling the nanotubes with an appropriate precursor (i.e., able to be sublimed, or melted [18, 19], or dissolved) that will later be transformed by a chemical reaction or by a physical interaction such as electron beam irradiation [16]. In the case of secondary chemical transformation, the reduction by H₂ is the most frequently used to obtain nanotubes filled with metals [20]. Sulfides can be obtained as well by using H₂S as reducing agent [20].

The wetting has a direct influence on the capillary action and the contact angle θ between the wetting liquid and the solid surface must be less than 90° (Fig. 2). θ can be measured experimentally. The Young–Laplace equation (Eq. 1):

$$\gamma_{SV} = \gamma_{SL} + \gamma_{LV} \cdot \cos\theta \tag{1}$$

describes the relation between γ_{SV} the interfacial tension between the solid and gas, γ_{SL} the interfacial tension between the solid and liquid and γ_{LV} the interfacial

Fig. 2 Contact angle θ of a liquid on a solid surface



tension between the liquid and gas. If θ is larger than 90°, the contact angle will be non-wetting. If θ is smaller than 90°, the liquid will spontaneously enter into the empty cavities of CNT [21]. The validity of the Young–Laplace equation at the nanometer scale may however be open to discussion.

In addition to the surface tension, the viscosity could be also considered as an important factor in the filling kinetics (although it usually decreases with increasing temperature).

2 The Filling of CNT from Solutions

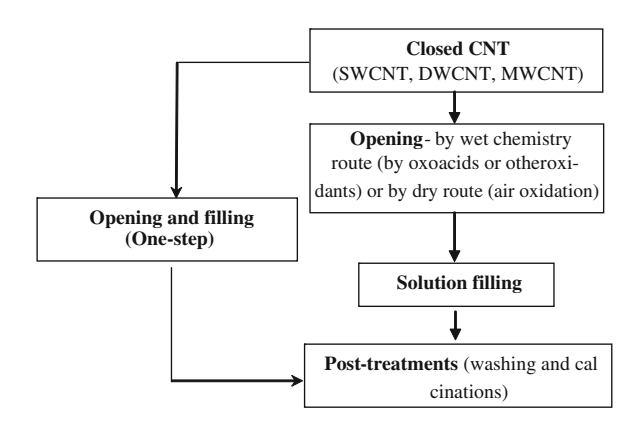
Introduction

The solution filling method is based on putting into contact a concentrated solution of the desired material (or generally a "precursor") with opened carbon nanotubes. The main advantage of the wet chemistry approach is its flexibility and the level of experimental control. This is a quite useful alternative method for filling CNT when the physical properties of the desired filling material are not suitable for filling from melted phases or via gas route. This method usually requires a few steps until filled CNT are obtained. The general description of the wet chemistry filling method is given in Fig. 3. The first way is to open and fill the CNT at the same time (one-step) and the second one is first to open the tubes and then to transfer them into the solution containing the filling material (two-step method).

Main Parameters Involved in Filling of CNT from Solutions

The most important factors for filling CNT are related to the diameter of the nanotubes, the physico-chemical properties of the material to be inserted (stability,

Fig. 3 Sketch of the main steps for the filling of CNT in solution



solubility, etc.) and the process itself (1 or 2 steps, need of thermal treatments in inert or redacting atmosphere, etc.). All these steps bring up many experimental variations and also many problems which have to be solved.

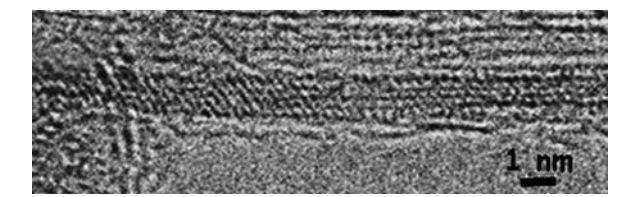
The diameter of the tubes used for filling has a very important place in the solution filling. The first information about filling of large sized MWCNT with metals from solution was given by Green et al. [22] in 1994 (filling details in II.3.1). MWCNT with inner diameter from 6 up to a few hundreds of nanometers are easier to fill [23–25], than the small sized SWCNT (ca. 1.22 nm) [26, 27] or DWCNT (ca. 1.5 nm) [28]. Since the discovery of this filling method, many efforts have been made to fill MWCNT for various applications in electronics [29–31], biology or material science [21, 32]. The domination of MWCNT for filling in solutions is evident from the number of published articles. Pederson and Broughton [11] calculated that increasing the tubular radius decreases the insertion energy and the overlap repulsion activation barrier at the open tip, from which they concluded that material encapsulation in narrow SWCNT via the liquid route should be unfavorable by comparison to larger MWCNT.

Many recent applications of carbon nanotubes (such as biomedical application, electronics, etc.) require going towards smaller tube diameters. So, recently, efforts have been made also to fill small diameter SWCNT and DWCNT. SWCNT display higher degree of uniformity with respect to their physical dimensions compared to MWCNT as they consist of one cylindrical graphitic layer and exhibit much less defects than MWCNT. SWCNT were first filled by wet chemistry with ruthenium chloride by Sloan et al. [33] (Fig. 4).

High-yield solution filling of SWCNT with ferromagnetic material like Fe was also reported [26]. Molecular dynamic simulation has shown that even DNA could be introduced inside SWCNT in an aqueous environment via an extremely rapid dynamic interaction process provided that the tube diameter exceeds a certain critical value of 1.08 nm [34].

DWCNT are a relatively new form of carbon nanotubes (although MWCNT have been produced for a long time, the selective synthesis of DWCNT is much more recent) but they are already successfully used for filling in solutions. It has been proved/shown by magnetic measurements that, by wet chemistry, α -Fe nanowires could be introduced into DWCNT [28]. This product could be very promising for applications as magnetic probes, AFM tips, memories, nanodevices for spin electronics and functionalized magnetic materials for biomedical applications. The method was also successfully used to fill DWCNT with crystalline AgCl nanowires in order to study the charge transfer phenomenon between the tubes and the filling material [35].

Fig. 4 HRTEM of the first example of metal@SWCNT [33] (RuCl₃ was initially introduced and then was chemically reduced to the metal)



Methods for Filling in Solution

In general, the methods for filling CNT in solution can be classified into two main types: one-step solution filling (opening and filling at the same time) and two-step solution filling (first opening and then filling).

One-Step Method

This was developed by Green and co-workers [22] from Oxford who successfully filled MWCNT this way. The procedure was performed by simultaneous opening and filling of CNT with a metal nitrate (nickel nitrate) in solution in concentrated nitric acid. Reflux at 140°C for a few hours makes the tubes more hydrophilic and attacks the tips of the tubes where the sp³ character is more pronounced, leading to their opening. This acid treatment also attacks the walls of the CNT where defects such as pentagon-heptagon pairs are located (functionalization). The opened tips allow the solution to enter inside the cavities and to fill the empty space. After filtration and washing, the filled CNT were heated at 450°C in a helium atmosphere in order to get the corresponding oxide. In the same study, oxides of Fe, Ni, Co and U were synthesized inside MWCNT using the same method. A few years later, still using the same method, the team from Oxford reported the one-step filling of MWCNT with different types of oxide crystals such as NiO, Sm₂O₃ and Nd₂O₃ (Fig. 5) [21]. It was observed that the use of nitric acid/Nd₂O₃ suspension created amorphous materials between the carbon layers, modifying the interlayer space by a few angstroms and also generating some defects. Carbon nanotubes containing oxides of the following elements Co, Pd, Cd, Fe, Y, La, Ce, Pr, Nd, Eu, U [36], Au and Pt [37] have been prepared using the same one-step method.

Another advantage of the one-step solution filling is the possibility to prepare stoichiometric mixed metal oxides containing ions of two different metals [36]. For example, FeBiO₃ was synthesized (after annealing) into the empty cavities of MWCNT suspended in a mixture of Fe(NO₃)₃·9H₂O and Bi(NO₃)₃·5H₂O dissolved into nitric acid and refluxed [21] (Fig. 6).

Another example using the one-step method is a direct synthesis of magnetic materials for nano-electromechanical systems applications (NEMS) like $Sm_2Fe_{17}N_x$ which has been introduced into the cavities of MWCNT [31]. The approach appears to have great promise although the yield is low.

Two-Step Method

The filling of CNT from a solution can also be realized first by the opening of the tubes (in an oxidizing solution) followed by the actual filling after transfer into a concentrated solution containing the precursor material. This method can be useful for filling of tubes with materials which are not stable at reflux temperature. The two-step methods may be classified depending on the opening agent used.

Fig. 5 HRTEM of MWCNT one-step filled with oxide crystals of **a** NiO, **b** Sm₂O₃ and **c** Nd₂O₃ intercalated crystalline in the bore and in the interlayer (*arrowed*) of nanotube [21]

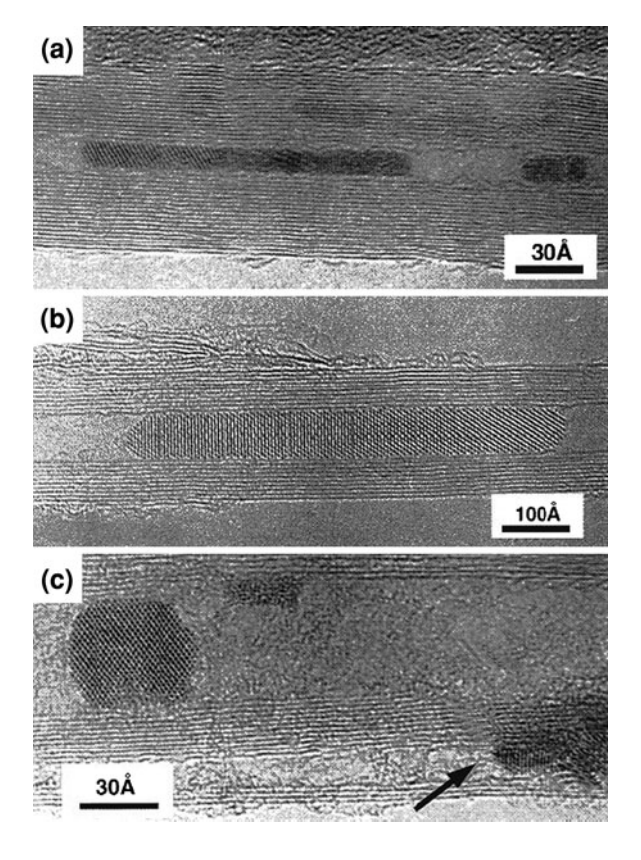
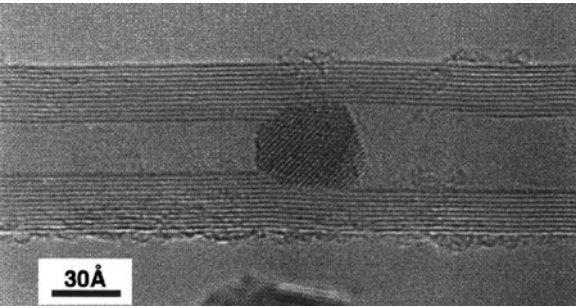


Fig. 6 HRTEM of MWCNT one-step filled with FeBiO₃ crystallite [21]



The very first filling reported using the two-step method was the filling of SWCNT with Ru from RuCl₃ [33]. As a first step the tubes were treated in concentrated HCl solution for few hours in order to open them, a finding which was contradicted by some authors who stated that hydrochloric acid does not attack the tubes and does not open them [38]. Since then, the two-step method has been widely used. Corio and co-workers [39] opened SWCNT in an aqueous solution of HCl and fill them with Ag from AgNO₃ aqueous solution resulting in significant changes in the Raman spectra of the SWCNT.

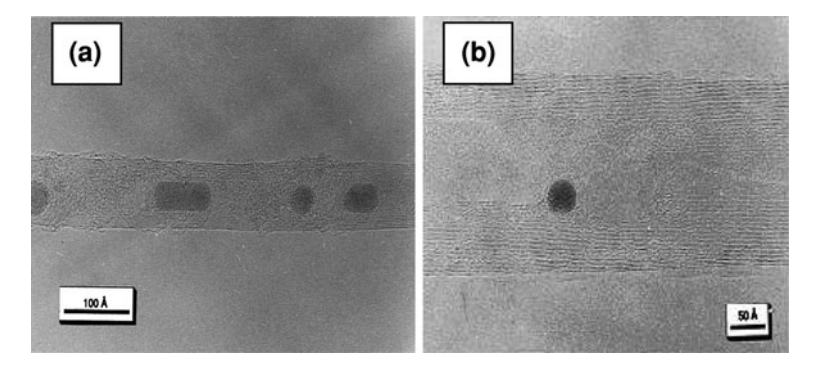


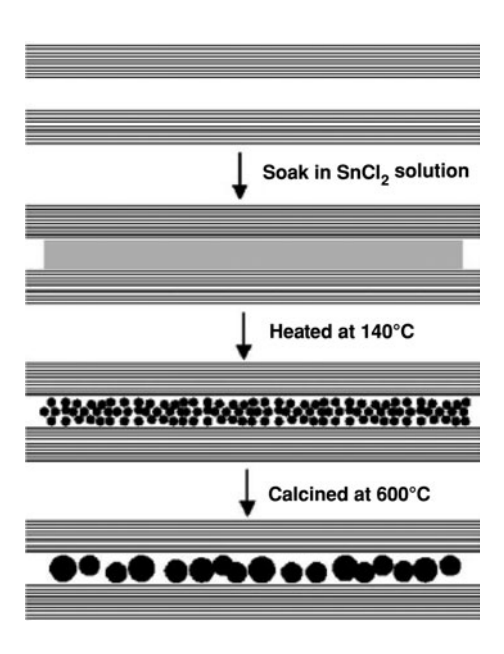
Fig. 7 HRTEM of two-step filled MWCNT with a silver and b gold [40]

Chu and co-workers [40] successfully opened MWCNT in concentrated HNO $_3$ and filled them with Ag crystals 35–85 Å in diameter (Fig. 7a). According to the low percentage of filled tubes usually achieved with this technique (20–30%) [21], an unusually high filling yield of 70% was estimated. In the same work, identical conditions were applied to fill MWCNT with small spherical Au crystals (diameter 10–50 Å) from AuCl $_3$ (Fig. 7b) but the filling yield was low.

In order not to damage CNT the optimum duration of reflux in conc. nitric acid (68%) is from 3 up to 24 h. Sloan et al. [41] from Oxford applied 24 h of reflux on MWCNT in conc. nitric acid and filled the tubes with spherical crystals of SnO (diameter 2-6 nm) from a SnCl₂·2H₂O/HCl solution. The same conditions for opening have been applied to fill MWCNT with different compounds like Fe [23] or CuO [42]. It was observed that the effect of oxidation and opening of MWCNT can be also obtained for shorter reflux times. Gao and co-authors [23] have reported the solution filling of pre-opened MWCNT with tin (IV) oxide (Fig. 8). MWCNT were first opened in concentrated nitric acid by reflux at 140°C for 3 h and then transferred into an aqueous/hydrochloric solution of SnCl₂ and stirred for 12 h. It was described that the amount of SnO₂ nanoparticles could be controlled by changing the concentration of SnCl₂ in the precursor which is a big advantage of the wet chemistry filling. After the opening, soaking and drying, heat treatment at 140°C for 3 h is required in order to form SnO₂ crystalline. Finally, calcination at 600°C in steam of argon was performed where nanocrystals in the inner cavities grew up until a spherical nanoparticle eventually appeared.

Conc. HNO_3 has been also used for two-step solution filling of MWCNT with different metals like Co, Fe or Ni [43]. Green and co-workers found that the two-step method is useful for filling tubes with materials which are neither soluble nor stable in refluxing nitric acid (one-step method). Filled MWCNT with dodecatungstosilicic acid ($H_4SiW_{12}O_{40}$) have been obtained after opening by reflux in conc. HNO_3 for 8–24 h and then stirring in concentrated $H_4SiW_{12}O_{40}$ aqueous solution [21]. MWCNT filled with RhCl₃, RuCl₃, PdCl₃, [NH₄]IrCl₆ and Co₂(CO)₈ have also been prepared by this method.

Fig. 8 Solution filling of MWCNT by SnO₂ [23]

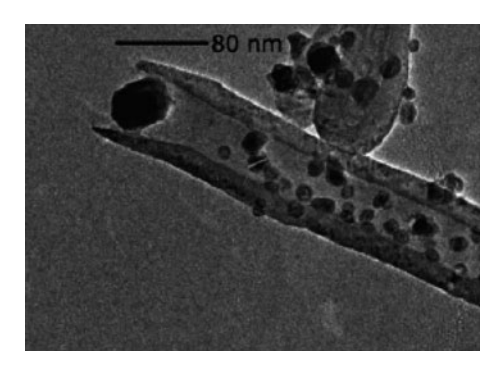


The wet chemistry method also gives possibilities to fill opened carbon nanotubes with thermally unstable materials: for example some organic compounds. Green and co-workers [44] reported filling of MWCNT with small proteins. The tubes were opened in nitric acid (24 h) and then suspended in protein (cytochrome C_3) aqueous solutions for 24 h. Large grey areas of about 13.5–17 nm in length, attributed to protein aggregates, were observed inside the CNT. The same conditions were used to fill MWCNT with proteins such as the cysteine-rich, beta-lactamase I flavocytochrome b_2 tetramer. The stability and catalytic activity studies of these materials were reported later [45].

Qu et al. [46] proposed another method for opening MWCNT in stronger acid solutions. MWCNT were cut into short pipes by chemical oxidation in a mixture of concentrated sulfuric and nitric acid (3:1) under ultrasonication for 8 h. The openended MWCNT were transferred into a saturated ferric nitrate solution for 12 h. The oxide precursor accumulated inside the tubes was decomposed into Fe₂O₃ during calcination at 450°C while iron ions absorbed and nucleated on the outer surface of the tubes were easily removed by washing before calcination.

Due to their single-wall structure, the conditions for opening SWCNT can be milder than those for MWCNT. Borowiak-Palen et al. [26, 47] have opened SWCNT in 2 M HNO₃ (reflux for 30 h at 130°C) and filled them with Fe from an over-saturated iron (III) chloride solution. High yield filling of SWCNT with Ag has been obtained with the same way of opening [27]. Mild chemical conditions for opening of DWCNT are also required. For DWCNT Jorje et al. [28] have reported the opening of DWCNT in 2 M HNO₃ by reflux for 30 h followed by

Fig. 9 TEM picture of MWCNT opened by permanganate/H₂SO₄ and filled with nanoparticles [32]



filling with ferromagnetic Fe from a concentrated iron (III) chloride solution. The acid treatment does not just open the tubes but also purifies them from the residual catalytic metal nanoparticles (Co in this case). Ferromagnetic nanowires with length between 50 and 100 nm were observed in the resulting product.

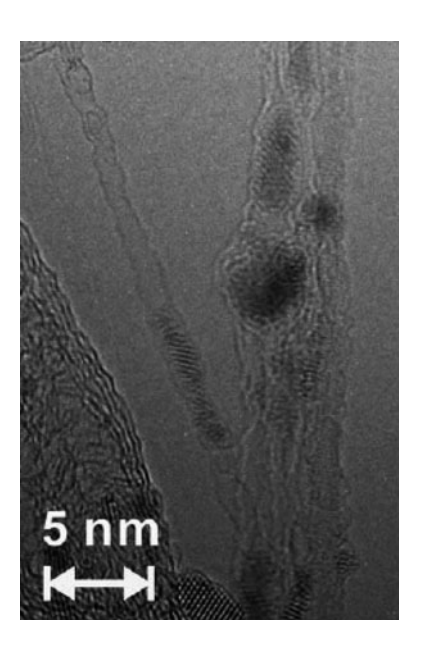
Use of oxidants in acid solutions gives another possibility to open CNT. Jain and Wilhelm [32] reported the opening of MWCNT in $KMnO_4/H_2SO_4$ solution followed by filling with organic-based ferrofluid (EMG-911) containing nanoparticles with an average size of 10 nm (Fig. 9). It was possible to observe that the tubes with diameter lower than 10 nm were less filled or remained empty.

Again using two-step filling, Shao and co-workers [48] proposed a new type of opening of CNT. They showed that SWCNT can be opened in an alkali or alkaline-earth hydroxide such as NaOH, KOH, CsOH·H₂O or Ba(OH)₂·8H₂O by heating in vacuum for 4 h at temperatures between 300 and 508°C, depending on the melting point of the selected hydroxide. After washing, the opened tubes were stirred in uranium oxide/conc. HNO₃ solution and successfully filled (Fig. 10).

Conclusion

To summarize, the solution filling route can be very useful as an alternative when the filling from gas route or molten phases is not possible, because of the physical properties of the desired filling material. Thanks to the large range of soluble materials, the method finds a large area of applications. One of the biggest advantages is that sensitive biomaterials can be easily dissolved and placed into CNT, which would be impossible with the other filling methods. Thanks to the simple preparation and the simple technical requirements, the method is found to be low-cost and attractive. The solution filling method also shows some disadvantages such as the need to open the CNT, usually in aggressive conditions where the tubes can be damaged and functionalised. Generally speaking, the filling yield obtained by using the solution method is rather low (scarcely above 20%). By decreasing the diameter of carbon nanotubes the filling yield decreases, making the task rather difficult in the case of SWCNT and DWCNT.

Fig. 10 HRTEM of SWCNT two-step filled with amorphous uranium compound in order to confirm the successful opening of the tubes [48]



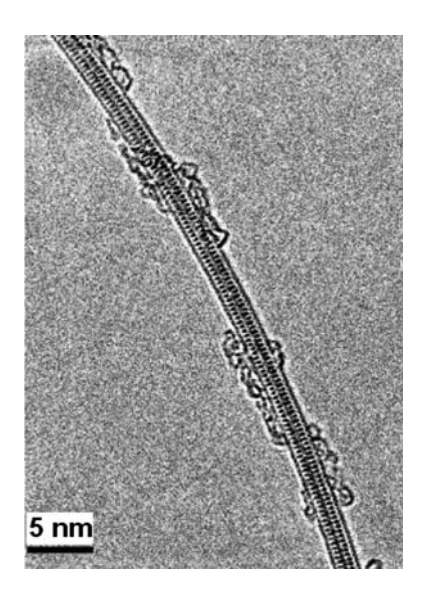
3 Filling of CNT from Melted Phases

A Bit of History

Filling with molten materials was among the first methods used to fill MWCNT. Four papers that reported some filling of MWCNT with various melted metals and compounds (PbO [12, 17], Y₃C and TiC [49], Bi₂O₅ [50] and Ni [51]) were published in 1993 in an attempt to obtain encapsulated inorganic nanowires. The first filling of carbon nanotubes with lead, reported by Ajayan and Iijima [12] was achieved in two steps: lead particles were deposited onto the tubes, following electron-beam evaporation of pure lead under a vacuum of 10⁻⁶ Torr, followed by an oxidation in air (400°C), which both opened the tips of the CNT and allowed Pb to get inside. Repeating the experiment with CNT already opened was unsuccessful and the identification of the phase inside the tubes indicated that the formation of an intermediate Pb–O–C compound seemed to be necessary (this compound would have a lower surface tension compared to that of the metal). Opening and filling seemed to have occurred simultaneously.

However, inner diameters of MWCNT are generally quite large (an average of 5–50 nm) and filling the much smaller inner cavity of SWCNT (range of 1–2 nm), that were discovered in 1993 [52, 53] appeared more challenging. The first work of a long series was done by the University of Oxford, which has thoroughly investigated the filling of SWCNT since then [54–56] making them the world leaders in the field.

Fig. 11 HRTEM image of ErCl₃@SWCNT [57]



A high filling yield of SWCNT ($\sim 90\%$) was recently obtained (Kitaura et al. [57]). These authors fabricated crystalline ErCl₃ nanowires into SWCNT cavities. Before the encapsulation reaction, the SWCNT were heated under dry airflow at 600°C for 30 min in order to remove the end-caps. Open-ended DWCNT together with anhydrous ErCl₃ were transferred into a quartz ampoule, vacuum-sealed at 10^{-7} Torr and then heated at 800°C for 72 h. At this temperature, ErCl₃ melted and became encapsulated within the core of SWCNT (Fig. 11). Two columns of dark spots arranged in a regular fashion were clearly observed in the ErCl₃@SWCNT sample.

Hence, encapsulating materials in CNT is likely to promote new phases, new structures, new properties, and/or new behaviors. Moreover, it is a certainty that any of these features are more interesting when the tube cavity diameter is of the order of 2 nm, as is encountered for most SWCNT and DWCNT [58, 59].

General Molten State Filling Procedure

The physical method involving a melted phase is more restrictive than the wet chemistry route, firstly because some materials may start to decompose when they melt, and secondly because the melting point has to be compatible with the nanotubes (i.e. thermal treatment temperature should remain below the temperature of transformation or damage of the nanotubes). Because the filling is occurring thanks to capillary forces, the surface tension of the molten materials has to be in the range from 100 to 200 N/cm² for MWCNT [17]. In a typical filling experiment, the CNT are closely mixed with the desired amount of filler by gentle

grinding, and the mixture is then vacuum-sealed in a silica ampoule. The ampoule is slowly heated to a temperature above the melting point of the filler, and then slowly cooled. The use of this method does not require any opening of the nanotubes prior to the heat treatment. The mechanism of nanotube opening is not yet established clearly, but it is certainly related to the chemical aggressiveness of the molten materials towards the carbon and more precisely towards the graphene defects in the tube structure.

Experimental results seem to indicate that it is difficult if not impossible to fill opened CNT which have not been submitted to an annealing treatment. The following hypotheses have been proposed to explain this phenomenon: (a) the presence of bulky carboxyl groups at the tips could obstruct the entrance of the CNT and thus hinder the filling; (b) the remains of the graphitic caps could be attracted inside the CNT during its opening. An annealing treatment at a temperature above 900°C (in vacuum) can degrade the carboxyl groups and it is thus suggested to facilitate the subsequent filling.

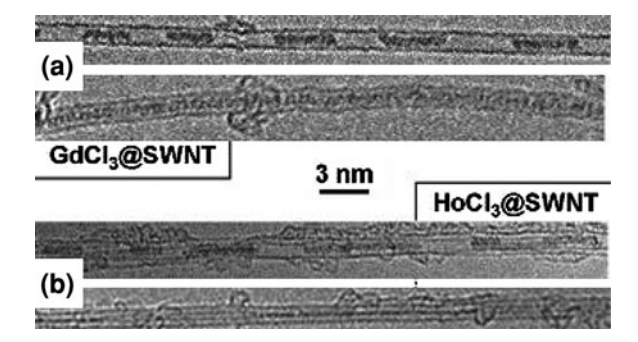
Estimation of the Filling Rate

As opposed to the solution method, the melting method allows high filling yields to be achieved even for SWCNT. One such example was the filling of SWCNT with lanthanide chlorides (Fig. 12) [15]. A quartz ampoule containing nanotubes along with the ground material was sealed under vacuum and was then heated for 24 h.

Filling materials formed both continuous nanowires [bottom images in Fig. 12a-b] or short segments somewhat periodically spaced [top images in Fig. 12a-b]. Filling yield as high as $\sim 80\%$ was reported for PbO in SWCNT [60, 61], although cumulative filling cycles were necessary to achieve the filling. This makes this method almost as efficient as the gas phase route, obviously, because, for both methods, only the desired filling material is entering the nanotube cavity (solvent free).

Generally speaking, the estimation of the filling yield (percent of filled tubes in all the sample) is problematic and most of the time is derived from the TEM

Fig. 12 HRTEM images of SWCNT filled with lanthanides chlorides: **a** GdCl₃@SWCNT obtained at 700°C. **b** HoCl₃@SWCNT obtained at 820°C [15]



observations, without any statistics on the number of the observed tubes. Moreover, as far as SWCNT are concerned, the fact that the nanotubes are gathered into bundles makes difficult the observation of the exact number of filled tubes, as well as the estimation of the filled length for each tube. Estimation of the filling yield is a difficult task and is subjected to controversy: should the proportion of total CNT containing some filling (whatever the length) be used? Or should it be the ratio of filled length to the total length of the observed CNT? Keeping in mind that this information can only be obtained using a high resolution transmission electron microscope (HRTEM), leading only to local observations, it seems that neither of these two methods can give the true filling yield for the whole sample. Global measurements of the filling yield have been proposed in the case of peapods, based on EELS or Raman spectroscopy but beyond that, there is still a need for a method for measuring global filling yield of the filled CNT samples.

Atomic Emission Spectroscopy (AES) is a method of chemical analysis that uses the intensity of light emitted from a flame, plasma, arc, or spark at a particular wavelength to determine the quantity of an element in a sample. The wavelength of the atomic spectral line gives the identity of the element, while the intensity of the emitted light is proportional to the number of atoms of the element. The problem of this method is that a global quantitative analysis of the filler compound in the whole sample with no distinction between the inside and the outside of CNT is obtained, making impossible a correct evaluation of the filling yield. Values reported in the literature should thus often be considered only as rough estimations.

Ballesteros et al. [56] reported the first methodology for the quantitative assessment of the amount of material encapsulated in filled carbon nanotubes. Single-walled carbon nanotubes were filled by molten phase capillary wetting with CuI, FeCl₂, and CuBr. A suitable solvent was used in each case to remove the large amount of external material present after the filling step. Thermogravimetric analyses in air were performed on the empty and filled nanotubes, and the data were used to obtain the filling yield for each sample.

During the TGA experiment on the filled samples in flowing air, the filling material may react with oxygen to form a solid residue, normally an oxide and/or may sublime or form a gaseous oxide. In any case, the filling yield (FY) can be accurately determined by the Eq. 2:

$$FY(wt\%) = 100 \times (R_2 - R_1) / (R_A - R_1)$$
 (2)

where R_1 , R_2 and R_A are the TGA residual quantities in air for the empty carbon nanotubes, the filled carbon nanotubes, and the bulk filling material (A), respectively. The obtained FY is an average value and does not make distinction between the filling efficiency of SWCNT of different diameters and lengths present in the sample. Calculations have to take into account the catalyst impurity in the nanotube samples.

Filling yield determination has special interest for the optimization of the filling experiments and for comparison of different filled samples, since differences in

properties of filled nanotubes will be related to different degrees of material encapsulation.

Filler Compounds (as Nanowires or Nanoparticles)

Filling CNT with compounds is a very important alternative when direct filling with chemical elements is not possible, typically because of a too high melting point and/or of a too high surface tension of the considered elements in the molten state [15]. Compounds are typically salts, among which halides are the most popular [56–59, 62, 63], for many reasons such as a high versatility. Many types of halides may be used for filling, i.e. fluorides, chlorides, bromides or iodides; in many cases, melting points are in a suitable temperature range (i.e., not too high, e.g. <1,000°C); there is good solubility in usual solvents (chloroform, water, etc.) in order to remove the excess of salt outside the nanotubes. Moreover, a great advantage in the case of the filling of CNT with iodides is the good contrast of the filled tubes on the HRTEM images (Fig. 13).

From 2001, oxides were also directly inserted into SWCNT, starting with CrO₃ [39] and Sb₂O₃ [64, 65], followed by others such as PbO [60] or Re_xO_y [66], sometimes with a fairly high filling yield (e.g., 80–90% for PbO). Although oxides can be interesting alternatives as intermediate compounds or can exhibit interesting intrinsic properties on their own (e.g., CrO₃ is electrically conductive), they will never become so popular as halides, because oxides have, generally, neither a high solubility in harmless solvents nor a reasonable melting temperature. Other

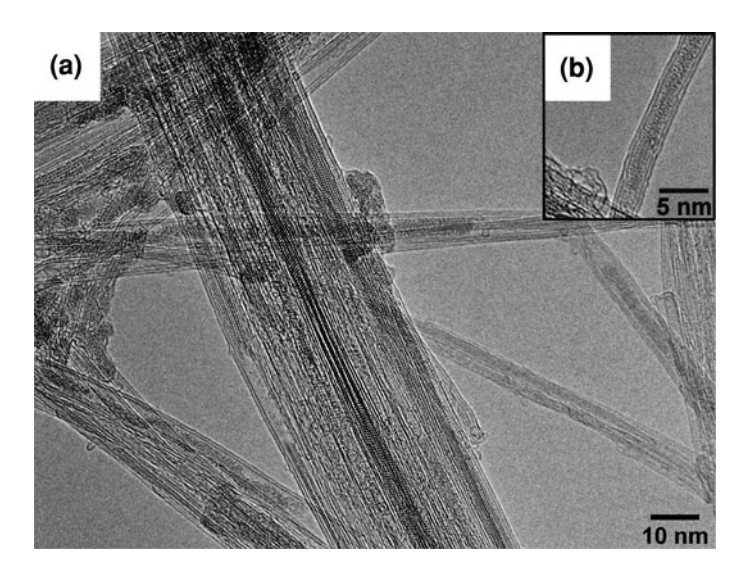
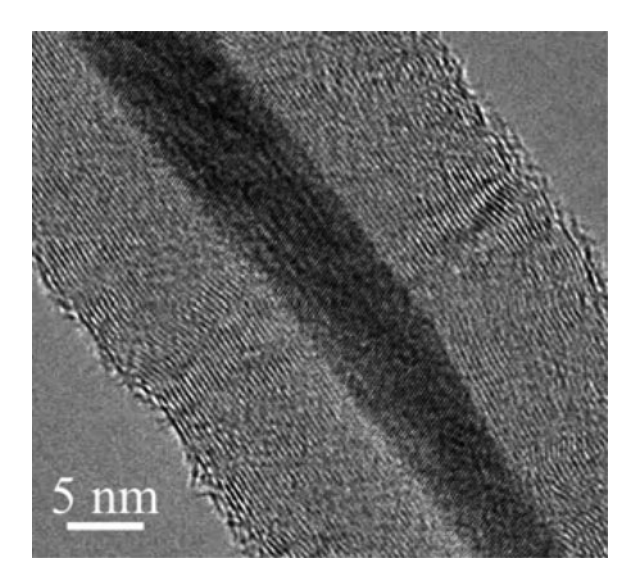


Fig. 13 HRTEM images of the FeI₂ filling within a a DWCNT bundle; b a single DWCNT [59]

Fig. 14 HRTEM image of iron filled MWCNT for hyperthermia application [73]



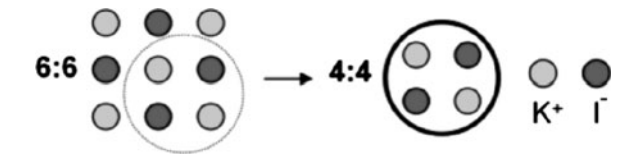
compounds that have been used in attempts to fill SWCNT are typically nitrates (specifically silver nitrate [39, 67, 68], bismuth nitrate [69], uranyl nitrate [70]), acetates (uranyl acetate [70]) and hydroxides (KOH and CsOH [70]).

The almost complete filling of CNT, which allows the production of metallic nanowires (Fig. 14) for electronic or magnetic devices, as well as for biomedical applications [71, 72] has been well-documented. In particular, CNT can be filled with magnetic nanoparticles. It is envisaged that external static magnetic fields could fix the ferromagnetic nanoparticles at a precise position in animal (human) tissues; gradient fields would move them and alternating (AC) fields lead to local heating. The latter can be utilized for the so-called "hyperthermia" [73], i.e. a therapeutic cell-killing anti-cancer treatment to raise the temperature of tumor tissue in vivo. This method applies the fact that a cancer cell-damaging effect is caused when a temperature above 41–42°C is maintained in the target volume.

Structural Modifications of Confined Matter

The main effect of confinement in a nanotube of only a few nanometers inner diameter is to decrease the coordination of the atoms (or ions) (Fig. 15) [74]. This

Fig. 15 The coordination of the K^+ and I^- ions decreases from 6:6 in the bulk structure to 4:4 when they are confined inside a CNT with an internal diameter of 1.4 nm [74]



58 P. Lukanov et al.

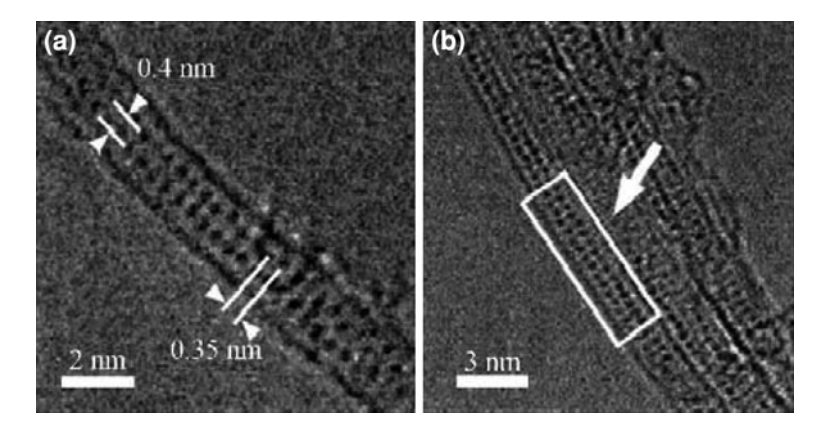


Fig. 16 HRTEM images of two layers of thick KI crystals formed within a a 1.4 nm diameter SWCNT, b a SWCNT bundle. Each *dark spot* corresponds to a two-ion K–I (or I–K) column [75]

happens because the inserted material is often reduced to only a few atomic layers when it is observed in perpendicular section to the CNT axis.

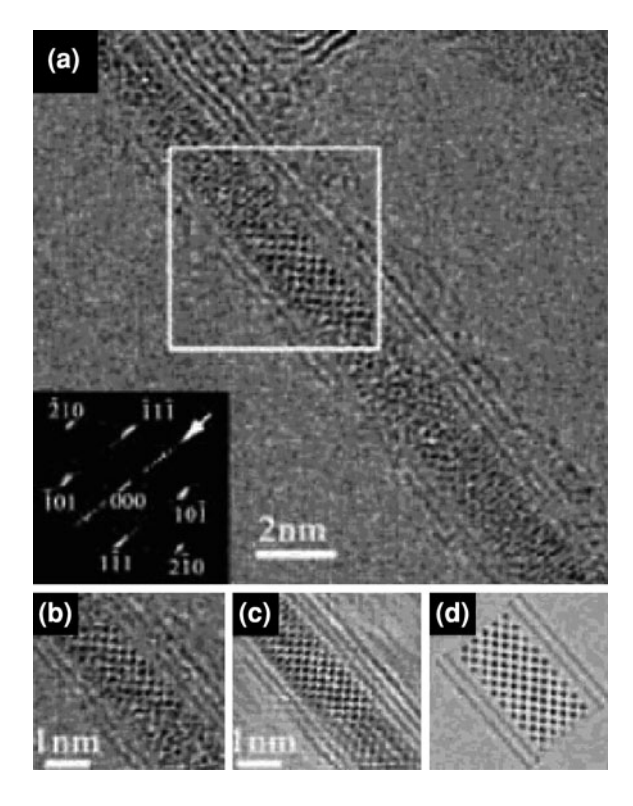
Confinement thus leads to 1D structure of atoms (or ions) of reduced coordination, which could be related—or not—to the bulk structure. We will now describe a series of examples to illustrate the effect of confinement. The effect of the inner diameter of the CNT will also be discussed.

The first example is that of KI@SWCNT [75]. KI has a face-centered cubic structure (a = 3.53 Å). The general methodology employed to determine the structure of confined crystals is the following: (a) HRTEM observation; (b) construction of a rough outline of the structural model from the HRTEM images; (c) simulation of the HRTEM image from the proposed structural model and comparison with the experimental data (the images are simulated at different focuses in order to match as well as possible the experimental image); (d) correction of the structural model and simulation until the fit with the experimental images is acceptable. In the case of KI@SWCNT (Fig. 16), the confined KI crystals retain a structure close to that of the bulk but distortions are observed. Along the axis, the d-spacing is 0.35 nm, as in the bulk; however, this spacing is increased by nearly 0.4 nm perpendicularly to the CNT axis (14% of extension).

In such a thin structure where all the ions are indeed "surface ions" (compared to the bulk structure), it seems that there is a strong interaction between the ions and the CNT inner wall. In the case of CNT with a large diameter, the situation is a bit more complex and slight distortions were brought to light both parallel and perpendicularly to the CNT axis. The measure of such small distortions was made possible by the use of the phase image restoration technique.

In the case of $PbI_2@DWCNT$ [76], similar crystal growth behavior was generally observed to occur in narrow nanotubes with inner diameters comparable to that of SWCNT. In this example, the PbI_2 crystal is oriented with the [1 2 1] direction parallel to the direction of the electron beam (Fig. 17). However, as the

Fig. 17 a HRTEM images of DWCNT continuously filled with PbI2. The inset Fourier transformation indicates that this crystal is being viewed in a [1 2 1] projection. **b** Detail from the boxed region in a. c An image produced by applying an adaptive filter followed by an inverse Fourier transformation produced from b. d The "best fit" image simulation obtained from the structural model [76]



diameter of the encapsulating capillaries increases, different preferred orientations are frequently observed.

The volume dimension available within the nanotubes thus somehow controls the crystal structure of the inserted materials. For instance, the structure and orientation of encapsulated PbI_2 crystals inside their capillaries were found to be different inside SWCNT and DWCNT with the same inner diameter [76]. In the case of SWCNT, most of the encapsulated one-dimensional PbI_2 crystals obtained exhibit a strong preferred orientation with their (110) plans, which make an angle of ca. 60° with the SWCNT axis as shown in Fig. 18a-b.

Due to the extremely small diameter of the nanotube capillaries, individual crystallites are often only a few polyhedral layers thick, as outlined in Fig. 18d–h. As a result of lattice terminations enforced by capillary confinement, the edging polyhedral must be of reduced coordination, as indicated in Fig. 18g–h.

Conclusion

To summarize, the melting method is the second preferred method to fill nanotubes because of the possibilities for high filling yields, simplicity (one to three steps,

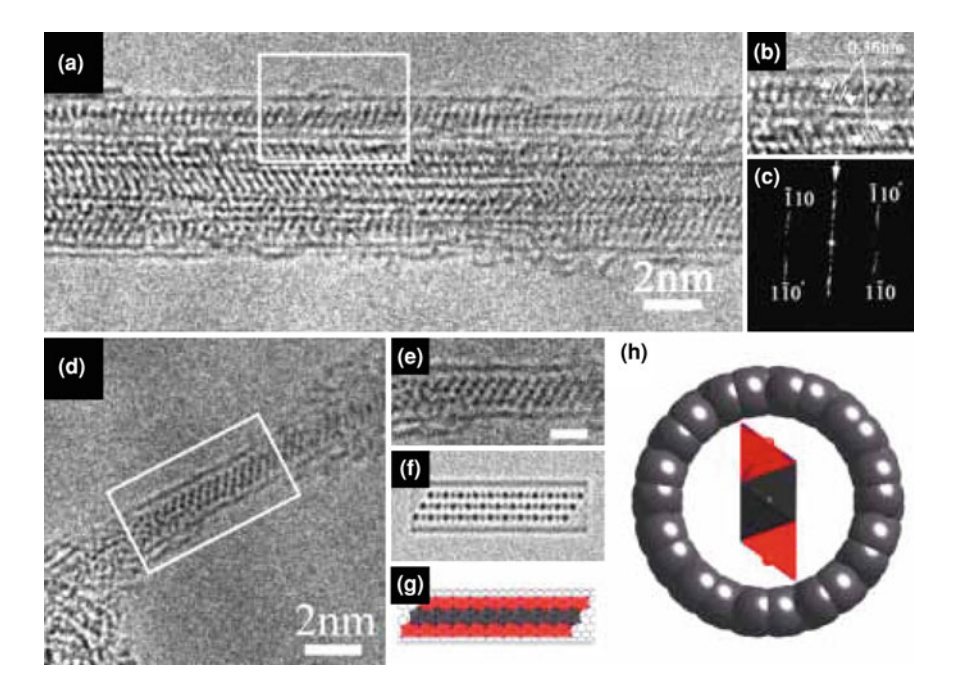


Fig. 18 (a) HRTEM image of a SWCNT bundle completely filled with PbI2. (b) Detail obtained from the boxed region in (a); 0.36 nm (or {110}) lattice planes of PbI2 are clearly visible in two adjacent tubules on the periphery of the bundle. (c) FFT obtained from a slightly larger region of bundle than (h). The indicated maxima correspond to lattice planes apparently related by a mirror plane (however, the planes occur in adjacent tubules). (d) HRTEM image of a discrete SWCNT filled with a 1D crystal of PbI2. (e) Detail from the boxed region in (d) showing the arrangement of the PbI2 polyedra, which appear as dark spots. (f) and (g) "last fit" image simulation and corresponding structural model conforming to a three polyhedral thick shah of PbI2. Edge terminating PbI5 squire pyramids are indicated in red. (h) End on view of SWCNT/PhI2 composite showing a1D chain of PbI6 octahedra bounded by two 1D chains of reduced coordination PbI5 squire pyramids [76]

depending on the goal and the material to fill) and versatility. Its main limitation is its requirement for selecting the materials to fill (or their compounds) among those exhibiting an acceptable surface tension in the molten state at the filling temperature.

4 About the Washing of Filled CNT

One of the most difficult parts of the filling is the washing of the tubes after filling. During the washing, a risk exists of emptying the already filled cavities. Usually, after filling in solution, the tubes can be washed as a wet material just after the filling process but many authors report that the percentage of the filling compound removed from inside the CNT is quite big [36, 41, 47]. There are some methods to

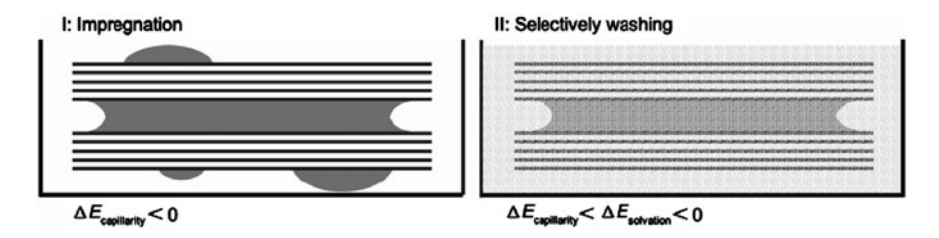


Fig. 19 Illustration of selective filling of carbon nanotubes with metals: filling of carbon nanotubes via impregnation (I) and selective washing (II) [43]

avoid this problem: for example drying the resulting mixture of X@CNT and then washing it [35] or washing the tubes after calcination [41]. In the case of filling with melted compounds, the risk of removing the filling material from inside the cavities is lower, but the problem could be the material which remains outside the tubes as a wall surface coating or as individual nanoparticles [56]. In either case, a certain amount of material will be left on the external walls of the CNT.

Green and co-workers [33] found that washing with water of CNT filled by aqueous solution of inorganic compounds may remove almost all materials from inside and outside the tubes.

In order to clean the outside walls and to keep a maximal filling, a simple strategy was suggested [43]. MWCNT were pre-opened in boiling nitric acid and then impregnated in aqueous nitrate solutions of iron, cobalt or nickel. A mixture of chloroform and 1-propanol was chosen as washing agent which can be efficient in removing the material sticking on the external walls, but also keeping the filling product in the internal cavity (Fig. 19). Such a mixture enables miscibility between the impregnation solution and the washing agent.

5 General Conclusion

The filling of CNT represents a remarkable example of matter manipulation at the nanometric scale. The experiments described here clearly give examples of the capacities and potential for nanofabrication of novel materials. Though filling is possible in situ during the synthesis of the CNT, a posteriori methods allow a better control. Whatever the method, the real filling yield is generally difficult to evaluate. The confinement of the matter inside CNT leads to more or less significant structural modifications, depending on both the bulk structure of the confined material and the CNT inner diameter. These modifications generally occur mainly perpendicularly to the axis of the CNT, where the influence of the interaction with the CNT inner wall is more pronounced. These structural changes are likely to lead to a modification of most of the physical properties (electrical, optical, mechanical, thermal) of the X@CNT composites, because of the strong interaction between the 1D nanocrystals and the CNT.

62 P. Lukanov et al.

References

- 1. Iijima, S.: Helical microtubules of graphite carbon. Nature **354**, 56–58 (1991)
- Smith, B.W., Monthioux, M., Luzzi, D.E.: Encapsulated C₆₀ in carbon nanotubes. Nature 296, 323–325 (1998)
- 3. Wang, Z., Zhao, Z., Qiu, J.: In situ synthesis of super-long Cu nanowires inside carbon nanotubes with coal as carbon source. Carbon 44, 1845–1869 (2006)
- Geng, F., Cong, H.: Fe-filled carbon nanotube array with high coercivity. Physica B 382, 300–304 (2006)
- Costa, S., Borowiak-Palen, E., Bachmatiuk, A., et al.: Filling of CNT for bio-applications. Phys. Status Solidi (B) 244, 4315–4318 (2007)
- 6. Liu, Z.J., Che, R., Xu, Z., et al.: Preparation of Fe-filled carbon nanotubes by catalytic decomposition of cyclohexane. Synth. Met. 128, 191–195 (2001)
- Schnitzler, M.C., Oliveira, M., Ugarte, D., et al.: One-step route to iron oxide-filled carbon nanotubes and bucky-onions based on the pyrolysis of organometallic precursors. Chem. Phys. Lett. 381, 541–548 (2003)
- 8. Costa, S., Borowiak-Palen, E., Bachmatiuk, A., et al.: Iron filled carbon nanostructures from different precursors. Energy Convers. Manag. **49**, 2483–2486 (2008)
- Kataura, H., Maniwa, Y., Kodama, T., et al.: High yield fullerene encapsulation in singlewall carbon nanotubes. Synth. Met. 121, 1195–1199 (2001)
- Brown, G., Bailey, S.R., Sloan, J.J., et al.: Electron beam induced in situ clusterisation of 1D ZrCl₄ chains within single-walled carbon nanotubes. Chem. Commun. 845–846 (2001)
- Pederson, M.R., Broughton, J.Q.: Nanocapillarity in fullerene tubules. Phys. Rev. Lett. 69, 2689–2692 (1992)
- 12. Ajayan, P.M., Iijima, S.: Capillarity-induced filling of carbon nanotubes. Nature **361**, 333–334 (1993)
- 13. Ebbesen, T.W.: Wetting, filling and decoration of carbon nanotubes. J. Phys. Chem. Solids 57, 951–955 (1996)
- Dujardin, E., Ebbesen, T.W., Krishnan, A., et al.: Wetting of single carbon nanotubes. Adv. Mater. 10, 1472–1475 (1998)
- 15. Monthioux, M., Flahaut, E., Cleuziou, J.P.: Hybrid carbon nanotubes: strategy, progress and perspectives. J. Mater. Res. 21, 2774–2793 (2006)
- Ugarte, D., Chatelain, A., Heer, W.A.: Nanocapillarity and chemistry in carbon nanotubes. Science 274, 1897–1899 (1996)
- 17. Dujardin, E., Ebbesen, T.W., Hiura, H., et al.: Capillarity and wetting of carbon nanotubes. Science **265**, 1850–1852 (1994)
- 18. Xu, C., Sloan, J., Brown, G., et al.: 1D lanthanide halide crystals inserted into single-walled carbon nanotubes. Chem. Commun. 2427–2428 (2000)
- 19. Bishop, C.L., Wilson, M.: The mechanism for filling carbon nanotubes with molten salts: carbon nanotubes as energy landscape filters. J. Phys. Condens. Matter. **21**, 1–7 (2009)
- Cook, J., Sloan, J.J., Green, M.L.H.: Opening and filling carbon nanotubes. Fuller. Sci. Technol. 5, 695–704 (1997)
- Chen, Y.K., Chu, A., Cook, J., et al.: Synthesis of carbon nanotubes containing metal oxides and metals of the d-block and f-block transition metals and related studies. J. Mater. Chem. 7, 545–549 (1997)
- 22. Tsang, S.C., Chen, Y.K., Harris, P.J.F., et al.: A sample chemical method of opening and filling carbon nanotubes. Nature **372**, 159–161 (1994)
- Zhao, I., Gao, L.: Filling of multi-walled carbon nanotubes with tin (IV) oxide. Carbon 42, 3251–3272 (2004)
- 24. Wu, S.W., Guo, J.X., Li, Y.L., et al.: The study of the filling behaviour carbon nanotubes using the radioactive-trace technique. Nanotechnology **14**, 1203–1207 (2003)

- Pham-Huu, C., Keller, N., Estournes, C.: Microstructural investigation and magnetic properties of CoFe₂O₄ nanowires synthesized inside carbon nanotubes. Phys. Chem. Commun. 5, 3716–3723 (2003)
- 26. Borowiak-Palen, E., Mendoza, E., Bachmatiuk, A., et al.: Iron filled single-wall carbon nanotubes—a novel ferromagnetic medium. Chem. Phys. Lett. **421**, 129–133 (2006)
- Borowiak-Palen, E., Ruemmeli, M.H., Gemming, T., et al.: Silver filled single-wall carbon nanotubes—synthesis, structural and electronic properties. Nanotechnology 17, 2415–2419 (2006)
- Jorge, J., Flahaut, E., Gonzalez-Jimenez, F., et al.: Preparation and characterization of a Fe nanowires located inside double wall carbon nanotubes. Chem. Phys. Lett. 457, 347–351 (2008)
- 29. Zhao, D.L., Li, X., Shen, Z.M.: Preparation and electromagnetic and microwave absorbing properties of Fe-filled carbon nanotubes. J. Alloys Compd. **471**, 457–460 (2009)
- 30. Hang, B.T., Hayashi, H., Yoon, S.H.: Fe₂O₃-filled carbon nanotubes as a negative electrode for a Fe-air battery. J. Power Sour. **178**, 393–401 (2008)
- 31. Seifu, D., Hijji, Y., Hirsch, G.: Chemical method of filling carbon nanotubes with magnetic material. J. Magn. Magn. Mater. **320**, 312–315 (2008)
- 32. Jain, D., Wilhelm, R.: An easy way to produce α -iron filled multiwalled carbon nanotubes. Carbon 45, 602–606 (2007)
- 33. Sloan, J.J., Hammer, J., Sibley, M.Z., et al.: The opening and filling of single walled carbon nanotubes (SWTs). Chem. Commun. 347–348 (1998)
- 34. Gao, H., Kong, Y., Cui, D.: Spontaneous insertion of DNA oligonucleotides into carbon nanotubes. Nano Lett. 3, 471–473 (2003)
- 35. Chen, G., Qiua, J., Qiu, H.: Filling double-walled carbon nanotubes with AgCl nanowires. Sci. Mater. **58**, 457–460 (2008)
- 36. Lago, R.M., Tsang, S.C., Lu, K.L., et al.: Filling carbon nanotubes with small palladium metal crystallites: the effect of surface acid groups. J. Chem. Soc., Chem. Commun. 1355–1356 (1995)
- 37. Satishkumar, B.C., Govindaraj, A., Mofokeng, J., et al.: Novel experiments with carbon nanotubes: opening, filling, closing and functionalizing nanotubes. J. Phys. B **29**, 4925–4934 (1996)
- 38. Flahaut, E., Peigney, A., Laurent, C., et al.: Gram-scale CCVD synthesis of double-walled carbon nanotubes. J. Mater. Chem. 10, 249–252 (2000)
- 39. Corio, P., Santos, A.P., Santos, P.S.: Characterisation of single walled carbon nanotubes filled with silver and with chromium compounds. Chem. Phys. Lett. **383**, 475–480 (2004)
- 40. Chu, A., Cook, J., Heesom, J.R., et al.: Filling of carbon nanotubes with silver, gold, and gold chloride. Chem. Mater. **8**, 2751–2754 (1996)
- 41. Sloan, J.J., Cook, J., Heesom, J.R., et al.: The encapsulation and in situ rearrangement of polycrystalline SnO inside carbon nanotubes. J. Cryst. Growth 173, 81–87 (1997)
- 42. Wu, H.Q., Wei, X.W., Shao, M.W., et al.: Synthesis of copper oxide nanoparticles using carbon nanotubes as templates. Chem. Phys. Lett. **364**, 152–156 (2002)
- 43. Qiang, F., Weinberg, G., Dang-Sheng, S.: Selective filling of carbon nanotubes with metals by selective washing. New Carbon Mater. 23, 17–22 (2008)
- Tsang, S., Davis, J.J., Green, M.L.H., et al.: Immobilization of small proteins in carbon nanotubes: high-resolution Transmission electron microscopy study and catalytic activity. J. Chem. Soc., Chem. Commun. 17, 1803–1804 (1995)
- 45. Davis, J.J., Green, M.L.H., Hill, H.A.O., et al.: The immobilization of proteins in carbon nanotubes. Inorg. Chim. Acta 272, 261–266 (1998)
- 46. Qu, S., Huang, F., Chen, G., et al.: Magnetic assembled electrochemical platform using Fe₂O₃ filled carbon nanotubes and enzyme. Electrochem. Commun. **9**, 2812–2816 (2007)
- 47. Borowiak-Palen, E., Bachmatiuk, A., Rümmeli, M.H., et al.: Iron filled single walled carbon nanotubes—synthesis and characteristic properties. Phys. Status Solidi (B) **243**, 3277–3280 (2006)

P. Lukanov et al.

48. Shao, L., Tobias, G., Huh, Y., et al.: Reversible filling of single walled carbon nanotubes opened by alkali hydroxides. Carbon 44, 2849–2863 (2006)

- 49. Seraphin, S., Zhou, D., Jiao, J., et al.: Yttrium carbide in nanotubes. Nature 362, 503-505 (1993)
- 50. Ajayan, P.M., Ebbesen, T.W., Ichihashi, T., et al.: Opening carbon nanotubes with oxygen and implications for filling. Nature **362**, 522–525 (1993)
- Saito, Y., Yoshikawa, T.: Bamboo-shaped carbon tube filled partially with nickel. J. Cryst. Growth 134, 154–156 (1993)
- 52. Iijima, S., Ichihashi, T.: Single-shell carbon nanotubes of 1-nm diameter. Nature 363, 603–605 (1993)
- 53. Bethune, D.S., Kiang, C.H., De Vries, M.S., et al.: Cobalt catalysed growth of carbon nanotubes with single-atomic-layer walls. Nature **363**, 605–607 (1993)
- 54. Sloan, J.J., Kirkland, A.I., Hutchison, J.L., et al.: Integral atomic layer architectures of 1D crystals inserted into single walled carbon nanotubes. Chem. Commun. 1319–1320 (2002)
- Sloan, J.J., Kirkland, A.I., Hutchison, J.L., et al.: Aspects of crystal growth within carbon nanotubes. C. R. Phys. 4, 1063–1074 (2003)
- Ballesteros, B., Tobias, G., Ward, M.A.H., et al.: Quantitative assessment of the amount of material encapsulated in filled carbon nanotubes. J. Phys. Chem. C 113, 2653–2661 (2009)
- 57. Kitaura, R., Ogawa, D., Kobayashi, K., et al.: High yield synthesis and characterization of the structural and magnetic properties of crystalline ErCl₃ nanowires in single-walled carbon nanotube templates. Nano Res. 1, 152–156 (2008)
- 58. Chikkannanavar, S.B., Taubert, A., Luzzi, D.E.: Filling single wall carbon nanotubes with metal chloride and metal nanowires and imaging with scanning transmission electron microscopy. Mater. Res. Soc. Symp. Proc. **706**, Z6.23.1–Z6.23.9 (2002)
- Tîlmaciu, C.M., Soula, B., Galibert, A.M., et al.: Synthesis of superparamagnetic iron(III) oxide nanowires in double-walled carbon nanotubes. Chem. Commun. (2009). doi: 10.1039/b909035e
- Hulman, M., Kuzmany, H., Costa, P.M.F.J., et al.: Light-induced instability of PbO-filled single wall carbon nanotubes. Appl. Phys. Lett. 85, 2068–2073 (2004)
- 61. Costa, M.F.J., Thamavaranukup, N., Rutherford, T., et al.: Structural and morphological variations of encapsulated metal oxides in single walled carbon nanotubes. Mater. Res. Soc. **901E**, 45.1–45.8 (2006)
- 62. Flahaut, E., Sloan, J.J., Friedrichs, S., et al.: Crystallization of 2H and 4H PbI₂ in carbon nanotubes of varying diameters and morphologies. Chem. Mater. **18**(8), 2059–2069 (2006)
- 63. Li, X., Yuan, G., Brown, A., et al.: The removal of encapsulated catalyst particles from carbon nanotubes using molten salts. Carbon 44, 1699–1705 (2006)
- 64. Friedrichs, S., Meyer, R.R., Sloan, J., et al.: Complete characterization of a Sb₂O₃/(21, 8)SWCNT inclusion composite. Chem. Commun. 929–930 (2001)
- Friedrichs, S., Sloan, J.J., Green, M.L.H., et al.: Simultaneous determination of inclusion crystallography and nanotube conformation for a Sb₂O₃/single-walled nanotube composite. Phys. Rev. B 64, 045406–045418 (2001)
- Costa, P.M.F.J., Sloan, J., Rutherford, T., et al.: Encapsulation of Re_xO_y clusters within single-walled carbon nanotubes and their in tubulo reduction and sintering to Re metal. Chem. Mater. 17, 6579–6582 (2005)
- 67. Govindaraj, A., Satishkumar, B.C., Nath, M., et al.: Metal nanowires and intercalated metal layers in single-walled carbon nanotube bundles. Chem. Mater. 12, 202–205 (2000)
- 68. Borowiak-Palen, E., Rummeli, M.H., Mendoza, E., et al.: Silver intercalated carbon nanotubes. In: Kuzmany, H., Fink, J., Mehring, M., Roth, S. (eds.) Electronic Properties of Novel Nanostructures. American Institute of Physics Proceedings Series, vol. 786, pp. 236–238
- 69. Kiang, C.H., Choi, J.S., Tran, T.T.: Molecular nanowires of 1 nm diameter from capillary filling of single walled carbon nanotubes. J. Phys. Chem. B **103**, 7449–7451 (1999)

- Thamavaranukup, N., Höppe, H.A., Ruiz-Gonzalez, L., et al.: Single-walled carbon nanotubes filled with M OH (M = K, Cs) and then washed and refilled with clusters and molecules. Chem. Commun. 1686–1689 (2004)
- Lamprecht, C., Danzberger, J., Lukanov, P., et al.: AFM imaging of functionalized doublewalled carbon nanotubes. Ultramicroscopy 109, 899–907 (2009)
- 72. Heister, E., Neves, V., Tîlmaciu, C., et al.: Triple functionalisation of single-walled carbon nanotubes with doxorubicin, a monoclonal antibody, and a fluorescent marker for targeted cancer therapy. Carbon 47, 2152–2161 (2009)
- 73. Klingeler, R., Hampel, S., Büchner, B.: Carbon nanotubes based biomedical agents for heating, temperature sensoring and drug delivery. Int. J. Hyperth. 24, 496–508 (2009)
- Loiseau, A., Launois, P., Petit, P.: Understanding carbon nanotubes. In: Béguin, F., et al. (eds.) Surface Properties, Porosity and Electrochemical Applications, pp. 528–529. Springer, Berlin (2006)
- 75. Sloan, J., Novotny, M.C., Bailey, S.R., et al.: Two layer 4:4 co-ordinated KI crystals grown within single walled carbon nanotubes. Chem. Phys. Lett. **329**, 61–65 (2000)
- 76. Flahaut, E., Sloan, J., Coleman, K.S.: 1D p-block halide crystals confined into single walled carbon nanotubes. Proc. Mater. Res. Soc. Symp. **633**, A13.15.1–A13.15.6 (2001)

Filling of Carbon Nanotubes: Containers for Magnetic Probes and Drug Delivery

E. Borowiak-Palen, C. Tripisciano, M. Rümmeli, S. Costa, X. Chen and R. J. Kalenczuk

Abstract Nanotechnology is a broad scientific field but one of the most explored materials in nanotechnology is carbon nanotube (CNT). A large proportion of research on CNTs is focused on their huge potential for biomedical applications. Within this context, the synthesis of carbon nanotubes filled with magnetic materials has been widely investigated, especially with iron due to its excellent ferromagnetic characteristics. Pure iron-filled carbon nanotubes (Fe-CNT) can be prepared following diverse routes. Here, an overview of the different preparation routes of Fe-CNT, using the chemical vapour deposition (CVD) synthesis method will be presented. Several working parameters were varied and investigated, the most significant being the pressure of the system, the iron and the carbon sources. The consequence of these modifications is reflected in the structure of the final material, which varies in respect of the amount of iron encapsulated in the cavity, tube diameter and the number of graphitic walls forming the CNT. The filling of hollow CNT through wet chemistry reactions (as a post-synthesis route) and CVD process (filling during the synthesis of CNTs) will also be addressed in this chapter.

E. Borowiak-Palen (🖾), C. Tripisciano (🖾), M. Rümmeli, S. Costa,

X.Chen and R. J. Kalenczuk

Centre of Knowledge Based Nanomaterials and Technologies,

Institute of Chemical and Environment Engineering,

West Pomeranian University of Technology, Szczecin, ul. Pulaskiego 10,

^{70-322,} Szczecin, Poland e-mail: eborowiak@zut.edu.pl

C. Tripisciano

e-mail: ctripisciano@zut.edu.pl

1 Iron Filled Carbon Nanotubes: An Overview of the Synthesis Techniques

Iron Filled Multiwalled Carbon Nanotubes (Fe-MWCNT)

The insertion of ferromagnetic compounds into the interior of carbon nanotubes gives rise to a system with unique magnetic properties. Moreover, the rolled-up graphene sheet can provide an effective barrier against oxidation, protecting the filler and ensuring the long-term stability of the core. Several investigations have been reported recently on the preparation of iron filled carbon nanotubes (Fe-CNT). Chemical vapour deposition is probably the most popular technique to synthesise such materials. The various production routes can be divided into two main categories: synthesis and simultaneous filling of the nanotubes (in situ process), where the nanotubes are grown already filled with iron [31], or a two-step process which involves the preliminary production of the hollow CNT which are then filled by chemical methods [43]. By varying the working conditions of a particular method, the properties of the resulting material can de controlled, such as the nanotube dimensions—diameter, number of walls, length and the quantity of filling—which can either be partial or total inside the nanotube cavity, as shown in Fig. 1.

Currently, many researchers are focusing their attention on the preparation of iron filled carbon nanotubes [9,31, 43]. So far, both singlewalled (SWCNT) and multiwalled carbon nanotubes (MWCNT) filled with iron have been prepared.

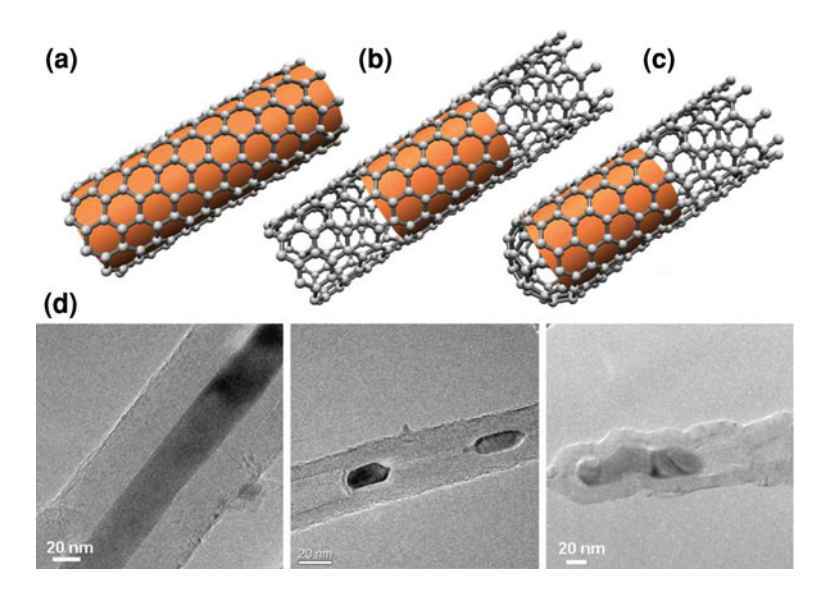


Fig. 1 Models of different iron filled carbon nanotubes: a totally filled [38], b partially filled [17], and c capped-tip-filled tube [28]; d real HR-TEM images of the different types of Fe-MWCNT

However, Fe filled MWCNT are, by far, the most often produced. The small cavity space difficulties encountered with SWCNT are generally overcome in the case of multiwalled carbon nanotubes. Even though filling mechanisms are similar to that for SWCNT, tube diameters of at least several nanometres facilitate the successful filling of MWCNT by magnetic materials.

Simultaneous Filling During the Synthesis

One of the advantages in the in-situ filling of CNT is the reduction in production time. Moreover, it enables a variation of several parameters during the process leading to the production of materials with different properties and characteristics. A diverse set of CVD experimental setups—such as doubled staged furnaces, injection assisted catalysts and liquid sources methods [8, 18, 33, 36, 45] can be used to obtain iron filled multiwalled carbon nanotubes (Fe-MWCNT).

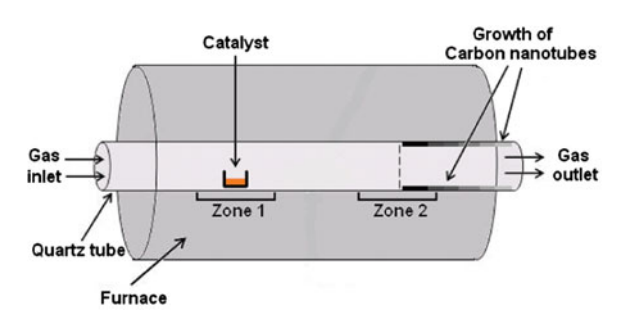
The so-called double staged systems consist of a furnace with two separate stages and each can be heated at different temperature (see Fig. 2). This type of system is commonly used for the combined synthesis and metal filling of MWCNT. In the first stage of the system the catalytic vaporisation of the metallic precursor occurs as it is heated to its sublimation point (lower temperature stage). The metallic particles are then carried to the second stage of the furnace by a carrier gas (Ar, He, N₂, either individually or in mixtures). The growth of the carbon nanotubes takes place in the second stage of the furnace where the carbon source is decomposed (higher temperature stage).

Costa et al. [9] employed ferrocene [bis(cyclopentadienyl)iron] as a catalyst and iron precursor in a double staged furnace to obtain Fe-MWCNT with high filling rate ($\sim 90\%$ of tubes were partially filled with iron) with only a single phase of iron, namely α -iron.

Mueller and his group have also often reported studies on the growth of Fe-MWCNT using a similar system. However, the growth occurs over substrates with different thin film coatings, leading to vertically aligned carbon nanotubes [37].

An alternative mode to introduce the catalyst is through an injection system attached to the CVD setup. The source of iron (e.g. ferrocene or acetyloferrocene)

Fig. 2 Illustration of a double staged furnace for the synthesis of Fe-MWCNT [31, 42]



70 E. Borowiak-Palen et al.

Fig. 3 Illustration of chemical injection CVD for the preparation of Fe-MWCNT [36]

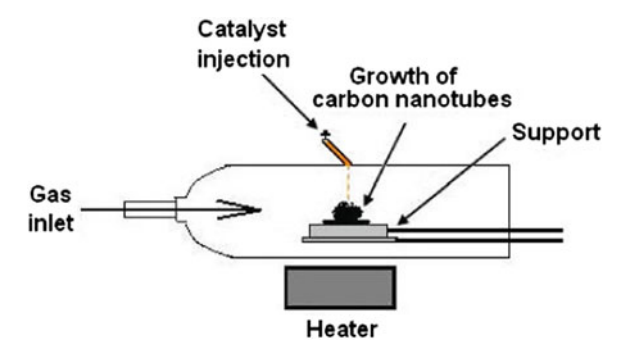
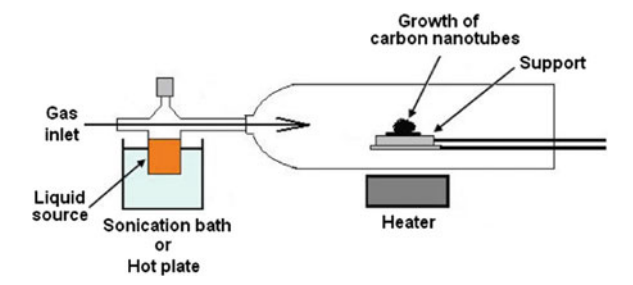


Fig. 4 Illustration of liquid source CVD system



is dissolved in a carbon feedstock and the mixture is injected directly into the high temperature zone of the furnace. This procedure enables control of the length of the carbon nanotubes to some degree, since the reaction can be finished at any time by stopping the injection of the sources [17]. The most widely reported catalyst/iron source is ferrocene due to its high solubility in different organic solvents such as xylene [17], dichlorobenzene [52] or toluene [45]. These solutions are commonly introduced to the reactor via an injector system. Figure 3 shows an illustration of the catalyst injection CVD system.

This method is simple and is a low cost means for the synthesis of CNT arrays, with Fe filling the inner cavity quasicontinuously over the entire length of the tubes [17]. The injection CVD method allows great control of the catalyst to carbon ratio. The nanotube diameter, length and alignment can be controlled by varying the reaction parameters [45].

Another possible route to synthesise Fe-MWCNT is to connect the furnace with a liquid source. This arrangement can provide both the iron and the carbon source, or just be the carbon feedstock with the catalyst placed in the centre of the furnace. A simple way to perform this experiment is to connect the liquid source directly to the furnace (see Fig. 4). In this method liquid is introduced into the furnace by a carrier gas, not by injection [33]. Costa et al., presented a systematic study on a system where the furnace was connected to a bottle containing the carbon source in the liquid form (ethanol or cyclohexane) [8]. A slightly different method was tested by Hampel et al. [18] where the furnace was connected with a moving band evaporator. The liquid source, ferrocene dissolved in cyclopentane, is directed to

the evaporator where evaporation of the solvent first occurs and later the ferrocene decomposes. The vapours are carried to the hot zone of the furnace by the carrier gas where the formation of Fe-MWCNT occurs.

Randomly grown and vertically aligned Fe-filled multiwalled nanotubes can be synthesised by decomposition of ferrocene in a liquid source CVD process. By varying the reaction parameters such as deposition time, reaction temperature and precursor concentration the influences on the length, diameter and filling yield of the carbon nanotubes is varied. The deposition time does not influence the sample morphology [18] contrary to the injection CVD method [17] where longer injection times lead to longer CNTs.

Alternative innovative methods have also been developed. In 2005, Lu et al. [35] investigated the use of an explosion induced method to produce iron filled carbon nanotubes and iron nanoparticles surrounded with carbon. Ferrocene dissolved in picric acid was used as both, the catalyst and carbon source. The detonation of the explosive was initiated by heating the mixture, evidenced by a pressure break inside the reaction vessel. During the explosion the temperature was calculated to be about 1,000°C, which is sufficient to promote CNT growth without any further heating.

The catalytic decomposition of ferrocene is widely used in different CVD methods. Ferrocene is an organometallic compound with the formula Fe(C₅H₅)₂. It is the prototypical metallocene, a type of organometallic chemical compound consisting of two cyclopentadienyl rings bound on opposite sides of a central metal atom (here an iron atom). Such organometallic compounds are also known as sandwich compounds. Therefore, ferrocene has one important advantage: it contains the metal (the catalyst initiating the MWCNT growth) and the carbon (the feedstock) within its structure. Müller et al. [38] showed that the operating conditions strongly influence the characteristics of the final product. The parameters, such as the deposition time and the use or not of a substrate for the nanotube growth, have a strong influence on the diameter size distribution and the quality of the products. Another important aspect was studied by Qiu et al. [39], who investigated the influence of the collection zone on the structure of the carbon materials. He showed that within the same synthesis process two different products were obtained. In the inlet area of the second stage area the product consisted of filled MWCNT, while outside this area the deposited materials were mainly composed of iron filled carbon nanocapsules (Fe-CNCap). Fe-CNCap are formed by the encapsulation of iron within a hollow graphitic cage. It does not have tubular characteristic typical for CNT.

The effect of ring substitution in the role of ferrocene as a catalyst was also investigated by Mohlala et al. [36]. This group performed a study using the injection of substituted ferrocenes dissolved in toluene. It was revealed that the substituent can affect the type of carbonaceous material formed and its diameter depends on the working conditions. The synthesis process with substituted ferrocenes leads to a mixture of carbon materials in the final product. The use of dimethylferrocene originated a combination of carbon fibers (tubular carbon structures without the hollow region), amorphous carbon and carbon nanotubes.

72 E. Borowiak-Palen et al.

Diethylferrocene leads to the formation of carbon nanocapsules (also termed microspheres) and acetylferrocene to a mixture of carbon nanofibers and carbon nanocapsules.

The choice of the carbon source also plays an important role in the preparation of carbon nanotubes. The group of Wang et al. [52] made an important modification in their method by the introduction of a chlorine-containing hydrocarbon. It was found that employing dichlorobenzene as the carbon source, together with a mixed Ar/H2 atmosphere leads to the reduction of the number of walls and consequently to thinner carbon nanotubes. It was found that the introduction of chlorine can slow down the growth rate of CNTs and consequently enhance the iron filling rate. Another interesting observation was obtained by Geng et al. [17]. It was found that the use of excessive catalyst injection leads not only to longer iron filled carbon nanotubes, but also causes changes in the direction of growth within the same tube.

Another important fact that should be highlighted is that very often the resulting as-grown material contains a mixture of iron filled carbon nanotubes and iron filled carbon nanocapsules [36]. By varying the synthesis parameters only Fe-CNCap or only Fe-CNT can be formed. A simple explanation of this phenomenon is the lack of the carbon supply during the growth of the carbon nanostructures, thus encapsulates are preferentially formed [42]. Lu et al. [35], obtained different mixtures of Fe-CNT and Fe-CNCap, while testing different ratios of the catalyst to support. Costa et al. [10], used acetylferrocene as catalyst in a double staged furnace to obtain homogeneous round shaped nanostructures, fully filled with iron. Due to their particular shape and dimensions as well as their potential to be functionalized, Fe-CNCap are also attractive materials for biomedical applications.

Filling Reactions via Wet Chemistry Methods

Wet chemistry reactions applied to encapsulate materials within the cavity of the carbon nanotube take advantage of capillarity forces. When a capillary is set in contact with a wetting fluid, the fluid spontaneously penetrates inside. However, only substances with low surface tension can be introduced. A more detailed explanation of the filling mechanism via liquid routes is provided in another chapter of this book (Lukanov et al.). A requirement for wet chemistry methods is that open-ended carbon nanotubes need to be employed. The chemical opening of carbon nanotubes has been widely reported and it can be performed through chemical reactions with acids [23], NaOH [40] or other oxygen containing compounds [26].

The filling of nanotubes with ferrofluid, like magnetite (Fe_3O_4), seems to be a good method when a magnetic filling is needed. Jain and Wilhelm [25] successfully obtained magnetite filled MWCNT using a organic based ferrofluid as a starting material. Further reduction of the filled MWCNTs resulted in tubes filled

with α -iron. The group also observed a nanotube diameter influence on the filling rate. Larger inner diameters led to higher filling within the tubes. Another method for Fe-MWCNT preparation was recently developed by Seifu et al., using a metal chelating polymer, chitosan, as an intermediate [43]. The nanotubes were soaked in chitosan hydrogel containing iron nitrate. A simpler method was used by Jorge et al. [26] to fill double walled carbon nanotubes, employing a highly concentrated iron chloride solution. DWCNT with encapsulated iron nanowires were obtained after a reduction step. This latter step is important to obtain the ferromagnetic form of iron, α -Fe.

Different Methods, Different Materials

The morphology of the nanostructured material is strongly influenced by the experimental parameters which determine the yield, homogeneity of the sample, or reproducibility of the results. However, the filling of MWCNT with magnetic particles and their multiwalled structures brings a big advantage. The external walls protect the internal ones, which also maintain the chemical and physical properties of the encapsulated materials. Therefore, identifying the best route to achieve a good sample depends on the definition of a good material for a particular application.

Table 1 shows some properties of iron filled carbon nanostructures evaluated by the several authors who explored different routes to prepare these materials. Even though the publications do not always report all the parameters with respect to the dimensions of the materials, it is possible to observe a trend in the parameters. The number of walls can vary between 2 and 80 walls and their distribution is usually narrow. The carbon nanotubes are usually a few microns long and the Fe-MWCNT diameter distributions can mostly be divided into two categories: small tubes with diameters up to 50 nm, and larger tubes with diameters above 100 nm.

The iron nanowires inside nanotube usually have a diameter matching the inner diameter of the tubes, and the Fe length varies and can reach even the length of the entire carbon nanotube. However, it is known that the dimensions of the nanotubes are easily influenced by the parameters of the synthesis setup. In 2006 Hampel et al. [18], published a study reporting the influence of the catalyst concentration, reaction time and temperature on the properties of the nanotubes. It was found that the length, diameter and the magnetic properties of such materials were highly dependent on these parameters.

Recently, Costa and Borowiak-Palen also reported a systematic study on the optimisation of the Fe-MWCNT preparation, for homogeneous and reproducible material. Parameters such as the catalyst ratio, reaction temperature, and hydrocarbon were tested in different combinations [8]. Both reports highlight the strong influence of the synthesis setup and experimental conditions on the resultant materials.

74 E. Borowiak-Palen et al.

Table 1 Properties of iron filled carbon materials obtained by different groups

Authors	Number of walls	Diameter (nm)		Length (µm)	
		Carbon material [#]	Iron nanoparticle	Carbon nanotubes	Iron wire
Carbon nanotu	bes#				
Costa et al.	70-80	60-120	_	_	60-360
Muller et al.	_	10-150	5-30	~15	-
Wang et el.	~15	_	~20	_	~2
Liu et al.	~23	Varies within the same tube		Up to 0.4	
Hampel et al.	_	70-110	_	_	_
-		35-60			
Costa et al.	10-45	10-55	_	_	_
Geng et al.	_	20-50	10-20	80	_
Monch et al.	5-20	20-60	5-30	0.1-1	>1
Leonhardt et al.	-	$2-60^{a}$	-	~30	-
Carbon Nanoca	apsules#				
Mohlala et al.	_	30-50 (CNT)	_	_	_
		20-25 (CNCap)		
Costa et al.	8-32	70–120	_	_	_
Sano et al.	2-40	11-30	_	_	_
Lu et al.	6-20	5-20	_	_	_
Qiu et al.	_	10-30	_	_	_
CNT + Ferroff	luid				
Seifu et al.	_	20-50		5-20	5-30
Jain et al.	_	_	8-18	_	_

Number of walls: number of walls in CNTs or capsule in CNcaps; Diameter (nm): carbon material, diameter of tubes or capsules; iron nanoparticle, diameter of wires in CNTs or spheres in CNcaps; Length refers only to the filled tubes: CNTs or iron nanowires

Conclusion I

Iron filled carbon nanotubes are materials with very promising properties. The carbon walls protect the iron cores enabling them to maintain their properties. This makes them stable and resistant magnetic structures.

Many studies have focussed on the preparation of the Fe-MWCNT, especially through the use of CVD. It is well known that the synthesis parameters strongly influence the resultant carbon nanotube morphology. Each setup requires optimization depending on the material requirements. Some of the CVD routes facilitate control, such as the length of the nanotubes, the formation or not of nanocapsules, and the amount of iron encapsulated. Even so, full control of the nanotube growth and preparation is still a work in progress. The applications of Fe-MWCNT as drug delivery systems or as local nano-heaters are attractive applications for these materials. These applications are addressed in more detail elsewhere in this book.

^a Presence of SWCNT

2 Carbon Nanotubes Biofunctionalization for Potential Biomedical Application

Summary

Cisplatin (*Cis*-Diamminedichloroplatinum, CDDP) is a compound with effective cell-killing properties. The side-effects of CDDP chemotherapeutic treatment arise due to its bonding to plasma proteins. This results in reduced renal excretion and consequent deposition in tissues. Additionally, CDDP is not stable in aqueous solution, so other solvents must be added to the solution when used for intravenous injections. A way to minimize these negative aspects is to reduce the circulation time into the human body, thus improving its efficiency. An attractive route to achieve this is to employ Carbon nanotubes as a transport vehicle. CNT potential biological application has been investigated since their discovery. They have many useful properties. To this purpose their mechanical strength, chemical inertness and above all their ability to enter a living cell by crossing the plasma membrane are particularly useful characteristics: CNT can be exploited as nano-sized containers ideally suited for filling with therapeutic drugs.

Several in vivo studies have been carried out regarding pristine CNT toxicological profile. Those studies show that CNT biocompatibility is dramatically improved when they undergo surface functionalization. This functionalization step is also essential to remove the main barrier to CNT manipulation, viz. their hydrophobicity. Here we discuss pertinent contemporary results on the encapsulation of drug molecules into both types of CNT, SWCNT and MWCNT.

Cisplatin: A Platinum Based Anticancer Drug

The harmful side effects occurring from chemotherapeutic treatment are due to the lack of selectivity of the chemotherapeutic agents. Simply put, they are powerful cell-killers without any cell-specificity, i.e. they do not distinguish between transformed cells and healthy ones.

Cisplatin is a platinum-based molecule identified for the first time in 1845 by Peyrone.

In the late 1960s its structure was clarified by X-ray analysis. In the same period, experiments conducted by B. Rosenberg on *E. Coli* and sarcoma and later in leukemia mice cells, revealed its cell-killing effect and thus paved the way to its medical application as a cancer therapy for humans [41].

The main target of cisplatin molecules inside cells is the deoxyribonucleic acid (DNA). Replication and transcription are inhibited by the platinum(II)-DNA complexes given by the inter- and intra-strand crosslinks [14, 15] formed through the covalent binding of DNA's purine basis and aquated form of CDDP.

Cisplatin can also bind proteins and these interactions can play an important role in its pharmacological and toxicological profile. For instance, the binding of cisplatin to plasma proteins can indeed induce the formation of high molecular weight complexes which can be not filtered from the Bowman capsules, thus causing the accumulation of platinum in the kidneys and consequent nephrotoxicity.

Therefore, despite cisplatin's high effectiveness, some limits must be overcome in order to improve the quality of its use. Cisplatin has a low water solubility and low stability due to the substitution of the chloride ions by water molecules. This replacement can be reduced by increasing the sodium chloride concentration thus improving the drug stability in aqueous media.

Currently, during chemotherapeutic treatment, cisplatin is administered to a patient by intravenous injection of an aqueous solution with the addition of sodium chloride (as a source of chloride ions), mannitol (as a weak renal vasodilator) and hydrochloric acid (as a pH maintainer). A way to avoid the side-effects, improving cisplatin's characteristics and avoiding the use of additional solvents, is to create delivery structures which can selectively transport the antitumor agent directly to the target cells. This is usually referred to as targeted drug delivery.

Several studies have been conducted in the last decades on the development of vectors made up of organic materials, such as liposomes structures or polymeric mycelles, so that the toxicity of cisplatin could be reduced. More recently the employment of carbon nanotubes as nano-vehicles for drugs in cancer therapy has been extensively studied. Compared to classical drug delivery systems, CNT possess an enormous aspect ratio; moreover, their stability(given by the chemical composition) ensures a prolonged circulation-time inside the body. The potential application of CNT in the bio-medical field has been investigated since their discovery. Due to their passive plasma membrane crossing, CNT can be thought as nano-sized carriers which can transport drugs to a selected region. This selectivity can be accomplished through labelling these nano-vectors with antibodies which can recognize antigens specifically expressed by the cancer cells. The cellular uptake depends on the tubes diameter and the type of functionalization: Different strategies, such as the energy-requiring endocytosis process [6-25] and the passive plasma membrane crossing [4-30], have been reported by different groups.

The possibility to use CNT as transport vehicles could increase the efficacy of cancer therapy enormously: Various strategies e.g. hyperthermia and drug delivery, could be both applied by developing a single multifunctional complex.

Hyperthermia treatment (or thermotherapy) is a cancer treatment based on the controlled and prolonged exposure of body tissues to a temperature range of 40–43°C. The effects consist of cancer cell necrosis and damage to proteins and structures of the cells [21] with minimal damage of the healthy tissue [51]. Among the effects are an increase of local blood flow and an increase of the cell membrane permeability. As a consequence hyperthermia is very often used along with other cancer therapies, such as radiation and chemotherapy [51, 53], enhancing the sensitivity of some cancer cells to radiation or the efficiency of the anti-cancer drugs by increasing the uptake from cells.

In this respect the magnetic properties of CNT can be used to localize them in a selected region and, by applying infrared radiation, rapid and effective heating can be induced. Thus, the use of CNT can improve cancer therapy not only by carrying

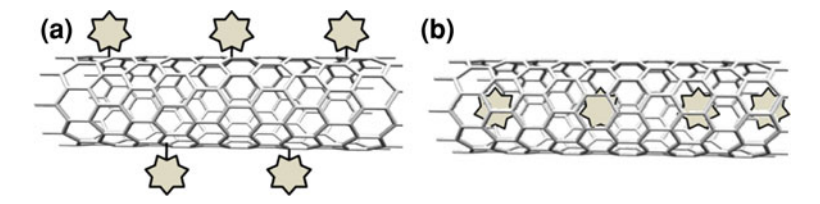


Fig. 5 Models of different carrier systems based on CNT. a The drug is loaded on the CNT external surface; b the drug molecules are inserted into CNT interior

the drug molecule selectively and preventing its undesired interaction with other proteins, but also enhancing its effect through hyperthermia [32].

Carbon Nanotubes as Nano-Sized Carriers

In order to safely employ CNT for medical applications, a large number of studies have been carried out on their potential toxic effects. In vitro [17, 29] and in vivo [11, 34] toxicological profiles of the pristine CNT have been extensively studied. They show that the CNT cytotoxicity is drastically reduced when they are surface functionalized. Several routes have been developed and analyzed to improve the solubility and biocompatibility of raw CNT.

The delivery application can be realized via loading (e.g. specific adsorption or covalent bonding) the therapeutic drug on the external surface (as reported by Feazell et al.) or placing it inside the tubes (see Fig. 5).

Feazell et al. developed a longboat delivery system where PEGylated SWCNT (Mn $\sim 2,000$) were conjugated with an inert platinum (IV) compound which was reduced to the active platinum (II) form after cell internalization. These drug carriers internalized via an endocytic pathway. The pH decrease of the cell endosomes was exploited to reduce the disulfide linkages releasing the lethal active cis-[Pt(NH₃)₂Cl₂] [16]. The study highlighted that the efficiency of the cisplatin active platinum form (II) is enhanced when carried and released from these sp² carbon derived vectors. They offer clear advantages, namely, drug inactivation or scarce circulation are avoided. In a more recent study [12] the same research group provided this longboat delivery system of a folic acid to specifically target folate receptor-enriched cancer cells. The as-produced system was evaluated to be stable at pH of 7.4 (similar to the bloodstream environment) and going through reduction with the decrement of pH value.

Another example of external CNT sidewall loading has been reported by Liu et al. [11]. Water soluble SWCNT non-covalently and covalently functionalized with PEG, were loaded with the anticancer drug Doxorubicin. Liu and co-workers found that the binding of the anticancer drug and its release are pH-dependent. Again, the pH decrease related to the endocytosis-mediated uptake mechanism is suitable for the controlled discharge within the cells of Doxorubicin, whose hydrophobic interaction with CNTs can be achieved instead with basic pH values

78 E. Borowiak-Palen et al.

(e.g. pH = 9). Moreover, the author's state that the loading depends on the tubes diameter, since the π -staking of the drug is stronger on tubes with larger diameter.

The first work in which a general method to open and fill carbon nanotubes with a variety of metal oxides using the wet chemistry was reported, was published by Tsang et al. [50] in 1994. This work paved the way for drug delivery applications with filled CNT.

Carbon nanotubes have been already used as containers for several organic molecules, such as β -Carotene [54], and fullerenes [44, 46].

The strong nanotube wall can provide the organic molecules with convenient protection from the surrounding environment [5, 47], since one of the disadvantages of some anticancer drugs (such as Cisplatin) includes instability or light sensitivity.

The inclusion of Cisplatin has already been explored in single-wall carbon nanohorns (SWCNH) which are graphitic nano-structures with cone shaped tips, typically forming spherical aggregates [1–3]. In these in vitro studies, the anticancer drug was found to maintain its cell-killing potentials, viz. the deactivation was prevented. The release analysis, evaluated in phosphate buffered saline solution (PBS), suggested that saturation of the solution with CDDP was reached after 50 h with 80% of discharge of the drug having been encapsulated in the SWCNH. Moreover, the works carefully analyzed the plug effects of oxygencontaining functional groups at edges, and a route to optimize the pore size in

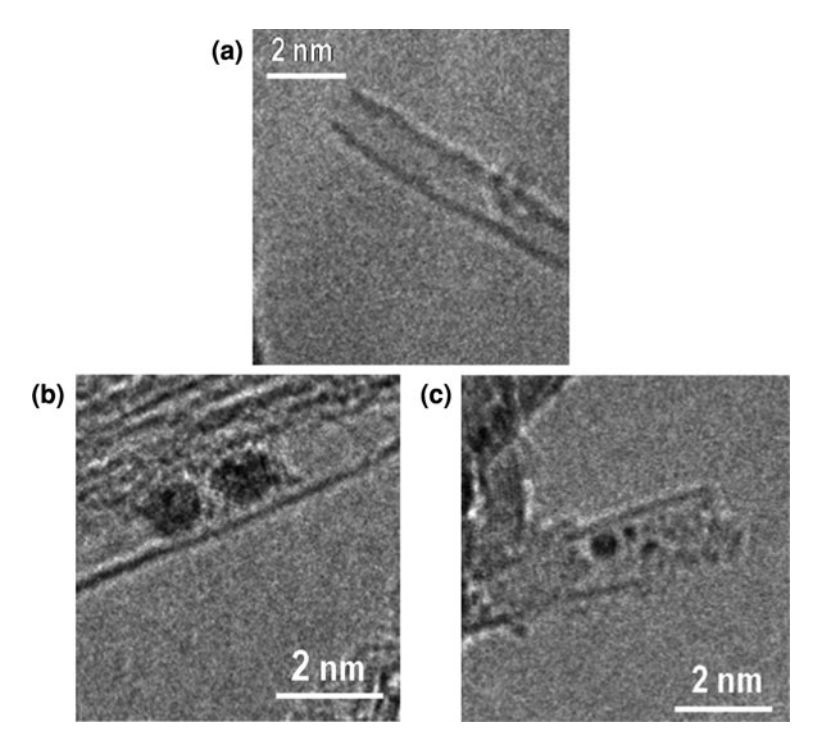


Fig. 6 TEM images of empty (a) and cisplatin filled SWCNTs (b, c)

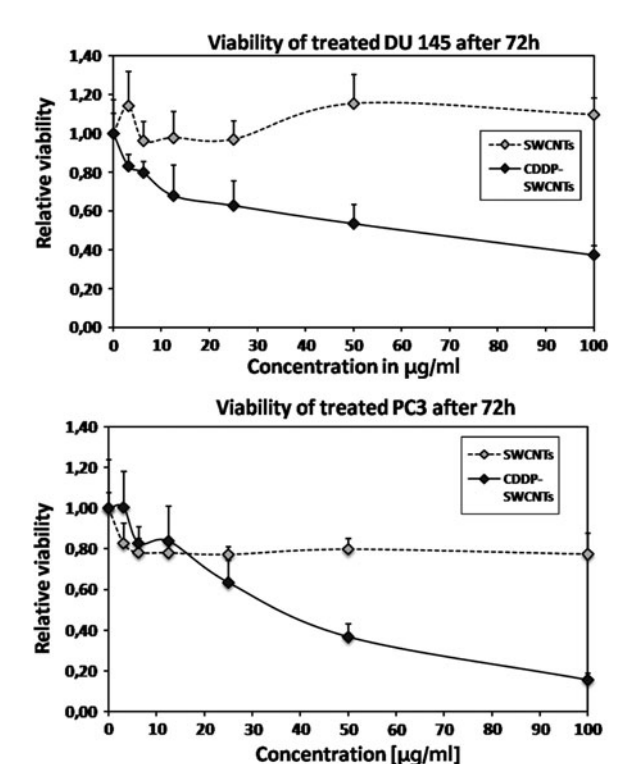
order to reduce the effect of the sodium attachment to the hole-edges moieties was presented.

Recently Tripisciano et al. presented a study of CDDP encapsulation into moieties-free SWCNT. In a previous work, the interaction between the anticancer drug molecules and the outer shell functional groups was indicated to occur when the tubes are exohedrally functionalized via strong acid treatment [48]. On the contrary, CDDP can be easily encapsulated into (Fig. 6) and liberated from the tubes core when there are no functional groups on the CNT shells [49].

The initial filling yield of the CNT was estimated to be 21 wt%. The release of the CDDP was evaluated over a period of 1 week. After 72 h most of the material had been released, i.e. 68% of the CDDP was found to have been released. A CDDP-filled SWCNTs concentration-dependent decrease of cell viability was reported (Fig. 7) for two different prostate cancer call lines, PC3 and DU145, although the authors state a possible partial interaction (and probable inactivation) of the drug molecules with the tubes inner sidewall or with groups remained at the defect sites generated on it by the harsh conditions used in the purification procedure.

The encapsulation of cisplatin in CNT has been theoretically calculated by Hilder and Hill [22], in particular the estimation of the minimum radius necessary for a nanotube to accept this drug molecule and the optimal radius that a nanotube should posses to internalize the maximum quantity of it. The authors used a hybrid discrete-

Fig. 7 Relative viabilities of DU 145 (upper panel) and PC3 (lower panel) cell lines treated with different concentration of empty SWCNTs and CDDP filled SWCNTs after 72 h of incubation [49]



80 E. Borowiak-Palen et al.

continuum model to express the interaction between CDDP and SWCNTs (representing CDDP as an irregularly shaped collection of atoms and nanotubes as a continuous distribution of carbon atoms). They calculated that the minimum radius of a CNT to accept all three orientations of the drug cisplatin must be 4.785 Å (that correspond to a diameter of 0.96 nm). Considering the suction energy as the energy that the drug molecules acquire from the tubes, which take them up into their hollow cavities, the maximum suction energy occurs when the tube radius is 5.3 Å (for all the CDDP orientations) that corresponds to a tube diameter of 1.06 nm.

A second-generation platinum compound with a broad spectrum of antineoplastic properties, Carboplatin, has been incorporated into MWCNTs by Hampel et al. [19]. MWCNTs have been preferred to SWCNTs because of the larger inner diameter and the yield of filling was measured to be the 30 wt% when the filling process was carried out at the temperature of 90°C. The impact of the produced carboplatin nanocarrier was tested on bladder cancer cells, revealing the cytotoxic effect of carboplatin filled tubes unlike the empty material, which barely affected the cell viability.

The validity of a nanotube-based drug delivery system depends on the environment where the drug will be discharged. The different system proposed (external uploading or internal filling) must overcome different limits. When the drug is carried as linked on the external tube sidewall, it is directly exposed to blood components: the main problem could be either the premature inactivation of the anticancer agent by enzymes or its premature, improper action. The solution is thus to prevent its active site before the nano-vector has reached the target cells.

When the drug molecules are placed inside the nanotubes the main disadvantage can be represented by the uncontrolled, early release. The remedy could be found in the enclosure of the tube open endings. If the release takes place late enough, the nano-carrier can reach the cytoplasm of tumour cells where the drug cytotoxic effect is required without the need of additional caps.

Conclusion II

The results obtained so far highlight the real potential of employing carbon nanotubes (and their derivatives) as nano-sized drug carriers and vectors. The reversibility of the filling process has been evaluated on different cancer cell lines. The studies show the cell-killing effect is preserved when embedded within CNT. Such systems can have a positive high impact in those negative aspects found with current cancer treatments can be avoided. Additionally, the therapeutic effect itself seems to be enhanced. The studies to date confirm the exciting potential of carbon nanotubes as drug delivery systems.

References

- 1. Ajima, K., et al.: Carbon nanohorns as anticancer drug carriers. Mol. Pharm. 2, 475–480 (2005)
- Ajima, K., et al.: Optimum hole-opening condition for cisplatin incorporation in single-wall carbon nanohorns and its release. J. Phys. Chem. B 110, 5773–5778 (2006a)

- Ajima, K., et al.: Effect of functional groups at hole edges on cisplatin release from inside single-wall carbon nanohorns. J. Phys. Chem. B 110, 19097–19099 (2006b)
- 4. Bianco, A., et al.: Biomedical applications of functionalised carbon nanotubes. Chem. Commun. 5, 571–7 (2005)
- 5. Borowiak-Palen, E.: Single-walled carbon nanotubes as nanotest tubes. Physica Status Solidi B **244**(11), 4311–4314 (2007)
- 6. Chin, S.-F., et al.: Amphiphilic helical peptide enhances the uptake of single-walled carbon nanotubes by living cells. Exp. Biol. Med. **232**, 1236–1244 (2007)
- Clare, B.W., Kepert, D.L.: Opening of carbon nanotubes by addition of oxygen. Inorg. Chim. Acta 343, 1–17 (2003)
- 8. Costa, S., Borowiak-Palen, E.: Comparative study on homogeneity, filling ration and purity of iron filled multiwalled carbon nanostructures. Eur. Phys. J. B (2010). doi: 10.1140/epjb/e2010-00070-1
- Costa, S., Borowiak-Palen, E., Bachmatiuk, A., Rummeli, M., Gemming, T., Kalenczuk, R.: Filling of carbon nanotubes for bio-applications. Physica Status Solidi B 244, 4315–4318 (2007)
- Costa, S., et al.: Iron filled carbon nanostructures from different precursors. Energy Convers. Manag. 49(9), 2483–2486 (2008)
- 11. Deng, X., et al.: The splenic toxicity of water soluble multi-walled carbon nanotubes in mice. Carbon 47, 1421–1428 (2009)
- 12. Dhar, S., et al.: Targeted single-wall carbon nanotube-mediated Pt(IV) prodrug delivery using folate as a homing device. J. Am. Chem. Soc. 130, 11467–11476 (2008)
- 13. Dumortier, H., et al.: Functionalized carbon nanotubes are non-cytotoxic and preserve the functionality of primary immune cells. Nano Lett. 6, 1522–1528 (2006)
- Eastman, A.: Interstrand cross-links and sequence specificity in the reaction of cisdichloro(ethylenediamine)platinum (II) with DNA. Biochemistry 25, 5027–5032 (1986a)
- Eastman, A.: Reevaluation of interaction of cis-dichloro(ethylenediamineplatinum(II) with DNA. Biochemistry 25, 3912–3915 (1986b)
- Feazell, R.P., et al.: Soluble single-walled carbon nanotubes as longboat delivery systems for platinum(IV) anticancer drug design. J. Am. Chem. Soc. 129(27), 8438–8439 (2007)
- 17. Geng, F., Cong, H.: Fe-filled carbon nanotube array with high coercivity. Physica B Condens. Matter **382**(1–2), 300–304 (2006)
- 18. Hampel, S., et al.: Growth and characterization of filled carbon nanotubes with ferromagnetic properties. Carbon 44(11), 2316–2322 (2006)
- 19. Hampel, S., et al.: Carbon nanotubes filled with a chemotherapeutic agent: a nanocarrier mediates inhibition of tumor cell growth. Nanomedicine 3, 175–182 (2008)
- Heller, D.A., et al.: Single-walled carbon nanotube spectroscopy in live cells: towards longterm labels and optical sensors. Adv. Mater. 17, 2793–99 (2005)
- 21. Hildebrandt, B., et al.: The cellular and molecular basis of hyperthermia. Crit. Rev. Oncol. Hematol. 43, 33–56 (2002)
- 22. Hilder, T.A., et al.: Modelling the encapsulation of the anticancer drug cisplatin into carbon nanotubes. Nanotechnology **18**, 275704–275712 (2007)
- Hu, C.-C., Su, J.-H., Wen, T.-C.: Modification of multi-walled carbon nanotubes for electric double-layer capacitors: tube opening and surface functionalization. J. Phys. Chem. Solids 68(12), 2353–2362 (2007)
- 24. Iijima, S., et al.: Carbon nanotube technology. Nec Tech. J. 2(1), 52–55 (2007)
- Jain, D., Wilhelm, R.: An easy way to produce [alpha]-iron filled multiwalled carbon nanotubes. Carbon 45(3), 602–606 (2007)
- Jorge, J., et al.: Preparation and characterization of [alpha]-Fe nanowires located inside double wall carbon nanotubes. Chem. Phys. Lett. 457(4–6), 347–351 (2008)
- Kam, N.W.S., et al.: Nanotube molecular transporters: internalization of carbon nanotubeprotein conjugates into mammalian cells. J. Am. Chem. Soc. 126, 6850–6851 (2004)
- 28. Kim, H., Sigmund, W.: Iron particles in carbon nanotubes. Carbon 43(8), 1743-1748 (2005)
- Kostarelos, K., et al.: Cellular uptake of functionalized carbon nanotubes is independent of functional group and cell type. Nat. Nanotechnol. 2, 108–113 (2006a)

30. Lacerda, L., et al.: Cell penetrating CNTs for delivery of therapeutics. Nanotoday 2, 38–43 (2007)

- 31. Leonhardt, A., et al.: Synthesis and properties of filled carbon nanotubes. Diam. Relat. Mater. 12(3–7), 790–793 (2003)
- Levi-Polyachenko, N.H., et al.: Multi-walled carbon nanotubes increase the efficiency of hyperthermic chemotherapy. Nanotech 2, 57–60 (2008)
- 33. Liu, Z.-J., et al.: Preparation of Fe-filled carbon nanotubes by catalytic decomposition of cyclohexane. Synth. Met. **128**(2), 191–195 (2002)
- 34. Liu, Z., et al.: Supramolecular chemistry on water-soluble carbon nanotubes for drug loading and delivery. ACS Nano 1(1), 50–56 (2007)
- 35. Lu, Y., Zhu, Z., Liu, Z.: Carbon-encapsulated Fe nanoparticles from detonation-induced pyrolysis of ferrocene. Carbon **43**(2), 369–374 (2005)
- 36. Mohlala, M.S., Liu, X.-Y., Coville, N.J.: Synthesis of multi-walled carbon nanotubes catalyzed by substituted ferrocenes. J. Organomet. Chem. **691**(22), 4768–4772 (2006)
- Muller, C., Leonhardt, A., Kutz, A.C., Büchner, B.: Growth aspects of iron-filled carbon nanotubes obtained by catalytic chemical vapor deposition of ferrocene. J. Phys. Chem. C 113, 2736–2740 (2009)
- 38. Müller, C., et al.: Iron filled carbon nanotubes grown on substrates with thin metal layers and their magnetic properties. Carbon **44**(9), 1746–1753 (2006)
- 39. Qiu, J., et al.: CVD synthesis of coal-gas-derived carbon nanotubes and nanocapsules containing magnetic iron carbide and oxide. Carbon **44**(12), 2565–2568 (2006)
- 40. Raymundo-Piñero, E., et al.: A single step process for the simultaneous purification and opening of multiwalled carbon nanotubes. Chem. Phys. Lett. **412**(1–3), 184–189 (2005)
- Rosenberg, B.: Some biological effects of platinum compounds. Platinum Metals Rev, 15, 42-51 (1971)
- 42. Sano, N., et al.: Separated synthesis of iron-included carbon nanocapsules and nanotubes by pyrolysis of ferrocene in pure hydrogen. Carbon **41**(11), 2159–2162 (2003)
- 43. Seifu, D., et al.: Chemical method of filling carbon nanotubes with magnetic material. J. Magn. Magn. Mater. **320**(3–4), 312–315 (2008)
- 44. Simon, F., et al.: Low temperature fullerene encapsulation in single wall carbon nanotubes: synthesis of N@C60@SWCNT. Chem. Phys. Lett. **383**, 362 (2004)
- 45. Singh, C., et al.: Production of aligned carbon nanotubes by the CVD injection method. Physica B Condens. Matter **323**(1–4), 339–340 (2002)
- 46. Smith, B.W., et al.: Carbon nanotube encapsulated fullerenes: a unique class of hybrid materials. Chem. Phys. Lett. **315**, 31–36 (1999)
- 47. Takenobu, T., et al.: Stable and controlled amphoteric doping by encapsulation of organic molecules inside carbon nanotubes. Nat. Mater. 2, 683–688 (2003)
- 48. Tripisciano, C., et al.: Cisplatin functionalized single-walled carbon nanotubes. Physica Status Solidi B **245**, 1979–1982 (2008)
- 49. Tripisciano, C., et al.: Single-wall carbon nanotubes based anticancer drug delivery system. Chem. Phys. Lett. **478**, 200–205 (2009)
- 50. Tsang, S.C., et al.: A simple chemical method of opening and filling carbon nanotubes. Nature **372**(6502), 159–162 (1994)
- 51. Van der Zee, J.: Heating the patient: a promising approach? Ann. Oncol. 13, 1173–1184 (2002)
- 52. Wang, W., et al.: Synthesis of Fe-filled thin-walled carbon nanotubes with high filling ratio by using dichlorobenzene as precursor. Carbon **45**(5), 1127–1129 (2007)
- 53. Wust, P., et al.: Hyperthermia in combined treatment of cancer. Lancet Oncol. 3, 487–497 (2002)
- 54. Yanagi, K., et al.: Highly stabilized β -carotene in carbon nanotubes. Adv. Mater. **18**, 437–441 (2006)

Part II Magnetically Functionalised Carbon Nanotubes for Medical Diagnosis and Therapy

Magnetic Nanoparticles for Diagnosis and Medical Therapy

Martin Sobik, Kirsten M. Pondman, Ben Erné, Bonny Kuipers, Bennie ten Haken and Horst Rogalla

Abstract Magnetic nanoparticles (MNPs) reveal promising opportunities for biomedical applications, potentially allowing minimally invasive diagnosis and therapeutic usage at several levels of human body organization (cells, tissue and organs). An increasingly broad collection of MNPs has been recently developed not only at the research level but also in some specific cases for medical applications. Superparamagnetic iron oxide (SPIO) nanoparticles are commonly used in clinical practice as contrast agents for magnetic resonance imaging (MRI) of liver and angiography. Carbon nanotubes (CNTs) are another type of nanomaterials with great potential for biomedical applications. Filled with ferromagnetic materials, an ensemble of aligned CNTs displays a highly non-linear, anisotropic and hysteretic magnetization behaviour due to their extremely high aspect ratio (length/diameter >100). The intrinsic properties of such ferromagnetic nanoparticles can potentially improve diagnosis and therapy of numerous diseases. Combining tailored biocompatible ferromagnetic nanomaterials with dedicated detection technology can provide a new approach leading to the exciting perspective of accurate medical imaging and medical therapy (magnetic hyperthermia, targeted drug delivery, etc.) at the cellular level. Elongated Fe-filled CNTs (Fe-CNTs) are foreseen as potential nanotools leading to minimally invasive, highly sensitive, and cost effective novel investigation routes for complete human body systems.

M. Sobik (M), K. M. Pondman, B. ten Haken and H. Rogalla Low Temperature Division, MIRA, Institute for Biomedical Technology and Technical Medicine, University of Twente, P.O. Box 217, 7500 AE, Enschede, The Netherlands e-mail: M.Sobik@tnw.utwente.nl

B. Erné and B. Kuipers Van't Hoff Laboratory, Debye Institute for Nanomaterials Science, University of Utrecht, Utrecht, The Netherlands

1 Introduction

During the last two decades dedicated magnetic nanoparticles (MNPs) have been developed for application in various fields in science and engineering. Different MNPs have been developed for various purposes, for example for immunoassays, cell separations, biosensing, and protein binding studies [1]. For several clinical procedures in vivo application of MNPs is approved. The fact that the human body is almost non-magnetic is crucial for these medical applications. These particles are used in a growing number of MRI applications such as angiography and liver imaging [2-4]. MNPs have been developed with a wide range of magnetic and hydrodynamic properties. The particles are designed to be easily movable in liquids, excited magnetically or detected inside non-magnetic tissue. Nanoparticles functionalised with a wide range of bio-compatible molecules have been internalized in cells. Most of the research has been focussed on one specific type of nanoparticles called SPIO nanoparticles. Most of these SPIO particles are spherical and consist of one or multiple magnetic cores and a shell with further functionalisations designed for specific biomedical applications. These MNPs display superparamagnetic properties, which render them useful and efficient for diagnosis of diseases. SPIO nanoparticles are also foreseen as a promising tool for in vitro immunoassays [5]. Another noteworthy type of MNP is gadolinium based nanoparticles, which show paramagnetic properties and are mainly used as contrast agents [6].

In the case of in vivo diagnosis as an MRI technique, SPIO nanoparticles are used as so-called contrast agents. The contrast agent can be used to image the blood flow immediately for angiography, for example to detect stenosis. The SPIOs can also be used for diagnosis of other health-related problems. While flowing in the bloodstream of a patient, the SPIO nanoparticles are recognized by the reticuloendothelial system, and after opsonisation, internalised by macrophages. This path will eventually transport the particles to the liver and spleen [5, 7]. This way, SPIO nanoparticles are successfully used to image accurately the lymphatic system and cancerous lesions in the liver or spleen of patients. Unfortunately, this passive route restricts the use of SPIO nanoparticles to a few organs, i.e. liver and spleen and limits the time window for angiography.

Active targeting of SPIO nanoparticles as a tool for magnetic drug delivery has not been successful in the past decades [8–15]. Due to their spherical shape, SPIO nanoparticles are subject to strong drag forces when injected into the blood flow of patients, while the magnetic response of the particles to clinically applicable magnetic fields is rather low. The particles can therefore not be easily trapped by a magnetic field at a specific area in the body. The spherical shape is a main drawback of SPIO nanoparticles and these have proven their limits [16]. To increase the potential of the MNP research has focused on the development of elongated MNPs; so-called magnetic nanowires or nanorods. Among these magnetic nanorods one new and unique type of MNPs is magnetic carbon nanotubes (CNTs). CNTs are quasi one dimensional anisotropic structures of rolled sheets of

graphene, that have shown their potential in various biomedical fields [17–21]. The carbon shell can be used for functionalisations that optimise the properties of the nanoparticles for the desired biomedical applications and render them biocompatible. In magnetic CNTs the carbon shell also protects the magnetic content from the external environment. The high potential of magnetic CNTs in medicine lies in the fact that the shape, size, surface chemistry and magnetic properties can be controlled.

2 Ferromagnetic Carbon Nanotubes

In most biomedical applications, the CNTs used do not contain any magnetic content, except for a small quantity of catalyst remaining from their synthesis process. These unfilled CNTs do therefore not show significant magnetic properties but only reflect the magnetism of the remaining catalyst (unfilled Fe-cat-CNTs). The absence of natural magnetism of carbon denotes that significant magnetization can only be accomplished through hybridization with magnetic materials, e.g. Co, Fe, Ni and alloys like Fe₃Co [22]. This hybridization can be achieved by encapsulation, incorporation within the walls or depositing the material on the outer surface of the nanotubes, both during the synthesis or in a subsequent process [23–25].

Due to the extremely high aspect ratio (length/diameter >100) of CNTs, an ensemble of aligned magnetic CNTs shows a highly non-linear anisotropic and hysteretic magnetisation curve [26]. Furthermore, individual magnetic CNTs have a strong magnetic moment with a preferred direction along their axis [27]. Exactly this property makes these magnetic CNTs exceptionally interesting for novel hyperthermia treatments, local temperature sensing and drug delivery [28, 29].

Fe-Filled Carbon Nanotubes

As other proposed methods will alter the properties of the CNTs, filling the CNTs is considered the most favourable method to add magnetic properties to the particles. Filling a CNT with magnetically susceptible liquids can be achieved by opening the CNTs and subsequent filling with magnetic materials. Another method is by simultaneous growth of CNTs with the chemical vapour deposition technique and growing a metallic nanowire within the CNT, rendering so-called Fe-filled multi-walled CNTs (Fe-MWCNTs or Fe-wire-filled MWCNTs) [30, 31].

When evaluating the magnetic properties of a sample of Fe-MWCNTs many aspects have to be taken into account as they influence the magnetic properties. First the length and diameter of the inner nanowire will determine the shape of the magnetization curve. Secondly, the number of walls will influence the mechanical stresses and therefore the magnetic properties. Furthermore, the alignment of the

88 M. Sobik et al.

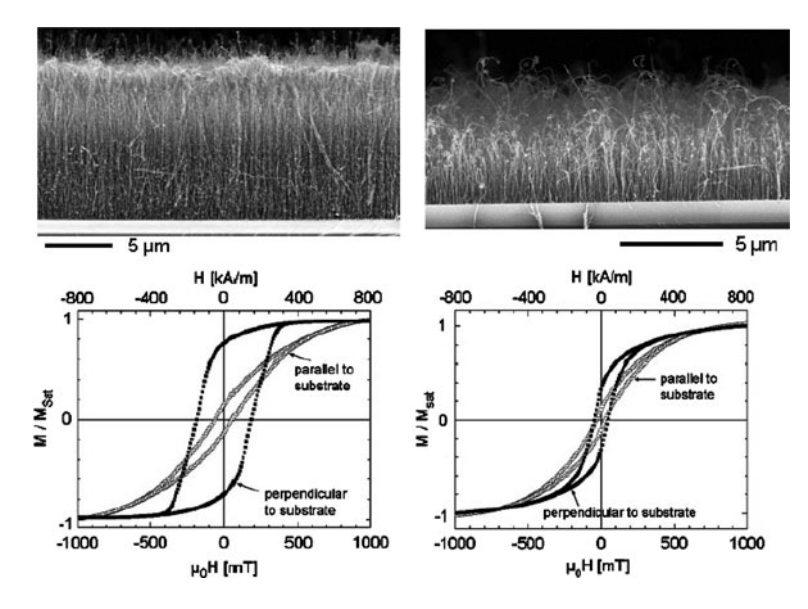


Fig. 1 Comparison of hysteresis loops of strong (left) and suboptimal (right) aligned filled CNTs at $T=300~{\rm K}$ [26]

nanotubes will have a large influence on the magnetization curve (Fig. 1) as randomly orientated nanotubes will be partly in a non-favourable orientation for magnetization.

The magnetic properties of the particles will also change when the particles are suspended in different media. The relaxation characteristics will change when particles are in suspension and able to show Brownian relaxation, or fixed in a matrix, such as frozen or in agar gel when only Néel relaxation is possible. These variations in relation to the medium are studied in our laboratory and will be discussed below. In this chapter, magnetisation characterisation of MWCNTs has been performed using a vibrating sample magnetometer (Model 10 Mark II VSM, Microsense). As for complex magnetic susceptibility a homemade set-up has been used [32].

Finally, not only the amount of filling but also the phase of the filling of the nanotube is important. For the Fe-MWCNTs mentioned in this work, the main component of the CNT filling is ferromagnetic α -Fe (bcc phase). Nevertheless, γ -Fe (fcc phase) and paramagnetic Fe₃C can also be found in insignificant proportions [31, 33, 34].

Pristine Fe-Filled Carbon Nanotubes

Prior to further studies on magnetic properties of elaborated Fe-MWCNTs based suspensions and phantoms, magnetisation of pristine Fe-MWCNTs and unfilled

Fe-cat-MWCNTs has been studied. It is noteworthy that unfilled MWCNTs have similar physical properties (average length, diameter, etc..) as Fe-MWCNTs, but they do not contain a magnetic filling with nanowires; remaining catalyst material is nevertheless present in measurable quantities (3 wt%) and causes a weak magnetisation of the unfilled Fe-cat-MWCNTs.

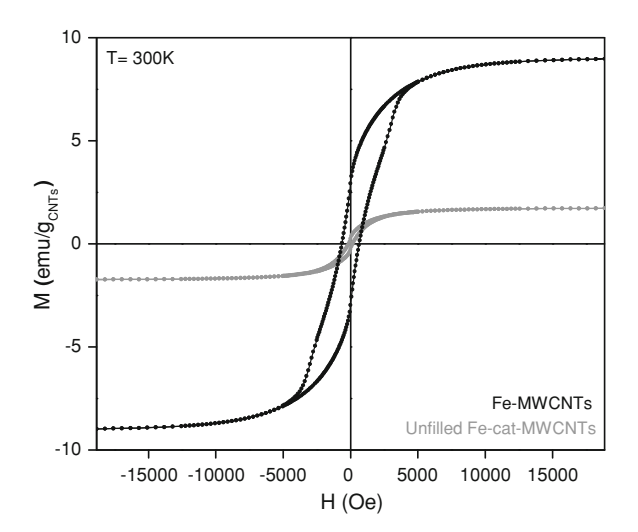
At room temperature (T = 300 K) magnetisation at saturation of pristine Fe-MWCNTs is determined to be 9 emu/g; whereas unfilled MWCNT magnetisation at saturation is a factor of 5 lower (Fig. 2). The magnetisation curve clearly indicates a ferromagnetic behaviour of pristine Fe-MWCNTs due to the highly non-linear anisotropic characteristics.

Suspensions of Fe-Filled Carbon Nanotubes

Pristine Fe-MWCNTs and unfilled MWCNTs were used as a starting material to obtain CNT suspensions. These suspensions are of great interest for the fundamental understanding of the properties and the behaviour of individually dispersed Fe-MWCNTs in biological media.

Pristine Fe-CNTs are difficult to disperse in water-based solutions. Furthermore, when brought into suspension, individual Fe-CNTs are hardly kept into stable suspensions over a significant period of time necessary to any biotechnological use. This is mainly due to the fact that individual Fe-CNTs are subject to attractive interaction (Van der Waals and magnetic dipolar forces) when they are dispersed in aqueous solutions. A way to prevent flocculation of Fe-MWCNTs is to create a repulsive (electrostatic or steric) interaction which will hinder

Fig. 2 Magnetisation curves of pristine Fe-MWCNTs and unfilled Fe-cat-MWCNTs at T = 300 K



90 M. Sobik et al.

aggregation of Fe-CNTs in large clusters and consequently their sedimentation due to gravity.

Stable suspensions of individually dispersed Fe-CNTs can be obtained using non-covalent functionalisation. This latter has been implemented for both pristine Fe-MWCNTs and unfilled MWCNTs (as a control). Several different biologically compatible dispersants (CMC-Na salt, polyphenylalanine—lysine (Lys:Phe, 1:1), PL-PEG-NH₂ and RNA) have been selected for this purpose. In aqueous media, all these dispersants feature a total electrostatic charge which generates a repulsive interaction between individually dispersed CNTs when non-covalently functionalised.

Stability of these different Fe-MWCNT suspensions was verified over several months using reliable and quantitative UV/Vis spectroscopy (data not shown). This analysis in combination with AFM and TEM imaging (Fig. 3) and studies of chemical properties [ζ -potential (data not shown)] of the suspensions indicated carboxymethylcellulose (CMC) Na salt as the dispersant leading to the most stable suspensions. For all following experiments, all the suspensions were prepared using CMC-Na salt as dispersant.

The magnetic properties of nanowire-filled Fe-MWCNT suspensions were studied at room temperature ($T=300~\rm K$). Suspensions of Fe-MWCNTs clearly possess a superparamagnetic-like (Fig. 4) behaviour, with a magnetization at saturation of 4.40 emu/g mL $^{-1}$. For comparison, unfilled Fe-cat-MWCNTs (Fig. 4) show a magnetization at saturation of 0.80 emu/g mL $^{-1}$. Therefore, the solubilisation process does not alter the ratio of the mass magnetization at saturation between both types of MWCNTs. Nevertheless, the solubilisation process that involves selection of individually dispersed MWCNTs reduces the mass magnetization at saturation by a factor of 2 for both types of MWCNTs.

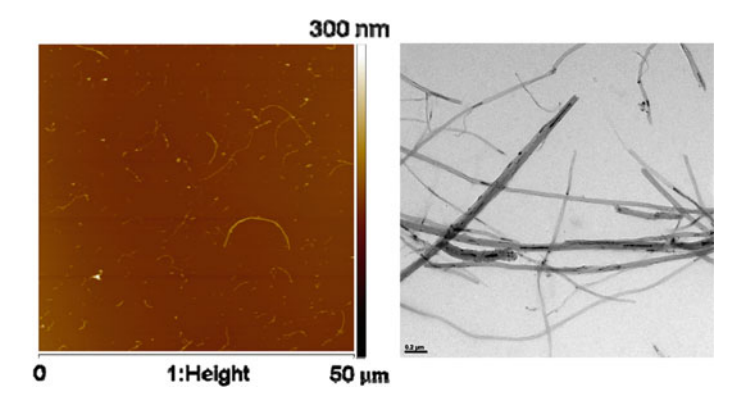


Fig. 3 AFM (left) and TEM (right) images of Fe-MWCNT suspensions using CMC-Na salt as dispersant

Fig. 4 Magnetisation curves of nanowire-filled Fe-MWCNTs and unfilled Fe-cat-MWCNTs suspensions at T = 300 K

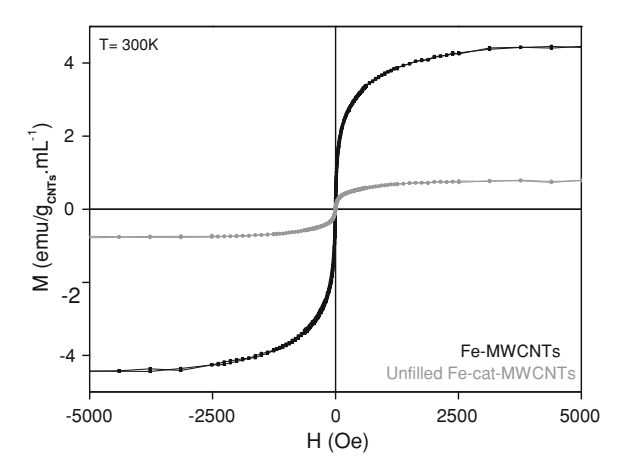
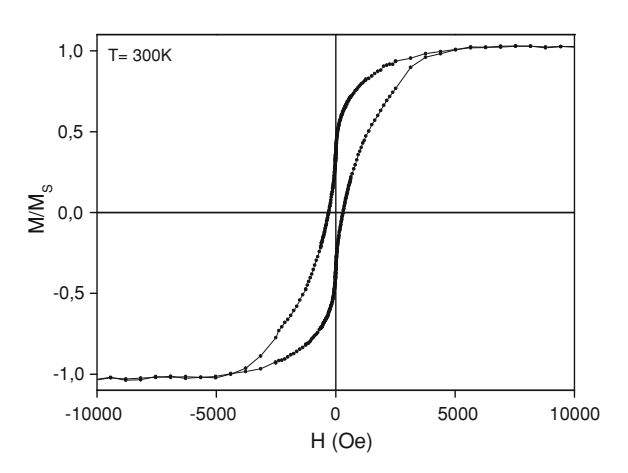


Fig. 5 Magnetisation curve of nanowire-filled Fe-MWCNTs in agar based phantoms at T = 300 K



Fe-Filled Carbon Nanotubes in Phantoms

Stable nanowire-filled Fe-MWCNT suspensions display superparamagnetic-like behaviour at $T=300~\rm K$ as seen previously (Fig. 4). When brought into agar based phantoms (from suspension) in order to mimic embedded Fe-CNTs in tissue, magnetic response is significantly changed when excited by an external magnetic field at $T=300~\rm K$. The main characteristic of the agar based phantoms is the high viscosity of the sample (gel-like sample), restricting freedom of movement of Fe-MWCNTs embedded in the phantom. Figure 5 shows how phantoms affect the magnetisation of Fe-MWCNTs. In this case, Fe-MWCNTs clearly display a ferromagnetic curve when they are homogeneously dispersed in phantoms. This is established by the data in Fig. 5 which shows the magnetisation curve of Fe-MWCNTs embedded in a phantom. The data clearly show a hysteretic

92 M. Sobik et al.

behaviour of Fe-MWCNTs at T = 300 K which is similar to the magnetisation curve of pristine Fe-MWCNTs in powder form (Fig. 2).

Mobility of Fe-Filled Carbon Nanotubes in Aqueous Media

As seen previously, nanowire-filled Fe-MWCNT suspensions display superparamagnetic-like behaviour when exposed to an external magnetic field. This is due to Brownian relaxation of the Fe-MWCNTs. The experimental data shown in Fig. 6 demonstrate that the complex magnetic susceptibility ($\chi = \chi' - j\chi''$) of Fe-filled MWCNTs goes to zero at frequencies above 1,000 Hz. Above 5 Hz, the real and imaginary components are the same, whereas below 5 Hz, the real component keeps increasing at decreasing frequency and the imaginary component possibly reaches a plateau around 0.3 Hz. The response is due to the rotational motion of the particles in the solvent, particles that apparently have a permanent magnetic dipole moment with a component along the long axis of the particles. Then, a frequency of the order of 0.3 Hz seems plausible for Fe-MWCNTs having a length of several micrometers.

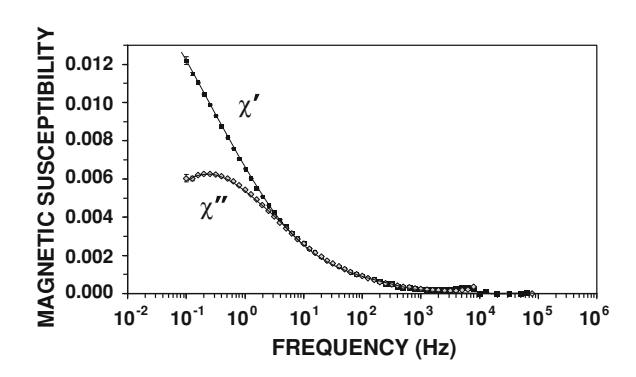
On the basis of

$$f_{\text{char}} = \frac{12k_{\text{B}}T\ln r}{\eta L^3} \quad [35]$$

where r is the aspect ratio, η is the viscosity (0.001 Pa s), and L is the length of the rods, assuming a diameter of 60 nm, the length corresponding to 0.3 Hz is 2.5 μ m. This does assume infinite dilution, which is not the case, giving an order of magnitude of several micron long Fe-MWCNTs.

The analyses of the complex magnetic susceptibility and relaxation of the magnetic particles can be used in biomedical applications especially non-invasive sensing. The variations in temporal response of Fe-MWCNTs to a rapidly changing magnetic field can be used to analyse interactions between the particles and the environment.

Fig. 6 Complex magnetic susceptibility of nanowire-filled Fe-MWCNTs in suspension at T = 300 K



3 Conclusion

Magnetic nanoparticles show promise for biomedical applications. Potential applications include minimally invasive diagnosis and therapy. Nanowire-filled Fe-MWCNTs are proposed as unique nanocontainers applicable for magnetic sensing and therapy in near future. The high potential of CNTs in medicine lies in the fact that these particles show anisotropic magnetic behaviour. Furthermore, their shape, size, magnetic properties and surface chemistry properties can be controlled potentially rendering CNTs biocompatible and inert to the environment.

Thus, these nanoparticles show a highly non-linear anisotropic and hysteretic magnetisation behaviour due to their extremely high aspect ratio. This behavior changes when the particles are brought into stable suspension. In this case, the suspensions show superparamagnetic-like behaviour with a mass magnetization at saturation approximately half of the value measured on the pristine MWCNTs. This decrease in magnetization at saturation is attributed to the fact that in the solubilisation process a selection is made on individually dispersed Fe-MWCNTs, which are likely to be smaller and less filled with Fe. On the other hand we analysed samples mimicking tissues. In these measurements the Fe-MWCNTs were not able to move or rotate with the applied magnetic field. Therefore the hysteresis curves are more open compared to the measurements on powder and especially suspensions.

These magnetic measurements were done as a first step potentially leading to new non-invasive sensing methods using Fe-MWCNTs in in vivo diagnosis. The application of nanotechnology and dedicated magnetic detection technique may permit cost efficient diagnosis and treatment of various diseases.

References

- Bjornerud, A., Johansson, L.: The utility of superparamagnetic contrast agents in MRI: theoretical consideration and applications in the cardiovascular system. NMR Biomed. 17(7), 465–477 (2004)
- Enpuku, K., et al.: Detection of magnetic nanoparticles with superconducting quantum interference device (SQUID) magnetometer and application to immunoassays. Jpn. J. Appl. Phys. 38(Part 2), 1102–1105 (1999)
- 3. Reimer, P., Balzer, T.: Ferucarbotran (Resovist): a new clinically approved RES-specific contrast agent for contrast-enhanced MRI of the liver: properties clinical development, and applications. Eur. Radiol. 13(6), 1266–1276 (2003)
- Bulte, J.W.M., Kraitchman, D.L.: Iron oxide MR contrast agents for molecular and cellular imaging. NMR Biomed. 17(7), 484–499 (2004)
- Salvador-Morales, C.: Study of the interaction between immune system proteins and carbon nanotubes. DPhil Thesis, University of Oxford, Oxford (2006)
- Reynolds, C.H., et al.: Gadolinium-loaded nanoparticles: new contrast agents for magnetic resonance imaging. J. Am. Chem. Soc. 122(37), 8940–8945 (2000)
- 7. Berry, C.C., Curtis, A.S.G.: Functionalisation of magnetic nanoparticles for applications in biomedicine. J. Phys. D Appl. Phys. **36**(13), R198–R206 (2003)

94 M. Sobik et al.

8. Lubbe, A.S., Alexiou, C., Bergemann, C.: Clinical applications of magnetic drug targeting. J. Surg. Res. **95**(2), 200–206 (2001)

- 9. Lubbe, A.S., et al.: Physiological aspects in magnetic drug-targeting. J. Magn. Magn. Mater. **194**(1–3), 149–155 (1999)
- 10. Lubbe, A.S., et al.: Preclinical experiences with magnetic drug targeting: tolerance and efficacy. Cancer Res. **56**(20), 4694–4701 (1996)
- 11. Lubbe, A.S., et al.: Clinical experiences with magnetic drug targeting: a phase I study with 4'-epidoxorubicin in 14 patients with advanced solid tumors. Cancer Res. **56**(20), 4686–4693 (1996)
- 12. Widder, K.J., Senyei, A.E.: Magnetic microspheres—a vehicle for selective targeting of drugs. Pharmacol. Ther. **20**(3), 377–395 (1983)
- 13. Crabtree, P.: Clinical trial fails; FeRx may close. In: The San Diego Union-Tribune. Union-Tribune Publishing Co., San Diego (2004)
- 14. Wilson, M.W., et al.: Hepatocellular carcinoma: regional therapy with a magnetic targeted carrier bound to doxorubicin in a dual MR imaging/conventional angiography suite—initial experience with four patients. Radiology **230**(1), 287–293 (2004)
- 15. Johnson, J., et al.: The MTC technology: a platform technology for the site-specific delivery of pharmaceutical agents. Eur. Cells Mater. 3, 12–15 (2002)
- 16. Pondman, K.M.: Investigation of rod-like nanoparticles as potential magnetic drug delivery carrier system. University of Twente (2010)
- 17. Foldvari, M., Bagonluri, M.: Carbon nanotubes as functional excipient for nanomedicines: II. Drug delivery and biocompatibility issues. Nanomedicine 4(3), 183–200 (2008)
- 18. Foldvari, M., Bagonluri, M.: Carbon nanotubes as functional excipients for nanomedicines: I. Pharmaceutical properties. Nanomedicine 4(3), 173–182 (2008)
- Heister, E., et al.: Triple functionalisation of single-walled carbon nanotubes with doxorubicin, a monoclonal antibody, and a fluorescent marker for targeted cancer therapy. Carbon 47(9), 2152–2160 (2009)
- 20. Lacerda, L., et al.: Carbon nanotubes as nanomedicines: from toxicology to pharmacology. Adv. Drug Deliv. Rev. **58**(14), 1460–1470 (2006)
- 21. Liu, Z., et al.: In vivo biodistribution and highly efficient tumour targeting of carbon nanotubes in mice. Nat. Nanotechnol. **2**(1), 47–52 (2007)
- Dresselhaus, M.S., Dresselhaus, G., Jorio, A.: Unusual properties and structure of carbonnanotubes. Annu. Rev. Mater. Res. 34, 247–278 (2004)
- 23. Flahaut, J.J., Gonzalez-Jimenez, F.: Preparation and characterization of a-Fe nanowires located inside double-walled carbon nanotubes. Chem. Phys. Lett. **457**, 347–351 (2008)
- 24. Grzelczak, M., et al.: Pt-catalyzed formation of Ni nanoshells on carbon nanotubes. Angew. Chem. Int. Ed. Engl. **46**(37), 7026–7030 (2007)
- Salgueirino-Maceira, V., et al.: Magnetic properties of Ni/NiO nanowires deposited onto CNT/Pt nanocomposites. Adv. Funct. Mater. 18, 616–621 (2008)
- 26. Leonhardt, A., et al.: Synthesis, properties, and applications of ferromagnetic-filled carbon nanotubes. Chem. Vapor Depos. **12**(6), 380–387 (2006)
- Wolny, S., et al.: Abnormal growth in mitochondrial disease. Acta Paediatr. 98(3), 553–554 (2009)
- 28. Vyalikh, A., et al.: A carbon-wrapped nanoscaled thermometer for temperature control in biological environments. Nanomedicine (Lond) **3**(3), 321–327 (2008)
- Klingeler, R., Hampel, S., Buchner, B.: Carbon nanotube based biomedical agents for heating. temperature sensoring and drug delivery. Int. J. Hyperth. 24(6), 496–505 (2008)
- Samouhos, S., McKinley, G.: Carbon nanotube-magnetite composites. With applications to developing unique magnetorheological fluids. J. Fluids Eng. Trans. ASME 129(4), 429–437 (2007)
- 31. Moench, I., Meye, A., Leonhardt, A.: Ferromagnetic filled carbon nanotubes as novel and potential containers for anticancer treatment strategies. In: Kumar, C.S.S.R. (ed.) Nanomaterials for Cancer Therapy, pp. 259–337. Wiley VCH Verlag, Weinheim (2006)
- 32. Kuipers et al.: Rev. Sci. Instrum. **79**(1), 013901 (2008)

- 33. Hampel, S., et al.: Growth and characterization of filled carbon nanotubes with ferromagnetic properties. Carbon 44(11), 2316–2322 (2006)
- 34. Mönch, I., et al.: Synthesis and characteristics of Fe-filled multi-walled carbon nanotubes for biomedical application. J. Phys. 61, 820–824 (2007)
- 35. Dhont, J.K.G.: An Introduction to Dynamics of Colloids, Elsevier, Amsterdam p. 211 (1996)

Feasibility of Magnetically Functionalised Carbon Nanotubes for Biological Applications: From Fundamental Properties of Individual Nanomagnets to Nanoscaled Heaters and Temperature Sensors

Matthias U. Lutz, Kamil Lipert, Yulia Krupskaya, Stefan Bahr, Anja Wolter, Ahmed A. El-Gendy, Silke Hampel, Albrecht Leonhardt, Arthur Taylor, Kai Krämer, Bernd Büchner and Rüdiger Klingeler

Abstract We discuss the prospects of applying the magnetic properties of magnetically functionalised carbon nanotubes to biomedical applications. The primary applications are use as a contactless local heating agent, as a standalone thermoablation treatment or in concert with remotely released anti-cancer drugs. Targeted heat treatment is an effective cancer treatment, as tumour tissue has a reduced heat tolerance. To understand the heating process in an applied alternating current (AC) magnetic field the basics of the ferro- and superparamagnetic heating mechanisms are described and brought into context with the material properties. The performance of various materials is compared with respect to heat output, and prospect of additional functionalisation. The actual heating output in AC magnetic fields is studied and discussed in this chapter. Hall magnetometry and Magnetic Force Microscopy are employed to study the magnetic properties of individual nano-ferromagnets, e.g. magnetisation reversal behaviour and domain configuration. NMR studies show that a non-invasive temperature control by virtue of a carbon-wrapped nanoscaled thermometer is feasible.

M. U. Lutz (

), K. Lipert, Y. Krupskaya, S. Bahr, A. Wolter, A. A. El-Gendy, S. Hampel, A. Leonhardt, B. Büchner and R. Klingeler Leibniz Institute for Solid State and Materials Research (IFW), Dresden, Germany e-mail: m.lutz@ifw-dresden.de

M. U. Lutz, K. Lipert, A. A. El-Gendy and R. Klingeler Kirchhoff Institute for Physics, University of Heidelberg, Heidelberg, Germany

A. Taylor and K. Krämer Department of Urology, Dresden University of Technology, Dresden, Germany

1 Introduction

Introducing nanoscaled magnets into biological systems represents a powerful tool as such artificial probes can be influenced by external magnetic fields. The great advantage of magnetic fields for biomedical applications is their biocompatibility and weak interaction with organic matter. Magnetic fields penetrate tissue non-invasively and without known adverse effects and hence reach deep layers of (human) tissue. However, at the receiving end nanoscale magnetic probes are needed, which can penetrate biological systems without adverse effects and with magnetic properties tailored for a particular purpose. In general, after being inserted, magnetic nanoparticles can be localized in deep tissue, external static magnetic fields can fix them at a precise position, gradient fields can move them and alternating fields lead to local heating of the magnetic probes. The last effect can be utilized for magnetic hyperthermia or thermoablation applications for an anti-cancer treatment. This method is based on the fact that the cancer cells are destroyed at elevated temperatures, i.e. either indirectly by hyperthermia ($\sim 42-45^{\circ}$ C) or directly through thermoablation (>46°C). In particular, local heating by means of nanosized probes not only reduces adverse effects on the healthy tissue present in conventional chemotherapeutical approaches but also increases the efficiency of concomitant radio- or chemotherapy. Much of the current research is focused on superparamagnetic iron oxide nanoparticles [1] which have proven their feasibility in animal experiments [2, 3] and are now under clinical trials [4]. Due to their particular magnetic properties, i.e. high coercivity and saturation magnetisation, metallic iron nanowires can generate heat more efficiently in comparison to superparamagnetic iron oxides since various mechanisms yield dissipative effects [5]. In practice, higher heating efficiency means that less nanoscale material would have to be introduced into the biological system in order to achieve the targeted hyperthermia effect. The use of nanoparticles made of iron, however, is hindered by the fact that oxidation in ambient or biological conditions has to be avoided. A promising way to overcome this problem appears to be the coating of the iron with a carbon shell by inclusion of the iron inside carbon nanotubes¹ and thereby protecting the biological environment and the filling material against each other. Degradation of filling materials is avoided and their possible toxicity and adverse effects are suppressed. In carbon-coated functional elements, therapeutically or diagnostically active materials are encapsulated by a protecting carbon shell so that, e.g., nanoscale magnetic heaters, drug carrier systems and sensors are made [6]. Note that, beyond the shielding effect against a biological environment, the carbon coating also offers an interface for exohedral functionalisation with suitable (bio-) molecules.

¹ Unless otherwise specified, we always use multiwalled carbon nanotubes (MWCNT) in our experiments.

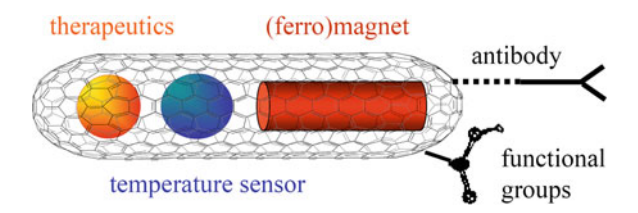


Fig. 1 Sketch of a filled carbon nanotube serving as multi-functional container for in vivo applications. A (ferro)magnet can induce heat in AC magnetic fields and a material with strongly temperature dependent nuclear magnetic resonance (NMR) signal might serve as a thermometer. Additional drug delivery can be envisaged. Exohedral functionalisation to achieve biocompatibility or targeting is sketched. Note that single-walled as well as multi-walled carbon nanotubes can be used

MWCNT form chemically and mechanically stable containers, thereby providing a nanoscale carrier system. A wide field of applications opens due to the fact that the carbon shells can be opened, filled with a functional material and closed again without losing their high mechanical and chemical stability. This is demonstrated by the example of local temperature control by virtue of functionalised MWCNT. Nanoscale carbon-coated temperature sensors suitable for contactless read-out by means of magnetic spectroscopy can be made using materials with strongly temperature dependent nuclear magnetic resonance (NMR) parameters. Such nanoscale temperature sensors can be envisaged for control of magnetic hyperthermia where, in practice, it may be difficult to provide uniform heating throughout the cancer tissue. This example already illustrates the great potential of functionalised MWCNT for biomedical applications. In general, the container feature of MWCNT allows simultaneous filling of MWCNT with different materials thereby combining multiple functionalities in a single carrier (Fig. 1). In this way MWCNT provide a smart carrier system on the nanometer scale which can be filled with tailored materials to address specific purposes. The container function is underlined by recent theoretical considerations [7] as well as experimental success in encapsulation of anticancer drugs into MWCNT and their transfer into living cells [8, 9].

In order to apply magnetically functionalised MWCNT for biomedical applications, their magnetic properties have to be understood in detail. In the following section we investigate the properties of individual ferromagnetic MWCNT as studied by means of Hall magnetometry and Magnetic Force Microscopy (MFM) in applied magnetic fields. These studies provide detailed information on the magnetisation reversal processes and the respective switching fields. Thereafter, investigations on ensembles of various magnetically functionalised as well as pure diamagnetic MWCNT are presented. The different response of fixed MWCNT and of those in aqueous suspension are analysed and brought into context with the heating mechanism. Further we show that insertion of NMR active substances provides nanoscale markers and sensors. In particular, we demonstrate non-invasive temperature control by virtue of a carbon-wrapped nanoscaled thermometer.

2 Magnetism of Individual Iron Nanowire Filled MWCNT

Carbon exhibits only a very weak diamagnetic behaviour which renders pure carbon nanotubes inappropriate for applications exploiting external magnetic fields. Therefore, magnetic functionalisation is essential in order to address MWCNT by an external magnetic field, i.e. for visualisation, fixation, moving or AC-magnetic heating as mentioned in Sect. 1. Note that pristine MWCNT are in general already magnetically functionalised due to the presence of nanosize magnetic catalyst particles used in the synthesis process. The magnetic properties of such pristine, iron-catalyst containing MWCNT (Fe-cat-MWCNT) will be described in Sect. 3. Functionalising with larger amounts of magnetic material is done by filling MWCNT with the desired materials, e.g., Fe, Co, or Ni, thereby forming carbon-coated ferromagnetic nanowires. The in situ synthesis process results in single crystal nanowires, described in detail elsewhere [10]. As mentioned above, the focus in this section lies on the magnetism of the iron nanowires encapsulated by MWCNT, neglecting the contribution of the catalyst particles. Note that the shape anisotropy (0.9 MJ m⁻³) dominates the magneto-crystalline anisotropy energy density (0.048 MJ m⁻³) for a long α -Fe nanowire. This implies that the magnetisation vector is aligned along the wire axis which therefore forms the hard magnetisation axis. As will be shown below, this behaviour is indeed observed in our experiments.

For any application, in particular in biomedicine, the properties of the individual objects have to be known and if necessary modified. We present two different experimental techniques, Hall magnetometry and magnetic force microscopy (MFM), which allow us to study the magnetism of individual nanomagnets. For both techniques, we present experimental investigations on individual iron nanowire filled MWCNT under applied external magnetic fields which enable us to determine their magnetic properties.

Magnetisation Measurements on Individual Iron Nanowire Filled MWCNT Probed with Hall Magnetometry

Hall magnetometry has proven to be a very sensitive and accurate technique to determine the magnetic properties of small magnetic objects [11–14]. Here, we study the magnetic properties of an individual nanometer-sized iron nanowire filled MWCNT by employing sub-micrometer sized ballistic Hall probes in a large temperature and magnetic field range.

The Hall sensor consists of a high mobility two-dimensional electron gas (2DEG) realized in a GaAs heterostructure. The square shaped active area of the sensor is patterned with electron beam lithography and has an area of approximately $800 \times 800 \text{ nm}^2$, located a few tens of nanometers below the surface of the sensor area. An individual iron nanowire with diameter of approximately 16 nm

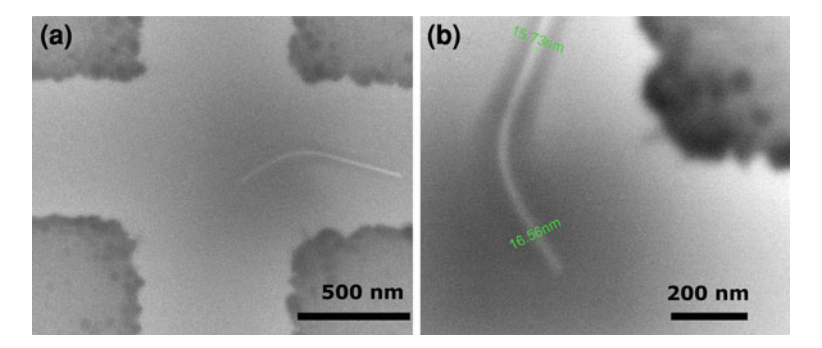


Fig. 2 a Scanning electron microscopy (SEM) image of a sub-micrometer sized Hall sensor with a single iron nanowire filled MWCNT on top of the device. **b** A closer look at the iron nanowire filled MWCNT before placement on the Hall sensor. The diameter of the homogenous Fe filling is around 15–17 nm

embedded in a MWCNT is placed onto the sensor, such that the magnetic stray field produced by the iron nanowire penetrates the active area of the sensor (Fig. 2).

In our experiments the external magnetic field could be applied in any direction within the surface plane of the sensor. The measured Hall voltage $U_{\rm H}$ is then given by

$$U_{\rm H} = R_{\rm H}IB. \tag{1}$$

 $R_{\rm H}$ is the Hall coefficient of the sensor which essentially depends on the electron density in the 2DEG. $R_{\rm H}$ lies in the range of 5 k Ω /Tesla and is almost independent of temperature and external magnetic fields. I denotes the electric current injected into the sensor (typically 2 μ A) and B is the magnetic stray field penetrating the sensor's active area.

Figure 3a shows a typical hysteresis loop at low temperatures where the external magnetic field was applied with an angle of $\alpha=-31^\circ$ with respect to the axis of the iron nanowire. The magnetisation curve has a nearly rectangular shape which is typical for the magnetisation reversal of a single-domain particle. In these magnetisation measurements we can clearly determine a single magnetic switching field, when the iron nanowire completely reverses its magnetisation. In highly anisotropic magnetic materials the two magnetic orientations are separated by an energy barrier that has to be overcome during the reversal process. This magnetisation reversal process is thermally activated and the magnetic switching field shows a quite large distribution, as shown in Fig. 3b. In order to determine the average switching field $H_{\rm SW}$ in a fixed experimental condition, we typically carried out a few hundreds of independent measurements and then calculated $H_{\rm SW}$ and $\Delta H_{\rm SW}$.

In order to elucidate the magnetisation reversal mechanism of our iron nanowire, we studied the angular dependence of the switching field H_{SW} with respect to the direction of the applied magnetic field as well as for different temperatures.

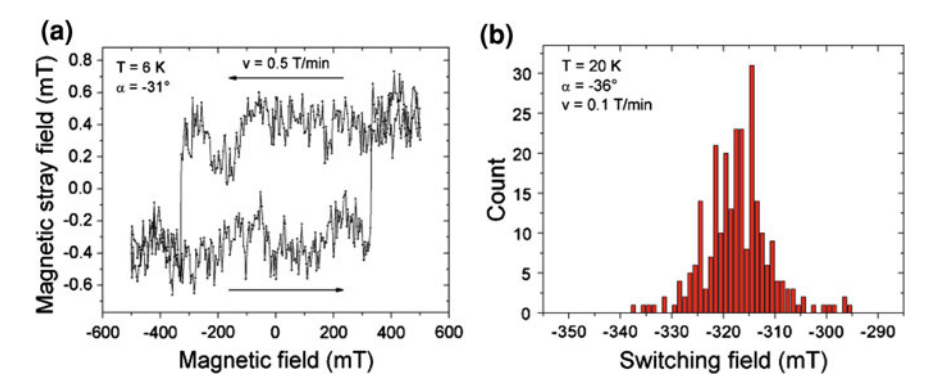


Fig. 3 a Hysteresis loop of a single iron nanowire encapsulated by MWCNT measured at T=6 K with Hall magnetometry. The external magnetic field was ramped at a rate of v=0.5 T/min with an angle of $\alpha=-31^{\circ}$ with respect to the axis of the nanowire. (b) Histogram of N=260 switching fields measured at T=20 K, $\alpha=-36^{\circ}$ and v=0.1 T/min

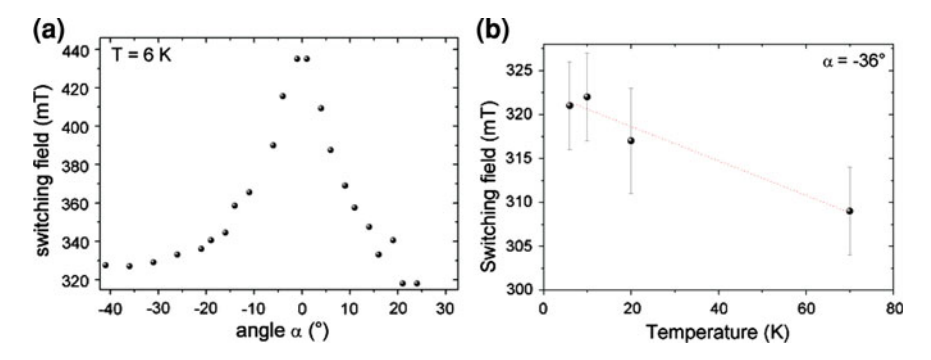


Fig. 4 a Angular dependence of the switching field of an individual iron nanowire measured at T=6 K. (b) Temperature dependence of the switching field with the external magnetic field applied under an angle of $\alpha=-36^{\circ}$

Figure 4a shows the angular dependence of $H_{\rm SW}$ at T=6 K. We observed a distinct increase of $H_{\rm SW}$ when the external magnetic field was applied along the tube axis. This behaviour of $H_{\rm SW}$ (α) can be understood in the framework of the Stoner–Wohlfarth model of uniform rotation of magnetisation [15]. In perfect nanowires, the transition from coherent rotation to non-coherent magnetisation reversal occurs at a critical diameter which in iron is around 11 nm [16–18]. However our experimental data show that even above this theoretically estimated value of the critical diameter, features of uniform magnetisation reversal can be observed, indicating that our long iron nanowire protected by a carbon shell shows a delocalized magnetisation reversal mode.

Therefore our results not only confirm the high homogeneity of the magnetic filling inside the MWCNT, but also open up the possibility to study in more detail

the crossover from delocalized magnetisation reversal to localized magnetisation reversal mechanisms in individual magnetic nanowires with high aspect ratio.

Figure 4b depicts the temperature dependence of $H_{\rm SW}$ when the external magnetic field is applied at an angle of $\alpha=-36^{\circ}$. At very low temperatures we observe switching fields around 320 mT, whereas at T=70 K we observe an average switching field of 309 mT. Theoretical considerations suggest the temperature dependence of the switching field is almost linear at high temperatures [19, 20]. Extrapolation of the switching field up to room temperature leads to $H_{\rm SW}\approx260$ mT, which corresponds quite well to switching field distributions of multiple wires observed at room temperature with magnetic force microscopy presented in the next section.

Magnetic Force Microscopy on Iron Nanowires Encapsulated by MWCNT in External Magnetic Fields

Magnetic force microscopy (MFM) is an established scanning probe technique for mapping the magnetic stray field of a small magnetic sample with high spatial resolution [21]. It can be applied to study any flat structure emitting a stray field, for example: domain walls in magnetic thin films [22] and patterned elements [23], nanowires [24] and vortices in superconductors [25].

In MFM, the signal is detected by scanning a magnetised tip at the end of a cantilever, oscillating at its resonance frequency, over a surface. MFM is a variant of the atomic force microscope (AFM) and is still capable of obtaining topographic information. However, the magnetic signal has to be recorded in the so-called

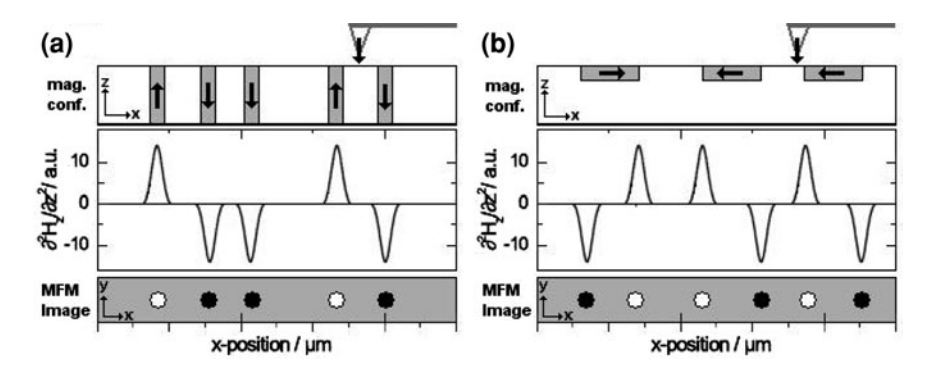


Fig. 5 Sketch of the MFM measurement technique for two different magnetic configurations. Top: Magnetic configuration of the sample, middle: 2^{nd} derivative of the stray field *z*-component $\partial^2 H_z/\partial z^2$, bottom: MFM contrast as seen in the final image. **a** In the case when the magnetisation of the sample is perpendicular to the scanned surface, the tip interacts with the positive (negative) magnetic pole of each magnetic object, which leads to a positive (negative) frequency shift in the final MFM image. **b** When the magnetisation is parallel to *xy*-surface, the two magnetic poles of each object can be distinguished in the final MFM image

non-contact mode, since the magnetic interactions are much weaker than the interactions with the surface. In the case of a rough surface one can apply the so-called lift mode, where at first the topography is recorded in tapping mode followed by a non-contact scan keeping the distance to the predetermined surface constant. The second measurement option is to scan the tip in a constant plane over the surface of a very flat sample. In both cases, the magnetic contrast is formed as described in Fig. 5. In the presence of stray field gradients a force will act on the tip. If the z-component of the stray field gradient is parallel (antiparallel) to the tip there will be an attraction (repulsion) leading to a negative (positive) frequency shift. In this way one can map the magnitude and sign of the z-component of the magnetic stray field over the area of interest, with white (black) representing a positive (negative) frequency shift. This enables one to reconstruct the spatially resolved magnetic structure of the sample. In the case at hand, the MFM is equipped with external magnetic fields so that field induced changes in the sample magnetisation can be detected.

Our data have been obtained by means of a high-resolution MFM (hr-MFM, NanoScan Ltd). The system is used in high vacuum, ensuring a high signal to noise ratio and thermal stability. A low-moment high-resolution tip has proven to minimize tip-sample interaction while at the same time providing an adequate signal strength and excellent resolution. For field dependent studies a permanent magnet is approached from below, resulting in a magnetic field parallel to the tip magnetisation. A MFM image is taken at each field strength. One can scan either with the field applied or retract the magnet before scanning.

In order to determine a large number of switching fields of α -Fe nanowires, an array of vertically aligned iron nanowire filled MWCNT was embedded in tetraethyl orthosilicate (TEOS). TEOS was deposited onto an as-grown iron nanowire filled MWCNT ensemble sticking on its substrate (so-called 'forest', cf. Fig. 10b) and then polished to a flat surface [26]. A typical MFM image of this ensemble is shown in Fig. 6a. Black and white spots indicate magnetic poles, i.e. the ends of embedded MWCNT-coated iron-nanowires. To be specific, white spots imply a repulsive force due to antiparallel arrangement of tip and wire magnetisation and black an attractive force implying parallel alignment. Note, that the behaviour of the nanowires can be studied without having to consider the catalyst particles.

The experiment starts by application of a large negative external magnetic field (typically $\mu_0 H = 0.6$ T) parallel to the long tube axis (perpendicular to the image plane) which causes all magnetisation vectors to point parallel to H, i.e. we observe only white spots in the MFM image. Upon application of a positive magnetic field, the magnetisation of each individual wire reverses at its corresponding switching field, seen as a white dot becoming black.

When applying a magnetic field parallel to the wires (from below), they gradually switch, where each individual switching event can be distinguished. The measured switching fields are displayed in Fig. 6b. Our data show that most wires switch between 200 and 400 mT.

These results are in good agreement with the room temperature extrapolation of the Hall magnetometry data. However, one has to be careful when comparing the

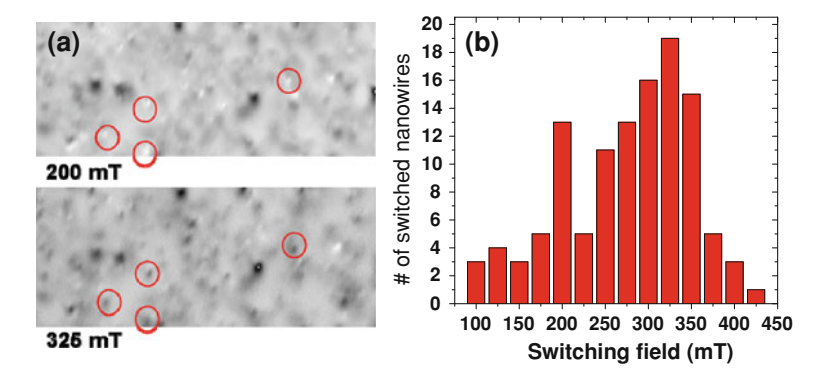


Fig. 6 (a) Top: MFM contrast of the area containing the 58 iron nanowires after applying a magnetic field of 200 mT. White (Black) dots represent magnetisation antiparallel (parallel) to the tip. Bottom: MFM contrast after applying 325 mT. Four examples of switched wires are highlighted by red circles. (b) Switching field distribution of 58 individual iron nanowires (absolute value for switching in positive and negative field for each wire). Adapted from [27]

two switching field distributions shown in Fig. 3b and Fig. 6b, respectively. The Hall magnetometry results represent multiple measurements of a single nanowire, where the switching field distribution is mainly due to thermal activation. The MFM results on the other hand are from 58 separate wires, each with its own intrinsic switching field. The variation between different wires is mainly due to a distribution of the wire diameters (12–26 nm). The two techniques complement each other nicely; MFM allows one to study multiple wires at once, whereas Hall magnetometry gives a more precise picture of the switching behaviour, with the possibility of angle and temperature dependent measurements.

3 Magnetism of Carbon Nanotube Ensembles

After addressing the switching behaviour of individual nanowires encapsulated by MWCNT, the magnetic response of ensembles will be elucidated. In the following, the different contributions to the bulk magnetic properties of the various components of the iron filled MWCNT system will be discussed in detail: the carbon nanotubes themselves, ferromagnetic catalyst particles and iron nanowires.

It is important to define precisely the terms used to describe carbon nanotubes, as their corresponding configuration has a crucial influence on the magnetic properties. The first part Sect. 3.1 introduces the magnetic properties of pure carbon nanotubes, i.e. without magnetic functionalisation. These properties are only accessible after either post-synthesis treatment of pristine iron catalyst containing MWCNT or by applying a non-magnetic rhenium catalyst for synthesis. The relevance of the catalyst particles on the magnetic response is emphasized in Sect. 3.2 which concerns iron catalyst containing MWCNT (Fe-cat-MWCNT),

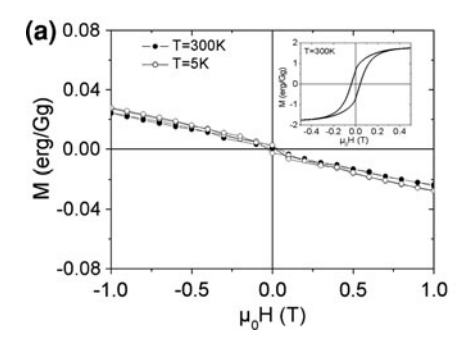
where ferromagnetic catalyst particles usually applied for the synthesis have to be taken into account. The section is concluded by examining ensembles of MWCNT deliberately grown with an additional ferromagnetic filling in the form of iron nanowires (Fe-wire-MWCNT).

The two primary tools used to investigate the magnetic behaviour of MWCNT ensembles are an alternating gradient magnetometer (AGM MicroMag Model 2900, Princeton Measurement Corporation) and a commercial Quantum Design MPMS-XL5 (Magnetic Property Measurement System) SQUID (Superconducting Quantum Interference Device) magnetometer.

Diamagnetism of Pure Carbon Nanotubes

Usually, MWCNT are synthesised by virtue of magnetic catalyst particles which affect the magnetic properties of the resulting material. Interestingly, from the variety of materials investigated as potential catalysts, the ferromagnetic ones such as iron, cobalt, nickel and their alloys exhibit the highest activity for catalyst based growth of carbon nanotubes [28–34]. On the other hand, pure carbon structures are supposed to exhibit only weak diamagnetic susceptibilities so that even an extremely small quantity of residual catalyst material present in the MWCNT would dominate the magnetic response. In particular, a ferromagnetic-like response is often observed in the pristine Fe-cat-MWCNT samples.

Even a purification process, e.g. washing the tubes in nitric acid after the synthesis, does not eliminate the catalyst contamination completely. This is illustrated, e.g., in the inset of Fig. 7a where a clear ferromagnetic hysteresis is seen superposing the expected diamagnetic properties of the pure material. In this example, the material contains Fe catalyst nanoparticles which had been utilized during synthesis. Taking into account the saturation magnetisation of bulk α -Fe



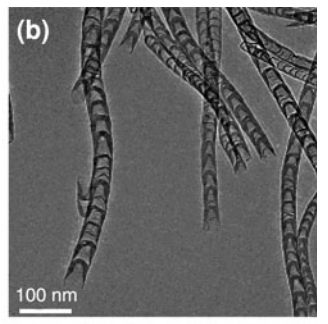


Fig. 7 a Diamagnetic behaviour of MWCNT grown with Fe-catalyst particles after annealing. *Inset* typical hysteresis loop of acid treated Fe-cat-MWCNT. **b** TEM image of Fe-catalyzed MWCNT, synthesized by using acetonitrile as solvent and after annealing at 2,500°C under argon. The TEM image confirms opened bamboo-like MWCNT with no catalyst particles visible [35]

 $[M_{\rm bulk}=212~{\rm erg/(G~g)}]$, we conclude that $m_{\rm Fe}/m_{\rm CNT}\approx 0.01$ in this particular case. Hence, even strongly purified MWCNT can exhibit a very large magnetic signal which renders them non-applicable for fundamental research on intrinsic magnetic properties and applications sensitive to ferromagnetic impurities. In order to study in detail the magnetic properties of a filling material or to utilize MWCNT as a highly pure nonmagnetic agent for biological environments, diamagnetic MWCNT are required. To obtain these nanotubes we have applied two different techniques: (1) post-synthesis evaporation of catalyst particles at extremely high temperatures and (2) usage of the nonmagnetic catalyst material rhenium.

The high temperature annealing process performed either in vacuum or under argon atmosphere is a unique approach to fully evaporate ferromagnetic catalyst particles from Fe-cat-MWCNT. After the annealing process performed in argon atmosphere at a temperature of 2,500°C, TEM images show no signature of Fe-catalyst particles as displayed in Fig. 7b. A much more sensitive method to confirm the absence of Fe-catalyst particles is, however, to measure the magnetisation of the material which indeed implies drastic changes (Fig. 7a). In particular, after the post synthesis treatment, the magnetisation decreases almost linearly upon increasing the external magnetic field.

This behaviour unambiguously implies a diamagnetic response and shows the absence of any measurable contribution of magnetic iron. We emphasize that the data at T=5 K strongly confirm the absence of any magnetic impurities since even diluted paramagnetic ions, e.g., individual Fe ions, would result in a Curielike increase in the magnetisation which is clearly not observed. Remarkably, the high-temperature treatment is non destructive and provides open nanotubes with intact crystal structure.

An alternative approach to achieve carbon nanotubes free of ferromagnetic impurities is to apply non-magnetic catalyst materials. Here, rhenium was used and the fixed bed method applied [36]. A TEM image of the Re-catalyzed carbon nanotubes is shown in Fig. 8b.

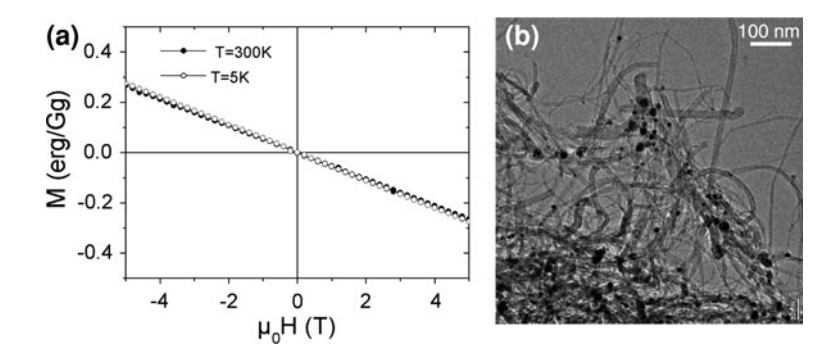


Fig. 8 a Diamagnetic response of Re-catalyzed MWCNT. After the synthesis procedure, the sample was annealed at 2,300°C. **b** TEM image of Re-catalyzed MWCNT after annealing at 2,300°C under vacuum. Re particles are still present in the material. Adapted from [35]

The magnetisation of Re-catalyzed MWCNT at T=300 K and at T=5 K is shown in Fig. 8a. Similarly as discussed above, the magnetic field dependence of the magnetisation is linear and exhibits a negative slope, which again demonstrates the diamagnetic properties of the material. Accordingly, also the temperature dependence of the magnetic susceptibility $\gamma = dM/dH$ is very weak.

Quantitatively, the magnetic susceptibility at $\mu_0 H = 0.5$ T and T = 300 K amounts to $\chi = (-2.7 \pm 0.5) \times 10^{-6}$ erg/(G^2 g) for the annealed nanotubes from approach (1) and to $\chi = (-4.6 \pm 0.1) \times 10^{-6}$ erg/(G^2 g) for the rhenium-catalyzed ones. These values are in agreement with the range of values previously reported for carbon structures [37–39].

Pristine MWCNT: Magnetism of Catalyst Nanoparticles

It has already been mentioned above that magnetisation measurements are sensitive to magnetic impurities and hence can provide information about their presence. In addition, magnetic measurements can be used as a very sensitive measure of the quantity of magnetic materials inside the sample while conventional methods such as Energy-dispersive X-ray spectroscopy (EDX), X-ray photoelectron spectroscopy (XPS) or X-ray diffraction (XRD) might fail to detect trace amounts of magnetic material.

Several different batches of empty carbon nanotubes were prepared using a variety of ferromagnetic catalyst materials and various synthesis methods. A set of seven different powder samples of MWCNT prepared with 50% FeCo alloy catalysts (sample 1) and pure iron catalyst (samples 2–7) were examined. The fixed bed method [40] was used in the synthesis of samples (1), (3) and (4), while aerosol assisted CVD was used for samples (2) and (5). In addition, commercially available single-walled carbon nanotubes (SWCNT) from Nanolab Inc. (sample 6) and MWCNT from Bayer MaterialScience (baytubes C150 HP) (sample 7) have been studied. Room temperature magnetic measurements were performed in magnetic fields up to 0.5 T employing the AGM and SQUID magnetometers. The results of these measurements are shown in Fig. 9.

The experimental data shown in Fig. 9 demonstrate ferromagnetic-like behaviour in all samples. In particular, diamagnetism of the carbon shells is masked by the magnetism of the catalyst particles formed during and remaining inside the carbon nanotubes after the synthesis procedure. The M(H) curves provide relevant characteristic parameters such as the coercive magnetic field (H_C) , the saturation magnetisation (M_S) and the remanent magnetic moment (M_R) . Indirectly, based on the saturation moment it is also possible to derive the amount of the magnetic material in the sample. The respective values are listed in Table 1. Note that the table includes also the mean diameter of the catalyst particles as extracted from TEM imaging. In addition we present the relative amount of ferromagnetic catalyst material in the sample, $m_{\rm cat}/m_{\rm CNT}$, which was deduced by comparing the measured saturation magnetisation with its corresponding bulk values.

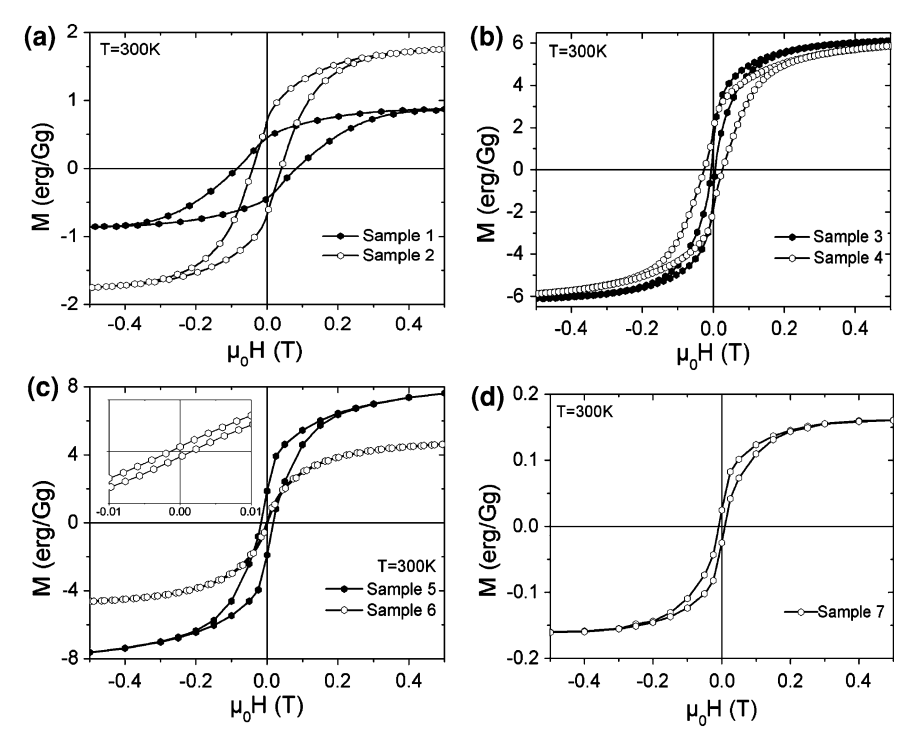


Fig. 9 Magnetisation versus magnetic field at $T=300~\rm K$ for **a** sample 1, MWCNT made by the fixed bed method with FeCo catalyst and sample 2, made by the AA-CVD method. **b** Sample 3, a single- and double-walled CNT mixture and sample 4, MWCNT, both made by the fixed bed method with Fe catalyst. **c** Sample 5, MWCNT by the AA-CVD method with Fe catalyst and sample 6, SWCNT from NanoLab synthesized by CVD with Fe as catalyst. **d** Sample 7, MWCNT from Bayer MaterialScience prepared by CVD with Fe as catalyst

Table 1 Summary of TEM and magnetisation analysis

Sample	Synthesis	Catalyst	d (nm)	$\mu_0 H_{\rm C} \ ({\rm mT})$	Ms [erg/(G g)]	$m_{\rm cat}/m_{\rm CNT}~(\%)$
1	Fixed bed	FeCo	10-15	84.2	0.87	_
2	AA-CVD	Fe	~10	36.9	1.76	0.8
3	Fixed bed	Fe	1-5	5.8	6.1	2.9
4	Fixed bed	Fe	8-15	26.1	5.93	2.8
5	AA-CVD	Fe	10-20	20.0	8.2	3.8
6	CVD	Fe	_	1.5	4.84	2.3
7	CVD	Fe	2-6	12	0.16	0.07

d denotes the diameter of the respective catalyst particles as taken from TEM imaging, $H_{\rm C}$ and $M_{\rm S}$ are the coercive field and saturation magnetisation from the data in Fig. 9. $m_{\rm cat}/m_{\rm CNT}$ is the relative amount of magnetic material in the sample

As the magnetic properties of MWCNT are usually governed by the response of the catalyst nanoparticles, in the following we discuss the coercivities $H_{\rm C}$ for samples (1) and (2). According to Table 1 the diameters of the catalyst particles

are below the single domain limit, 12 nm for Fe [41] and 41 nm for bcc FeCo [42]. According to the model of Néel [43] the coercivity of our single domain, randomly oriented nanoparticles with cubic anisotropy is proportional to the magnetocrystalline anisotropy constant K_1 , i.e. $H_C \sim K_1$. The values of K_1 found experimentally at room temperature are $K_1 = 4.8 \times 10^4$ J/m³ and $K_1 = -1 \times 10^5$ J/m³ for α -Fe and disordered BCC 50% FeCo alloy, respectively [44]. While the particle size is similar, we observe H_C (Sample 2) $\sim 2H_C$ (Sample 1) which is consistent with the Néel model.

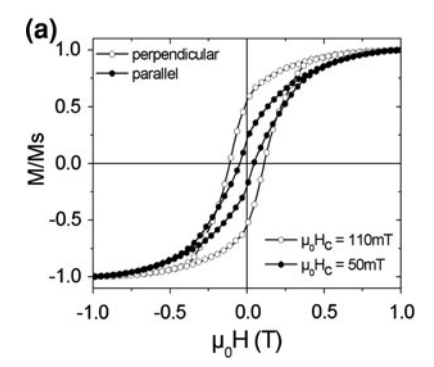
To be specific, coercivity is strongly associated with the size of the magnetic nanoparticles. Two regions can then be distinguished, one for which the particle diameter is smaller than the single domain limit (12 nm for Fe), the other for larger multidomain particles. The coercive force in the single domain region is proportional to $\sim d^6$ [45]. Indeed, a rapid increase of the critical field with diameter is evident for samples (3), (7), (2) where $H_{\rm C}$ increases from 5.8 up to 36.9 mT. In contrast, for particles in the multidomain limit with diameters above 12 nm, $H_{\rm C}$ becomes smaller for larger particles, i.e. $H_{\rm C} \sim 1/d$ [46]. This situation is seen in samples (2), (4), and (5), where the coercivity decreases from 36.9 to 20 mT with increasing particle size.

Iron Nanowire Filled MWCNT

Further magnetic functionalisation can be achieved by filling MWCNT with a magnetic material. This yields ferromagnetic nanowires coated by carbon shells the diameter of the nanowire being determined by the inner diameter of the MWCNT. Depending on the filling ratio, either very long micrometer-sized nanowires are formed or several shorter ones separated by hollow space. Here, we discuss the case of in situ iron nanowire filled MWCNT (Fe-wire-MWCNT) and their magnetic properties which have already been addressed by the studies on individual nanomagnets in Sect. 2.

Iron filled carbon nanotubes are prepared by means of thermal-catalytic chemical-vapour deposition (CVD) with ferrocene as precursor as described in several reviews, e.g. in [47]. This method produces filled carbon nanotubes with a filling of more than 40%, consisting of α -Fe, γ -Fe, and Fe₃C in different ratios depending on the sample preparation. Only α -Fe and Fe₃C exhibit ferromagnetic behaviour at room temperature while γ -Fe is paramagnetic. The iron filling forms single crystal nanowires of lengths up to 20 μ m. A scanning electron microscopy (SEM) image of such homogenous ensembles of Fe-wire-MWCNT grown onto a silicon substrate is shown in Fig. 10b.

The magnetisation was measured by means of the AGM at room temperature parallel and perpendicular to the oxidised silicon substrate (Fig. 10a). Fe-wire-MWCNT tend to grow perpendicular to the substrate plane and form an almost homogenous 'forest' of nanotubes (see Fig. 10b). The ferromagnetic α -Fe nanowires encapsulated by carbon nanotubes exhibit uniaxial magnetic anisotropy with



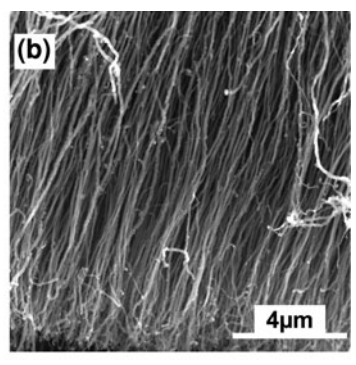


Fig. 10 a Magnetisation curve M versus H of Fe-wire-MWCNT grown on a silicon substrate measured at room temperature parallel and perpendicular to the substrate. b SEM image of the same material

the easy axis parallel to the long axis of the nanowires, leading to an enhanced magnetic coercivity ranging up to ~ 110 and ~ 50 mT in perpendicular and parallel direction to the substrate, respectively. The coercivity measured when the magnetic field was applied almost parallel to the long axes of the nanowires is about four times smaller then the switching field measured along the easy axis for an individual iron nanowire (see Fig. 6a). This can be explained by the fact that the single wire measurements were conducted on MWCNT deliberately chosen for their long and homogeneous filling, resulting in a large shape anisotropy with corresponding high switching fields. Such wires are estimated to contain a minority of the iron found in the whole sample. The rest is made up of short and/or inhomogeneous wires and catalyst particles, all of which have a much lower switching field. The response of the ensemble is therefore only of limited value for shedding light on the magnetic properties of the nanowires.

In order to determine the relative amount of iron in the Fe-wire-MWCNT by means of magnetometry, these MWCNT were removed from the substrate and measured as a dry powder. Figure 11 provides an example of a M(H) curve measured on the powder sample. At room temperature, Fe-wire-MWCNT powder shows a coercivity $\mu_0 H_C = 50$ mT and a saturation magnetisation $M_S = 14.8$ erg/ (G g_{CNT}). Comparison with the saturation magnetisation of bulk iron $M_{\text{bulk}} = 212$ erg/(G g) reveals a mass ratio of iron in Fe-wire-MWCNT of 6.8%. In comparison, EDX spectroscopy shows an iron concentration of around 7.6 ± 1 weight %. Remarkably, a comparison between Fe-wire-MWCNT and Fe-cat-MWCNT discussed in the previous subsection implies that the amount of ferromagnetic iron inside the Fe-wire-MWCNT is only two times higher. However, although it is known that catalyst material is also present in the Fe-wire-MWCNT, the amount of catalysts cannot be assessed. One might speculate that iron nanowires form at the expense of some catalyst material but a separation of the magnetic signal of Fewire-MWCNT into the response of nanowires and catalyst, respectively, is not possible by means of the data at hand.

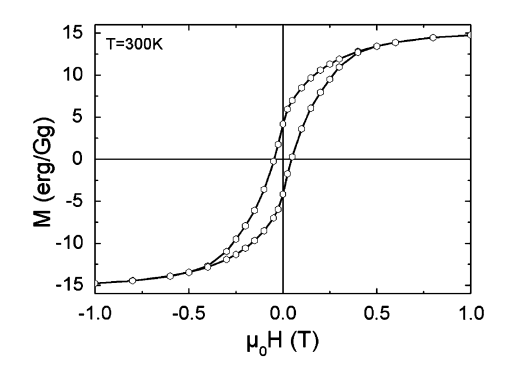
Magnetic Behaviour of Iron Containing MWCNT in Liquid Media

As seen in Figs. 9 and 11, fixed iron-containing MWCNT reveal pronounced hysteresis loops indicating a ferromagnetic state of the encapsulated iron irrespectively of whether nanoscale catalyst particles or iron nanowires are made. For usage in biological systems, however, the material is dispersed in liquid media which in general affects the magnetic response significantly [48]. In this section we will briefly discuss the case of magnetically functionalised MWCNT in aqueous suspension. Note that exohedral functionalisation, i.e. attaching side groups either non-covalently or covalently to the outer shells of the MWCNTs in order to render them dispersible in liquid media [49], does not in itself affect the magnetic properties considerably. The main reason for changes in the magnetic properties after dispersion is the strongly enhanced mobility of the particles. Possibly, changes in the mean distance of the nanoparticles are also relevant.

Figure 12 demonstrates how dispersion in liquid affects the magnetisation curve of Fe-cat-MWCNT, i.e. MWCNT with Fe-catalyst particles. While the powders exhibit a clear hysteresis and a spontaneous moment (see Fig. 9c, sample 5), the material behaves superparamagnetically after being dispersed in an aqueous medium (Fig. 12a). It is straightforward to associate these changes to the motion of initially ferromagnetic nanoparticles in liquid under exposure to magnetic fields. This is corroborated by the data in Fig. 12b which shows the magnetisation curve of the same dispersion after freezing at $T=260~\rm K$. The data imply a magnetic hysteresis similar to the powder sample.

This observation indicates that the superparamagnetic behaviour of Fe-cat-MWCNT in liquid is caused by the Brownian relaxation of the magnetic particles. This scenario is supported by AC susceptibility measurements in the frequency range f=0–10 kHz (Fig. 13). The AC susceptibility of Fe-cat-MWCNT in dispersion is significantly larger than in powder, which again indicates the motion of MWCNT in liquid under exposure to AC magnetic fields. In general, maximal energy losses for Brownian relaxation are observed when the condition $f=f_{\rm max}=(2\pi~\tau_{\rm Br})^{-1}$ is fulfilled, where $\tau_{\rm Br}$ is the Brownian relaxation time.

Fig. 11 Magnetisation curve *M* versus *H* of Fe-wire-MWCNT powder at room temperature



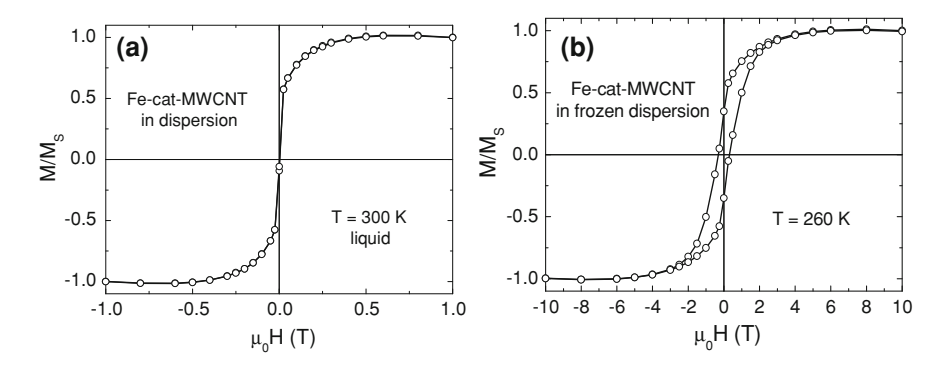
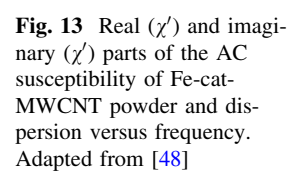
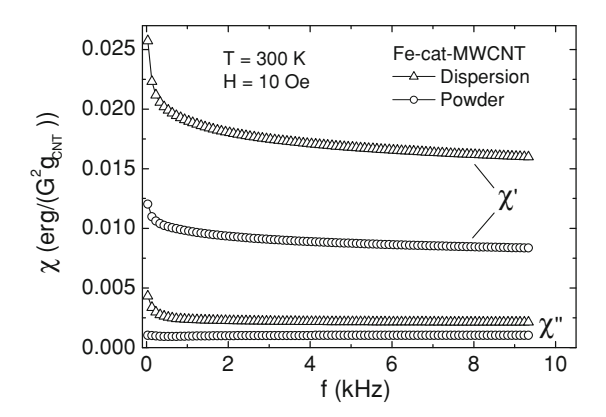


Fig. 12 Magnetisation curves of Fe-cat-MWCNT $\bf a$ in aqueous dispersion at $T=300~\rm K$ and $\bf b$ after freezing the dispersion at $T=260~\rm K$. Adapted from [48]





That is, the imaginary part of the AC susceptibility τ'' exhibits a maximum at $f_{\rm max}$. The Brownian relaxation time $\tau_{\rm Br}$ and hence $f_{\rm max}$ depend on the viscosity of the liquid medium and on the hydrodynamic radius of the particle [50, 51]. For spherical iron oxide nanoparticles in liquid dispersion (with the viscosity of water $\eta = 1.01 \times 10^{-3} \ {\rm kg \ m^{-1} \ s^{-1}}$) the maximum energy losses have been observed at $f_{\rm max} \approx 1.8 \ {\rm kHz}$ which implies a mean hydrodynamic particle diameter of 61 nm [50]. In the case of Fe-cat-MWCNT, the data in Fig. 13 display a maximum of χ'' at very low frequencies ($f_{\rm max} < 0.2 \ {\rm kHz}$). Such very long relaxation times are in agreement with the relatively big size and the elongated shape of MWCNT in comparison to iron oxide nanoparticles.

4 Heating of Magnetically Functionalised CNT with AC Magnetic Fields

AC magnetic heating, i.e. dissipation of energy due to magnetisation reversal of magnetic materials in alternating magnetic fields, is a general feature in

ferromagnetic and ferromagnetic-like systems. The particular advantage of magnetic nanoparticles concerns (1) their size which renders them applicable for nanomedical therapies and (2) significant heating at small field amplitudes which are safe to apply to the human body. In order to discuss the response of magnetic nanoparticles to high-frequency magnetic fields, different dissipation mechanisms will be introduced. In general, there are various possibilities for the heating of magnetic particles in AC magnetic fields: ferromagnetic (hysteresis) losses, superparamagnetic (relaxation) losses, eddy currents, etc. [52–54].

Magnetic Dissipation in Alternating Magnetic Fields

Hysteresis losses appear in ferromagnetic particles which possess hysteretic magnetic properties. In this case, alternating magnetic field induced magnetisation reversal causes dissipation of energy. The amount of dissipated energy $P_{\rm FM}$ can be determined according to Eq. 2, where the area of the hysteresis loop is multiplied by the frequency f.

$$P_{\rm FM} = \mu_0 f \oint H \mathrm{d}M. \tag{2}$$

In the particular case of single domain particles, no minor loops can be utilized for heating and dissipation only occurs upon complete switching of the magnetisation vectors, i.e. at external magnetic fields larger than the magnetic switching field $H_{\rm C}$.

Superparamagnetic or relaxation losses provide an alternative mechanism of magnetically induced heating in an AC field. The term superparamagnetism was introduced by Elmore in 1938 [55] in order to describe the magnetic behaviour of colloidal systems containing iron oxide particles. When such a colloidal system is removed from a magnetic field, its magnetisation relaxes back to zero due to the thermal energy. This relaxation of the magnetisation can be either associated with the physical motion of the nanoparticles (Brownian relaxation) or with the rotation of the magnetisation vector within each particle (Néel relaxation). Both kinds of relaxation lead to the dissipation of the magnetic field energy. In the case of non-interacting superparamagnetic particles the dissipated energy $P_{\rm SPM}$ can be described by

$$P_{\text{SPM}} = \mu_0 \pi f \chi'' H^2 \tag{3}$$

Here, χ'' is the out-of-phase component of the complex magnetic susceptibility. Physically, Eq. 3 implies that if the magnetisation lags the magnetic field there is a positive conversion of magnetic energy into internal energy [52].

Note, that in general also eddy currents might cause energy losses in AC magnetic fields. This effect is applied, e.g., in induction furnaces for melting metallic materials. In the case of nanoscaled metals used for magnetic

hyperthermia, particles are too small and AC field frequencies are too low for the generation of substantial eddy currents [39]. For Fe-cat-MWCNT studied here, this was proven experimentally using non-magnetic metal nanoparticles (see Sect. 4.2).

Heating of Fe-cat-MWCNT in Alternating Magnetic Fields

Inductive heating of Fe-cat-MWCNT (i.e. MWCNT synthesised with Fe-catalyst particles partly remaining in the material after synthesis) in an alternating magnetic field has been studied for different strengths and frequencies of the magnetic field. The experimental setup for these studies consists of a high-frequency generator with an impedance matching network and a magnetic coil system, providing AC magnetic fields of 0-100 kA/m strength with frequencies between 100 kHz and 300 kHz. The water-cooled copper coil has 5 turns with an inside bore diameter of 30 mm into which the sample is placed; the height of the coil is 40 mm. The sample is insulated by its container, an evacuated glass Dewar flask placed in the coil. The temperature of the sample during the measurements is determined by means of a fiber-optic temperature controller (Luxtron One) connected to a computer for data storage. Note that the fiber-optic thermometer is not affected by alternating magnetic fields. Inductive heating studies were performed on Fe-cat-MWCNT in liquid media. In order to obtain a stable dispersion, MWCNT were mixed in a 1:1 weight ratio with human serum albumin and dispersed in phosphate buffered saline (PBS) using ultrasonication. The concentration of Fe-cat-MWCNT in the dispersion was 5 mg/ml [48].

Calorimetrical measurements on Fe-cat-MWCNT dispersion in AC magnetic fields show a substantial heating capability of this material (see Fig. 14a). A significant increase of the temperature was observed in AC magnetic fields with

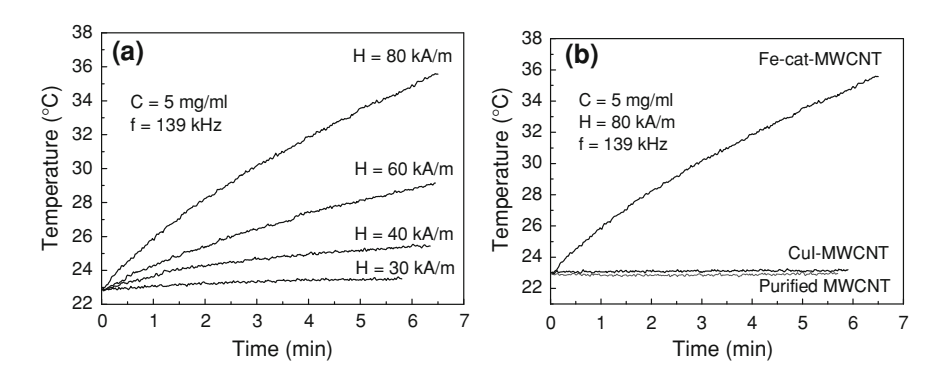


Fig. 14 Calorimetrical measurements on the Fe-cat-MWCNT dispersion in AC magnetic fields. **a** Fe-cat-MWCNT dispersion in different magnetic fields. **b** Comparison of Fe-cat-MWCNT to non-magnetic control materials (see the text). Adapted from [48]

frequency of 139 kHz and magnetic field strengths H above 30 kA/m. In particular, at H=80 kA/m the heating effect reaches 3°C/min. As control materials we used non-magnetic pure MWCNT [35], CuI-filled MWCNT [56], and C-coated Cu nanoparticles [57]. The calorimetric measurements on the control materials in AC magnetic fields did not reveal any significant temperature increase. This confirms the expectation that the heating effect of Fe-cat-MWCNT is connected to the presence of iron in the sample and thus implies its purely magnetic nature. To be specific, neither pure MWCNT nor MWCNT filled with a non-magnetic salt show any heating effect (see Fig. 14b). In addition, measurements performed on C-coated Cu nanoparticles experimentally prove that the observed heating effect of Fe-cat-MWCNT is not related to eddy currents occurring in the nanosized material under study.

Quantitative characterization of the heating effectiveness of the Fe-cat-MWCNT dispersion was achieved by determining the specific absorption rate (SAR) from the initial slopes of the temperature versus time curves. The SAR (in W/g) is the mass normalized rate of energy absorption which can be determined according to

$$SAR = c \frac{dT}{dt} \bigg|_{t \to 0}.$$
 (4)

Here, c is the specific heat capacity of the sample, which in the case at hand is equal to water ($c=4.186~\rm J~g^{-1}~K^{-1}$). The data of the SAR depending on the magnetic field strength are shown in Fig. 15a. The SAR shows a quadratic dependence on the applied magnetic field strength H, which is in agreement with the fact that the magnetic field energy is proportional to H^2 . For better comparability of Fe-cat-MWCNT to other magnetic materials the SAR was normalized to the mass of Fe-cat-MWCNT (SAR_{MWCNT}) and the mass of the active material iron (SAR_{Fe}). At the maximum magnetic field strength of 100 kA/m, SAR_{MWCNT} and SAR_{Fe} amount to 71.4 W/g_{MWCNT} and 1,879 W/g_{Fe}, respectively. Fig. 15b presents SAR_{MWCNT} and SAR_{Fe} versus H^2 confirming the quadratic dependence on the magnetic field strength. This quadratic dependence is in agreement with Eq. 3,

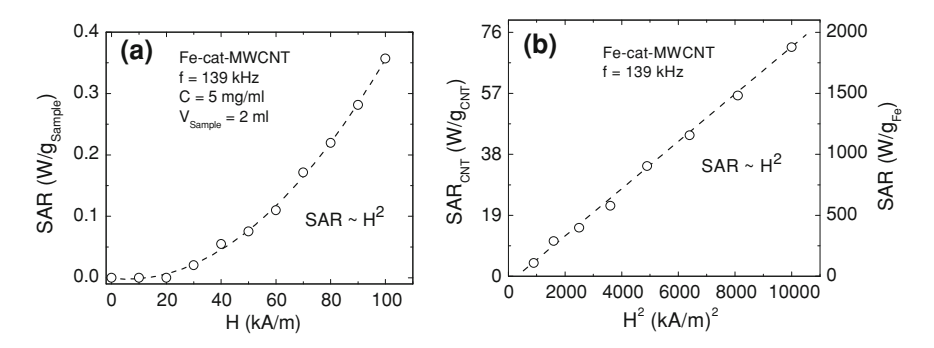


Fig. 15 a Specific absorption rate SAR of Fe-cat-MWCNT dispersion versus AC magnetic field strength H. b SAR normalised to the mass of Fe-cat-MWCNT (SAR_{MWCNT}) and to the mass of iron (SAR_{Fe}) in the dispersion versus H^2 . Adapted from [48]

assuming that χ'' is independent of the magnetic field strength. Under this assumption, the imaginary part of the AC susceptibility χ'' for the frequency f=139 kHz can be calculated from SAR_{MWCNT} according to Eq. 3. This calculation yields $\chi''=1\times 10^{-3}$ erg/(G²g_{MWCNT}). Note that this value is of the same order of magnitude as the measured χ'' at the frequencies of around 10 kHz (see Fig. 13). As discussed before, in the case of the Brownian relaxation the maximal energy losses are observed at $f_{\rm max}=(2\pi\tau_{\rm Br})^{-1}$. Therefore, the experimental observation of similar losses at applied frequencies of 139 kHz and 10 kHz implies both frequencies do not fulfil this condition.

While significant heating effects do occur in Fe-cat-MWCNT, large switching fields observed in iron nanowire-filled MWCNT (see Sect. 2) do not suggest this material for AC-magnetic heating. In general, rather than increasing the magnetic field strength, a higher applied frequency seems to be a promising solution to obtain high dissipation. So instead of activating the hysteresis loss heating mechanism in iron nanowires by applying stronger magnetic fields, a possible solution would be to use nanowires with a greatly reduced coercivity. This is indeed feasible since the iron filling is present in two ferromagnetic phases, α -Fe and Fe₃C. Contrary to α-Fe, described above, Fe₃C has a strong magneto-crystalline anisotropy (0.394 MJm³) which dominates over the shape anisotropy (0.3 MJm³), causing the magnetisation vector to point along the easy c-axis of crystalline Fe₃C. In all iron carbide tubes imaged so far the Fe₃C filling is singlecrystalline and the b-axis is found to be parallel to the long axis of the filling, resulting in soft magnetisation *perpendicular* to the long axis [58]. Remarkably, the competing anisotropies result in a very low effective anisotropy and in low switching fields of 30–90 mT (24–72 kAm⁻¹). Hence, using such low coercivity wires might allow one to retain the advantages of filled MWCNT (protection of and from bio-environment, biofunctionalisabilty, additional filling with anti-cancer drugs and temperature sensor) while enabling clinical application (lower field strength).

5 Filled Carbon Nanotubes for NMR-Based Thermometry at the Nanoscale

In the following we focus on the potential application of MWCNT for a contactless in vivo temperature control on the cellular level which can be used to control temperature in various hyperthermia treatments including the magnetic fluid hyperthermia (MFH) [1] therapy. Such a contactless thermometer consists of a MWCNT and a filling material with strongly temperature-dependent NMR parameters like the spin–lattice or the spin–spin relaxation, resonance frequency, dipolar or scalar couplings, and electrical quadrupole coupling at 290–330 K (\sim 20–60°C).

Conventional magnetic resonance (MR) thermometry based on a temperature-dependent proton resonance frequency shift of the water molecule enables

temperature control in combination with a good spatial resolution [59–62]. However, accurate temperature control with high spatial resolution is a challenging research topic in nano- and biotechnology. In particular, the application of magnetic nanoparticles for hyperthermia in cancer therapy raises the issue of precise thermometry on the cellular level where conventional methods usually fail. For example, in magnetic hyperthermia like the so-called MFH, high doses of unshielded nanomagnets prevent the application of conventional local non-invasive thermometry due to magnetic field inhomogeneities, i.e. proton-based magnetic resonance thermometry [60]. Hence, novel methods such as nanomaterial-based thermometry have to be applied [63, 64]. The development of an accurate nanoscale thermometer with high resolution is however not only a matter of size, but also requires materials with novel physical properties which can be exploited at this length scale [65–67]. Current developments cover various approaches such as thermal sensors using molecular and biological moieties [68] and nanoscale superstructures [69]. Another approach utilizes the flexibility of tailoring carbon-protected nanoscale functional materials by filling MWCNT. The general feasibility of MWCNT-based sensors for thermometry has been demonstrated recently [70, 71].

We have applied cuprous halides as filling material which exhibit pronounced temperature dependencies for various NMR parameters [72]. By inserting this filling into MWCNT, (1) a shielding of the sensor from local field inhomogeneities, e.g. induced by ferromagnetic particles nearby, is provided and (2) degradation of the filling material is avoided, and their potential toxicity and adverse effects are suppressed. There is also the possibility to modify the outer shell of MWCNT, e.g., with cancer-specific binding agents in order to facilitate attachment to a target tissue. This way, temperature detection is possible with a high accuracy even in more challenging situations with, e.g. ferromagnetic particles nearby.

In order to study the family of cuprous halides systematically, $CuCl_2$, CuBr, and CuI have been filled into MWCNT and investigated by NMR [71, 73]. Here, both the copper and halide nuclei have NMR active isotopes with a high natural abundance, allowing NMR studies on two different probing nuclei for all three materials. The NMR measurements have been done in a solid state NMR spectrometer in an external magnetic field of 7.05 T on powdered material. Both ^{63}Cu and $^{35}Cl/^{81}Br/^{127}I$ NMR spectra obtained from the Fourier transformed echo signals represent a single resonance line between 10 K and 320 K, indicating a vanishing static quadrupolar coupling due to a highly symmetric tetrahedral crystallographic environment. The spin–lattice relaxation T_1 was measured employing an inversion recovery pulse sequence. The decay of ^{63}Cu and $^{35}Cl/^{81}Br/^{127}I$ longitudinal magnetisation was analyzed following a standard equation for the nuclear spin I = 3/2 (^{63}Cu , ^{35}Cl , ^{81}Br), and I = 5/2 (^{127}I), correspondingly. In all cases the magnetisation curve follows an exponential law characterized by a single spin–lattice relaxation time. Similar experiments at room temperature on powdered reference material (pure commercially available cuprous

halide powder) result in no remarkable differences in line width, resonance frequency and spin-lattice relaxation.

The ⁶³Cu NMR spectra exhibit only a small increase of the resonance frequency in the temperature range of biological interest, which strongly contrasts with the NMR shift on the halide nucleus indicating much stronger temperature dependence. The most promising results, however, are provided by the spin-lattice relaxation rates T_1^{-1} , which are presented in Fig. 16. Although the 63 Cu T_1^{-1} dependencies are similar to the halide data, the slope of its T_1^{-1} rate is much smaller providing a lower accuracy in temperature determination. The T_1^{-1} dependencies for all nuclei are found to be in very good agreement with the law $T_1^{-1} \propto T^2$ that is expected for a Raman two-phonon quadrupolar process [74]. This is consistent with the view that the spin-lattice relaxation is driven by a quadrupolar mechanism in this compound, which at a first glance might appear to be unusual, since CuI crystallizes in the zinc blende structure [75]. However, timedependent quadrupolar interactions can arise from time-dependent distortions of the nuclear environment by the lattice vibrational modes, although in a perfect crystal of CuCl₂, CuBr and CuI no static, secular interaction between the nuclear electric quadrupole moment and the crystalline electric field gradient are expected. This behaviour is observed over the entire temperature range implying no contributions from impurities which might appear at low temperatures and from ionic

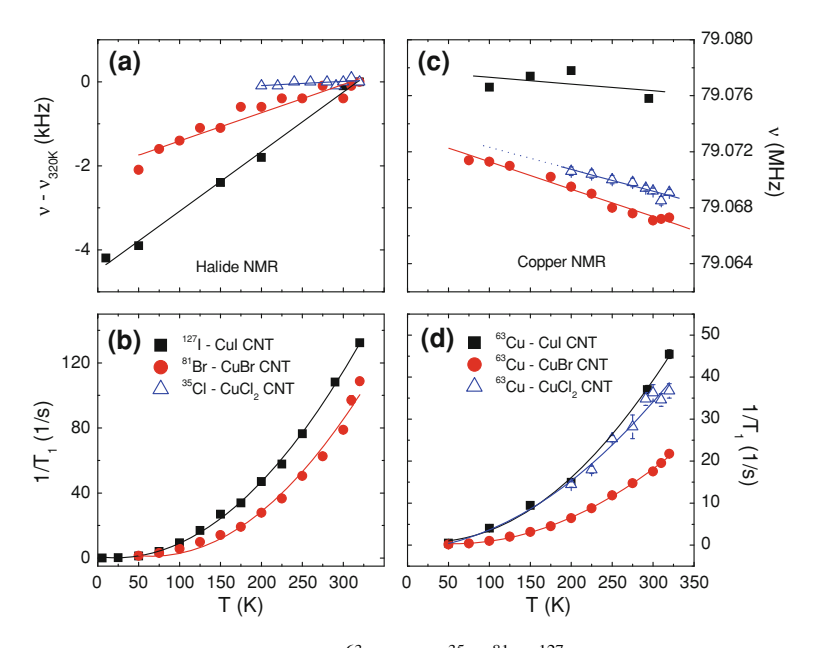


Fig. 16 Temperature dependencies of ⁶³Cu and ³⁵Cl/⁸¹Br/¹²⁷I nuclear magnetic resonance parameters measured on cuprous-halide-filled carbon nanotubes. (**a, c**) Nuclear magnetic resonance frequency. (**b, d**) Nuclear spin–lattice relaxation rate. The *symbols* represent the experimental data. The *solid lines* are the fits (see text)

diffusion which might be observed in the high temperature range. The temperature dependent data are well fitted with the quadratic function $T_1^{-1} = a + bT + cT^2$. Here, the mean squared errors of the fitting coefficients provide an estimate of the accuracy of the temperature determination for the nanothermometer, resulting in an optimal temperature accuracy of 2 K by means of 127 I spin–lattice relaxation measurement in CuI-filled MWCNT in the temperature range of biological interest (i.e. 290–320 K).

The absolute values for the temperature sensitivity parameters are given in Table 2 for all three cuprous halide filled MWCNT and respective probing nuclei. A clear tendency is visible from this table, showing that upon stepping forward from ³⁵Cl to ⁸¹Br to ¹²⁷I in the periodic system of the elements, the temperature sensitivity increases for both NMR parameters, i.e. NMR frequency and 1/T₁-relaxation rate, as well as for both nuclei, i.e. copper and halide nuclei. This implies that the best temperature accuracy of 2 K is observed for CuI-filled MWCNT, which is a promising result and a good starting point for a smart way to look for further filling materials in order to increase the accuracy of temperature determination in the future.

The potential of carbon-wrapped nanoscale thermometers for a non-invasive temperature control is demonstrated by our detailed temperature dependent NMR studies. The basic principles of MRI-based thermometry also apply for the carbon-wrapped nanothermometer. However, compared to the conventional approach using naturally abundant protons in the body of the patient as probing nuclei, our sensor material (probing nucleus other than ¹H) is shielded by the carbon container. Therefore, in the case of a sensor based relaxation-weighted imaging even large doses of unshielded magnets which are nearby—such as in nanoparticle-based hyperthermia treatments—and which introduce magnetic field inhomogeneities will not reduce MRI contrastivity.

A valuable extension of this approach for the future is spatially resolved NMR, i.e., magnetic resonance imaging (MRI) of MWCNT-based nanosensors on the cellular level. One example is the rapidly growing field of cellular and molecular MR imaging, which enables us to visualize cells and inserted MWCNT in order to track cancer cells and to control therapies on the cellular level such as magnetic hyperthermia. Here, the container feature of MWCNT is extensively utilized if a heating element (ferromagnet), a temperature sensor and a contrast agent are either confined within the same nanocontainer or differently filled MWCNT are mixed.

Table 2 Temperature sensitivity parameters of several filled MWCNT

Material	Nucleus	dv_{res}/dT (Hz/K)	$d(T_1^{-1})/dT \text{ (Hz/K)}$
CuCl ₂ -MWCNT	⁶³ Cu	15	0.23
	³⁵ Cl	1	_
CuI-MWCNT	⁶³ Cu	_	0.27
	^{127}I	14	0.86
CuBr-MWCNT	⁶³ Cu	19	0.15
	$^{81}{ m Br}$	7	0.75

Such a combination of different functionalities on a nanoscale would provide simultaneous heating, temperature control by means of MRI and high spatial resolution of the image. Furthermore, if clinical usage of the static magnetic field is contra-indicated and MR imaging is no longer suitable, then the technology proposed here addresses materials with temperature dependent nuclear quadrupolar resonance NQR (e.g. cuprous oxide) or zero-field NMR (e.g. Co-based compounds) parameters that demonstrates versatility of this approach for biomedical applications.

6 Summary

Magnetically functionalised carbon nanotubes provide a multifunctional material in which magnetic properties can be tailored to address various functionalities. Carbon-coating of active material such as superparamagnetic heaters and temperature sensors provides a multifunctional biocompatible carrier system in which particular properties can be exploited for therapeutical or diagnostical usage. Our AC magnetic field studies imply the promising potential of magnetically functionalised MWCNT for magnetic hyperthermia, in particular, if multiple functionalities are addressed. This is particularly highlighted by NMR studies showing feasibility of a non-invasive temperature control by virtue of a carbon-wrapped nanoscale thermometer. In general, however, nanotechnologically relevant magnetic materials demand elaborate understanding of the magnetic properties of individual entities, e.g. magnetisation reversal behaviour and domain configuration, which is a precondition to tailor the material appropriately. Here, Hall magnetometry and Magnetic Force Microscopy are employed to elucidate fundamental properties of the single particle. Understanding the interplay between intrinsic magnetic properties and behaviour as an ensemble is vital for future application. Especially the behaviour in liquid media is of utmost importance in the frame of biomedical applications. Our studies hence demonstrate how fundamental research on a technologically relevant nanomaterial opens prospects to applications.

Acknowledgements This work was supported by the Europeon Community through the Marie Curie Research Training Network CARBIO under contract No. MRTN-CT-289 2006-035616 and by the DFG via WO 1532/1.

References

- 1. Jordan, A., Scholz, R., Wust, P., Fahling, H., Felix, R.: Magnetic fluid hyperthermia (MFH): cancer treatment with AC magnetic field induced excitation of biocompatible superparamagnetic nanoparticles. J. Magn. Magn. Mat. **201**, 413–419 (1999)
- Johannsen, M., Thiesen, B., Jordan, A., Taymoorian, K., Gneveckow, U., Waldöfner, N., Scholz, R., Koch, M., Lein, M., Jung, K., Loening, S.A.: Prostate 283, 64 (2005)

3. Matsuoka, F., Shinkai, M., Honda, H., Kubo, T., Sugita, T., Kobayashi, T.: Hyperthermia using magnetite cationic liposomes for hamster osteosarcoma. Biomagn. Res. Technol. 2, 3 (2004)

- Johannsen, M., Gneveckow, U., Taymoorian, K., Thiesen, B., Waldöfner, N., Scholz, R., Jung, K., Jordan, A., Wust, P., Loening, S.A.: Morbidity and quality of life during thermotherapy using magnetic nanoparticles in locally recurrent prostate cancer: results of a prospective phase I trial. Int. J. Hyperth. 23, 315–323 (2007)
- 5. Dale, L.H.: Synthesis, properties, and applications of iron nanoparticles. Small 1, 482 (2005)
- Klingeler, R., Hampel, S., Büchner, B.: Carbon nanotube based biomedical agents for heating, temperature sensoring and drug delivery. Int. J. Hyperth. 24, 496–505 (2008)
- 7. Hilder, T.A., Hill, J.M.: Nanotechnology 18, 275704–275712 (2007)
- 8. Wu, W., Wieckowski, S., Pastorin, G., Benincasa, M., Klumpp, C., Briand, J.-P., Gennaro, R., Prato, M., Bianco, A.: Angew. Chem. Int. Ed. 44, 6358 (2005)
- Hampel, S., Kunze, D., Haase, D., Rauschenbach, M., Kraemer, K., Ritschel, M., Leonhardt, A., Thomas, J., Oswald, S., Hoffmann, V., Buechner, B.: Carbon nanotubes filled with a chemotherapeutic agent—a nanocarrier mediates inhibition of tumor cell growth. Nanomedicine 3, 175–182 (2008)
- Leonhardt, A., Mönch, I., Meye, A., Hampel, S., Büchner, B.: Adv. Sci. Technol. 49, S74– S78 (2006)
- 11. Kent, A.D., von Molnar, S., Gider, S., Awschalom, D.D.: J. Appl. Phys. 76, 6656 (1994)
- Gider, S., Shi, J., Awschalom, D., Hopkins, P., Campman, K., Gossard, A., Kent, A., von Molnar, S.: Appl. Phys. Lett. 69, 3269 (1996)
- 13. Geim, A.K., Dubonos, S.V., Lok, J.G.S., Grigorieva, I.V., Maan, J.C., Hansen, L.T., Lindelof, P.E.: Appl. Phys. Lett. **71**, 2379 (1997)
- Li, Y., Xiong, P., von Molnar, S., Wirth, S., Ohno, Y., Ohno, H.: Appl. Phys. Lett. 80, 4644 (2002)
- Stoner, E.C., Wohlfarth, E.P.: Philos. Trans. R. Soc. Lond. Ser. A Math. Phys. Sci. 240, 599 (1948)
- 16. Aharoni, A.: Phys. Status Solidi 16, 3 (1966)
- 17. Sellmyer, D.J., Zheng, M., Skomski, R.: J. Phys. Condens. Matter 13, R433 (2001)
- 18. Skomski, R.: J. Phys. Condens. Matter 15, R841 (2003)
- 19. Meier, J., Doudin, B., Ansermet, J.: J. Appl. Phys. 79, 6010 (1996)
- Zeng, H., Skomski, R., Menon, L., Liu, Y., Bandyopadhyay, S., Sellmyer, D.J.: Phys. Rev. B. 65, 134426 (2002)
- 21. Martin, Y., Wickramasinghe, K.: Appl. Phys. Lett. 50, 1455–1457 (1987)
- 22. Göddenhenrich, T., Hartmann, U., Anders, M., Heiden, C.: J. Microsc. **152**, 527–536 (1988)
- Gomez, R.D., Luu, T.V., Pak, A.O., Kirk, K.J., Chapman, J.N.: J. Appl. Phys. 85, 6163 (1999)
- 24. O'Barr, R., Schultz, S.: J. Appl. Phys. **81**, 5458 (1997)
- 25. Moser, A., et al.: Phys. Rev. Lett. 74, 1847 (1995)
- 26. Müller, C., Elefant, D., Leonhardt, A., Büchner, B.: J. Appl. Phys. 103, 034302 (2008)
- Lutz, M.U., Weissker, U., Wolny, F., Müller, C., Löffler, M., Mühl, T., Leonhardt, A., Büchner, B., Klingeler, R.: JPCS 200, 072062 (2010)
- 28. Peigney, A., Laurent, C., Dobigeon, F., Rousset, A.: J. Mater. Res. 12, 613 (1997)
- Dai, H., Rinzler, A.G., Nikolaev, P., Thess, A., Colbert, D.T., Smalley, R.E.: Chem. Phys. Lett. 260, 471 (1996)
- Hafner, J., Bronikowski, M.J., Azamian, B.R., Nikolaev, P., Rinzler, A.G., Colbert, D.T., Smith, K.A., Smalley, R.E.: Chem. Phys. Lett. 296, 195 (1998)
- 31. Nagaraju, N., Fonseca, A., Konya, Z., Nagy, J.B.: Mol. Catal. A. Chem. 181, 57 (2002)
- 32. Lee, S.Y., Yamada, M., Miyake, M.: Sci. Technol. Adv. Mater. 6, 420 (2005)
- 33. Cassell, A.M., Raymakers, J.A., Kong, J., Dai, H.: Phys. Chem. B 103, 6484 (1999)
- 34. Mabudafhasi, M.L., Bodkin, R., Nicolaides, C.P., Liu, X.Y., Witcomb, M.J., Coville, N.J.: Carbon 40, 2737 (2002)

- Lipert, K., Kretzschmar, F., Ritschel, M., Leonhardt, A., Klingeler, R., Büchner, B.: J. Appl. Phys. 105, 063906 (2009)
- Ritschel, M., Leonhardt, A., Elefant, D., Oswald, S., Büchner, B.: J. Phys. Chem. C 111, 8414 (2007)
- 37. Heremans, J., Olk, C.H., Morelli, D.T.: Phys. Rev. B 49, 15122 (1994)
- 38. Tsui, F., Jin, L., Zhou, O.: Appl. Phys. Lett. 76, 1452 (2000)
- 39. Byszewski, P., Baran, M.: Europhys. Lett. 31, 363 (1995)
- 40. Leonhardt, A., Ritschel, M., Elefant, D., Mattern, N., Biedermann, K., Hampel, S., Müller, Ch., Gemming, T., Büchner, B.: J. Appl. Phys. 98, 074315 (2005)
- 41. Skomski, R.: J. Phys. Condens. Matter 15, 841 (2003)
- 42. Hütten, A., Sudfeld, D., Ennena, I., Reiss, G., Wojczykowski, K., Jutzi, P.: J. Magn. Magn. Mater. 293, 93 (2003)
- 43. Neel, L.: Compt. Rend. (Paris) 224, 1488 (1947)
- 44. O'Handley, R.C.: Modern magnetic materials. John Wiley and Sons, New York (2000)
- 45. Herzer, G.: J. Magn. Magn. Mater. 112, 258 (1992)
- 46. Kersten, M.: Z. Phys. 44, 63 (1943)
- 47. Hampel, S., Leonhardt, A., Selbmann, D., Biedermann, K., Elefant, D., Mueller, C., Gemming, T., Buechner, B.: Carbon 44, 2316 (2006)
- 48. Krupskaya, Y., Mahn, C., Parameswaran, A., Taylor, A., Krämer, K., Hampel, S., Leonhardt, A., Ritschel, M., Büchner, B., Klingeler, R.: JMMM 321(24), 4067–4071 (2009)
- Heister, E., Neves, V., Tîlmaciu, C., Lipert, K., Sanz Beltrán, V., Coley, H., Silva, S.R.P., McFadden, J.: Carbon 47(9), 2152–2160 (2009)
- Hergt, R., Hiergeist, R., Hilger, I., Kaiser, W.A., Lapatnikov, Y., Margel, S., Richterd, U.: J. Magn. Magn. Mater. 270, 345–357 (2004)
- 51. Rosensweig, R.E., Magn, J.: Magn. Mater. **252**, 370–374 (2002)
- Pankhurst, Q.A., Connolly, J., Jones, S.K., Dobson, J.: J. Phys. D. Appl. Phys. 36, R167–R181 (2003)
- 53. Farle, M.: Magnetism goes nano, C4, Forschungszentrum Juelich (2005)
- 54. Kumar, C.S.S.R.: Nanomaterials for cancer therapy. Wiley-VCH, pp 291–296 (2006)
- 55. Elmore, W.C.: The magnetisation of ferromagnetic colloids. Phys. Rev. **54**, 1092–1095 (1938)
- 56. Vyalikh, A., Wolter, A.U.B., Hampel, S., Haase, D., Ritschel, M., Leonhardt, A., Grafe, H.-J., Taylor, A., Krämer, K., Büchner, B., Klingeler, R.: Nanomedicine 3(3), 321–327 (2008)
- Haase, D., Hampel, S., Leonhardt, A., Thomas, J., Mattern, N., Büchner, B.: Surf. Coat. Technol. 201, 9184–9188 (2007)
- 58. Weissker, U., Löffler, M., Wolny, F., Lutz, M.U., Scheerbaum, N., Klingeler, R., Gemming, T., Mühl, T., Leonhardt, A., Büchner, B.: J. Appl. Phys. 106, 054909 (2009)
- 59. Grimault, S., Lucas, T., Quellec, S., Mariette, F.: Quantitative measurement of temperature by proton resonance frequency shift at low field: a general method to correct non-linear spatial and temporal phase deformations. J. Magn. Res. **170**, 79–87 (2004)
- 60. Ye, X., Ruan, R., Chen, P., Chang, K., Ning, K., Taub, I., Doona, C.: Accurate and fast temperature mapping during ohmic heating using proton resonance frequency shift MRI thermometry. J. Food. Eng. **59**, 143–150 (2003)
- Kahn, T., Harth, T., Kiwit, J.C.W., Schwarzmaier, H.J., Wald, C., Mödder, U.: In vivo MRI thermometry using a phase-sensitive sequence: preliminary experience during MRI-guided laser-induced interstitial thermotherapy of brain tumors. J. Magn. Reson. Imaging 8, 160–164 (1998)
- Smith, N.B., Merrilees, N.K., Hynynen, K., Dahleh, M.: Control system for an MRI compatible intracavitary ultrasound array for thermal treatment of prostate disease. Int. J. Hyperth. 17, 271–282 (2001)
- Popescu, V.: Senzori de temperatură pe bază de filme de PbS nanostructurate. Rev. Chim. 55, 983–985 (2004)
- 64. Tan, C.M., Jia, J., Yu, W.: Temperature dependence of the field emission of multiwalled carbon nanotubes. Appl. Phys. Lett. **86**, 263104 (2005)

- 65. Murphy, C.J.: Nanocubes and nanoboxes. Science 298, 2139–2141 (2006)
- Nel, A., Xia, T., M\u00e4dler, L., Li, N.: Toxic potential of materials at the nanolevel. Science 311, 622–627 (2006)
- 67. Klostranec, J.M., Chan, W.C.W.: Quantum dots in biological and biomedical research: recent progress and present challenges. Adv. Mater. 18, 1953–1964 (2006)
- Narberhauser, F., Waldminghaus, T., Chowdhury, S.: RNA thermometers. FEMS Microbiol. Rev. 30, 3–16 (2006)
- 69. Lee, J., Govoroy, A.O., Kotov, N.A.: Nanoparticle assemblies with molecular springs: nanoscale thermometer. Angew. Chem. Inter. Ed. 117, 7605–7608 (2005)
- 70. Gao, Y., Bando, Y., Liu, Z., Golberg, D., Nakanishi, H.: Temperature measurement using a gallium-filled carbon nanotube nanothermometer. Appl. Phys. Lett. 83, 2913–2915 (2003)
- Vyalikh, A., Wolter, A.U.B., Hampel, S., Haase, D., Ritschel, M., Leonhardt, A., Grafe, H.-J., Taylor, A., Krämer, K., Büchner, B., Klingeler, R.: A carbon-wrapped nanoscaled thermometer for temperature control in biological environment. Nanomedicine 3, 321–327 (2008)
- 72. Becker, K.D.: Temperature dependence of NMR chemical shifts in cuprous halides. J. Chem. Phys. 68, 3785–3793 (1978)
- Wolter, A.U.B., Klingeler, R., Büchner, B.: Thermometry on the nanometre-scale for biomedical applications using NMR spectroscopy. J. Biomed. Nanosci. Nanotechnol. (2010) (in print)
- 74. Abragam, A. (ed.): Principles of Nuclear Magnetism. Oxford University Press (1961)
- 75. Andrew, E.R., Hinshaw, W.S., Tiffen, R.S.: Nuclear spin-lattice relaxation in solid cuprous halides. J. Phys. C Solid. State. Phys. 6, 2217–2222 (1973)

Nuclear Magnetic Resonance Spectroscopy and Imaging of Carbon Nanotubes

Vijav K. Anuganti and Aldrik H. Velders

Abstract Nuclear magnetic resonance (NMR) spectroscopy is one of the most versatile and powerful analytical tools developed in the last century and have been proven to be a suitable means for the elucidation of structural properties as well as physico-chemical characteristics in chemistry and material sciences. In the first part of this chapter a review is given on the investigation of different types of carbon nanotube (CNT) structures and properties by solution-state NMR, solid state NMR and high-resolution magic angle spinning (HR-MAS) NMR spectroscopy. (Nuclear) Magnetic resonance imaging (MRI) is one of the most powerful noninvasive diagnostic techniques used in clinical medicine for in vivo assessment of anatomy and biological functions. CNTs are unique materials that can be used as a platform for the synthesis of hybrid construct molecules capable of enabling multiple biomedical applications in vitro and in vivo as molecular transporters for drug delivery, and potential new therapeutics. In the second part of this chapter the potential use of CNTs as contrast-enhancing agent for MRI, in vitro, ex vivo and in vivo, is reviewed.

1 Introduction

Carbon nanotubes (CNTs) are unique tubular structures of nanometer size diameters and large length/diameter ratio. The nanotubes may consist of one up to tens or even hundreds of concentric shells of carbons with adjacent shells separated by

V. K. Anuganti (⋈) and A. H. Velders (⋈)

Supramolecular Chemistry and Technology Group, University of Twente, P.O. Box 217,

7500 AE, Enschede, The Netherlands e-mail: V.K.Anuganti@tnw.utwente.nl

A. H. Velders

e-mail: a.h.velders@utwente.nl

 ~ 0.34 nm. The tubular structures and CNTs were observed for the first time in carbon fibers in the 1970s [1]. It came to light when Kroto et al. discovered C_{60} , called fullerene or buckyball in honor of Buckminster Fuller, in 1985 [2]. However, the structures started to attract intensive attention only after Iiiima observed multi-walled CNTs (MWCNTs) in transmission electron microscopy in 1991 [3]. In 1993 Iijima and Bethune [4, 5] independently observed single-walled CNTs (SWCNTs). Since then, the unique structures and properties of CNTs have inspired researchers in physics, chemistry and material science to exploit their properties. CNTs have unique properties which offer a wide range of opportunities and application potential also in biology and medicine. For example, the rich electronic properties of CNTs have been explored for the development of highly sensitive and specific nanoscale biosensors. The optical absorption of CNTs in the near-infrared has been used for laser heating cancer therapy. CNTs are currently being considered to be suitable substrates for the growth of cells for tissue regeneration, as delivery systems for a variety of diagnostic or therapeutic agents or as vectors for gene transfection [6].

Many techniques have been used to characterize the structure and properties of CNTs. It has been proved that NMR spectroscopy is also a useful tool to study the structure of fullerene [7] and nanotube [8] materials, but the application of NMR spectroscopy to nanotubes has been more difficult, with substantial progress being made only in the last few years. CNTs are difficult to separate from the carbonaceous and catalytic metal impurities that are co-produced during synthesis. Advances in SWCNT synthesis and purification have allowed for the observation of the ¹³C resonance for SWCNT by solid-state NMR spectroscopy and recently ¹H NMR was used to measure water inside SWCNTs.

Nuclear magnetic imaging is a noninvasive technique, which is capable of producing images of arbitrarily oriented slices through optically nontransparent objects. Biological tissues, plants, food stuffs and many synthetic materials can be penetrated by RF waves and the signal is hardly attenuated by absorption and emission of RF energy at the resonance frequencies of the nuclear spins. The noninvasive and apparently hazard-free nature of NMR imaging techniques has inevitably led to their application in the study of biological systems, including man.

The aim of this chapter is to provide an overview of NMR spectroscopy and imaging studies of CNTs. In the first part of the chapter an overview is given on solution-state, solid state and high-resolution magic angle spinning (HR-MAS)–NMR spectroscopy of CNTs. In the second part of this chapter a brief introduction is given to NMR Imaging and an overview on application of CNTs as contrast agents in NMR imaging.

2 Nuclear Magnetic Resonance Spectroscopy of CNTs

Nuclear magnetic resonance (NMR) spectroscopy is obviously one of the most desirable instrumental methods for studying the structures and properties of raw

and functionalized CNTs, and there is increasing interest in the applications related to NMR spectroscopic investigations of CNTs. Below the major topics are subdivided into three different sections, and regard spectroscopic analyses of CNTs by solution-state NMR spectroscopy, solid state NMR spectroscopy and HR-MAS NMR spectroscopy.

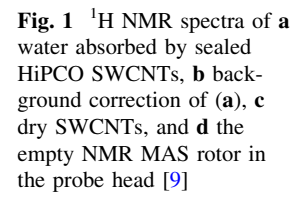
Solution-State NMR Spectroscopy of CNTs

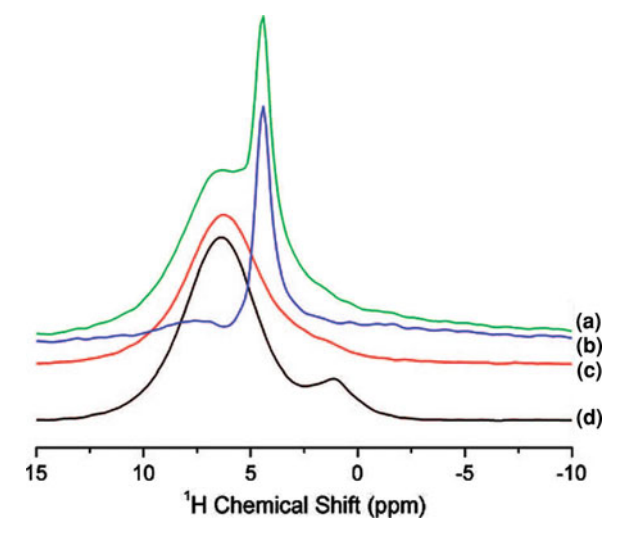
Solution-state NMR spectroscopy is a widely used technique for characterizing organic compounds, from small compounds to biomacromolecules, e.g. 100 kDa sized proteins. The nuclei of certain isotopes possess spin angular momentum ("spin") and the interaction of this spin with radio frequency radiation in the presence of a magnetic field provides a probe which is uniquely sensitive to the chemical environment of the nucleus. Information can be obtained not only about the chemical environment of the various nuclei present, but also about their connectivity and topology. In solution-state NMR spectroscopy of CNTs, the major applications are, ¹H NMR spectroscopy of CNTs, diffusion ordered spectroscopy (DOSY) of CNTs, 2D correlation spectroscopy (COSY) of CNTs and ¹³C NMR spectroscopy of CNTs.

¹H NMR Spectroscopy of CNTs

Pure CNTs obviously lack protons, so ¹H NMR spectroscopy is not the first tool of choice to investigate CNTs themselves. However ¹H NMR spectroscopy is (for example) a technique used to study the properties of H₂O inside the CNTs under nanoscale confinement (Fig. 1) [9–12], and can also give information on outer surface of functionalized CNTs [13, 14]. For example, Chen et al. [15] reported the use of ¹H NMR results to validate their proposed noncovalent d-stacking mechanism for the functionalization of SWCNTs with polymers. Holzinger et al. [14] used ¹H NMR to characterize their SWCNT samples functionalized by various substituted oxycarbonyl nitrenes. The NMR signals from the functional groups on SWCNTs are often broader than those from the free functionalization material, with generally similar patterns but sometimes upfield shifting of the signals [14, 15].

Chen et al. proved that, even after Q-factor correction, the proton signal from the empty NMR MAS rotor in the probe head (Fig. 1d) is noticeably different from that of the rotor packed with SWCNTs (Fig. 1c). Thus, background subtraction of proton signal from empty and packed rotors it would be unreliable in studying water adsorption by SWCNTs, either qualitatively or quantitatively. This subtraction method might work if factors such as the pulse length and power strength were taken into account. However, as they are concerned only with interrogating the absorbed water in the samples and not other sources of protons, all spectra





associated with water treated SWCNTs are referenced to those obtained before adding liquid water (the "dry" spectrum). The effectiveness of this method of subtracting the "dry" background can be seen by comparing (Fig. 1a, b), before and after subtracting the "dry" background from the SWCNTs dosed with about 100 wt % water [9].

Ghosh et al. reported that it is also possible to study the freezing phenomena of confined water inside SWCNTs in the temperature range of 300–200 K. This can be achieved because the transverse (spin–spin) relaxation time of mobile water (approximately a few seconds) compared with solid water, i.e. ice (\sim 6 μ s) can be used to monitor the process of freezing, through a signal that emerges upfield, or at lower ppm relative to bulk water, which was attributed to water inside SWCNTs [16].

¹H NMR spectroscopy has not been among the main tools for characterization of organically modified carbon nanostructures. ¹H NMR analysis of CNTs covalently modified with small organic molecules is limited by the low number of organic functionalities introduced, which improves only slightly the dispersibility of the derivatives in both organic solvents and aqueous solutions [17]. A few years ago, Prato and coworkers characterized the conformation of peptides covalently linked to the sidewalls of SWCNTs using 2D NMR spectroscopy [18]. In most cases, the interpretation was made particularly difficult by the weakness and broadness of the signals of the attached peptides, often below noise levels. The signals become negligible compared to the intensity of the solvent signals, and therefore very long experimental times are needed to obtain structural information [13]. Recently, to overcome these limitations, Prato et al. [19] have investigated the applicability of ¹H NMR spectroscopy based on gradient-edited diffusion pulse sequences [1D DOSY] in the characterization of CNT derivatives.

DOSY is a recently rediscovered NMR experiment allowing separation of the NMR signals from species of different sizes (hydrodynamic radii) on the basis of their apparent diffusion coefficients. In a typical DOSY experiment, a series of spectra is recorded with incremented magnetic field gradient (PFG) in a pulsed-field gradient spin-echo (PFGSE) or stimulated echo (PFGSTE) experiment. The 1D spectra are then converted into a pseudo-2D spectrum by fitting the decay of the signal as a function of PFG amplitude to the appropriate theoretical expression (1) and constructing a second, diffusion, dimension with Gaussian line shapes centered on the calculated diffusion coefficient (*D*). The decay of the signal in an ideal pulsed-field gradient echo experiment is described by the Stejskal–Tanner equation [20–22]

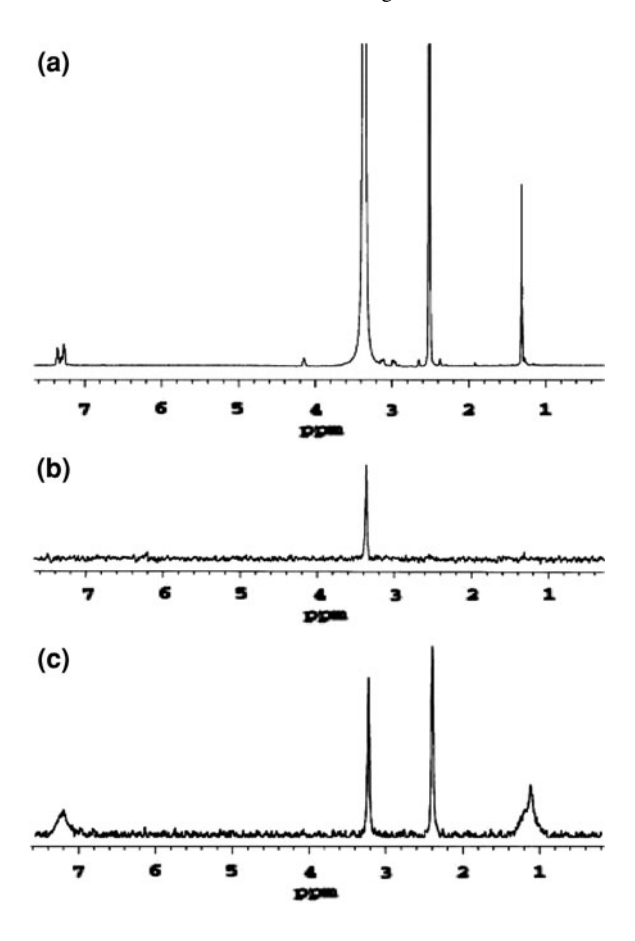
$$S = S_0 e^{-D\gamma^2 \delta^2 g^2 \Delta} \tag{1}$$

where 'S' is the signal amplitude, ' S_0 ' is the echo amplitude that would have resulted had there been no diffusion, 'D' is the diffusion coefficient, ' δ ' is the gradient pulse width, ' γ ' is the magnetogyric ratio, 'g' is the gradient amplitude, and ' Δ ' is the diffusion time corrected for the effects of finite gradient pulse width

Prato et al. used a small set of CNT derivatives covalently linked via an amide bond to organic amines starting from oxidized SWCNTs (ox-SWCNTs). These derivatives show moderate dispersability in some organic solvents such as chloroform, dimethyl formamide and dimethyl sulfoxide and were thus suitable for NMR analysis in deuterated solvents. To confirm the covalent attachment of the amines to the nanotubes, ¹H and 1D DOSY spectra of ox-SWCNT-Phe-*O-t*Bu were compared to those obtained by mixing ox-SWCNTs and HCl·H-Phe-*O-t*Bu, without using coupling reagents (Fig. 2a, b). Also the Kaiser test has been used together with the DOSY to confirm the formation of covalent derivatives of ox-SWCNTs. It was proposed [19] that this analytical techniques can be extended to other types of functionalized CNT with moderate dispersibility.

Nelson et al. reported COSY NMR experiments of 4-chlorophenyl-SWCNT, to facilitate analysis and reveal aromatic spin–spin coupling, which appears to be the first such spectrum reported for a covalently side wall functionalized SWCNT [13]. As shown in Fig. 3, the ¹H NMR spectrum of 4-chlorophenyl-SWCNT has two rather broad signals in the aromatic region at 8.12 and 7.94 ppm. This broadness could be due to short relaxation times, resulting from the large SWCNT size, or due to the aromatic functionalities associating with other SWCNTs or other aromatic groups on the same or other SWCNTs. Ju et al. [23] previously reported a 2D COSY spectrum of SWCNT with diacetylenic amine physisorbed on the surface, but not covalently bound. The COSY spectrum of 4-chlorophenyl-SWCNT (Fig. 3) reveals that the two aromatic signals are coupled and 0.18 ppm apart. Nelson et al. [13] demonstrated that 2D correlation NMR spectroscopy (COSY) can be applied to characterize functionalities covalently attached to SWCNT sidewalls.

Fig. 2 a ¹H NMR and **b** 1D DOSY spectra of the mixture of ox-SWCNTs and HCl·H-Phe-O-tBu at 36.5 G cm⁻¹, and **c** 1D DOSY spectra of ox-SWCNTs-Phe-tBu at 36.5 G cm⁻¹ [19]



¹³C NMR Spectroscopy of CNTs

Although some research has been going on NMR investigations of functionalized CNTs, still several technical difficulties have hindered ¹³C NMR spectroscopy of the functionalized CNT itself in solution. The limitations comprise limited sample solubility and the presence of impurities, among others, together with the intrinsic low sensitivity of natural-abundance of the ¹³C isotope. Kitaygorodskiy et al. reported the solution-phase ¹³C NMR study of ¹³C isotropically enriched functionalized CNTs. High nanotube dispersibility was achieved via functionalization of SWCNTs with diamine-terminated oligomeric poly (ethylene glycol). The residual metal catalysts were effectively removed from the functionalized nanotube sample in solution via repeated magnetic separation. The solution-phase NMR results have been compared with those from solid-state NMR measurements (Fig. 7). The partially resolved nanotube carbon signals in the NMR spectra are discussed in terms of theoretically predicted difference in chemical shifts between semiconducting and metallic SWCNTs [24, 25].

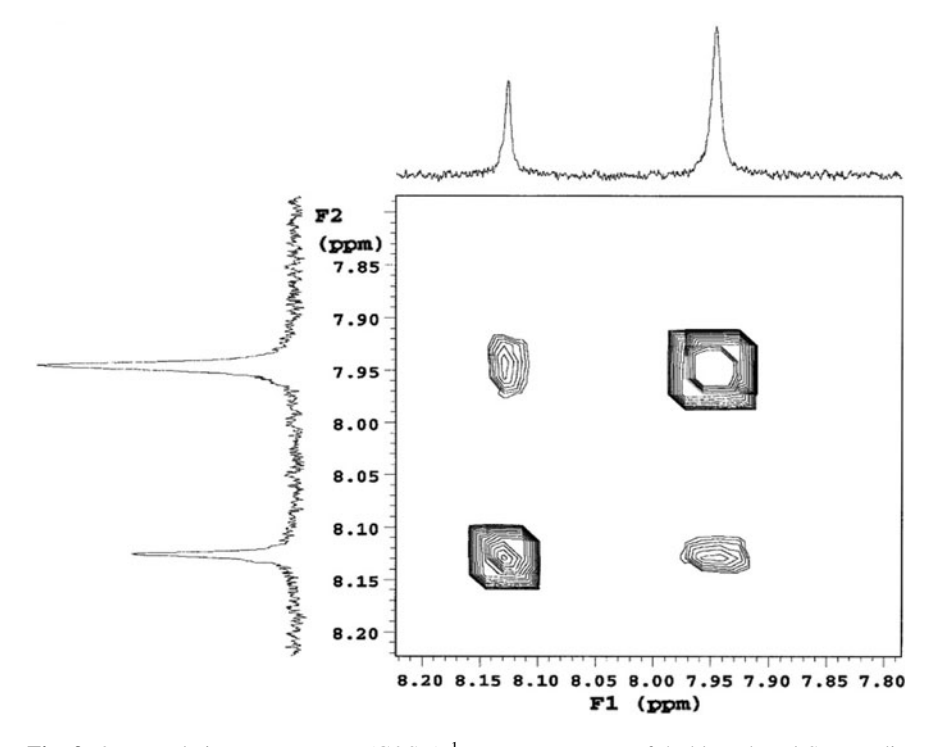
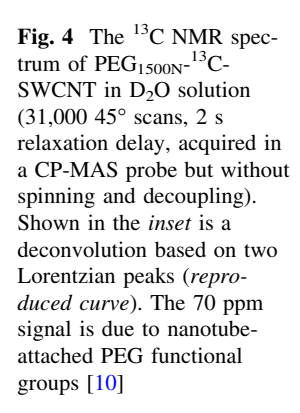
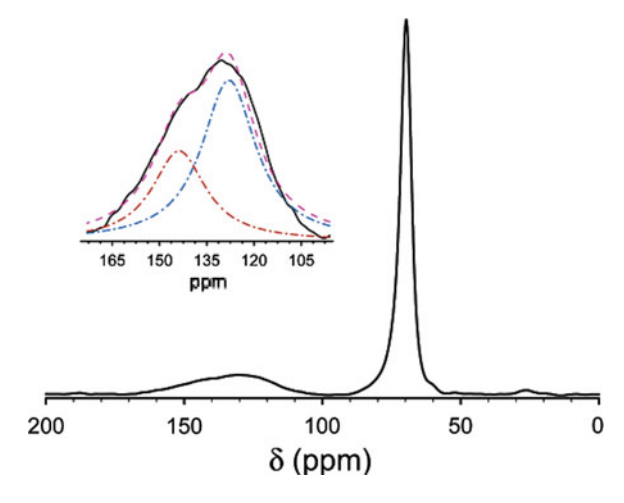


Fig. 3 2D correlation spectroscopy (COSY) ¹H NMR spectrum of 4-chlorophenyl-SWNT displays coupling of aromatic peaks at 8.12 and 7.94 ppm [13]





As shown in the Fig. 4, for $PEG_{1500N}^{-13}C$ -SWCNT in D_2O (suspension concentration ~ 36 mg ml⁻¹ SWCNT equivalent), the nanotube sp^2 carbons exhibit a broad signal centered at ~ 132 ppm [full width half maximum ~ 28 ppm], which

is consistent with theoretical predictions and close to what is observed in solidstate NMR [26]. So, nanotube carbons can be detected by ¹³C NMR in solution, and the broadness in the signals reflects the chemical shift dispersion of nanotube carbons, which are likely inhomogeneous due to different nanotube chiralities, lengths, adjacent defects, etc. However, there are some distinctive features in the broad signals, which through deconvolution (resolving the curve into underlying peaks) can be represented by two Lorentzian peaks of similar line widths of ~ 20 ppm. The ratio of area under the peak centered at 128 ppm to that at ~ 144 ppm is ~ 1.8 . A variation of relaxation delay time from 3 to 0.4 s had little effect on the signal shape, with similar line widths and chemical shifts, and, see (Fig. 8), the two peaks were tentatively assigned to semiconducting (upfield) and metallic (downfield) SWCNTs. In fact, the difference in their chemical shifts (16 ppm) is in reasonable agreement with what has been predicted by Goze-Bac et al. [24, 25] in their theoretical calculations, suggesting that there should be an approximately 12 ppm upfield shift for the semiconducting nanotube carbons from their metallic counterparts due to the localized ring currents.

Solid State NMR Spectroscopy of CNTs

Solid-state NMR spectroscopy rarely produces resolution that is as high as that from solution-state NMR. This difference is due to anisotropic interactions such as dipolar couplings, chemical shift anisotropy (CSA) and quadrupolar couplings and the fact that, in the solid state, chemically equivalent nuclei might be in different magnetic environments and thus have different resonance frequencies [27–29]. These anisotropic interactions, on the one hand have the significant disadvantage of hindering the resolution of distinct sites, but on the other hand, contain valuable structural and dynamic information. Specifically, the CSA and quadrupolar interactions provide insight into electronic structure and bonding, while the dipolar coupling offers direct access to internuclear distances. Moreover, all three anisotropic interactions are formidable probes of dynamic features. In solution, fast isotropic tumbling of the molecules causes the averaging to zero of the line broadening due to the anisotropic interactions. Rather than requiring random isotropic motion of each molecule, it can be shown that a physical rotation (typically 10-25 kHz) of the whole sample around an axis inclined at an angle of $\arctan(\sqrt{2})$ (viz. 54.7°, referred to as the magic angle) to B_0 suffices to average any second-order tensor interaction to zero. MAS is as successful as a means of line narrowing, and it is first necessary to recognize that the CSA, dipolar, and first-order quadrupolar interaction all have basically the same orientational dependence. Solid state NMR spectroscopy has been used to study different types of CNTs. In this section we briefly discuss ¹³C MAS NMR spectra of CNTs, ¹²⁹Xe and ¹³¹Xe NMR studies and ⁵⁹Co and ⁵⁷Fe NMR studies on filled CNTs.

¹³C NMR Spectroscopy of CNTs

There have been extensive recent investigations on the detection of CNTs by ¹³C NMR spectroscopy. In ¹³C NMR spectroscopy of CNTs, the following interactions are taken into consideration; chemical shift interaction, Knight Shift interaction, bulk magnetic susceptibility and dipole–dipole interaction [24, 30–34].

Figure 5 shows the static spectrum of SWCNTs as well as static and MAS spectra of ¹³C enriched double-walled CNTs (DWCNTs). Singer et al. have calculated the mass fraction belonging to the enriched phase relative to the total sample mass from the integrated NMR signal by comparing it to the NMR signal of 89% ¹³C enriched fullerene. They found that the mass ratio of inner tubes as compared to the total sample mass is 15%, obtained from the SWCNT purity (50%), $\approx 70\%$ volume filling in highly filled samples, and the mass ratio of encapsulated fullerenes to the mass of the SWCNTs. The measured mass fraction of the highly enriched phase is very similar to that of the calculated fraction of inner tubes. They suggest that the NMR signal derives nominally from inner tubes and that other carbon phases such as amorphous or graphitic carbon are not enriched [35]. Tang et al. [8] reported the static and MAS-NMR spectra of purified CNTs (10% enriched in ¹³C), and determined an isotropic shift of 124 ppm for these samples. Later on, Latil et al. [32] concluded that the presence of paramagnetic or ferromagnetic impurities in bundles of SWCNTs broaden the NMR response at 126 ppm and Hayashi et al. [30] have reported the synthesis of SWCNTs by catalytic decomposition of enriched ¹³C methane (99.9%) over Fe catalysts at 1,073 K. The ¹³C isotropic shift estimated was 116 ppm. Two

Fig. 5 NMR spectra normalized by the sample mass: **a** static spectrum for non enriched SWCNT enlarged by a factor of 15, **b** static and **c** MAS spectra of ¹³C_{0.89}-DWCNT. *Smooth curve* is a simulated CSA powder pattern. Spinning sidebands at 8 kHz are marked with *asterisks*. Frequency reference is TMS (tetramethylsilane) line [35]

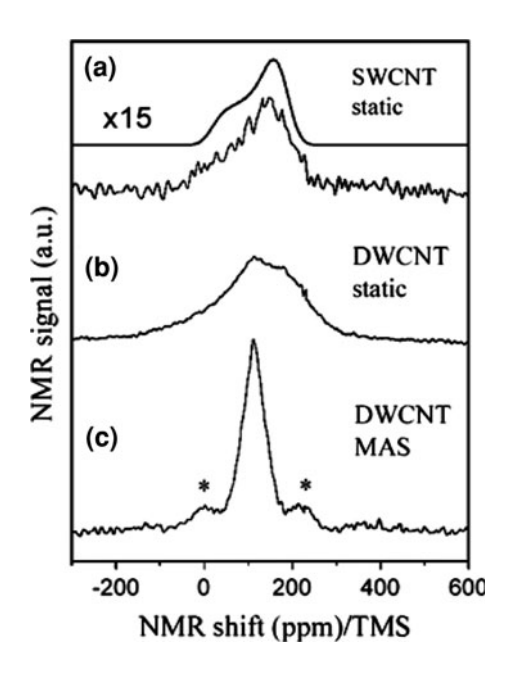
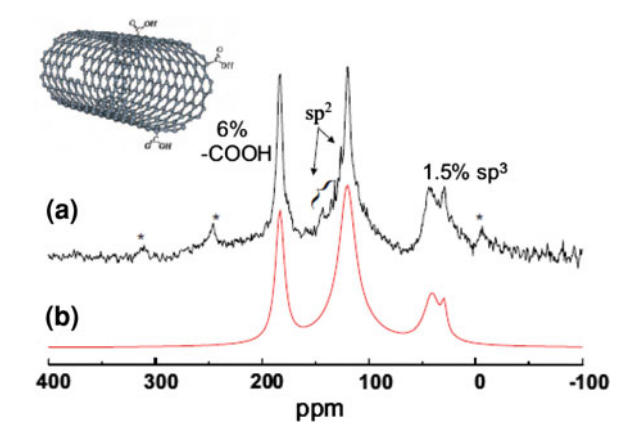


Fig. 6 ¹³C proton decoupled MAS–NMR spectrum of functionalized SWCNT (a) and its deconvolution with five Lorentzian lines (b) [24]

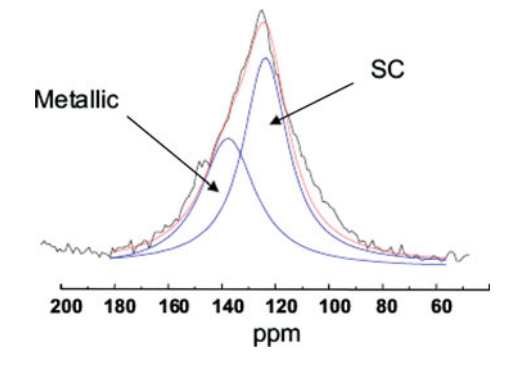


additional bands at 171 and 152 ppm were detected and ascribed to carbon oxidized species at defects or edges after purification with nitric acid treatments.

Goze-Bac et al. reported the high-resolution 13 C MAS-NMR spectra of purified and functionalized SWCNT recorded with proton-decoupling in order to remove 13 C NMR line broadenings due to dipolar coupling (Fig. 6). The disadvantage of SWCNT purification is the modification of the electronic properties of SWCNT due to nanotube-sidewall functionalization, the formation of defects in the SWCNT and even the possibility of nanotube-opening by oxidative end-cap removal. Upon SWCNT purification with 65% nitric acid treatment the NMR line structure drastically changed. Besides a modification of the sp^2 carbon signal, the appearance of an additional –COOH line as well as an sp^3 line is observable. This is a clear signature of SWCNT functionalization and existence of a large variety of defects. Even though reversibility of the functionalization by high temperature treatment was proven, a regeneration of removed SWCNT end-caps is rather improbable [24, 25].

Theoretical calculations have shown that the total degree of carbon sp^2 – sp^3 -rehybridization required to form the curvature of a nanotube surface is rather small, constant and independent of nanotube chiralities. Therefore, the Pople part contribution to chemical shifts in SWCNT should be more or less negligible [36]. This is different from the chemical shift behavior in fullerides, where the hybridization Pople part is dominant [24]. Furthermore, the Knight shift (observable in metallic compounds and arises from electron nuclear spin–spin hyperfine interactions) contribution in pristine SWCNT is rather small and negligible [37]. It depends on the density of states at the Fermi level which accounts only for about $\eta(\varepsilon F) \sim 0.015$ states/eV · spin · atom in metallic SWCNT [38]. Therefore, the difference between the isotropic line position of isolated metallic and semiconducting SWCNT is solely determined by the London ring-current shift contribution. This leads to a calculated isotropic line splitting of 12 ppm (Fig. 7) [24]. However, this splitting of metallic and semiconducting SWCNT ¹³C NMR lines

Fig. 7 Isotropic ¹³C NMR line at 126 ppm and its deconvolution with two Lorentzian lines attributed to metallic and semiconducting SWCNT [25]



should be rather difficult to observe, since paramagnetic impurities and defects in SWCNT will broaden NMR spectra.

¹²⁹Xe and ¹³¹Xe NMR Studies on CNTs

Nuclear magnetic resonance spectroscopy of adsorbed xenon is a relatively new NMR technique, which is able to provide independent information on the structure of porous adsorbents and catalysts. Using xenon in natural isotopic abundance allows for studying both ¹²⁹Xe and ¹³¹Xe, and chemical shifts are related to xenon's physical state of matter (gas, liquid, or solid), relaxation time measurements reveal information about the nature of the adsorption process and related activation energies. The chemical shift of xenon gas is pressure and temperature dependent and is the same for both nuclear isotopes ¹²⁹Xe and ¹³¹Xe. The resonance frequency of free xenon gas is linearly dependent on gas density with a shift close to 0 ppm [39], and xenon gas extrapolated to zero density is thus used as the chemical shift reference. Solid xenon resonates at around 300 ppm, and liquid xenon, which appears as a narrow peak, resonates around 240 ppm. NMR signals arising from physisorbed xenon can be observed even at room temperature. For weaker interactions, the adsorbed phase signal becomes visible only at lower temperatures as observed for oxidatively purified multi-walled CNTs [40]. 129Xe and ¹³¹Xe NMR has been rarely used to probe the properties of carbon materials and carbon-based catalysts [41, 42].

Clewett and Pietras [41] reported the study of adsorption of xenon gas on single-walled and multi-walled CNTs with ¹²⁹Xe and ¹³¹Xe NMR spectroscopy. Overall, the adsorption was weak, with slightly stronger interaction between xenon and multi-walled nanotubes. Figure 8 shows the ¹²⁹Xe and ¹³¹Xe NMR spectra of SWCNTs and MWCNTs at various temperatures. As shown in Fig. 8a, b, in the case of MWCNTs, the Xe gas peak close of 0 ppm is observed in the temperature range from 213 K, below this temperature its shifts downfield due to increased interactions with the sample surface. This effect is most obvious in the ¹²⁹Xe NMR of MWCNTs, indicating stronger interaction than in SWCNTs (see vertical lines in

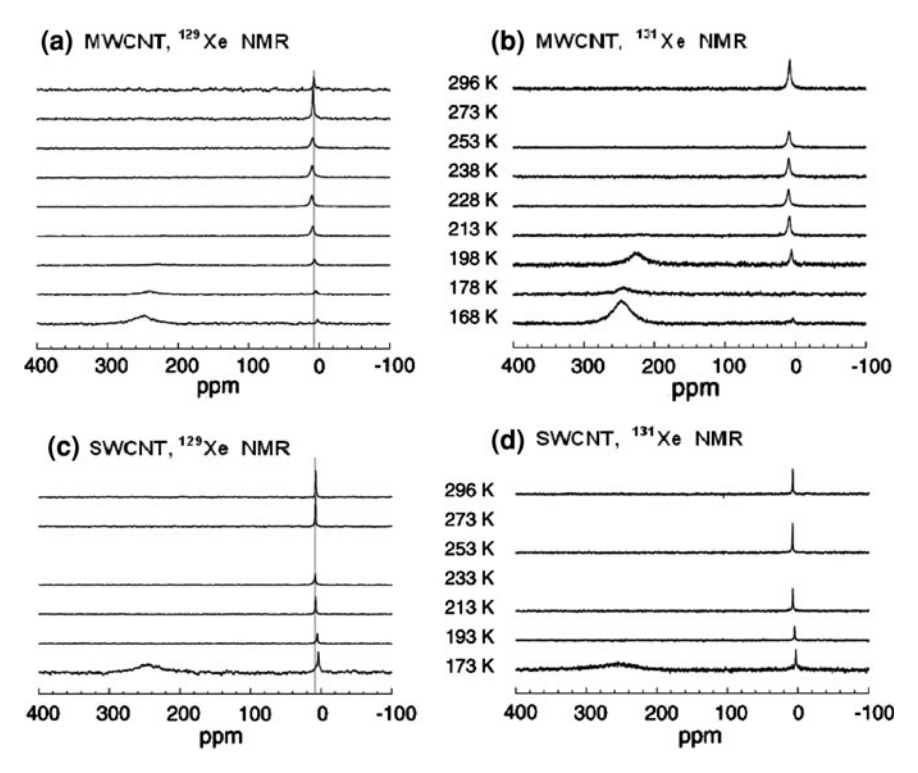


Fig. 8 129 Xe and 131 Xe spectra of xenon on single-walled and multi-walled carbon nanotubes at various temperatures. The *vertical lines* in the 129 Xe spectra highlight the shift of the gas phase resonance. Signal intensities have been scaled to account for the different number of scans used at different temperatures, resulting in different noise levels. The relaxation delay was optimized based on T_1 . **a** 129 Xe NMR, MWCNT, **b** 131 Xe NMR, MWCNT, **c** 129 Xe NMR, SWCNT and **d** 131 Xe NMR, SWCNT [41]

Fig. 8c, d). It has been hypothesized that, on single-walled nanotubes, xenon preferentially adsorbs on the metal particles that give rise to rapid Korringa relaxation, rendering adsorbed xenon invisible due to extreme line broadening. As more layers build up at colder temperatures, the xenon becomes observable by NMR as a multilayer, bulk-like phase. For the multi-walled tubes, xenon preferentially adsorbs onto defect sites which become rapidly saturated due to their smaller size, and more xenon remains detectable by NMR.

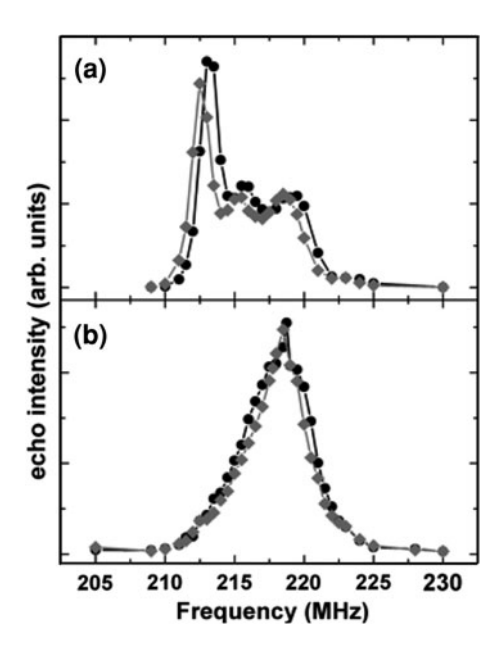
⁵⁹Co/⁵⁷Fe NMR Spectroscopy of CNTs

There is an increasing interest in using filled (Fe/Co) CNTs for biomedical applications, therapeutics and diagnostics. Vyalikh et al. [43] describe ⁵⁹Co and ⁵⁷Fe NMR studies on filled CNTs. Dujardin et al. [44] also carried out ⁵⁹Co

NMR experiments to show that non-metallic cobalt as well as the Co–Ni alloy are still present in the purified samples of CNTs. Vyalikh et al. proposed that 59 Co NMR has an advantage because various NMR active isotopes can be probed within one substance and different NMR characteristics can be investigated (e.g. NMR shift, relaxation times, J-coupling, quadrupolar splitting or line width). Due to very low sensitivity and low abundance in nature of a 57 Fe nucleus only a weak 57 Fe NMR signal can be observed in iron-filled CNT even after few hours of accumulation time at room temperature. The long measurement time and the low signal-to-noise ratio makes 57 Fe NMR spectroscopy an inefficient tool for thermometry, particularly in the temperature range of the biological interest, i.e. $\sim 300-320$ K [43].

Vyalikh et al. have shown the variable temperature ⁵⁹Co NMR spectra of Co-filled CNT (Fig. 9) together with the spectra measured on the reference metallic cobalt powder. Their measurements show the remarkably intense signals resulting from the 100% natural-abundance and high sensitivity of a ⁵⁹Co nucleus. A temperature shift of the highest peak in the ⁵⁹Co NMR spectrum (Fig. 9a) arising from domains in hexagonal close packed (hcp) cobalt renders a high temperature sensitivity parameter of 26 kHz K⁻¹ that provides a prerequisite for the application of Co-based nanothermometers. However, the ⁵⁹Co NMR spectrum of Co-CNT (Fig. 9b) is broadened and unresolved due to the distribution of the resonance frequencies due to distribution of sizes and shapes of encapsulated cobalt [43].

Fig. 9 ⁵⁹Co NMR spectra of a metallic Co powder and **b** Co-filled MWNT. *Dark symbols* and *line* correspond to spectra at 295 K, *light ones* to spectra at 320 K [43]



HR-MAS-NMR Spectroscopy of CNTs

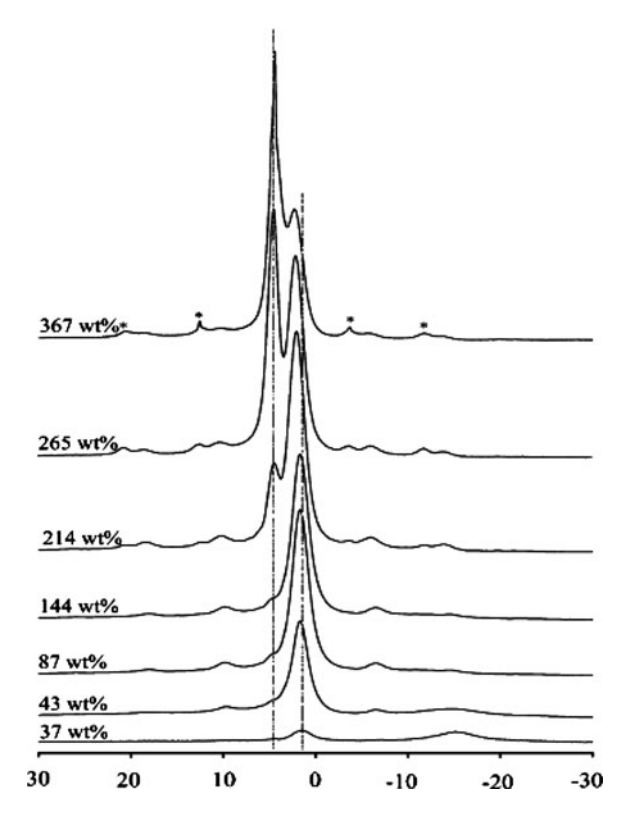
High-resolution magic angle spinning NMR spectroscopy has become an extremely versatile tool to study heterogeneous systems. HR-MAS relies on MAS of semi-solid or dispersed samples to average out to zero magnetic susceptibility differences in the sample and to obtain resonance line widths approaching those of liquid-state NMR spectroscopy [45]. HR-MAS experiments are usually performed on standard liquid-state NMR spectrometers equipped with an HR-MAS probe that allows spinning the sample at the magic angle typically at few kilohertz. Since the radio frequency circuits of these probes are designed to withstand only the power classically available on liquid-state NMR spectrometers, they cannot be used to perform standard solid-state type experiments. They are usually fitted with a gradient coil generating a linear field gradient along the magic angle axis that allows performing coherence selection experiments. Typically the rotors made of ZrO₂ are used to put the sample, these rotors can withstand the strong centrifugal forces created by high spinning speeds. To optimize the sensitivity of the probe, the rotor is fitted with Teflon inserts to define a 20–100 µl volume that matches the detection volume of the solenoidal coil.

¹H NMR Spectroscopy of CNTs

The behavior of water confined in nanoscale environments is of great interest, and CNTs furnish an ideal system to study the water confined spaces. Sekhaneh et al. [46] reported the ¹H HR-MAS studies of water confined in, and adsorbed on, single-wall CNTs (SWCNTs). The ¹H NMR spectrum, which shows at least two different chemical shift ranges for water, strongly depends on the amount of absorbed water, the temperature and the amount of remaining catalyst in the sample. Mao et al. [12] reported the water adsorption of isotherms at room temperature in SWCNTs. Ghosh et al. [16] also reported the water confinement in SWNTs as a function of temperature from 210 to 300 K.

Figure 10 shows the ¹H spectra of water in SWCNTs as a function of increasing amount of water. The spectra show that at lowest water loading (37 wt%), there are two lines around 1.3 and -15.1 ppm. Upon increase of the amount of water, the line at -15 ppm weakens and the line at 1.3 ppm grows in intensity, and also shifts to low field with increasing amount of water, possibly because of exchange with the new line that appears at 4.6 ppm around 214 wt% of water. Sekhaneh et al. [47] also reported that since the inter-tube distance of SWCNT bundles are 0.34 nm, the water cannot penetrate inside the inter-tube void. Therefore, the water should remain inside the tubes or outside the bundles It has been observed that the line at 4.6 ppm, very near to that of free water (4.8 ppm), becomes stronger and stronger by adding more and more water and at very high water content completely overwhelms the other lines. This is a strong indication that the water resonating at 4.6 ppm is due to the water present outside the nanotubes.

Fig. 10 ¹H HR-MAS spectra in SWCNTs as a function of increasing amount of water [46]



NMR spectroscopy is very sensitive in detecting the difference between the liquid and the solid phase of water [16, 48]. The resonance of ice is approximately 50,000 Hz wide [49], which corresponds to 125 ppm at 400 MHz spectrometer. A transition from water to ice caused the complete disappearance of the water line from their spectra. Sekhaneh et al. also reported the proton spectra of the SWCNTs at water loadings of 87, 214 and 318 wt% as a function of temperature. It has been shown that the line at around 4.6 ppm disappears at temperatures at around 250 K, but the water responsible for the line at around 1.3 ppm is liquid down to a temperature of at least 244 K for 87% of water and down to at least 220 K for 214–366% of water. This finding strongly supports the assignment of the 4.6 ppm resonance to more or less free water, adsorbed at the outside of the nanobundles and the 1.3 ppm line to water inside the nanotubes.

At low water content, except for the unassigned line at -15 ppm, Mao et al. detected one line at 1.3 ppm [12]. Ghosh et al. also shows two lines, but their behavior with temperature differs from that of their two lines at 4.6 and 1.3 ppm at higher water loadings; the high field line disappears first when the temperature is lowered, and assigned [16] assigned these two resonances to water outside and inside SWCNTs, respectively. With this assignment, the spectra confirm that the

first water absorbed by dry SWCNTs is absorbed inside the tubes; moreover, the water inside the tube freezes at temperatures far below 273 K [50].

3 NMR Imaging of CNTs

Magnetic resonance imaging is a powerful diagnostic noninvasive technique which can penetrate deep into tissue (unlike optical approaches), provides excellent soft tissue contrast with sub-millimeter resolution on clinical scanners (far better than nuclear imaging techniques), and does not employ ionizing radiation (like γ- and X-ray imaging). The majority of non-MR-based techniques used for imaging or for in vivo studies involve ionizing radiation in one form or another. For example, computer-assisted tomography (CT) uses X-rays, and positron emission tomography (PET) involves the administration of radioactive tracers. Imaging can be performed using planar gamma cameras (scintigraphy) or single photon emission computed tomography (SPECT) systems. Therefore the use of (N)MR imaging instead of traditional radioisotope techniques, not only minimizes the exposure of radioactivity to the patient but also eliminates the cost of the disposal of radioactive materials. Targeted contrast agents add molecular specificity to the rich anatomical and functional information already attainable by MRI. The major challenge for molecular MR imaging is sensitivity. In clinical MRI, water is imaged and contrast arises because of differences in water content among tissues or differences in the relaxation times, T_1 and T_2 , of the hydrogen nuclei. Contrast agents catalytically shorten T_1 and T_2 of water molecules encountering the agent. Despite high relaxation efficiencies, micromolar concentrations of Gd^{III} are required to cause detectable T_1 change in 55 M bulk water. This concentration requirement makes detecting proteins by MRI a challenge, but the attributes of MRI (resolution, no radiation, and shelf-stable contrast agents) make this challenge worth meeting. Relaxivity $(r_1 \text{ or } r_2)$ is the change in the relaxation rate $(\Delta = 1/T_{1 \text{or } 2})$ normalized to the concentration of the contrast agent (CA) expressed in millimolar. The observed relaxation rate is given by Eq. 2.

$$[T_i]^{-1} = [T_i^0]^{-1} + r_i[CA] \quad i = 1, 2$$
 (2)

 T_i^0 is the relaxation time in the absence of a contrast agent. The signal is proportional to $1/T_1$ and thus depends upon both the concentration of the agent and its relaxivity. This differs from nuclear and X-ray agents, which only depend upon the concentration [51].

The current MRI contrast agents in clinical use are in the form of either paramagnetic complexes [52] or superparamagnetic nanoparticles [53]. Paramagnetic complexes, which are usually gadolinium (Gd^{3+}) or manganese (Mn^{2+}) chelates, accelerate the longitudinal (T_1) relaxation of water protons and therefore exhibit bright contrast where they localize. Gadolinium diethylenetriaminepentaacetate (Gd-DTPA) has been the most widely used T_1 contrast agent. On the other

hand, superparamagnetic iron oxide nanoparticles accelerate the transverse (T_2) relaxation of water protons and exhibit dark contrast. Commercially used T_2 contrast agents of iron oxide nanoparticles are synthesized in the aqueous phase via a co-precipitation method and stabilized with hydrophilic polymers, such as dextran.

The start of MR imaging is attributable to Lauterbur, who generated the first two-dimensional MR image which depicted the proton (1 H) density and the NMR spin lattice relation time (T_1) distribution in two 1-mm tubes containing water, and proved the relation between location and frequency by causing linear variations of resonance frequencies using a spatial gradient of the static field B_0 [54]. Earlier, Gabillard [55] investigated one-dimensional distributions of the NMR signal, and Damadian patented a device for detecting cancer by NMR after discovery that the T_1 s of cancerous tissues are longer than those of healthy tissue [56]. In 1979, Hinshaw [57] demonstrated NMR imaging in biological systems. In 1977 Damadian [58] performed the first MRI scan of the human body, and Ernst (Nobel Prize, in 1991), suggested the use of phase and frequency encoding and Fourier transformation which are routinely used in MRI [59]. In 2003 Lauterbur and Mansfield [60, 61] were awarded the Nobel Prize for their discoveries concerning MRI.

In this last section we give an overview of the potential use of CNTs filled and functionalized with metal complexes as contrast-enhancing agents for MRI of biological systems. Below we report on fullerenes, single-walled CNTs, Fe-enriched SWCNTs and MWCNTs as MRI contrast agents.

Fullerenes as MRI Contrast Agents

Fullerenes are molecules composed entirely of carbon, in the form of a hollow sphere, ellipsoid, tube, or plane. Spherical fullerenes are also called buckyballs, and cylindrical ones are called CNTs or buckytubes. Because of shape, structure and properties it was speculated that fullerenes might be used to safely encapsulate and carry medically useful metals to different parts of the body where they could then be used for diagnostic or therapeutic purposes. The use of fullerene molecules as cages or carriers for diagnostic or therapeutic entities was first proposed by Watson et al. [62]. In an MRI study by Sitharaman et al. [63] polycarboxylated GdC₆₀ derivatives were tested in vitro in mouse stromal cells and NIH 3T3 mouse fibroblast cells. Similarly in vivo MRI scans with polycarboxylated gadofullerene revealed that this gadofullerene acted as an effective MRI contrast-enhancing agent with a biodistribution similar to Gd(III) based MRI contrast agents with weaker reticuloendothelial system (RES) uptake [64]. Besides metal encapsulated fullerenebased contrast agents, other NMR active isotopes such as ¹⁹F fluorinated fullerene, a perfluorinated metallofullerene ($C_{60}F_{60}$), have also been proposed for MRI studies. These contrast agents afford the possibility of conducting direct ¹⁹F MR imaging studies [65]. However, owing to the increased tissue toxicity due to high fluorine and metal concentrations, only a low concentration of the contrast agent can be used. As a result, the sensitivity and signal strength represent a significant challenge for applications in vivo. The solubility of $C_{60}F_{60}$ is also an impeding factor which renders this agent impractical as an MRI contrast agent for use in vivo. In addition these fullerene agents are still toxic which prevents the ultimate use in vivo but efforts to render them non-toxic are ongoing.

MR Imaging of SWCNTs

Single-walled CNTs possess unique characteristics desirable for biomedical applications, potential drug and contrast agent carrier systems. These nanocarriers are natural successors for α , β and γ cyclodextrins and dendrimers, which have been widely investigated for their potential use as pharmaceutical carrier systems. The similarity between α , β and γ cyclodextrins and nanotubes lies in their internal structure and inclusion techniques. CNTs are tubular objects with a high aspect ratio and a diameter in the nanoscale range [66]. The length of SWCNTs ranges from few nanometers to few hundred microns, but ultra-short nanotubes (US tubes) (20–100 nm) are well suited for cellular uptake, biocompatibility, and elimination from circulation. Additionally, the US-tube exterior surface provides a versatile scaffold for attachment of solubilizing groups and targeting ligands, while its interior space allows for encapsulation of atoms, ions, and even small molecules (Fig. 11) [67, 68].

Sitharaman et al. [69] first reported the application of Gd³⁺-functionalized CNT-based contrast agent in MRI imaging called a "gadonanotube". Their research demonstrated the ability of US tubes to encapsulate smaller ions or molecules within their framework by successfully loading and confining Gd³⁺ ion clusters within US tubes. Relaxometry and magnetometry studies revealed that these Gd³⁺ ultra small tube species are linear superparamagnetic molecular magnets with MRI efficacies 40–90 times larger than any current Gd³⁺ based contrast agent in clinical use. As such, gadonantubes, with their embedded 2–5 nm

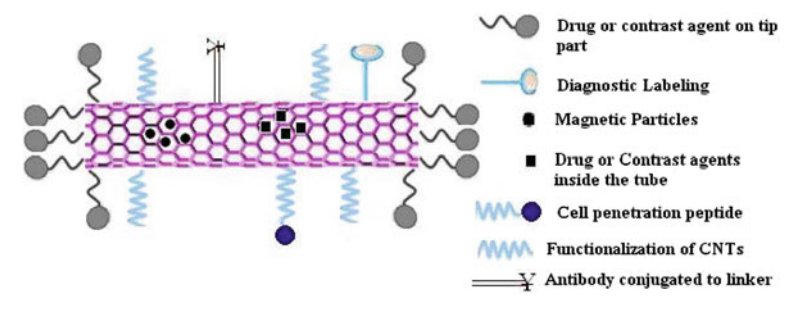


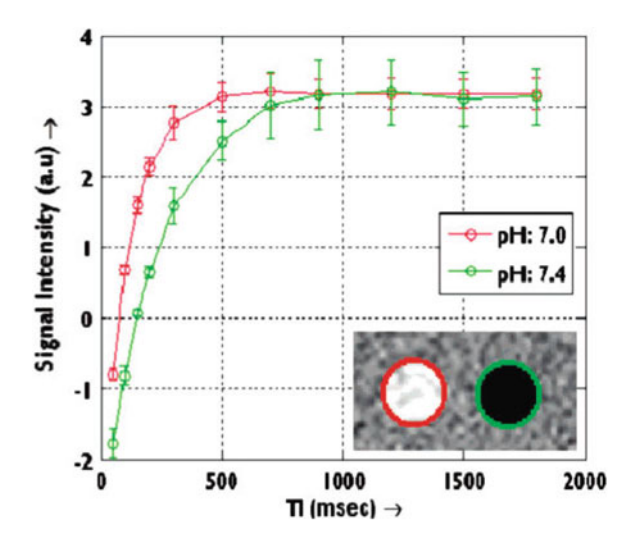
Fig. 11 Different strategies associated with carbon nanotubes (CNTs) to be used as a carrier system for various types of drugs and contrast agents

super paramagnetic Gd³⁺ ion clusters, demonstrate potential as a completely new strategy for the development of high performance MRI contrast agents. These nanotubes could represent a versatile tool for engineering a safer and more effective contrast agent. Moreover, targeting moieties can be added to specifically direct the nanotubes to a certain type of cell and/or tumor tissues.

Another study, conducted by Hartman et al. [70] describes nanoscalar, superparamagnetic Gd³⁺ ion clusters confined within pH-sensitive surfactant-suspended ultra-short (20-80 nm) single-walled CNTs. In that study, gadonanotubes have also been shown to maintain their integrity when challenged ex vivo by phosphatebuffered saline solution, serum, heat, and pH cycling. Furthermore, the synthesized gadonanotubes possessed ultra sensitive pH-smart probes characteristics with their r_1 /pH response. In fact, at the pH value of 7.4 or below, the r_1 relaxivity of gadonanotubes, 180 mM⁻¹ s⁻¹, is an order of magnitude greater than for any other MR contrast agent. As shown in Fig. 12, to confirm its pH-dependent properties of gadonanotubes, samples were divided into two parts, in which one part was adjusted to a pH of 7.0 and a second to a pH of 7.4. A T₁-weighted inversionrecovery scan confirmed a large relaxivity difference between the two samples (Fig. 12), which differed by a mere 0.4 pH units. The relaxivities from the images were calculated to be 200 mM $^{-1}$ s $^{-1}$ (pH 7.0) and 98 mM $^{-1}$ s $^{-1}$ (pH 7.4) at 25°C. This suggests that novel contrast agents composed of nanotubes might be excellent candidates for the development of clinical agents for the early detection of cancer where the extracellular pH of tumors can drop to pH = 7 or below. Unfortunately, the in vivo application of these nanoparticles to any of the gynecological malignancies is yet to be explored.

Al Faraj et al. [71] carried out a noninvasive follow up study to evaluate the biodistribution and effect of nanotube deposition after exposure directly in vivo. Combined helium-3 and proton magnetic resonance imaging (MRI) were used in a rat model to evaluate the biodistribution and biological impact of raw single-wall

Fig. 12 An inversion-recovery scan at a 150 ms time slice of the gadonanotubes at pH 7.0 (*inset*, *left*) and pH 7.4 (*inset*, *right*) at 1.5 T and 25 C; $T_1 = 110$ ms at pH = 7.0 and $T_1 = 219$ ms at pH = 7.4. The *circles* around the *inset slices* are not analyzed regions of interest, but are present only to indicate coordination with the proper relaxivity fit [70]



CNTs (raw-SWCNTs) and super purified SWCNTs (SP-SWCNTs). A gradientecho imaging sequence was used to evaluate the presence of SWCNTs in systemic organs. Since most of the nanomaterials exhibit high uptake in RES, contrast-tonoise ratios (CNRs) was measured in liver, spleen, and kidneys, and chosen as an index of SWCNT deposition [71]. Within the liver, ROIs were drawn around apparent vascular structures and these regions subtracted out of the map to retain liver parenchyma only. ROIs encompassing the whole spleen and the two kidneys were manually selected for signal measurement. Figure 13 shows the CNR values were statistically identical over the 2 weeks of investigation in both raw- and SP-SWCNT exposed animals. In the raw-SWCNT injected group, a two- to threefold decrease of CNR (corresponding to proton NMR signal attenuation) in the spleen and kidneys was observed up to 24 h after injection. This effect decreases gradually with time, and CNR values become comparable to control groups 2 weeks after instillation Susceptibility effects (decrease of proton signal intensity) were measured as well in the animal group injected with raw-SWCNT. These findings indicate that nanotube impurities can be used for the detection of CNTs in systemic organs using standard proton MR techniques.

Major disadvantage of MRI is its inherent low sensitivity, which can only be partially compensated by working at higher magnetic fields (4.7–14 T), acquiring data for much longer time periods, and using exogenous contrast agents. Although

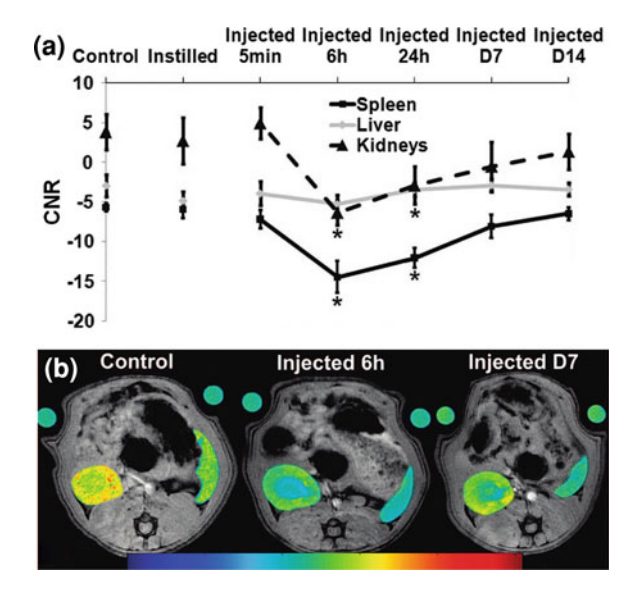


Fig. 13 a Graph showing CNR variation of control, instilled (averaged over the 2-week investigation) and injected animals 6, 24 h, 1 week, and 2 weeks after raw-SWCNT injection in spleen, liver, and kidneys. *Asterisks* indicate statistically different values from the control group (p < 0.05). **b** Proton MR images of an injected rat: (1) before, (2) 6 h after, and (3) 7 days after injection showing signal variation in the spleen and kidneys. The superimposed signal intensity color maps over kidneys and spleen indicate the MR signal intensity drops post injection [71]

proof-of-principle studies have been reported for several targets [72], whether molecular MRI can significantly improve patient management remains to be elucidated in future studies. Currently, it is unclear whether Gd³⁺ containing SWCNTs can be molecularly targeted and perform well in animal studies, which needs to be demonstrated before any clinical applications can be in place.

MR Imaging of Fe-Enriched SWCNTs

Choi et al. [73] demonstrated for the first time the multifunctionality of functionalized single-walled CNT/iron oxide nanoparticle complexes as dual magnetic and fluorescent imaging agents. Figure 14 shows a MR image of macrophage cells incubated with the Fe-enriched SWCNTs. The image (7.68 \times 1.92 mm) is generated on a T_2 -weighted spin-echo multislice sequence (SEMS) with a pulse repetition time (T_R) of 1.2 s and an echo time (T_R) of 10 ms. The macrophages are specifically chosen because they are involved in the immune defense systems of vertebrate animals by engulfing pathogens and can easily incorporate extraneous particles via phagocytosis. The cells were incubated with the Fe-enriched sample for a nanotube concentration of 10 mg l⁻¹ of the cell medium. After 7 h incubation, the exact amount of the nanostructures engulfed by the cells is unknown, but the MR image clearly shows the cells as dark spots. Because the iron oxide nanoparticles are T_2 contrast agents, the nanoparticles enhance the negative image

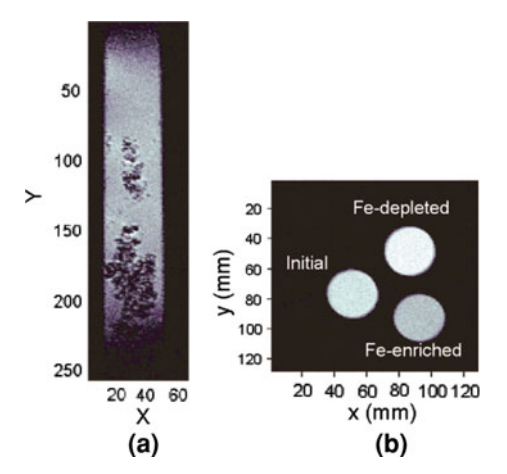


Fig. 14 a Vertical MR image of murine macrophage cells with the Fe-enriched SWCNT sample. A T_2 -weighted spin-echo multislice sequence is used with a pulse repetition time (T_R) of 1.2 s and an echo time (T_R) of 10 ms. There are 256 pixels in the y axis and 64 pixels in the x axis. Each pixel has 30 \times 30 μ m in plane and 250 μ m in depth. **b** Transverse MR image of the initial, Fe-enriched, and Fe-depleted nanotube samples in water ($T_R = 1$ s, $T_E = 13$ ms). A discrete contrast is observed according to the concentration of the iron oxide nanoparticles [73]

contrast. In the control experiments with the Fe-depleted samples and also without any nanomaterials, no image contrast has been seen.

Choi et al. also imaged the cross-sections of capillary tubes containing the three nanotube samples in pure water (Fig. 14b). This image was obtained based on a T_2 -weighted SEMS with $T_{\rm R}=1$ s and $T_{\rm E}=13$ ms. There is a differences in the image contrast: the dark, intermediate, and light-gray areas correspond to the Feenriched, initial, and Fe-depleted samples, respectively [73]. Choi et al suggested if the Fe-enriched SWCNT are suspended or further functionalized with monoclonal antibodies to target specific receptor sites, the complexes could be used as targeted agents to provide molecular-level contrast and biosensing. Finally, the potential exists for these complexes to achieve phototherapy and hyperthermia effects in cells and tissue through NIR laser radiation and the high-speed rotation of the nanomaterials upon application of an external magnetic field modulated at a high frequency.

MR Imaging of MWCNTs

Richard et al. reported noncovalent functionalization of the outer surface of CNTs by amphiphilic gadolinium Gd(III) chelates (GdL) and their effect on water proton relaxation in vitro and in vivo. Figure 15 shows the MRI Images of MWCNTs/GdL complexes with different weightings and concentrations. Figure 15a displays a reference proton density image, where all MWCNT/GdL samples and water reference sample have a high intensity signal.

In the T_1 -weighted image, the nanotube samples containing higher GdL concentration are in hypersignal compared to the water reference sample (Fig. 15b). On the other hand, in the T_2 - and T_2^* -weighted images (Fig. 15c, d, respectively) the tubes with higher GdL concentrations appear in hyposignal, as predicted by the T_1 and T_2 values previously measured. T_2^* values were too small to be quantified (suggesting a short value inferior to 5–10 ms). Clearly, the T_2 and T_2^* effects are

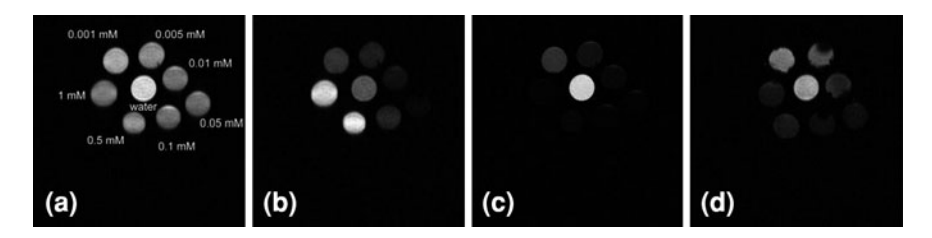
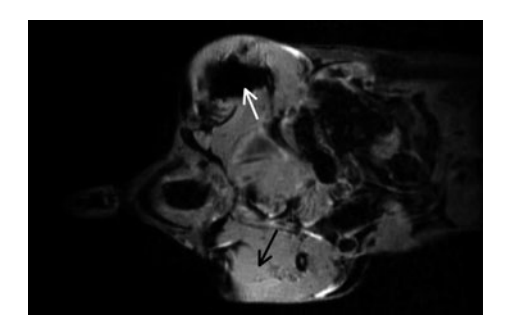


Fig. 15 MRI images of the MWCNT/GdL complex with different weightings and concentrations measured at 300 MHz. **a** Rho-weighted SE TR/TE = 15 s/10 ms, **b** T_1 -weighted SE TR/IR/TE = 15 s/10 ms with hypersignal for the Gd concentrated complex, **c** T_2 -weighted SE TR/TE = 15 s/33 ms with hyposignal for the concentrated Gd complex, and **d** T_2^* -weighted with relative signal intensity as (**c**) GE TR/TE = 15 s/9 ms, FOV = 5 cm, final 256 × 256 matrix resolution [74]

Fig. 16 T_2^* -weighted gradient-echo sequence. Coronal in vivo MR image of mouse legs after MWCNT/L injection (*left leg, white arrow*) and lipid L injection (*right leg, black arrow*) [74]



predominant as compared to the T_1 effect. A sufficient T_1 contrast would require considerably high GdL concentrations (here >0.1 mM in vitro). Consequently, T_2 weighting was privileged for further in vivo experiments.

To evaluate the efficiency of this novel system for in vivo applications, Richard et al. performed experiments by injecting 50 μ L of the less concentrated suspension (MWCNT/L at L concentration of 0.05 mM) into the muscle of the leg of anesthetized mice. As is clearly visible in Fig. 16, a negative contrast is easily detected as a dark area (white arrow) at the site of injection. When 50 μ l of a solution of the lipid L alone (at identical concentration as above, but without nanotubes) were injected, no contrast appeared (black arrow). Similar results were obtained if a suspension of MWCNT/L was injected in the liver. These nanomaterials were well tolerated by the mice. No apparent side effects were observed and 100% survival of the animals was obtained after more than 1 month.

4 Conclusions

In this chapter we have given a review of the many NMR spectroscopic techniques used to characterize and study the structure and properties of different types of raw and functionalized CNTs. Although ¹³C is the nucleus of choice for identifying CNTs, many other isotopes can be useful as well in specific investigations, Even though pure CNTs lack protons, it has been shown, for example, that ¹H NMR spectroscopy is a powerful tool to investigate the molecular structures and particularly functionalization, of CNTs by solution-state, solid-state and HR-MAS-NMR techniques. We have also reviewed different strategies associated with CNTs to be used as a drug carrier and, filled and functionalized with metal complexes, as MRI contrast agents. These systems hold the promise of overcoming many hurdles typically encountered by contrast agents that can enable the early detection of disease. In contrast, these CNTs are still toxic which prevents their ultimate use in vivo but efforts to render them non-toxic are ongoing. Thus, much more research is expected to be done in the field of NMR spectroscopy and imaging of CNTs for biomedical applications.

References

- Oberlin, A., Endo, M., Koyama, T.: High resolution electron microscope observations of grap hitized carbon fibers. Carbon 14(2), 133–135 (1976)
- 2. Kroto, H.W., et al.: C60: Buckminsterfullerene. Nature **318**(6042), 162–163 (1985)
- 3. Iijima, S.: Helical microtubules of carbon nanotubes. Nature 354(6348), 56-58 (1991)
- Bethune, D.S., et al.: Cobalt-catalysed growth of carbon nanotubes with single-atomic-layer walls. Nature 363(6430), 605–607 (1993)
- Iijima, S., Ichihashi, T.: Single-shell carbon nanotubes of 1-nm diameter. Nature 363(6430), 603–605 (1993)
- Chen, X., et al.: Interfacing carbon nanotubes with living cells. J. Am. Chem. Soc. 128(19), 6292–6293 (2006)
- Tycko, R., et al.: Molecular orientational dynamics in solid C70: investigation by one- and two-dimensional magic angle spinning nuclear magnetic resonance. J. Chem. Phys. 99(10), 7554–7564 (1993)
- Tang, X.P., et al.: Electronic structures of single-walled carbon nanotubes determined by NMR. Science 288(5465), 492–494 (2000)
- Chen, Q., et al.: Identification of endohedral water in single-walled carbon nanotubes by 1H NMR. Nano Lett. 8(7), 1902–1905 (2008)
- Kitaygorodskiy, A., et al.: NMR detection of single-walled carbon nanotubes in solution.
 J. Am. Chem. Soc. 127(20), 7517–7520 (2005)
- 11. Yu, I.S., Lee, J., Lee, S.: NMR of hydrogen adsorbed on carbon nanotubes. Phys. B Condensed Matter 329, 421–422 (2003)
- 12. Mao, S.H., Kleinhammes, A., Wu, Y.: NMR study of water adsorption in single-walled carbon nanotubes. Chem. Phys. Lett. **421**(4–6), 513–517 (2006)
- Nelson, D.J., Rhoads, H., Brammer, C.: Characterizing covalently sidewall-functionalized SWNTs. J. Phys. Chem. C 111(48), 17872–17878 (2007)
- 14. Holzinger, M., et al.: Functionalization of single-walled carbon nanotubes with (*R*-)oxycarbonyl nitrenes. J. Am. Chem. Soc. **125**(28), 8566–8580 (2003)
- 15. Chen, J., et al.: Noncovalent engineering of carbon nanotube surfaces by rigid, functional conjugated polymers. J. Am. Chem. Soc. **124**(31), 9034–9035 (2002)
- Ghosh, S., Ramanathan, K.V., Sood, A.K.: Water at nanoscale confined in single-walled carbon nanotubes studied by NMR. Europhys. Lett. 65(5), 678–684 (2004)
- 17. Tasis, D., et al.: Chemistry of carbon nanotubes. Chem. Rev. 106(3), 1105–1136 (2006)
- Pantarotto, D., et al.: Synthesis, structural characterization, and immunological properties of carbon nanotubes functionalized with peptides. J. Am. Chem. Soc. 125(20), 6160–6164 (2003)
- Marega, R., et al.: Diffusion-ordered NMR spectroscopy in the structural characterization of functionalized carbon nanotubes. J. Am. Chem. Soc. 131(25), 9086–9093 (2009)
- Stejskal, E.O., Tanner, J.E.: Spin diffusion measurements: spin echoes in the presence of a time-dependent field gradient. J. Chem. Phys. 42(1), 288–292 (1965)
- Loening, N.M., Keeler, J., Morris, G.A.: One-dimensional DOSY. J. Magn. Reson. 153(1), 103–112 (2001)
- 22. JohnsonJr, C.S.: Diffusion ordered nuclear magnetic resonance spectroscopy: principles and applications. Prog. Nucl. Magn. Reson. Spectrosc. **34**(3–4), 203–256 (1999)
- Ju, S.Y., et al.: NMR study of organization of diacetylenic amine on single-wall carbon nanotubes. In: Abstracts of papers of the American Chemical Society, vol 229, p. 119-POLY (2005)
- 24. Goze Bac, C., et al.: 13C NMR investigation of carbon nanotubes and derivatives. Curr. Appl. Phys. 1(2-3), 149-155 (2001)
- Goze-Bac, C., et al.: Magnetic interactions in carbon nanostructures. Carbon 40(10), 1825– 1842 (2002)

- 26. Peng, H., et al.: Sidewall carboxylic acid functionalization of single-walled carbon nanotubes. J. Am. Chem. Soc. **125**(49), 15174–15182 (2003)
- 27. Mehring, M.: Principles of High Resolution NMR in Solids. Springer, Berlin (1983)
- Schmidt-Rohr, K.a.S., H.W.: Multidimensional NMR and Polymers. Academic Press, New York (1994)
- Steven, P.B., Lyndon, E.: Solid-state NMR. In: Gauglitz, G. (ed.) Handbook of Spectroscopy, pp. 269–326 (2005)
- 30. Hayashi, S., et al.: C-13 NMR studies of C-13-enriched single-wall carbon nanotubes synthesized by catalytic decomposition of methane. Carbon **41**(15), 3047–3056 (2003)
- 31. He, H.: 13C solid-state MAS NMR studies of the low temperature phase transition in fullerene C60. PCCP **2**(2), 2651–2654 (2000)
- 32. Latil, S., et al.: C-13 NMR chemical shift of single-wall carbon nanotubes. Phys. Rev. Lett. **86**(14), 3160–3163 (2001)
- 33. Perez-Cabero, M., et al.: C-13 MAS-NMR study of carbon nanotubes grown by catalytic decomposition of acetylene on Fe-silica catalysts. Carbon **43**(12), 2631–2634 (2005)
- 34. Alemany, L.B., et al.: Solid-state NMR analysis of fluorinated single-walled carbon nanotubes: assessing the extent of fluorination. Chem. Mater. **19**(4), 735–744 (2007)
- 35. Singer, P.M., et al.: NMR study of spin excitations in carbon nanotubes. Phys. Status Solid B Basic Solid State Phys. **243**(13), 3111–3116 (2006)
- 36. Pennington, C.H., Stenger, V.A.: Nuclear magnetic resonance of C60 and fulleride superconductors. Rev. Modern Phys. **68**(3), 855 (1996)
- 37. Knight, W.D.: Solid State Physics, vol. 2, p. 93. Academic Press, New York (1956)
- Mintmire, J.W., White, C.T.: First-principles band structures of armchair nanotubes. Appl. Phys. A Mater. Sci. Process. 67(1), 65–69 (1998)
- 39. Cynthia, J.J., Jameson, A.K., Sheila, M.C.: Temperature and density dependence of [sup 129]Xe chemical shift in xenon gas. J. Chem. Phys. **59**(8), 4540–4546 (1973)
- 40. Kneller, J.M., et al.: TEM and laser-polarized 129Xe NMR characterization of oxidatively purified carbon nanotubes. J. Am. Chem. Soc. **122**(43), 10591–10597 (2000)
- 41. Clewett, C.F.M., Pietrass, T.: Xe-129 and Xe-131 NMR of gas adsorption on single- and multi-walled carbon nanotubes. J. Phys. Chem. B **109**(38), 17907–17912 (2005)
- 42. Romanenko, K.V., et al.: Xe-129 NMR study of Xe adsorption on multiwall carbon nanotubes. Solid State Nucl. Magn. Reson. **28**(2–4), 135–141 (2005)
- 43. Vyalikh, A., et al.: A nanoscaled contactless thermometer for biological systems. Phys. Status Solid. B Basic Solid State Phys. **244**(11), 4092–4096 (2007)
- 44. Dujardin, E., et al.: Interstitial metallic residues in purified single shell carbon nanotubes. Solid State Commun. **114**(10), 543–546 (2000)
- 45. Piotto, M., et al.: Practical aspects of shimming a high resolution magic angle spinning probe. J. Magn. Reson. **173**(1), 84–89 (2005)
- 46. Sekhaneh, W., et al.: High resolution NMR of water absorbed in single-wall carbon nanotubes. Chem. Phys. Lett. **428**(1–3), 143–147 (2006)
- 47. Marti, J., Gordillo, M.C.: Structure and dynamics of liquid water adsorbed on the external walls of carbon nanotubes. J. Chem. Phys. 119(23), 12540–12546 (2003)
- 48. Kolesnikov, A.I., et al.: Anomalously soft dynamics of water in a nanotube: a revelation of nanoscale confinement. Phys. Rev. Lett. **93**(3), 1–035503 (2004)
- Barnaal, D.E., Lowe, I.J.: Experimental free-induction-decay shapes and theoretical second moments for hydrogen in hexagonal ice. J. Chem. Phys. 46, 4800–4809 (1966)
- 50. Gogotsi, Y., et al.: In situ multiphase fluid experiments in hydrothermal carbon nanotubes. Appl. Phys. Lett. **79**(7), 1021–1023 (2001)
- 51. Caravan, P.: Protein-targeted gadolinium-based magnetic resonance imaging (MRI) contrast agents: design and mechanism of action. Acc. Chem. Res. **42**(7), 851–862 (2009)
- 52. Caravan, P.: Strategies for increasing the sensitivity of gadolinium based MRI contrast agents. Chem. Soc. Rev. **35**(6), 512–523 (2006)
- 53. Jeff, W.M.B., Dara, L.K.: Iron oxide MR contrast agents for molecular and cellular imaging. NMR Biomed. 17(7), 484–499 (2004)

- Lauterbur, P.C.: Image formation by induced local interactions: examples employing nuclear magnetic resonance. Nature 242(5394), 190–191 (1973)
- Gabillard, R.: A steady state transient technique in nuclear resonance. Phys. Rev. 85(4), 694 (1952)
- 56. Damadian, R.: Tumor detection by nuclear magnetic resonance. Science **171**(3976), 1151–1153 (1971)
- 57. Hinshaw, W.S., Bottomley, P.A., Holland, G.N.: A demonstration of the resolution of NMR imaging in biological systems. Cell. Mol. Life Sci. **35**(9), 1268–1269 (1979)
- 58. Damadian, R., Goldsmith, M., Minkoff, L.: NMR in cancer: XVI. FONAR image of the live human body. Physiol. Chem. Phys. **9**(1), 97–100, 108 (1977)
- 59. Kumar, A., Welti, D., Ernst, R.R.: NMR Fourier zeugmatography. J. Magn. Reson. 18(1), 69–83 (1975)
- Wehrli, F.W.: On the 2003 Nobel Prize in medicine or physiology awarded to Paul C. Lauterbur and Sir Peter Mansfield. Magn. Reson. Med. 51(1), 1–3 (2004)
- Mansfield, P.: Snapshot magnetic resonance imaging (Nobel Lecture). Angew. Chem. Int. Edn. 43(41), 5456–5464 (2004)
- 62. Watson, A.D., J.K., Jamieson, G.C., Fellmann, J.D., Vogt, N.B.: Use of fullerenes in diagnostic and/or therapeutic agents, USA (1994)
- 63. Sitharaman, B., et al.: Gadofullerenes as nanoscale magnetic labels for cellular MRI. Contrast Media Mol. Imaging 2(3), 139–146 (2007)
- 64. Bolskar, R.D., et al.: First soluble M@C60 derivatives provide enhanced access to metallofullerenes and permit in vivo. Evaluation of Gd@C60[C(COOH)2]10 as a MRI contrast agent. J. Am. Chem. Soc. 125(18), 5471–5478 (2003)
- Neumann, W.L., Cacheris, W.P. (eds): Fullerene compositions for magnetic resonance spectroscopy and imaging. US Patent 5,248,498, 1993
- 66. Haddon, R.C.: Carbon nanotubes. Acc. Chem. Res. 35(12), 997–997 (2002)
- Mackeyev, Y.A., et al.: Stable containment of radionuclides on the nanoscale by cut singlewall carbon nanotubes. J. Phys. Chem. B 109(12), 5482–5484 (2005)
- 68. Suenaga, K., et al.: Element-selective single atom imaging. Science **290**(5500), 2280–2282 (2000)
- 69. Sitharaman, B., et al.: Superparamagnetic gadonanotubes are high-performance MRI contrast agents. Chem. Commun. **31**, 3915–3917 (2005)
- 70. Hartman, K.B., et al.: Gadonanotubes as ultrasensitive pH-smart probes for magnetic resonance imaging. Nano Lett. 8(2), 415–419 (2008)
- 71. Al Faraj, A., et al.: In vivo imaging of carbon nanotube biodistribution using magnetic resonance imaging. Nano Lett. **9**(3), 1023–1027 (2009)
- 72. Sosnovik, D.E., Weissleder, R.: Emerging concepts in molecular MRI. Curr. Opin. Biotechnol. **18**(1), 4–10 (2007)
- 73. Choi, J.H., et al.: Multimodal biomedical imaging with asymmetric single-walled carbon nanotube/iron oxide nanoparticle complexes. Nano Lett. **7**(4), 861–867 (2007)
- 74. Richard, C., et al.: Noncovalent functionalization of carbon nanotubes with amphiphilic Gd3+ chelates: toward powerful T_1 and T_2 MRI contrast agents. Nano Lett. **8**(1), 232–236 (2008)

Part III Interaction with Biological Systems

Exploring Carbon Nanotubes and Their Interaction with Cells Using Atomic Force Microscopy

Constanze Lamprecht, Andreas Ebner, Ferry Kienberger and Peter Hinterdorfer

Abstract At present, atomic force microscopy (AFM) offers a unique solution to study biological specimens on the nanometer scale under near-physiological conditions without the need for rigorous sample preparation, staining or labelling. We expect new and significant biophysical insights into the delivery process and transport mechanism of CNTs into cells employing AFM. Here we give an overview for the application of AFM to characterize and assess CNT surface biofunctionalization. Moreover, we show how topographic AFM imaging can be used to study the binding of functionalized single walled carbon nanotubes (SWCNTs), double walled carbon nanotubes (DWCNTs) and multi walled carbon nanotubes (MWCNTs) to various relevant biological membranes, including nuclear membranes and cell surfaces.

1 Introduction

Since its invention in the late 1980s [1], the atomic force microscope (AFM) has evolved into a powerful research instrument to study most diverse specimens in nearly every scientific field from material science to molecular biology. The main application of AFM is imaging of surfaces on scales from micro- to nanometres with the objective to visualize and properly characterize surface textures and shapes. Today, the AFM has successfully complemented electron microscopy (EM) studies of biological membranes and cells. Unlike EM, AFM yields three-dimensional maps with an exceptionally good vertical resolution, and without the

C. Lamprecht (\boxtimes), A. Ebner, F. Kienberger and P. Hinterdorfer Institute of Biophysics, J Kepler University, Altenberger Straße 69, 4040 Linz, Austria e-mail: Constanze.Lamprecht@jku.at

need for extensive sample preparation, staining or labelling. Not only is AFM capable of resolving structures of native membranes in the sub-nanometre range [2–4], most importantly, it allows the visualization of biological samples in buffers that preserve their structure and function over an extended period of time. When applied to living cells, new cellular surface structures and their physiological functions have been identified [5–7]. In addition to high-resolution imaging, interand intramolecular interactions can be studied directly at the molecular level. [8]. The capability of AFM to resolve nm-sized details, together with its force-detection sensitivity, has led to the development of molecular recognition imaging [9]. By combining topographical imaging with force measurements, receptor sites are localized with nanometre accuracy. Topography and recognition of target molecules are thereby simultaneously mapped.

Altogether, the AFM offers a versatile tool-box to study, investigate and characterize multifunctional carbon nanotubes, and their interaction with biological systems under physiological conditions. We expect new and significant bio-physical insights into transport mechanisms of multifunctional CNTs into cells by employing the AFM. In the following an overview will be given for the application of AFM to characterize and assess differently bio-functionalized CNTs in respect to their surface coating, bundling and aggregation behaviour. Moreover, we present some of the first AFM experiments towards an understanding of the internalisation pathway of functionalized CNTs into cells [10]. In these studies AFM imaging has been used to show binding of CNTs to various biological membranes.

2 Principles of Atomic Force Microscopy

In AFM imaging a micro cantilever with a very sharp tip at the end scans horizontally line by line over a sample generating a topographic image of the surface. Due to the interaction of the tip with the surface the cantilever is deflected. The deflection is monitored by a laser which is focused on the very end of the cantilever and from there reflected into a four quadrant photodiode. The movement of the laser spot on the photodiode causes an electric signal, which is used in a feedback loop in order to keep the force exerted on the sample by the AFM tip constant.

Within the feedback loop voltage is applied to a piezo electric scanner which moves either the sample or the tip up and down by retracting or extending, thereby controlling the distance between sample surface and AFM tip. The surface topography is then reconstructed from the vertical movements of the piezo (Fig. 1). Today, high precision piezo electric scanners allow for a sub-nanometre resolution in *z*-axis.

According to experimental requirements, topographical imaging can be done in various modes. In contact-force mode, the tip is always in physical contact with the sample. The scanner traces the tip over the sample and the contact forces cause the cantilever to bend upon changes in topography. With this technique

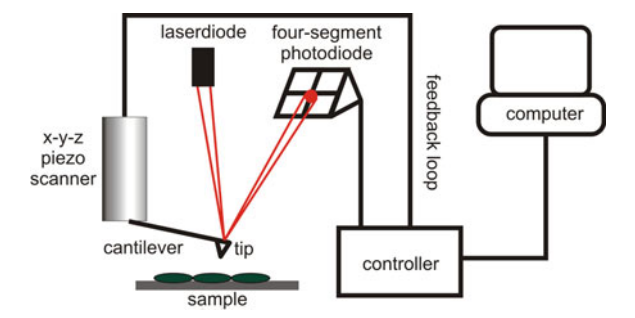


Fig. 1 Schematic to illustrate the principles of atomic force microscopy. A sample is probed by an ultra-sharp tip mounted on a cantilever, which scans laterally over the sample surface. A reflected laser beam amplifies and reports deflections of the cantilever to a split photodiode. The deflection signal is fed into a feedback loop that controls the piezo movement by which the tip is lifted from or lowered to the surface in order to adjust tip sample interaction. A topographic image of the sample is then reconstructed from the piezo-movement

high-resolution images of biological samples are easily achieved [11–13]. In dynamic force microscopy (DFM) imaging, however, the AFM tip is oscillated near its resonant frequency while it scans over the surface. Here, the tip touches the sample surface only at the very end of its downward movement, which reduces lateral forces acting on the sample. In DFM not the deflection but the amplitude reduction upon intermittent tip–surface contact is held constant by the feedback-loop. DFM imaging is of advantage when imaging soft biological samples like native membranes and loosely attached specimen [14–16]. For application in biosciences a major advantage of the AFM over other high-resolution microscopic techniques is the possibility to operate in liquid [16, 17] without the need for a rigorous sample preparation or labelling. Thus the AFM provides ideal conditions for measurements under near physiological conditions [18].

3 Characterization of Functionalized CNTs Employing AFM

Topographical Imaging of Functionalized CNTs

Pristine CNTs are inherently hydrophobic and thus have a strong tendency to aggregate (Fig. 2). Substantial van der Waals attractions among them make CNTs practically insoluble in any kind of solvent. The ability to form a stable suspension in aqueous media, however, is a fundamental prerequisite for potential biological and biomedical applications. The strategies to disperse CNTs to form stable suspensions can be divided into two main categories: covalent and non-covalent functionalization of the outer CNT surface.

For the non-covalent dispersal method surfactant molecules like nucleic acids [19–22], proteins and peptides [23–30] or polymers [31–37] are used to adsorb onto

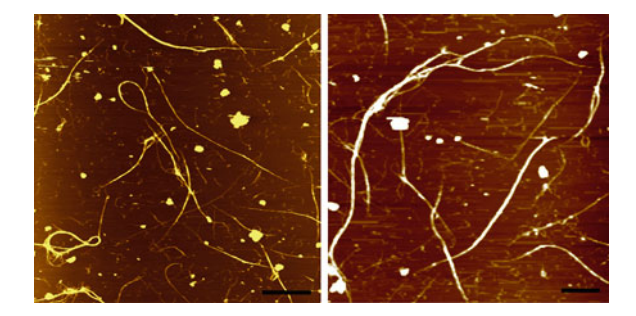


Fig. 2 Pristine carbon nanotubes are inherently hydrophobic. Thus, dry CNTs are practically indispersible in any kind of solvent. For contact mode AFM imaging a small amount of dry DWCNTs was dispersed in 1, 2-dichloroethane under strong sonication and deposited on mica. Mostly big aggregates and bundles of DWCNTs are visible. The lengths of individual DWCNTs vary between several 100 nm and a few μm with diameters ranging from 1.4 to 3.4 nm. As bundles they form long ropes of more than 20 μm length and several 100 nm height. AFM images: $scale\ bar\ 2\ \mu m$

the CNT surface by means of hydrophobic interactions. Their hydrophilic parts impart the water-solubility of the CNTs. The non-covalent dispersion procedures usually involve ultrasonication, centrifugation and filtration to remove excess surfactant molecules. They are quick and easy, achieving debundling of CNTs, dispersion in water and increased biocompatibility in one step, and they do not alter the surface composition of the CNT itself. Topographical imaging with the atomic force microscope can be used to visualize the surface coating of individual DWCNTs by biomolecules and to determine the degree of debundling and dispersion.

In a comparative study of several non-covalent approaches to non-covalently functionalize DWCNTs, the ability of RNA, BSA and the polymer DSPE-PEG₂₀₀₀-NH₂, as well as a combination thereof, to coat the surface of purified DWCNTs was investigated [38]. Height profiles along individual nanotubes indicated an increase in the diameter of the respective DWCNTs depending on the surfactant used for functionalization and revealed adsorption of single molecules onto the nanotubes (Fig. 3).

That way, RNA could clearly be seen wrapping around the DWCNT (Fig. 3a). The height of the RNA-wrapped DWCNTs ranged between 3 and 5 nm, indicating that most tubes are likely to be wrapped with only a single strand of RNA (diameter about 0.5–1 nm). For BSA coated DWCNTs (Fig. 3b) bright dot-like structures were observed decorating the nanotubes densely along the entire length. From the cross-section profiles along the tubes peak heights of 1–2 nm were obtained, suggesting the adsorption of single Bovine serum albumin (BSA) molecules. In comparison, DSPE-PEG₂₀₀₀-NH₂ appeared to wrap DWCNTs more uniformly (Fig. 3c) adding about 1 nm to the DWCNT height. Finally, for the BSA DSPE-PEG₂₀₀₀-NH₂ bi-conjugated DWCNTs (Fig. 3d) BSA (dot-like structures on the nanotube surface) was found not to cover the entire DWCNT. Instead, also segments with uniform and soft appearing features were visible on the DWCNTs suggesting the adsorption of DSPE-PEG₂₀₀₀-NH₂ on the same DWCNT.

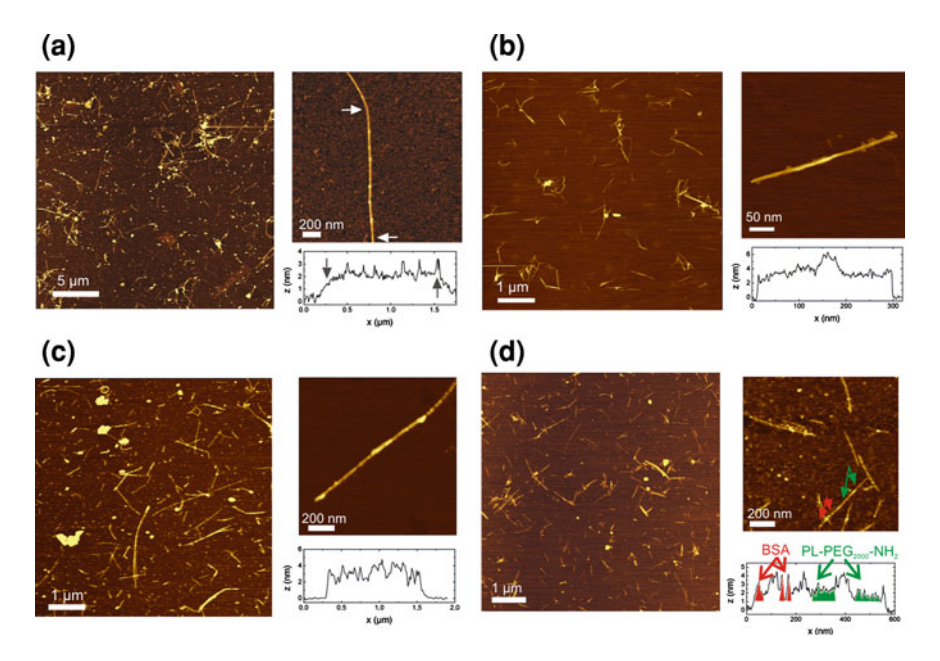


Fig. 3 Topographical AFM images and height-profiles of biomolecule conjugated CNTs. Dispersion of CNTs in aqueous media is a fundamental prerequisite for potential biomedical applications. A common strategy to disperse CNTs in water is the non-covalent coating with surfactant molecules like nucleic acids (**a**) protein (**b**) or synthetic polymer (**c**). The dispersion procedures usually involve ultrasonication, ultra-centrifugation and filtration. Debundling, dispersion in water and biocompatibility can be achieved in one step. **a** DWCNTs wrapped with yeast-RNA. **b** BSA-coated DWCNTs. **c** DWCNTs coated with the bio-polymer DSPE-PEG₂₀₀₀-NH₂. **d** DWCNT conjugated to BSA and DSPE-PEG₂₀₀₀-NH₂

Topographical imaging showed well dispersed and separated CNTs after proper functionalization. But it also clearly illustrated that the different coating methods differ in their abilities to successfully debundle and disperse CNTs, as can be seen in the overview scans in Fig. 3. The functionalization with BSA alone resulted mainly in smaller bundles instead of well isolated individual DWCNTs. In comparison, the use of DSPE-PEG₂₀₀₀-NH₂ yielded a higher degree of debundling. The combination of protein and polymer produced a stable suspension of mostly individual functionalized DWCNTs and thus proved most efficient for dispersion of purified DWCNTs.

When preparing carbon nanotubes for Covalent functionalisation of CNTs of molecules, reactive binding sites are required, which are not present on pristine carbon nanotubes. Reactive groups are usually generated on the CNT surface by a rigorous treatment with chemicals, which alter the surface composition and destroy the regular carbon network [39–46]. A popular method to create binding sites, primarily in the form of carboxylic groups, is the treatment with a mixture of concentrated nitric acid (HNO₃) and sulphuric acid (H₂SO₄). This process additionally renders the nanotubes dispersible in water. Several studies have shown

that acid oxidation of carbon nanotubes creates molecular debris, which covers the surface of oxidised CNTs [46–48]. This debris is known to consist of partially oxidised polyaromatic fragments and can be removed from the CNT surface by washing with an aqueous base [49].

A recent study [50] shows that the presence of molecular debris significantly changes the dispersibility qualities of different types of oxidised SWCNTs, DWCNTs and MWCNTs. The oxidised CNT samples and corresponding reference (unoxidised) samples were washed with sodium hydroxide (NaOH) and were characterized by spectroscopic and microscopic techniques including topographic AFM imaging (Fig. 4). From the AFM images it could be observed that after oxidation all CNTs were well dispersed in water, but the tubes were completely decorated with globular fragments. In contrast, the amount of debris on the CNT sidewall was much lower after extensive washing with NaOH-solution, though increased sedimentation of NaOH-washed oxidized CNTs in aqueous suspensions was observed. In fact, highly oxidised debris acts as a surfactant and improves the aqueous dispersion of CNTs. Hence, after removal of this debris the stability of oxidized CNTs in water can be reduced.

In summary, topographical AFM imaging has proven to be an indispensable technique as a fast and direct method to assess and characterize functionalized CNTs. Not only CNT dispersions can be studied but more importantly structural and surface properties of functionalized CNTs can be visualized with sub-nanometre resolution.

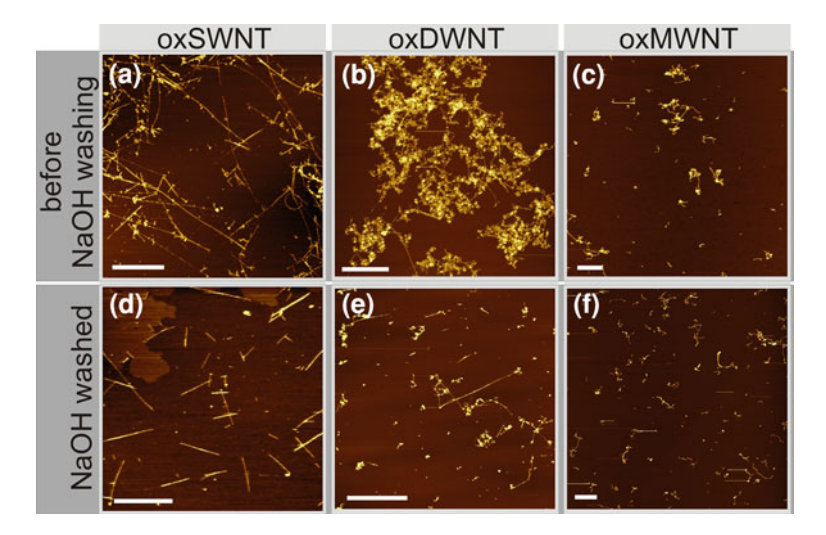


Fig. 4 Exohedral functionalization of SWCNTs (\mathbf{a} , \mathbf{d}), DWCNTs (\mathbf{b} , \mathbf{e}) and MWCNTs (\mathbf{c} , \mathbf{f}) by acid treatment (surface oxidation). Acid oxidation creates molecular debris, which covers the CNT surface (\mathbf{a} - \mathbf{c}). The debris is known to consist of partially oxidised polyaromatic fragments and can be removed by washing with an aqueous base (here sodium hydroxide—NaOH) (\mathbf{d} - \mathbf{f}). AFM images were aquired by contact mode imaging in air at a scan rate of 2 lines/s with a very soft cantilever (spring constant k = 0.03 N/m), all *scale bars* 1 μ m

Addressing the Bio-Functionalization of CNTs

With the aim to create multifunctional entities for medical applications which specifically target or sense cognate receptors, CNTs are conjugated (non-covalently or covalently) to a wide range of bio-molecules [51, 52]. Analytical techniques to determine molecular recognition comprise immunological assays (e.g. ELISA) and spectroscopic methods as well as electrophoresis techniques (gels, blots). These common methods are ensemble-averaging techniques which do not give insight into the ability of an individual functionalized CNT to recognize or bind to a target molecule or receptor. The atomic force microscope offers an alternative analytical tool to visualize and determine molecular recognition on a single molecule level.

The avidin–biotin complex is often regarded as the prototype of a receptor ligand pair, due to its enormously high affinity ($K_{\rm D}=10^{-13}$ M) and long bond lifetime (τ (0) = 80 days) [53]. Thus biotin functionalized CNTs, which specifically bind avidin and streptavidin, were used to demonstrate the possible applications of the AFM to study CNT surface functionalization.

Figure 5a shows topographical images of DWCNTs non-covalently functionalized with biotinylated BSA (biotin-BSA DWCNTs), which were exposed to a solution of streptavidin. The corresponding height profile analysis for individual nanotubes showed a peak height of 3–4 nm above the DWCNT baseline while iotin-BSA DWCNTs without streptavidin have a peak height of 1–2 nm, only (Fig. 3c).

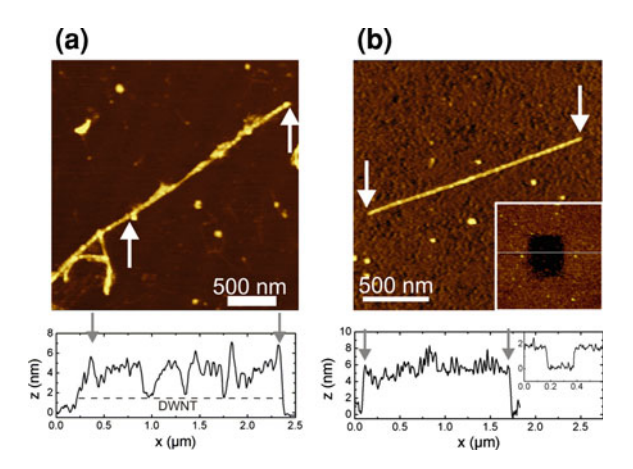


Fig. 5 Non-covalently functionalized CNTs for specific binding of molecules. The bio-molecules, conjugated to the CNT surface, mostly retain their properties and hence can be used to specifically recognize and bind cognate ligands. a Topographic AFM image and corresponding profile of biotin-BSA functionalized CNTs after specific binding of streptavidin to biotin-BSA, as obtained by contact mode imaging in air. b Specific immobilization of biotin-BSA-functionalized DWCNTs to a dense layer of avidin on mica. The image was captured while operating in buffer solution. Insets: a rectangular hole was scratched into the avidin layer to expose bare mica. From the cross-section profile the layer height was determined to be ~ 1.5 nm

The strong and specific interaction of biotin and avidin has also been successfully applied for a tight immobilization of CNTs to a support to enable imaging of CNTs under physiological conditions, i.e. in buffer solution, without any tip-induced displacement [10, 38]. A dense layer of avidin molecules was prepared and subsequently incubated with biotin- BSA CNTs. The sample was rigorously washed to remove loosely bound CNTs. Topographic images (Fig. 5b) showed that the CNTs were entirely covered by bright dots representing biotin-BSA adsorbed to the nanotubes.

4 Visualization of CNT on Biological Membranes with the AFM

CNT on a Nuclear Membrane

Due to their nano-sized dimensions CNTs have the potential to access into various cellular compartments including the nucleus. Only recently Porter et al. [54] provided direct evidence that SWCNT translocated across the nuclear membrane and could be found in the nucleus. Thus CNTs are promising candidates to deliver bioactive molecules (such as DNA or siRNA) which exert their therapeutic action only inside the nucleus. Since the transport of biomolecules, such as regulatory proteins, rRNA, or mRNA into the nucleus is governed by the nuclear pore complexes (NPC) [55], it is of particular interest to visualize binding of individual CNTs to these NPCs.

Figure 6a shows topographic AFM images of the cytoplasmic side of the nuclear membrane spanned with a special preparation method [56] on a glass slide. In a zoom-in the typical ring structures of the NPC embedded in the nuclear membrane is visible with the inner diameter of about 40 nm and a typical outer diameter of 120 nm. Figure 6b shows the nuclear membrane with tightly packed NPC and a net of individual RNA coated DWCNTs and smaller bundles on top. The average roughness of the underlying NPC area was 4–5 nm, while the height of individual DWCNTs ranged from 2 to 4 nm and the height of bundles from 6 to 15 nm. Here the visualization of single DWCNTs on the nuclear membrane was achieved while, at the same time, resolving individual nuclear pore complexes at high resolution. The images demonstrate the potential of the AFM to monitor the transport of individual CNTs through single nuclear pore complexes with high lateral resolution.

CNT on Cells

Understanding the internalization pathway of multifunctional CNTs into living cells is crucial for future clinical utilization. Several groups have studied the

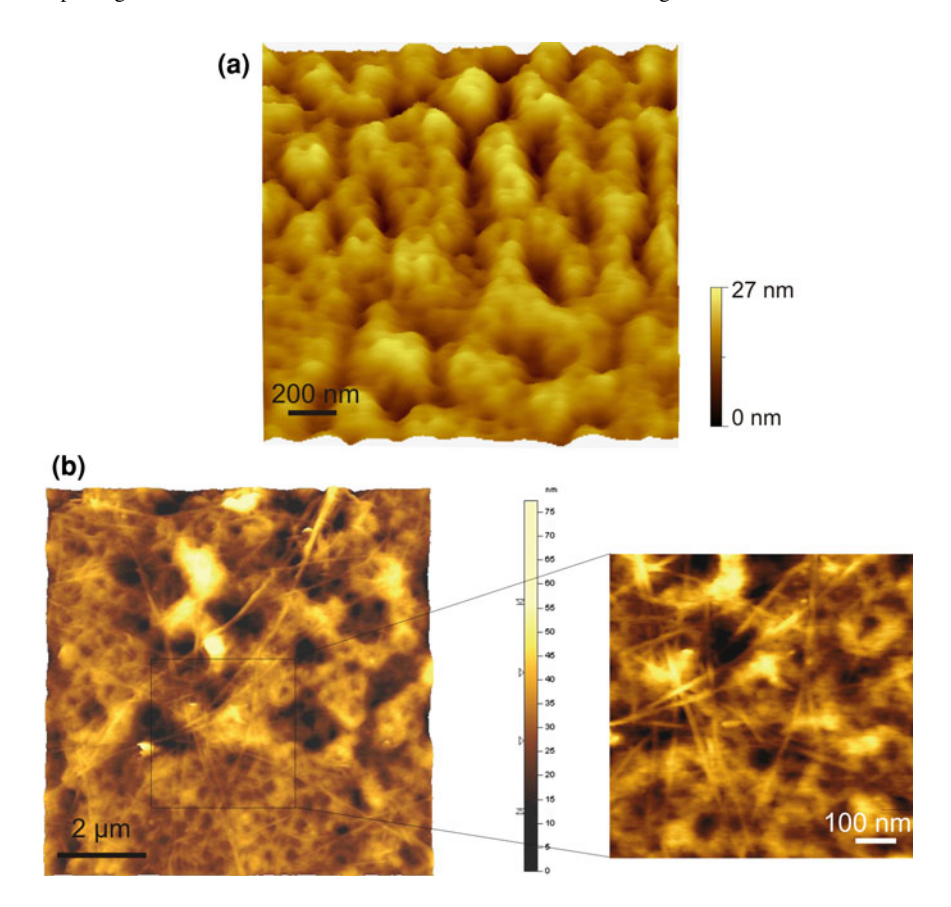


Fig. 6 RNA coated carbon nanotubes on a nuclear membrane. **a** The nuclear envelope of the cell nucleus is perforated by nuclear pore complexes (NPCs). The image shows the cytoplasmic side of the nuclear envelope of a *Xenopus laevis* oocyte with a high density of NPCs. The inner diameter of an NPC is about 40 nm, the outer diameter is about 150 nm. **b** RNA-coated DWCNTs on nuclear membrane as observed in contact mode imaging in air. A 2 μl droplet of an aqueous suspension of RNA-coated DWCNTs (~0.01 mg/ml) was placed on a preparation of nuclear envelope. The medium-scale image and the zoom-in show a dense net of DWCNTs on closely packed NPCs

uptake of biofunctional CNTs in order to elucidate the uptake route and the transport mechanism inside mammalian cells [19, 21, 57–62]. Experiments addressing CNT uptake usually make use of fluorescent labelling of carbon nanotubes and subsequent detection of the dyes by means of fluorescence microscopy. Label-free observation of SWCNT bundles, internalized inside cells, has been achieved by energy-filtered transmission electron microscopy (TEM) in combination with electron energy loss (EEL) spectrum imaging on sliced cell sections [54]. In comparison to this technique, the AFM has the advantage of combining nanometre resolution with the ability to operate in liquid media without the need for extensive sample preparation. With the AFM, measurements can be

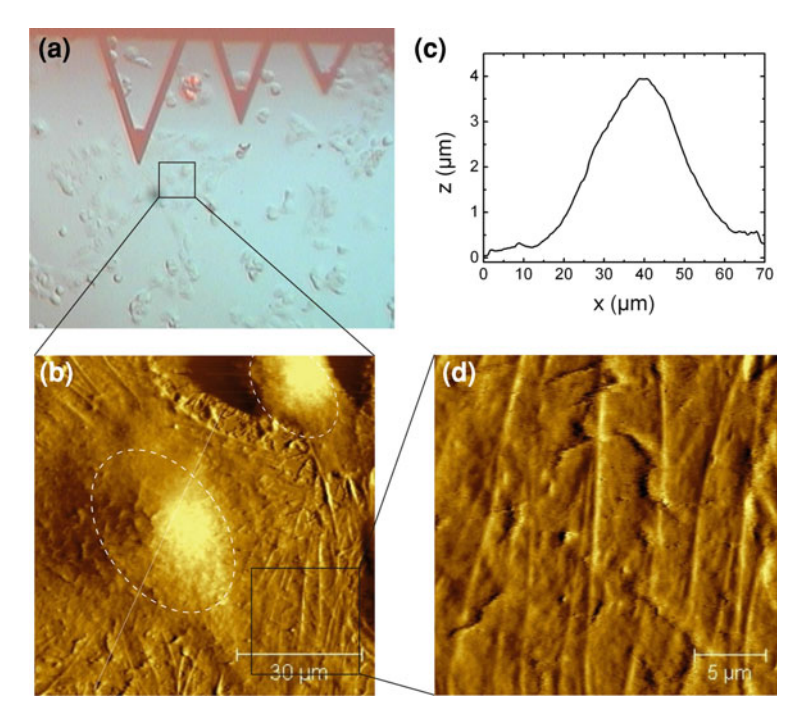


Fig. 7 AFM imaging of live ECV cells. a Camera snapshot of AFM cantilevers scanning over a cell sample. b AFM deflection image of an overview scan showing two live ECV cells. The dashed lines mark the high areas where the nucleus and most organelles of a cell are located. Typical ECV cells have a size of $50-80~\mu m$. The nucleus region has a height of $\sim 3~\mu m$, as indicated in the height profile (c) while the cytoplasmic area around the nucleus area is rather flat with a roughness of less than 100~n m. The fine lines drawn through the cell are the cytoskeleton which stabilizes the cell and gives its shape. It consists of microtubules ($\sim 25~n m$), intermediate filaments ($\approx 11~n m$) and actin filaments ($\approx 7~n m$). d Zoom-in on a flat region of the cell, where the most prominent features are the microtubules of the cytoskeleton under the cell surface

performed on live cells under near physiological conditions revealing details and substructures of native cellular surfaces (Fig. 7).

Figure 8 shows topographic images of HeLa cells after incubation with RNA-coated SWCNTs over a period of 3 h. To inhibit further uptake and/or release of RNA-SWCNTs the cells were fixed prior to AFM imaging. Individual SWCNTs were found lying in close proximity to the cell border and even partially extending onto the cell surface. However, imaging directly on the cell surface, no RNA-SWCNTs were observed.

Imaging small diameter CNTs on a soft (and rough) cell surfaces is a particular challenge. Using flat cells, which exhibit a low surface roughness and form widespread flat regions can be advantageous. ECV cells, a derivative of human urinary bladder carcinoma cells, grow in culture as an adherent monolayer. AFM imaging showed that typical sizes of ECV cells range between 50 and 80 µm. The

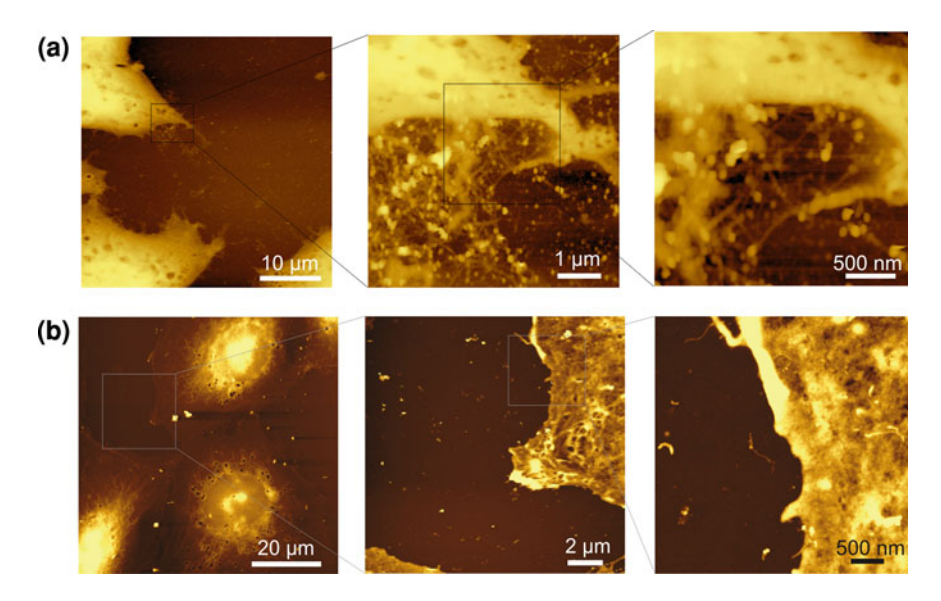


Fig. 8 Topographic AFM images of dry cells after incubation with RNA wrapped CNTs. In contrast to a flat support like mica, native biological membranes and especially cells are rarely homogeneously structured and exhibit a high surface roughness. Resolving individual CNTs even on dry cells is a particular challenge. **a** HeLa cells were incubated with RNA-SWCNTs for 3 h and dried after fixation with paraformaldehyde. Stepwise zooming-in on the border of a cell reveals a network of tangled SWCNTs. (Images taken from [10]) **b** ECV cells were exposed to RNA-coated MWCNTs after fixation and subsequently dried. MWCNTs can be seen as fine lines on the cell surface and next to the cell on the underlying glass slide

nuclear region has a height of about 3 μ m while the surrounding cytoplasmic area is rather flat, with an overall surface roughness of less than 50 nm (Fig. 7b, d).

The ECV cells presented in Fig. 8b were exposed to RNA-coated MWCNTs after fixation. Following CNT exposure the cells were washed and left for drying before imaging the sample in air. Gradually zooming-in on the cell border revealed individual MWCNTs (white arrows) on the dry cell surface, on the cell border and next to the cell on the underlying glass slide.

AFM images of ECV cells incubated with BSA–DWCNTs are shown in Fig. 9. The images were acquired with contact mode AFM under near physiological conditions in buffer solution. Larger bundles of CNTs with heights of 30–80 nm were observed on the cell surfaces. Some CNT bundles even appeared to be sticking in the cell surface suggesting possible internalization into the cell. Beneath the CNT bundles also cellular substructures like filaments from the cytoskeleton were visible (Fig. 9b, c). The cytoskeleton consists of microtubules (~25 nm diameter), intermediate filaments (roughly 10 nm) and actin filaments (~10 nm). In comparison, the size of individual SWCNTs and DWCNTs ranges between 1–3 and 2–4 nm, respectively (without bio-functionalization). Accordingly, it is difficult to discriminate unequivocally individual SWCNTs/DWCNTs from cellular filaments.

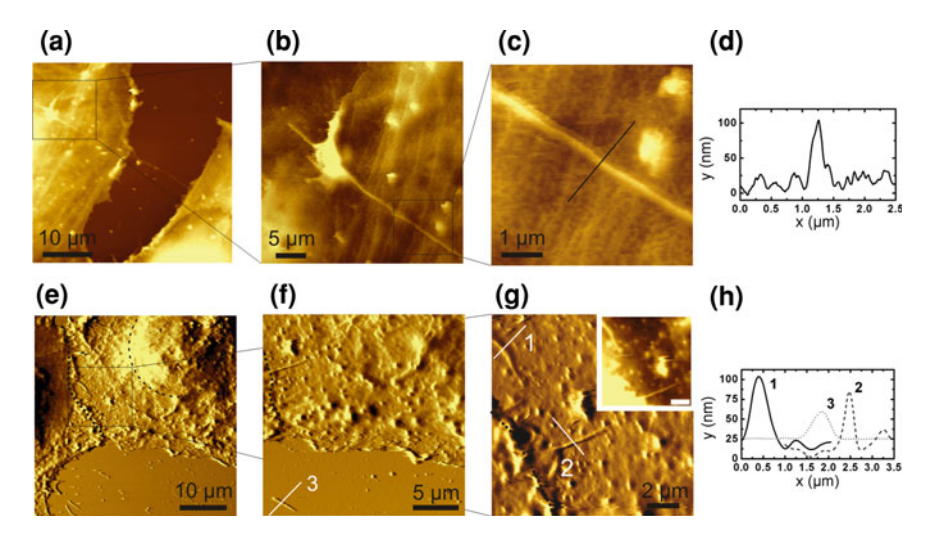


Fig. 9 AFM images of fixed cells after exposure to BSA conjugated DWCNTs, captured with contact mode under buffer conditions. Corresponding cross-section profiles indicate the size of observed DWCNT bundles. **a−c** Topographic images of ECV cells which were exposed to BSA–DWCNTs after fixation. A large DWCNT bundle of 80 nm in height (cross section in **c**) is visible lying across the cell. The filamentous structures beneath the bundle show the interlaced network of the cell cytoskeleton. **e−g** Cantilever deflection images of two ECV cells, which were incubated with BSA–DWCNT over a period of 3 h prior to fixation. Cell nuclei are marked with *black dashed line*, and cell–cell contact regions are marked by a *dotted line*. Subsequent zooming-in on the contact region revealed DWCNT bundles of ~70 nm sticking in the cell surfaces. (Images taken from [10])

The results of the experiments described seem to indicate limitations for the AFM to study binding of individual carbon nanotubes to the cell surface and furthermore their CNT uptake into the cell under physiological conditions. However, complementary techniques, namely the combination of fluorescence microscopy and AFM imaging [63] and simultaneous topographical and recognition imaging (TREC) [64, 65] with a ligand functionalized AFM tip, could facilitate the localization of functionalized carbon nanotubes on the cell surface and enable time resolved uptake studies.

5 Summary and Outlook

In this chapter we have introduced the atomic force microscope as a versatile instrument to study carbon nanotubes and their interaction with biological systems. We presented in detail the technique of topographic imaging to visualize and investigate bio-functionalized CNTs alone and in contact with biological membranes.

We first showed how to determine and assess the effect of different non-covalent and covalent functionalization methods on the surface structure of individual CNTs and their bundling and aggregation behaviour. Subsequently, Biotin-BSA-functionalized DWCNTs were shown to specifically bind streptavidin. Moreover the tight immobilization of biotin-BSA DWCNTs to a dense layer of mica-bound avidin presents a method for high-resolution topographical imaging of bio-functionalized DWCNT in buffer solution. In the future the new and emerging technique of simultaneous topographical and recognition imaging (TREC) could be used to directly visualize functional groups on the sidewall of an individual CNT.

Next we focussed on the application of AFM imaging to study binding of functionalized CNTs to relevant biological membranes. We presented high-resolution topographical images of CNTs bound to the nuclear membrane. Individual CNTs could be resolved demonstrating the potential of the AFM to monitor the transport of individual CNTs through single nuclear pore complexes with high lateral resolution.

We then showed topographical images of CNTs bound to cell surfaces. The images were obtained first under dry conditions and second in a near physiological environment in buffer solution, thus illustrating a key advantage of the AFM with its ability to operate in liquid media without the need for extensive sample preparation. Yet, the detection and resolution of individual CNTs on a nanometre scale on cells in buffer seemed to be impaired by the softness of the cells. Here, complementary techniques, such as the combination of fluorescence microscopy and AFM imaging or the simultaneous topographical and recognition imaging (TREC) with a ligand functionalized AFM tip, may turn out to be promising for localization of functionalized CNTs on the cell surface. In addition, more insight into the binding event itself between functionalized CNTs and cell receptors could be gained by employing the method of AFM force spectroscopy.

In summary, the AFM represents an indispensable tool to properly characterize CNTs and explore their interaction with biological systems under physiological conditions. Topographical imaging has already yielded new and interesting results in that matter and additional AFM techniques like force spectroscopy and TREC are promising methods to gain further knowledge about CNT functionalization and CNT-cell interaction.

References

- Binnig, G., Quate, C.F., Gerber, C.: Atomic force microscope. Phys. Rev. Lett. 56(9), 930–933 (1986)
- Horber, J.K.H., Miles, M.J.: Scanning probe evolution in biology. Science 302(5647), 1002–1005 (2003)
- 3. Muller, D.J., et al.: Observing structure, function and assembly of single proteins by AFM. Prog. Biophys. Mol. Biol. **79**(1–3), 1–43 (2002)

 Scheuring, S., Levy, D., Rigaud, J.L.: Watching the components of photosynthetic bacterial membranes and their in situ organisation by atomic force microscopy. Biochim. Biophys. Acta Biomembr. 1712(2), 109–127 (2005)

- 5. Jeremic, A., et al.: Reconstituted fusion pore. Biophys. J. **85**(3), 2035–2043 (2003)
- Franz, C.M., Muller, D.J.: Analyzing focal adhesion structure by atomic force microscopy. J. Cell Sci. 118(22), 5315–5323 (2005)
- 7. Zaman, M.S., et al.: Imaging and analysis of *Bacillus anthracis* spore germination. Microsc. Res. Tech. **66**(6), 307–311 (2005)
- 8. Allison, D.P., Hinterdorfer, P., Han, W.H.: Biomolecular force measurements and the atomic force microscope. Curr. Opin. Biotechnol. **13**(1), 47–51 (2002)
- 9. Kienberger, F., et al.: Molecular recognition imaging and force spectroscopy of single biomolecules. Acc. Chem. Res. **39**(1), 29–36 (2006)
- 10. Lamprecht, C., et al.: AFM imaging of functionalized carbon nanotubes on biological membranes. Nanotechnology **20**(43), 7 pp. (2009) Article Nr.: 434001
- 11. Hoh, J.H., et al.: Structure of the extracellular surface of the gap junction by atomic-force microscopy. Biophys. J. **65**(1), 149–163 (1993)
- 12. Muller, D.J., et al.: Imaging purple membranes in aqueous-solutions at subnanometer resolution by atomic-force microscopy. Biophys. J. **68**(5), 1681–1686 (1995)
- 13. Schabert, F.A., Henn, C., Engel, A.: Native *Escherichia coli* Ompf porin surfaces probed by atomic-force microscopy. Science **268**(5207), 92–94 (1995)
- 14. Kienberger, F., et al.: Dynamic force microscopy imaging of native membranes. Ultramicroscopy **97**(1–4), 229–237 (2003)
- 15. Putman, C.A.J., et al.: Tapping mode atomic-force microscopy in liquid. Appl. Phys. Lett. **64**(18), 2454–2456 (1994)
- 16. Han, W.H., et al.: Kinked DNA. Nature **386**(6625), 563–563 (1997)
- Marti, O., Drake, B., Hansma, P.K.: Atomic force microscopy of liquid-covered surfaces atomic resolution images. Appl. Phys. Lett. 51(7), 484–486 (1987)
- 18. Muller, D.J., et al.: Electrostatically balanced subnanometer imaging of biological specimens by atomic force microscope. Biophys. J. **76**(2), 1101–1111 (1999)
- 19. Becker, M.L., et al.: Length-dependent uptake of DNA-wrapped single-walled carbon nanotubes. Adv. Mater. 19(7), 939 (2007)
- Jeynes, J.C.G., et al.: Generation of chemically unmodified pure single-walled carbon nanotubes by solubilizing with RNA and treatment with ribonuclease A. Adv. Mater. 18(12), 1598–1602 (2006)
- Kam, N.W.S., Liu, Z.A., Dai, H.J.: Carbon nanotubes as intracellular transporters for proteins and DNA: an investigation of the uptake mechanism and pathway. Angew. Chem. Int. Ed. 45(4), 577–581 (2006)
- 22. Zheng, M., et al.: DNA-assisted dispersion and separation of carbon nanotubes. Nat. Mater. **2**(5), 338–342 (2003)
- 23. Chen, R.J., et al.: Noncovalent functionalization of carbon nanotubes for highly specific electronic biosensors. Proc. Natl Acad. Sci. USA 100(9), 4984–4989 (2003)
- Kam, N.W., Dai, H.: Carbon nanotubes as intracellular protein transporters: generality and biological functionality. J. Am. Chem. Soc. 127(16), 6021–6026 (2005)
- 25. Nepal, D., Geckeler, K.E.: Proteins and carbon nanotubes: close encounter in water. Small 3(7), 1259–1265 (2007)
- 26. Shim, M., et al.: Functionalization of carbon nanotubes for biocompatibility and biomolecular recognition. Nano Lett. **2**(4), 285–288 (2002)
- 27. Strano, M.S., et al.: The role of surfactant adsorption during ultrasonication in the dispersion of single-walled carbon nanotubes. J. Nanosci. Nanotechnol. **3**(1–2), 81–86 (2003)
- 28. Valenti, L.E., et al.: The adsorption-desorption process of bovine serum albumin on carbon nanotubes. J. Colloid Interf. Sci. **307**(2), 349–356 (2007)
- 29. Vyalikh, A., et al.: A carbon-wrapped nanoscaled thermometer for temperature control in biological environments. Nanomedicine **3**(3), 321–327 (2008)

- 30. Zorbas, V., et al.: Preparation and characterization of individual peptide-wrapped single-walled carbon nanotubes. J. Am. Chem. Soc. 126(23), 7222–7227 (2004)
- 31. Liu, Z., et al.: siRNA delivery into human T cells and primary cells with carbon-nanotube transporters. Angew. Chem. Int. Ed. **46**(12), 2023–2027 (2007)
- 32. Moore, V.C., et al.: Individually suspended single-walled carbon nanotubes in various surfactants. Nano Lett. 3(10), 1379–1382 (2003)
- 33. Nakayama-Ratchford, N., et al.: Noncovalent functionalization of carbon nanotubes by fluorescein-polyethylene glycol: supramolecular conjugates with pH-dependent absorbance and fluorescence. J. Am. Chem. Soc. **129**(9), 2448–2449 (2007)
- 34. O'Connell, M.J., et al.: Reversible water-solubilization of single-walled carbon nanotubes by polymer wrapping. Chem. Phys. Lett. **342**(3–4), 265–271 (2001)
- 35. Petrov, P., et al.: Noncovalent functionalization of multi-walled carbon nanotubes by pyrene containing polymers. Chem. Commun. **23**, 2904–2905 (2003)
- 36. Prencipe, G., et al.: PEG branched polymer for functionalization of nanomaterials with ultralong blood circulation. J. Am. Chem. Soc. **131**(13), 4783–4787 (2009)
- 37. Richard, C., et al.: Supramolecular self-assembly of lipid derivatives on carbon nanotubes. Science **300**(5620), 775–778 (2003)
- 38. Lamprecht, C., et al.: AFM imaging of functionalized double-walled carbon nanotubes. Ultramicroscopy **109**(8), 899–906 (2009)
- 39. Bahr, J.L., Tour, J.M.: Covalent chemistry of single-wall carbon nanotubes. J. Mater. Chem. 12(7), 1952–1958 (2002)
- Hou, P.X., Liu, C., Cheng, H.M.: Purification of carbon nanotubes. Carbon 46(15), 2003–2025 (2008)
- 41. Klein, K.L., et al.: Surface characterization and functionalization of carbon nanofibers. J. Appl. Phys. 103(6), (2008)
- 42. Lin, T., et al.: Chemistry of carbon nanotubes. Aust. J. Chem. **56**(7), 635–651 (2003)
- 43. Martinez, M.T., et al.: Modifications of single-wall carbon nanotubes upon oxidative purification treatments. Nanotechnology **14**(7), 691–695 (2003)
- 44. Sinnott, S.B.: Chemical functionalization of carbon nanotubes. J. Nanosci. Nanotechnol. 2(2), 113–123 (2002)
- 45. Zhang, J., et al.: Effect of chemical oxidation on the structure of single-walled carbon nanotubes. J. Phys. Chem. B **107**(16), 3712–3718 (2003)
- 46. Nagasawa, S., et al.: Effect of oxidation on single-wall carbon nanotubes. Chem. Phys. Lett. **328**(4–6), 374–380 (2000)
- 47. Hu, H., et al.: Nitric Acid Purification of Single-Walled Carbon Nanotubes. Phys Chem. B **107**(50), 13838 (2003)
- 48. Rosca, I.D., et al.: Oxidation of multiwalled carbon nanotubes by nitric acid. Carbon **43**(15), 3124–3131 (2005)
- 49. Verdejo, R., et al.: Removal of oxidation debris from multi-walled carbon nanotubes. Chem. Commun. 5, 513–515 (2007)
- 50. Heister, E. et al.: Higher dispersion efficacy of functionalized carbon nanotubes in chemical and biological environments. Acs. Nano. 4, 2615–2626 (2010)
- 51. Portney, N.G., Ozkan, M.: Nano-oncology: drug delivery, imaging, and sensing. Anal. Bioanal. Chem. **384**(3), 620–630 (2006)
- Prato, M., Kostarelos, K., Bianco, A.: Functionalized carbon nanotubes in drug design and discovery. Acc. Chem. Res. 41(1), 60–68 (2008)
- 53. Kamruzzahan, A.S.M., et al.: Antibody linking to atomic force microscope tips via disulfide bond formation. Bioconj. Chem. **17**(6), 1473–1481 (2006)
- 54. Porter, A.E., et al.: Direct imaging of single-walled carbon nanotubes in cells. Nat. Nanotechnol. **2**(11), 713–717 (2007)
- 55. Suntharalingam, M., Wente, S.R.: Peering through the pore: nuclear pore complex structure, assembly, and function. Dev. Cell **4**(6), 775–789 (2003)
- Kramer, A., et al.: A pathway separate from the central channel through the nuclear pore complex for inorganic ions and small macromolecules. J. Biol. Chem. 282(43), 31437–31443 (2007)

57. Chen, X., et al.: Interfacing carbon nanotubes with living cells. J. Am. Chem. Soc. 128(19), 6292–6293 (2006)

- Kam, N.W.S., et al.: Carbon nanotubes as multifunctional biological transporters and nearinfrared agents for selective cancer cell destruction. Proc. Natl Acad. Sci. USA 102(33), 11600–11605 (2005)
- 59. Kostarelos, K., et al.: Cellular uptake of functionalized carbon nanotubes is independent of functional group and cell type. Nat. Nanotechnol. **2**(2), 108–113 (2007)
- 60. Lacerda, L., et al.: Cell-penetrating CNTs for delivery of therapeutics. Nano Today 2(6), 38–43 (2007)
- 61. Pantarotto, D., et al.: Translocation of bioactive peptides across cell membranes by carbon nanotubes. Chem. Commun. 1, 16–17 (2004)
- 62. Liu, Z., et al.: In vivo biodistribution and highly efficient tumour targeting of carbon nanotubes in mice. Nat. Nanotechnol. **2**(1), 47–52 (2007)
- 63. Madl, J., et al.: A combined optical and atomic force microscope for live cell investigations. Ultramicroscopy **106**(8–9), 645–651 (2006)
- 64. Ebner, A., et al.: Determination of CFTR densities in erythrocyte plasma membranes using recognition imaging. Nanotechnology **19**(38) 6 pp. (2008) Article Nr. : 384017
- 65. Tang, J.L., et al.: High-affinity tags fused to S-layer proteins probed by atomic force microscopy. Langmuir **24**(4), 1324–1329 (2008)

Uptake, Intracellular Localization and Biodistribution of Carbon Nanotubes

V. Neves, H. M. Coley, J. McFadden and S. R. P. Silva

Abstract Carbon nanotubes (CNTs) exhibit unique size, shape and physical properties, which make them promising candidates for biomedical applications. In particular, carbon nanotubes have been intensively studied for conjugation with pre-existing therapeutic agents for more effective targeting, as a result of their ability to cross cell membranes. However, to utilise them effectively in biological systems it is extremely important to understand how they behave at the cellular level and their distribution in vivo. Additionally, in order to consider carbon nanotubes as candidate delivery systems of therapeutic agents it is important to ascertain their fate in vivo, but also take into account many factors, such as solubility, stability and clearance. Issues surrounding their short term and long term safety are currently the subject of toxicology testing. Herein, we propose to summarize the main findings on the uptake, trafficking and biodistribution of carbon nanotubes, with special focus on functionalized carbon nanotubes for delivery of therapeutic agents.

1 General Considerations on Uptake and Distribution of Nanoparticles

The clinical administration of therapeutic agents has been limited by multiple factors such as low solubility, stability and rapid clearance. With the goal of improving the bioavailability and reducing side effects, the approach of conjugating pharmacological agents with nanoparticles has met with great interest from

V. Neves (⋈), H. M. Coley, J. McFadden and S. R. P. Silva Faculty of Health and Medical Sciences, University of Surrey, Guildford, GU2 7XH, UK e-mail: V.Neves@surrey.ac.uk

the medical research community [1-3]. There are many examples of nanoparticles being used in current clinical practice and also at various stages of clinical development [4-6]; these complexed agents show improved pharmacological and toxicological properties versus the parent non-complexed counterparts. The circulating half-life of the drug complex, maximal tolerated dose (MTD), and target selectivity are the most important factors culminating in a high therapeutic index. The therapeutic load is typically conjugated to the surface of nanoparticles, or encapsulated and protected inside the core. The nanoparticle can also be designed to provide either controlled or triggered release of the therapeutic molecule [7]. The particle surface can then functionalized by various methods with the objective of increasing the circulating half-life, and by reducing nonspecific distribution in some cases by targeting tissue with specific cell surface antigens with a targeting ligand (peptide, aptamer, antibody, small molecule). Surface functionalization can address the major limiting factor of long-circulating nanoparticles, notably protein absorption. Proteins adsorbed on the surface of the nanoparticle promote opsonization, leading to aggregation with subsequent rapid clearance from the bloodstream [8–10]. The resultant rapid clearance is due to phagocytosis by the mononuclear phagocyte system (MPS) in conjunction with the liver and spleen filtration network. Typically, the majority of opsonized particles are cleared by a receptor-mediated mechanism within minutes due to the high concentration of phagocytic cells in the liver and spleen or alternatively they may be excreted [9].

Numerous biological barriers exist to protect the human body from invasion by foreign particles. The biodistribution of any nanoparticle is primarily ruled by their ability to transverse biological barriers [11]. These barriers include: the reticuloendothelial system (RES), endothelial/epithelial membranes, complex networks of blood vessels, abnormal flow of blood and interstitial gradients. Endothelia composing the blood vessels have been classified as continuous, fenestrated, or discontinuous, depending on the morphological features and organ location. Continuous endothelium morphology appears in arteries, vessels [12], and the lungs [13]. In contrast, fenestrated endothelium appears in glands [14], digestive mucosa, and kidney (wherein fenestrae form pores of approximately 60 nm). Discontinuous endothelium is a characteristic of the liver (fenestrae of 50–100 nm) [15]. Endothelial cells from the blood vessels are able to respond to the physiological environment, resulting in angiogenic activity. Angiogenesis pertaining to tumour biology has been well characterized in many studies. During tumor growth, angiogenesis results in defective hypervasculature and a deficient lymphatic drainage system, which explains the concept of passive targeting of nanoparticles to tumors through the "enhanced permeability and retention" (EPR) effect [16, 17]. The EPR is a unique tumour-related feature, which allows macromolecules or nanoparticles (cutoff size of >400 nm) to preferentially accumulate and diffuse within tumor tissues [18].

Additionally, boundaries exist at a cellular level, for example, the cell membrane and the different organelles inside the cell, in particular the nuclear envelope and endosomes [19]. For example, if internalization of nanoparticles is via

receptor-mediated endocytosis, it is usually through the endosome/lysosome pathway and can lead to the therapeutic agent to be trapped in the organelle or be degraded.

More recently, carbon nanotubes have been considered for biomedical applications and a number of groups are currently involved in elucidating their uptake and biodistribution.

2 Uptake and Intracellular Localization of Carbon Nanotubes

Pantarotto and colleagues published the first evidence that carbon nanotubes translocate across cell membranes [20]. In that particular study, water-soluble, amino-functionalized single walled carbon nanotubes (SWCNTs) were conjugated to a fluorescent dye via either a short organic linker or a peptide. When incubated with fibroblasts (Human 3T6 and murine 3T3) both conjugates were internalized but the peptide- SWCNTs were found to accumulate in the nucleus, whereas the directly labeled SWCNTs were solely confined to the cytoplasm. The uptake mechanism described was shown to be endocytosis-independent given that internalization was unaffected by temperature or presence of endocytosis inhibitors. Thus, it was proposed that carbon nanotubes behave like cell penetrating peptides (CPPs) and related synthetic oligomers [20]. Following this study, uptake of carbon nanotubes was also demonstrated by means of gene expression [21], for the use of CNTs for gene delivery. The interaction of SWCNTs with HeLa cells (human cervical cancer) was reported using transmission electron microscopy (TEM) with evidence of nanotubes crossing the plasma membrane barrier. A mechanism whereby carbon nanotubes pass through the cell membrane as "nanoneedles" without loss of cell viability, was proposed [21]. The hypothesis was put forward that the cationic functional groups bind the nanotubes to the cell membrane and this facilitates a spontaneous insertion mechanism allowing them to pass through the biomembrane. Additionally, it was demonstrated that various types of functionalized carbon nanotubes can be taken up by a wide range of cells, some of which were deficient in phagocytotic function (i.e. fibroblasts) or lacked the capacity to undergo endocytosis (e.g. fungi, yeast and bacteria) [22]. Hence the term "nanosyringe", was adopted to describe these properties and this was further explored by Lopez et al. They proposed a model whereby nanotubes interact with lipid bilayers via a diffusion process directly through the biomembrane. The mechanism involves a two-step process in which the nanotubes are first associated onto the membrane surface and then reoriented to adopt a transmembrane configuration [23].

As an alternative to the "nanoneedles" mechanism, Kam et al. subsequently reported uptake of SWCNT and SWCNT-streptavidin by human promyelocytic leukemia (HL60) and human T cells (Jurkat) via an endocytic pathway. In that study, not only is it shown that carbon nanotubes are taken up by cells but they can also carry large cargos such as streptavidin (MW \approx 60 kDa) [24]. To elucidate

the mechanism of entry of carbon nanotubes into cells, a membrane/endosome marker FM 4-64, and reduced temperature were used. By adding both endosome marker and nanotube conjugates co-localization was observed which provided direct evidence for the endocytotic uptake. A later study from the same group further demonstrated uptake of carbon nanotubes conjugated with different labeled proteins: streptavidin, protein A, bovine serum albumin and cytochrome c in various adherent and suspension cell line cultures. Data obtained were in support of an endocytic pathway, showing co-localization of nanotubes with an endosomal marker but absence of nuclear localisation [25]. To investigate the release of nanotubes by the endosomes they added chloroquine to cell medium during incubation of cells with protein- SWCNT conjugates. Chloroquine is a membrane permeable base capable of localizing inside endosomes, increasing pH giving rise to endosomal rupture. With chloroquine addition it was shown that the intracellular fluorescence signal was more diffuse and uniform as opposed to a more punctate staining pattern. To assess the role of Clathrin coated vesicles, further experiments were carried out in the presence of sucrose and potassium-depleted medium, which revealed a significantly reduced level of CNT uptake [26]. The study also demonstrated that the nanotubes were not internalized via the caveolae or lipid-raft pathway. Moreover, using filipin and nystatin treatment, known to perturb the cholesterol distribution on the cell membrane had no influence on uptake of carbon nanotubes. In conclusion, SWCNT, complexed with proteins and nucleic acids, penetrate cell membranes following a Clathrin-dependent endocytotic process.

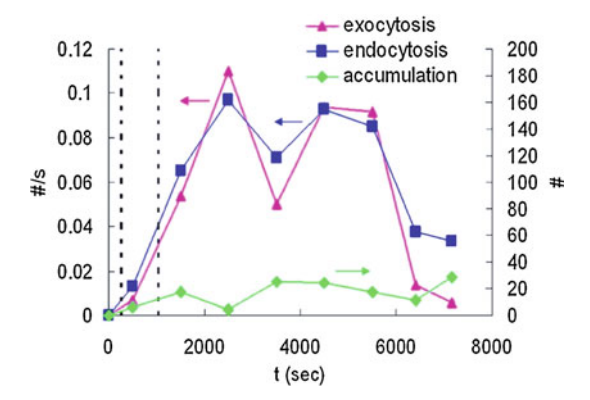
In the approaches described before carbon nanotube uptake was studied by visualizing internalization by covalently linkage of a visible-wavelength fluorophore. Caution should be exercised when considering this approach with respect to parameters such as: chemical linkage which resist enzymatic cleavage, the emission from the visible-wavelength fluorophore which must be detected above background endogenous fluorescence. Further, the chemical processing of nanoparticles may dramatically change their biological fate. Cherukuri et al. [27] presented a technique that permits the observation of pristine, hydrophobic SWCNTs in biological media by near-infrared (NIR) fluorescence. Carbon nanotubes present a unique NIR intrinsic fluorescence making them advantageous for use in biological systems as there is minimal background autofluorescence from cells, tissues, and other biological molecules in this spectral range. Furthermore, biological tissues facilitate high transmission penetration of NIR light (near $\sim 1 \mu m$) for detection within an organism or under the surface of tissues [28]. Using this technique mouse macrophage-like cells can be seen to actively engulf significant quantities of SWCNT, with an average ingestion rate of approximately one nanotube per second per cell. They also revealed that incubating cells at a reduced temperature of 27°C caused a reduction of uptake of nanotubes of 60% compared with incubation at 37°C, suggesting an active ingestion of the nanotubes [27]. Another uptake study involving spectroscopic measurement of DNA-wrapped carbon nanotubes indicated a length-selective uptake of nanotubes. The assay determined an approximate uptake threshold of

approximately 189(±17) nm. After 16 h incubation 32% of nanotubes remained in solution, suggesting that only a proportion of nanotubes available may be ingested [29]. Heller et al. used a combined approach of NIR and Raman spectroscopy for assessment of cellular uptake [30]. Raman spectroscopy is a general, rapid (~1 min per spectrum) non-destructive technique that operates at standard room temperature (~300 K) and pressure conditions, and uses readily available Raman characterization instrumentation [31]. Due to electronic structure and diameter of carbon nanotubes strong resonance-enhanced Raman bands are produced at 150-300, ~ 1.350 , 1.590-1.600, and ~ 2.600 cm⁻¹ away from the excitation wavelength [32]. The first, termed the Raman: Radial breathing modes (RBMs), are caused by uniaxial vibrations and depend linearly on the nanotube diameter; then the tangential mode (or G band), which is caused by stretching along the C-C bonds of graphene [32–34]; the $\sim 1,350 \text{ cm}^{-1}$ for the disorder-induced D band, and at $\sim 2.900 \text{ cm}^{-1}$ for its second-order harmonic, the G' band [32]. After incubation, of Murine myoblast stem cell and 3T3 fibroblast cells, with DNAwrapped SWCNT, persistent Raman scattering and a parallel marked decrease in intensity in fluorescence (relative to Raman was observed) due to internalisation of nanotubes. The deposition of the nanotubes could be determined up to 3 months in culture. Raman signal of cells incubated with DNA- SWCNT left in culture for 48 h and 8 days showed that the nanotubes concentrated near, but outside, the nuclei of cells. This perinuclear accumulation of nanotubes was confirmed by TEM where it is shown that carbon nanotubes formed uniaxial, ordered bundles inside vesicles located near the nucleus, but not within the nuclear envelope. In view of these observations it was suggested that there was an endocytic transport mechanism for DNA-SWCNT aggregates. Interestingly, it was also reported that aggregates remained in cells during repeated cell divisions [30]. By use of Raman spectroscopic measurement of, carbon nanotube uptake was also analysed in SWCNT dispersed in media containing fetal bovine serum or a peptide (nano-1), demonstrated this to be a time- and temperature-dependent process [35]. Measurements of the G band in different regions within the cell were performed showing that it was detected in both the cytoplasm and nucleus. However, it was suggested that the localisation was more realistically associated with carbon nanotubes at the perinuclear region and/or in the cytoplasm immediately above or below the nucleus. It was proposed that the intensity of the G band produced was due to an active uptake of CNTs, as incubation at 4°C resulted in a 98% decrease in intensity [35]. Yehia et al. conducted a similar study with time-dependent uptake studied using Raman spectroscopy in conjunction with TEM to examine intracellular distribution. They reported that CNTs were not associated with mitochondria, Golgi bodies or the nucleus, but they accumulated in cytoplasmatic vacuoles [36].

Another label-free approach for visualizing CNT uptake is by AFM. Lamprecht et al. demonstrated that AFM could be used to visualize non-covalently functionalized single walled (SWCNT) and double walled carbon nanotubes (DWNT) immobilized on different biological membranes, such as plasma membranes and nuclear envelopes, as well as on a monolayer of avidin molecules [37].

V. Neves et al.

Fig. 1 A comparison of net internalisation (endocytosis) and exocytosis rates (#/s) and net accumulation (#/cell) over time by single particle tracking. This results in NIH3T3 fibroblast cells, shows that the data imply that endocytosis and exocytosis rates for DNA- SWCNT are closely regulated



Jin and co-workers [38] reported the first evidence of exocytosis; by single particle tracking (SPT) they demonstrated that the rate of exocytosis closely matches that for endocytosis. NIH-3T3 fibroblast cells were exposed to DNA-SWCNTs for approximately 16 min, followed by media perfusion for a period of approximately 2 h. Endocytosis took place throughout the duration of the experiment at a slow rate, with uptake of CNT aggregates occurring as a later event. It has been suggested that the DNA- SWCNT could be recycled back to the membrane together with its receptors. The endocytotic rate is highest initially, and the exocytosis rate closely matched with a negligible temporal offset (Fig. 1). Given that Au nanoparticles of diameters from 14 to 100 nm undergo exocytosis according to a size associated linear relationship, with the larger particles being less likely to be exocytosed [39]. Those data were in agreement with the previously reported agglomeration observed within cell (as above). However it should be noted that the accumulation observed represented a small fraction of SWCNT processed by the cell, as illustrated in Fig. 1. The basis for the endocytotic mechanism is explained by adsorption of proteins from the media to the surface of functionalized SWCNT, confirmed by electrophoretic mobility and zeta potentials of DNA- SWCNT in water and in media [38]. Additionally, the same group has recently published a study on size-dependent uptake and expulsion of SWCNT using the same methodology (SPT) [40]. This study comprises a mathematical model for size dependent uptake and shows that for SWCNT a optimal endocytosis rate occurs around 25 nm [40].

Neves et al. also describe expulsion of carbon nanotubes, in a study of uptake and release of RNA-wrapped oxidized DWNT in PC3 cells. The data not only illustrate, by Raman mapping, the distribution of RBM band inside the cells due to the internalization of CNTs (Fig. 2), but also provide evidence that nanotubes are not simply located at the cell surface. This evidence is provided by experiments performed on whole cell lysate preparations at different time points from 30 min to 24 h. CNT uptake and CNT release occurred within 24 h with no significant changes on cellular structures or a loss in cell viability. The highest intensity occurred at 3 h with a peak of 50% of cells with internalized CNTs. Cells gradually released CNTs, with a marked fourfold decrease in cellular accumulation

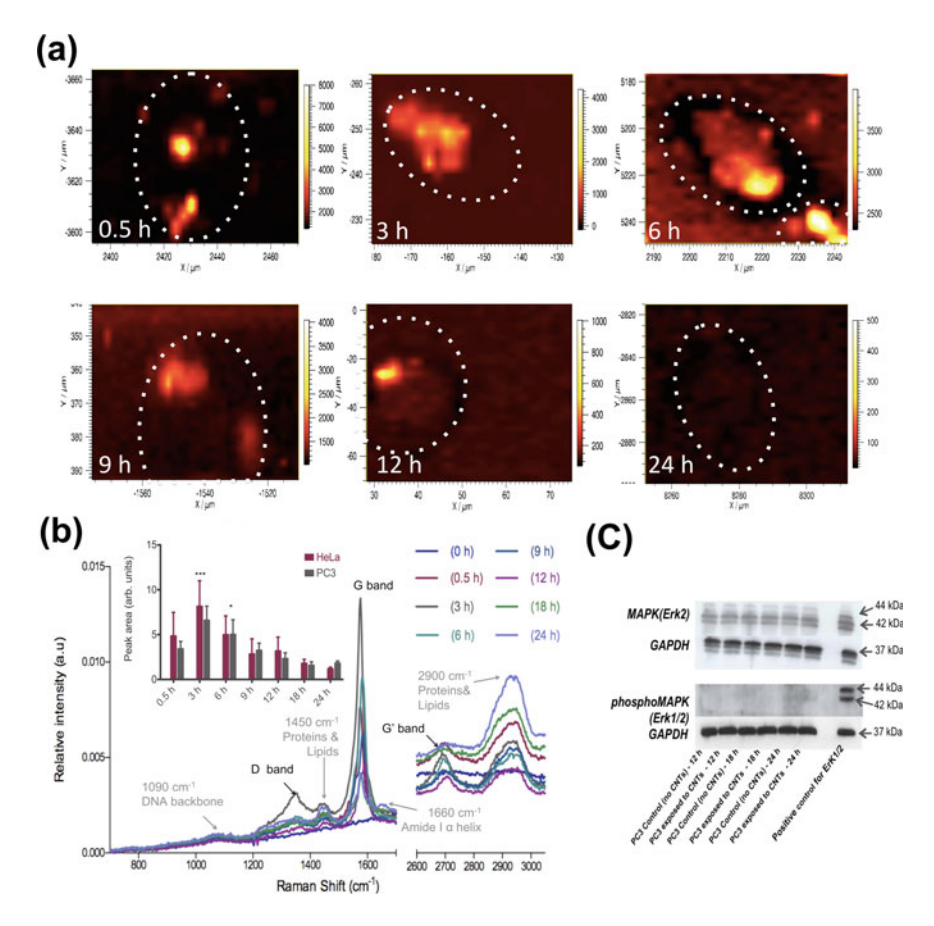


Fig. 2 Time-dependent uptake and release of RNA-wrapped, oxidized double walled carbon nanotubes (oxDWNT-RNA) by Raman in intact PC3 cells (**a**) and in PC3 cell lysates (**b**) with no induced stress response (**c**). **a** Single cell mapping of whole PC cell showing the distribution of nanotubes inside the cells at different time points, from 0.5 to 24 h. **b** Raman intensity of PC3 cell lysates at the various time points, G band intensity exhibits a maximum at 3 h with a consequent decrease with the release of nanotubes. **c** MAPK (Erk2) and phosphorylated MAPK (Erk 1/2) expression on cells exposed to carbon nanotubes

seen, after 12 h incubation. At 24 h the intensity associated with the presence of carbon nanotubes was negligible. These findings were supportive of the use of CNTs as non-toxic carriers of pharmaceutical agents for use in many biomedical settings, such as cancer therapy. Moreover, it was established that protein and DNA was being synthesized and that no induced stress was evident after exposure to CNTs. Stress response was evaluated by means of activation of mitogen-activated protein kinase (MAPK) revealing that cells exposed to carbon nanotubes do not present a significant increase in its phosphorylated form (phospho-MAPK).

Intracellular trafficking of CNTs was firstly described by Lacerda et al. [41]. The previously described "nanoneedle" carbon nanotubes (SWCNT-NH³⁺).

V. Neves et al.

which contain a luminescence signal due to the functionalization method, were incubated with A549 cells (human lung carcinoma) and free cellular stainings. The results demonstrated that uptake of nanotubes leads to perinuclear accumulation with no effect on cell viability. As this set of experiments was not performed under standard tissue culture conditions (absence of serum), which was different from the experimental conditions used in the exocytosis experiments this could explain the effects seen on intracellular accumulation [41].

In summary, progress has been made towards our understanding of how nanotubes interact with cell. However, it is important to note, that besides different mechanisms of uptake described, there are many variations on experimental design and methodologies used,—such as functionalization of the material, concentration etc.

3 Biodistribution of Carbon Nanotubes

Elucidating the pharmacological profiles of in vivo administered CNTs, is very important when considering their potential for medical use. Potential harmful effects associated with nanotubes, due to their nanoscale dimensions and carbon backbone, may arise from their ability to readily enter the respiratory tract, deposit in the lung tissue, redistribute from their site of deposition, escape from the normal phagocytic defenses, and modify the structure of proteins. Therefore, nanotubes might potentially activate inflammatory and immunological responses, affecting normal organ function [42].

Initial studies of biodistribution of CNTs focused on their toxicological profile in vivo [43–49]. Studies focused on the effects of CNTs in terms of pulmonary toxicity following inhalation, intratracheal instillation [45, 46], and pharyngeal aspiration [47], in addition to their effects on skin toxicity after topical application [43], and subcutaneous administration [48, 49]. These reports cited acute pulmonary toxicity effects, induction of granulomas, and inflammatory reactions to CNT. However, all of those particular studies used pristine, non-functionalized CNT, usually dispersed in an aqueous buffer with the aid of a surfactant such as Tween 80 [46]. In contrast, toxicity of acid-treated CNT of two different lengths (200 and 825 nm) subcutaneously administered to rats showed, no severe inflammatory response such as necrosis, tissue degeneration, or neutrophil infiltration [49]. Thus, functionalization and aqueous solubility contribute significantly to biocompatibility of these materials, improving dramatically the in vitro toxicity profile [50, 51].

The first in vivo study on functionalized CNT biodistribution was reported by Wang et al. using mice treated with intraperitoneally (i.p.) administered short hydroxylated single walled CNTs. SWCNTs were shown to accumulate mainly in the liver and kidney, lesser so in the spleen and lung, and excreted mainly by the kidney within 18 days [52]. In another study, using intravenous administration (i.v.) it was demonstrated that functionalized SWCNT with a chelating molecule diethylenetriaminepentaacetic (DTPA) and labeled with indium (111 In)—[111 In]DTPA- SWCNT, followed by radioactivity tracing using gamma

scintigraphy, resulted in no retention in any RES organs (liver or spleen) and were rapidly cleared from the systemic blood circulation again via renal excretion [42]. In addition this study allowed a comparison of the biodistribution of two types of functionalization: the first with no free amino groups and a second one with 40% free amino groups resulting in surface charge. Both functionalized SWCNTs were found in kidney, muscle, skin, and blood after 30 min. However the surfacecharged SWCNTs led to a higher affinity for kidney, muscle, skin, and lung, leading to their rapid clearance from all tissues. As rapidly as 3 h the nanotubes were cleared from all organs down to levels of 1-2% (relative to the 30 min time point). TEM analysis of urine samples indicated high levels of intact functionalized CNTs showing that they are rapidly cleared from the systemic circulation via the kidney [42]. Subsequently, Lacerda et al. presented an elimination mechanism for CNT complexes using [111In]DTPA-MWCNT. The CNT complexes tail vein injected showed very rapid entry into the systemic blood circulation followed by rapid urinary clearance (Fig. 3) [53]. The reason for rapid elimination observed here, when compared to with surfactants functionalization is that once in the blood these surfactants desorbed from the CNTs which leads to bundles circulating and

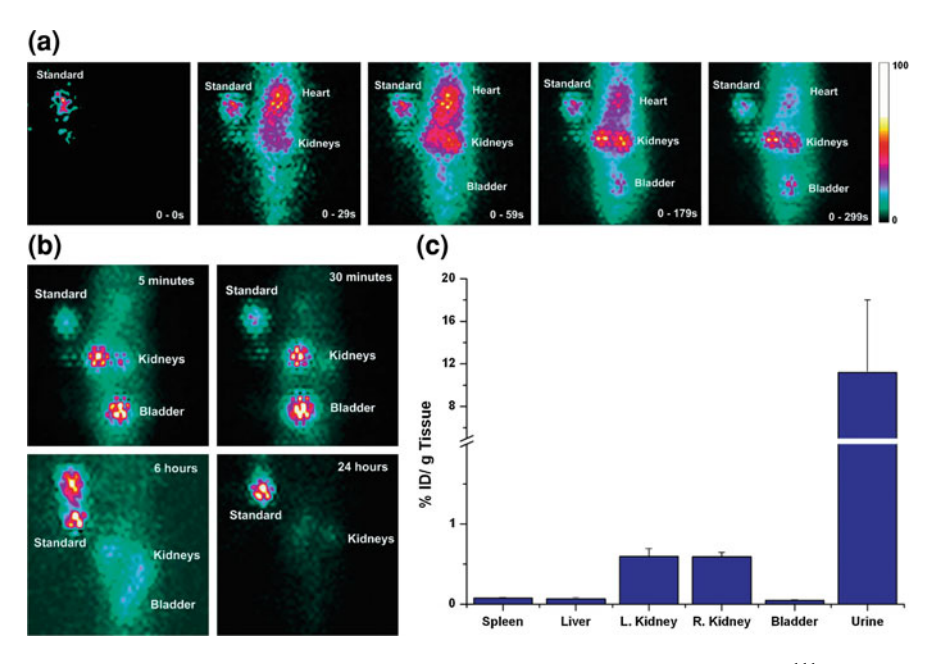


Fig. 3 Rat distribution of radioactive labeled multi-walled carbon nanotubes ([111 In]DTPA-MWCNT). **a** Dynamic anterior planar images of whole body distribution of [111 In]DTPA-MWCNT within 5 min after intravenous administration in rats. **b** Static anterior planar images of whole body distribution of [111 In]DTPA-MWCNT within 5 min, 30 min, 6 h and 24 h post-injection. **c** %ID radioactivity per gram tissue at 24 h after intravenous administration of [111 In]DTPA-MWCNT quantified by gamma counting (n = 3 and *error bars* for standard deviation) [53]

consequent accumulation in the liver tissue. The mechanism of [111In]DTPA-MWCNT eliminations has been shown to be via the kidney glomerular filtration system. It is important to note that [111In]DTPA-MWCNT complexes used in this study were considerably larger than the dimensions of the glomerular capillary wall. Hence, the length does not appear to be a critical parameter in their renal clearance. The mechanism by which CNTs pass through the glomerular filtration system is believed to involve the acquisition of a conformation in which the longitudinal dimension of the nanotube is perpendicular to the glomerular fenestrations (cross section is between 20 and 30 nm) and small enough to allow permeation through the glomerular pores [53]. This hypothesis was later confirmed by TEM imaging, where individualized, well-dispersed MWCNTs were observed in the renal capillary lumen. During their translocation through the glomerular filtration barrier their longitudinal axis was shown to be vertically oriented to the endothelial fenestrations [54]. Moreover, histological examination of the different tissues confirmed that those MWCNT complexes did not induce any physiological abnormality after 24 h post-injection [55].

Systemic clearance of SWCNT was also demonstrated by NIR fluorescence (near-IR). SWCNTs were dispersed in a solution of Pluronic F108 surfactant and injected in rabbits showing that the concentration of nanotubes in the blood serum decreased exponentially with a half life of 1 h. Moreover, near-IR fluorescence microscopy on tissue revealed that only SWCNTs in the liver were detected at significant levels at 24 h [56].

Considering the safety and efficacy of CNT-complexes for medical applications its not only relevant that they are cleared rapidly from the body. They need to achieve good biodistribution and show good target specificity in order to have therapeutic efficacy. The targeted accumulation of CNTs in vivo was first demonstrated by Lui et al. using PEGylated SWCNT linked to an arginine-glycineaspartic acid (RGD) peptide [57]. They generated U87MG human glioblatoma and HT-29 human colorectal tumour models by injecting 5×10^6 cells in PBS into front legs of mice and allowed to reach a tumour volume of 200-300 mm³. Furthermore, with the purpose of increasing the circulating half-life, two different lengths of PEG chains were used (molecular weight of PEG chains = 2,000 and 5,400, respectively). The lengths of the PEG molecule influenced biological behaviour, with the longer PEG chain leading to increased blood levels and reduced RES uptake when compared with the shorter chain complex. The explanation for this was suggested to be due to the fact that PEG₅₄₀₀ renders SWCNT more hydrophilic and resistant to protein non-specific binding (NSB). These properties were not seen with the CNT complex involving functionalization with PEG₂₀₀₀, which was unable to prevent protein NSB to SWCNT. In addition, the linking of the RGD peptide, which is a ligand for cell-surface integrins, led to an increased in uptake into the tumor, with PEG5400 achieving higher tumor accumulation due to its increased plasma half-life. Moreover, the study used Raman spectroscopy to directly detect SWCNT in the various murine tissues. The analysis revealed the existence of SWCNT in the liver and tumor samples with high G band Raman intensities, proving the tumor uptake of the complex [57]. Subsequently, Raman spectroscopy was also used to image the localization of SWCNT in live rodents [58]. Similar to the previous study, increased accumulation of RGD-SWCNT in tumor was demonstrated as opposed to plain- SWCNT. These findings demonstrated the ability of Raman spectroscopy to non-invasively localize targeted SWCNT in vivo [58]. The biodistribution and long-term fate of CNTs injected intravenously in vivo, was later studied, using the same technique, of Raman spectroscopy [59]. Besides the enhancement in blood half-life of CNTs (up to 15 h), SWCNT have also been detected in various organs and tissues of mice ex vivo over a period of up to 3 months. To study in depth the excretory pathway CNTs were injected at high dose in mice and urine and faeces collected at different time points. There was evidence for CNTs in faeces and intestine revealing excretion via the hepato-biliary pathway. The Raman signal was measured in the kidney and bladder after 24 h, suggesting SWCNTs are also excreted through the renal pathway, as demonstrated in other studies. Since the average of lengths used in that study exceeded the renal excretion threshold and the majority of CNTs accumulated in the liver, it was suggested the urinary excretion occurs for a small percentage of CNTs of very short length (<50 nm in length, diameter 1–2 nm). The overall conclusion from these studies is that in fact CNTs are excreted chiefly via the biliary pathway, with faecal elimination [59]. In addition, necropsy, histology and blood chemistry reveal no toxicity in mice injected with SWCNT with no impact on body weight or mortality [59].

The findings described above have revealed that CNTs can be designed in many ways to form pharmaceutical complexes, which allow them to enter blood circulation, target cells, deliver pay-loads, be exocytosed and finally eliminated from the body. A variety of approaches have been described above, for example, chemical modification via functionalization, which increased circulatory half-life and led to enhanced tumor accumulation. As a nanoparticle for medical applications, the carbon nanotube, shows promise in offering lower toxicity with enhanced efficacy.

References

- Zhang, L., et al.: Nanoparticles in medicine: therapeutic applications and developments. Clin. Pharmacol. Ther. 83(5), 761–769 (2008)
- Shaffer, C.: Nanomedicine transforms drug delivery. Drug Discov. Today 10(23–24), 1581– 1582 (2005)
- 3. Alexis, F., et al.: New frontiers in nanotechnology for cancer treatment. Urol. Oncol. **26**(1), 74–85 (2008)
- 4. James, N.D., et al.: Liposomal doxorubicin (Doxil): an effective new treatment for Kaposi's sarcoma in AIDS. Clin. Oncol. (R Coll. Radiol.) 6(5), 294–296 (1994)
- 5. Muggia, F.M.: Doxil in breast cancer. J. Clin. Oncol. 16(2), 811-812 (1998)
- 6. Schluep, T., et al.: Preclinical efficacy of the camptothecin-polymer conjugate IT-101 in multiple cancer models. Clin. Cancer Res. **12**(5), 1606–1614 (2006)
- 7. Pridgen, E.M., Langer, R., Farokhzad, O.C.: Biodegradable, polymeric nanoparticle delivery systems for cancer therapy. Nanomedicine **2**(5), 669–680 (2007)

V. Neves et al.

8. Romberg, B., Hennink, W.E., Storm, G.: Sheddable coatings for long-circulating nanoparticles. Pharm. Res. **25**(1), 55–71 (2008)

- 9. Moghimi, S.M., Hunter, A.C., Murray, J.C.: Long-circulating and target-specific nanoparticles: theory to practice. Pharmacol. Rev. **53**(2), 283–318 (2001)
- Owens 3rd, D.E., Peppas, N.A.: Opsonization, biodistribution, and pharmacokinetics of polymeric nanoparticles. Int. J. Pharm. 307(1), 93–102 (2006)
- 11. Ferrari, M.: Cancer nanotechnology: opportunities and challenges. Nat. Rev. Cancer 5, 161–171 (2005)
- 12. Simionescu, M., Simionescu, N., Palade, G.E.: Morphometric data on the endothelium of blood capillaries. J. Cell Biol. **60**(1), 128–152 (1974)
- 13. Brigham, K.L.: Estimations of permeability properties of pulmonary capillaries (continuous endothelium). Physiologist **23**(1), 44–46 (1980)
- 14. Ryan, U.S., et al.: Fenestrated endothelium of the adrenal gland: freeze-fracture studies. Tissue Cell **7**(1), 181–190 (1975)
- 15. Braet, F., et al.: Contribution of high-resolution correlative imaging techniques in the study of the liver sieve in three-dimensions. Microsc. Res. Tech. **70**(3), 230–242 (2007)
- Maeda, H.: The enhanced permeability and retention (EPR) effect in tumor vasculature: the key role of tumor-selective macromolecular drug targeting. Adv. Enzyme Regul. 41, 189–207 (2001)
- 17. Greish, K.: Enhanced permeability and retention of macromolecular drugs in solid tumors: a royal gate for targeted anticancer nanomedicines. J. Drug Target. **15**(7–8), 457–464 (2007)
- 18. Hobbs, S.K., et al.: Regulation of transport pathways in tumor vessels: role of tumor type and microenvironment. Proc. Natl. Acad. Sci. USA **95**(8), 4607–4612 (1998)
- Sanhai, W.R., et al.: Seven challenges for nanomedicine. Nat. Nanotechnol. 3(5), 242–244 (2008)
- 20. Pantarotto, D., et al.: Translocation of bioactive peptides across cell membranes by carbon nanotubes. Chem. Commun. (1), 16–17 (2004)
- Pantarotto, D., et al.: Functionalized carbon nanotubes for plasmid DNA gene delivery. Angew. Chem. Int. Ed. 43, 5242–5246 (2004)
- Kostarelos, K., et al.: Cellular uptake of functionalized carbon nanotubes is independent of functional group and cell type. Nat. Nanotechnol. 2(2), 108–113 (2007)
- Lopez, C.F., et al.: Understanding nature's design for a nanosyringe. Proc. Natl. Acad. Sci. USA 101(13), 4431–4434 (2004)
- 24. Kam, N.W.S., et al.: Nanotube molecular transporters: internalization of carbon nanotube-protein conjugates into mammalian cells. J. Am. Chem. Soc. **126**(22), 6850–6851 (2004)
- Kam, N.W.S., Dai, H.J.: Carbon nanotubes as intracellular protein transporters: generality and biological functionality. J. Am. Chem. Soc. 127(16), 6021–6026 (2005)
- Kam, N.W.S., Liu, Z.A., Dai, H.J.: Carbon nanotubes as intracellular transporters for proteins and DNA: an investigation of the uptake mechanism and pathway. Angew. Chem. Int. Ed. 45(4), 577–581 (2006)
- Cherukuri, P., et al.: Near-infrared fluorescence microscopy of single-walled carbon nanotubes in phagocytic cells. J. Am. Chem. Soc. 126(48), 15638–15639 (2004)
- 28. Meinke, M., et al.: Chemometric determination of blood parameters using visible-near-infrared spectra. Appl. Spectrosc. **59**(6), 826–835 (2005)
- Becker, M.L., et al.: Length-dependent uptake of DNA-wrapped single-walled carbon nanotubes. Adv. Mater. 19(7), 939–945 (2007)
- Heller, D.A., et al.: Single-walled carbon nanotube spectroscopy in live cells: towards longterm labels and optical sensors. Adv. Mater. 17, 2793–2799 (2005)
- 31. Jorio, A., et al.: Structural (n, m) determination of isolated single-wall carbon nanotubes by resonant Raman scattering. Phys. Rev. Lett. **86**(6), 1118–1121 (2001)
- 32. Saito, R., Dresselhaus, G., Dresselhaus, M.S.: Physical Properties of Carbon Nanotubes. Imperial College Press, London (1998)
- 33. Strano, M.S., et al.: Assignment of (n, m) Raman and optical features of metallic single-walled carbon nanotubes. Nano Lett. **3**(8), 1091–1096 (2003)

- 34. Doorn, S.K., et al.: Resonant Raman excitation profiles of individually dispersed single walled carbon nanotubes in solution. Appl. Phys. A Mater. Sci. Process. **78**(8), 1147–1155 (2004)
- 35. Chin, S.F., et al.: Amphiphilic helical peptide enhances the uptake of single-walled carbon nanotubes by living cells. Exp. Biol. Med. **232**(9), 1236–1244 (2007)
- 36. Yehia, H., et al.: Single-walled carbon nanotube interactions with HeLa cells. J. Nanobiotechnol. 5(1), 8 (2007)
- 37. Lamprecht, C., et al.: AFM imaging of functionalized carbon nanotubes on biological membranes. Nanotechnology **20**(43), 434001–434007 (2009)
- 38. Jin, H., Heller, D.A., Strano, M.S.: Single-particle tracking of endocytosis and exocytosis of single-walled carbon nanotubes in NIH-3T3 cells. Nano Lett. 8(6), 1577–1585 (2008)
- Chithrani, B.D., Chan, W.C.W.: Elucidating the mechanism of cellular uptake and removal of protein-coated gold nanoparticles of different sizes and shapes. Nano Lett. 7(6), 1542–1550 (2007)
- Jin, H., et al.: Size-dependent cellular uptake and expulsion of single-walled carbon nanotubes: single particle tracking and a generic uptake model for nanoparticles. ACS Nano 3(1), 149–158 (2009)
- 41. Lacerda, L., et al.: Intracellular trafficking of carbon nanotubes by confocal laser scanning microscopy. Adv. Mater. **19**(11), 1480–1484 (2007)
- 42. Singh, R., et al.: Tissue biodistribution and blood clearance rates of intravenously administered carbon nanotube radiotracers. Proc. Natl. Acad. Sci. USA 103, 3357–3362 (2006)
- Maynard, A.D., et al.: Exposure to carbon nanotube material: aerosol release during the handling of unrefined single-walled carbon nanotube material. J. Toxicol. Environ. Health. A 67(1), 87–107 (2004)
- 44. Huczko, A., et al.: Combustion synthesis as a novel method for production of 1-D SiC nanostructures. J. Phys. Chem. B **109**(34), 16244–16251 (2005)
- 45. Lam, C.W., et al.: Pulmonary toxicity of single-wall carbon nanotubes in mice 7 and 90 days after intratracheal instillation. Toxicol. Sci. 77, 126–134 (2004)
- 46. Warheit, D.B., et al.: Comparative pulmonary toxicity assessment of single-wall carbon nanotubes in rats. Toxicol. Sci. 77, 117–125 (2004)
- Shvedova, A.A., et al.: Unusual inflammatory and fibrogenic pulmonary responses to singlewalled carbon nanotubes in mice. Am. J. Physiol. Lung Cell. Mol. Physiol. 289(5), L698– L708 (2005)
- 48. Yokoyama, A., et al.: Biological behavior of hat-stacked carbon nanofibers in the subcutaneous tissue in rats. Nano Lett. **5**(1), 157–161 (2005)
- 49. Sato, Y., et al.: Influence of length on cytotoxicity of multi-walled carbon nanotubes against human acute monocytic leukemia cell line THP-1 in vitro and subcutaneous tissue of rats in vivo. Mol. Biosyst. 1(2), 176–182 (2005)
- Sayes, C.M., Fortner, J.D., Guo, W., Lyon, D., Boyd, A.M., Ausman, K.D., Tao, Y.J., Sitharaman, B., Wilson, L.J., Hughes, J.B., West, J.L., Colvin, V.L.: The differential cytotoxicity of water-soluble fullerenes. Nano Lett. 4(10), 1881–1887 (2004)
- 51. Sayes, C.M., et al.: Functionalization density dependence of single-walled carbon nanotubes cytotoxicity in vitro. Toxicol. Lett. **161**(2), 135–142 (2006)
- 52. Wang, H., et al.: Biodistribution of carbon single-wall carbon nanotubes in mice. J. Nanosci. Nanotechnol. 4(8), 1019–1024 (2004)
- 53. Lacerda, L., et al.: Dynamic imaging of functionalized multi-walled carbon nanotube systemic circulation and urinary excretion. Adv. Mater. **20**(2), 225–230 (2008)
- Lacerda, L., et al.: Carbon-nanotube shape and individualization critical for renal excretion.
 Small 4(8), 1130–1132 (2008)
- Lacerda, L., et al.: Tissue histology and physiology following intravenous administration of different types of functionalized multiwalled carbon nanotubes. Nanomedicine 3(2), 149–161 (2008)

V. Neves et al.

 Cherukuri, P., et al.: Mammalian pharmacokinetics of carbon nanotubes using intrinsic nearinfrared fluorescence. Proc. Natl. Acad. Sci. USA 103(50), 18882–18886 (2006)

- 57. Liu, Z., et al.: In vivo biodistribution and highly efficient tumour targeting of carbon nanotubes in mice. Nat. Nanotechnol. **2**(1), 47–52 (2007)
- 58. Zavaleta, C., et al.: Noninvasive Raman spectroscopy in living mice for evaluation of tumor targeting with carbon nanotubes. Nano Lett. **8**(9), 2800–2805 (2008)
- Liu, Z., et al.: Circulation and long-term fate of functionalized, biocompatible single-walled carbon nanotubes in mice probed by Raman spectroscopy. Proc. Natl. Acad. Sci. USA 105(5), 1410–1415 (2008)

Recognition of Carbon Nanotubes by the Human Innate Immune System

Malgorzata J. Rybak-Smith, Kirsten M. Pondman, Emmanuel Flahaut, Carolina Salvador-Morales and Robert B. Sim

Abstract A major function of the human innate immune system is to recognize non-self: i.e., invading microorganisms or altered, damaged self macromolecules and cells. Various components of the human immune system recognize foreign synthetic materials, including carbon nanotubes (CNTs). The complement system proteins in blood, and the collectins, SP-A and SP-D in the lungs bind to carbon nanotubes, in competition with other plasma proteins, and may influence their subsequent adhesion to and uptake by cells and their localization in the body. Modification of the surface chemistry of carbon nanotubes alters their binding to complement proteins and collectins, and provides information on the mechanism by which binding of these proteins occurs.

M. J. Rybak-Smith, K. M. Pondman and R. B. Sim (🖂)

Department of Pharmacology, University of Oxford, Mansfield Road,

Oxford, OX1 3QT, UK

e-mail: bob.sim@bioch.ox.ac.uk

K. M. Pondman

Faculty of Science and Technology, University of Twente, P.O. Box 217 Hogekamp 4240, 7500 AE, Enschede, The Netherlands

E. Flahaut

Institut Carnot Cirimat, Université de Toulouse; UPS, INP, 118, route de Narbonne, 31062, Toulouse Cedex 9, France

E. Flahaut

CNRS, Institut Carnot Cirimat, 31062, Toulouse, France

C. Salvador-Morales and R. B. Sim Department of Biochemistry, MRC Immunochemistry Unit, South Parks Rd, Oxford, OX1 3QU, UK

Present Address:

C. Salvador-Morales

Harvard-MIT Health Sciences and Technology, 77 Massachusetts Avenue, Cambridge, MA 02139, USA

1 The Innate Immune System

Multicellular living organisms have developed very varied systems to protect themselves from attack by organisms of other species. One aspect of these protective mechanisms is an immune system, which has evolved to protect multicellular organisms from attack by small parasites or from infectious microorganisms, such as bacteria, viruses and fungi. Most multicellular organisms also have to solve a problem, which occurs as they grow and develop: this is to remove their own obsolete, dying or damaged cells. Parts of the immune system appear to have evolved to take on this role also, so that the immune system can recognize not only foreign microorganisms, but also altered or damaged host cells and macromolecules. Recognition of these foreign or altered particles is mediated by specific proteins, which bind to the foreign or altered particle (target); then trigger downstream reactions, which lead to the destruction of the target.

Vertebrate animals, including humans, have sophisticated immune systems, which can conveniently be divided into two parts: innate immunity and adaptive immunity. In innate immunity, recognition of the target is mediated by proteins which are encoded directly by genes of the host organism, and are usually present at all times in the blood, body fluids or tissues of the host, throughout its life-span. For adaptive immunity, however, new recognition proteins are created in response to a challenge by an invading microorganism, by rearrangement and mutation of genes in specialized cells (lymphocytes) of the host. This is called somatic mutation and creates antibodies (B cell receptors) and T cell receptors.

In this review, we will discuss only the innate immune system, which has evolved generalized mechanisms to recognize, on the surface of targets, repetitive patterns of chemical groupings, which are not present in healthy host cells [1]. In this way, the innate immune system can distinguish between "self" and foreign or altered-host materials. However, since many synthetic materials are polymer-based and have repetitive surface chemical groupings, the innate immune system can recognize these also. Carbon nanotubes, as discussed below, are one of many synthetic polymers recognized by vertebrate innate immune systems [2, 3].

Innate immune system components include:

- 1. Soluble proteins (in the blood or other body fluids). The complement system and collectins are the major protein systems involved.
- 2. Cells, of many types but mainly phagocytes (macrophages and neutrophils in the body fluids or in tissues), with their repertoire of surface receptors. The main receptor types involved in innate immune recognition are the toll-like receptors (TLRs), scavenger receptors, integrins, and sugar-binding receptors (lectins), such as the mannose receptor or dectin.

A common feature of recognition of targets by innate immune system components is "multiple low-affinity binding" [4]. In such binding, a site on the recognition protein binds weakly to (recognizes) a molecular motif, such as a small charge cluster (2 or 3 negative charges), a single neutral sugar (monosaccharide),

vicinal hydroxyl groups (vicinal diols), or single acetyl groups. This one-to-one weak interaction is not enough to hold the target and recognition protein together, nor is it enough to confer specificity (distinction of self from non-self). These problems are overcome by polymerization or multivalency, so that the recognition protein takes the form of a polymer, presenting multiple binding sites, which can recognize multiple similar or identical motifs on a target surface. The multiple binding gives high avidity, strong interaction, and the geometric spacing of the motifs recognized confers specificity. Alternatively, the recognition protein may not polymerize, but may be present in hundreds of copies on a cell surface, which can engage simultaneously hundreds of motifs on the target surface.

2 Complement

The complement system is a group of over 40 soluble and cell surface proteins which interact together to recognize and opsonize foreign and altered-self materials [4–6]. Complement system recognition proteins bind to the target and trigger activation of proteases (see Fig. 1) [7, 8]. Activation occurs by any of three different pathways (classical, alternative or lectin) each of which recognizes a different spectrum of targets. In the classical pathway, the recognition protein C1q binds to charge clusters or hydrophobic patches on targets. When it binds, two

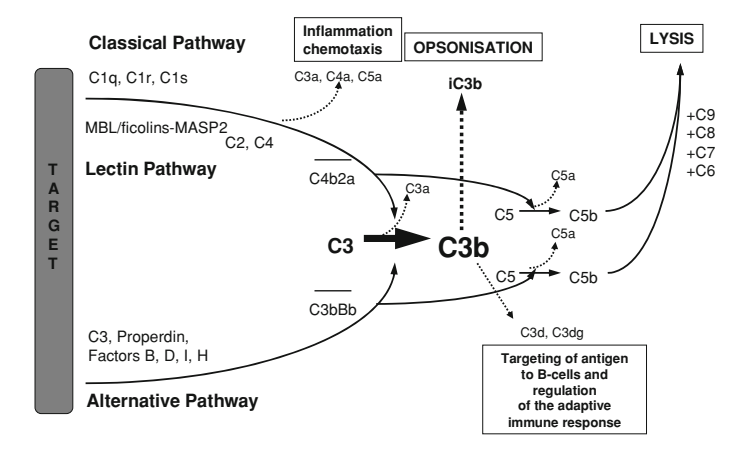


Fig. 1 The complement system. As discussed in the text, complement proteins C1q, MBL or ficolins recognize and bind to "foreign" materials, activate proteases including C1r, C1s and MASP2, which in turn activate the protease C4b2a, which cleaves C3. Many molecules of C3b bind covalently to the target, and mediate opsonization (mostly via a breakdown product iC3b) or interaction with the adaptive immune response (via the breakdown product C3d or C3dg). Fixation of C3b onto C4b2a also allows C5 to be activated, which leads to the formation of a C5b, 6, 7, 8, 9 complex [the membrane attack complex (MAC)] which can lyse cellular targets. The alternative pathway has a more complex initiation procedure, but goes through similar steps up to the activation of C3

proteases (C1r and C1s) which are bound to C1q are activated, and C1s in turn activates the complement proteins C4 and C2. They form a complex protease, called C4b2a, which activates C3, the most abundant complement protein. Activated C3 (called C3b) binds covalently to the surface of the target, and when hundreds of copies of C3b are bound, the target is opsonized. Phagocytic cells have surface receptors for C3b (and a further breakdown product iC3b) and so the C3b/iC3b-coated target binds strongly to the phagocyte and is ingested, then digested in the lysosomes of the cell. During C3 activation, one C3b will bind covalently onto C4b2a, forming C4b2a3b, which binds and activates the next complement protein, C5. Activated C5 (C5b) forms a large protein complex C5b-C6-C7-C8-C9 (C5b-9), the membrane attack complex (MAC), which can insert into lipid bilayers and will lyse targets which have a lipid bilayer.

In the lectin pathway, the recognition proteins are MBL (mannose-binding lectin) or the ficolins, of which there are three (L-, H- and M-ficolin) [9]. MBL binds to vicinal diols on sugars, such as mannose, fucose or glucosamine. The target recognition specificity of the ficolins is not well established, but L-ficolin will bind to many acetylated species, such as *N*-acetyl galactosamine or *N*-acetyl glucosamine, and some sialic acids [10]. L-Ficolin does bind several bacteria and parasites, such as *Mycobacterium tuberculosis* and *Trypanosoma cruzi* [11, 12].

When MBL or the ficolins bind to a target, a protease called MASP-2 (similar to C1s) is activated, and cleaves C4 and C2, starting off the same series of complement protein reactions as described for the classical pathway [8, 13].

C1q, MBL and the ficolins are all multimeric proteins [13–15], which bind to targets by multiple low-affinity binding. The general structure of these proteins is shown in Fig. 2. C1q is made up of three homologous polypeptide chains, A, B and C, each about 23 kDa. The N-terminal part of each chain has collagen-like amino acid sequence (repeating Gly-X-Yaa triplets, where X can be any amino

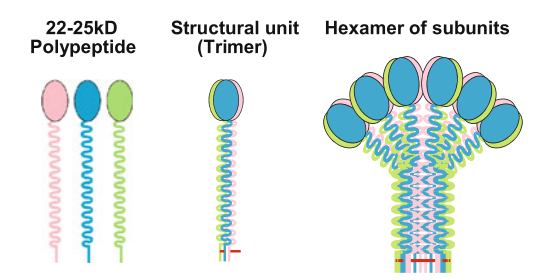


Fig. 2 The structure of C1q. Three homologous polypeptide chains, A, B and C combine to form a trimeric subunit, which then polymerizes to form a six-headed "bunch-of tulips" shape. Each of the six globular heads contains three lobes, derived from the homologous A, B, C chains. Each of these lobes recognizes a different spectrum of targets (with some overlap). The structures of MBL, ficolins and SP-D are similar except that each is a homopolymer, i.e. contains only 1 type of polypeptide. SP-A contains two types of polypeptide. MBL, the ficolins and SP-D assemble on average to a four-headed structure, not six-headed as for C1q and SP-A. In each protein, the polypeptides are made up of a globular region, and an extended collagen-like sequence. Figure provided by Mayumi Bradley

acid, and Yaa is often proline or hydroxyproline). The C-terminal part is a globular domain, which binds to targets mainly via charge interactions. These chains associate together to form a trimeric subunit, and the collagenous regions form a collagen triple helix. The subunits then polymerize, with some disulphide bridging between them, to form a hexamer of subunits.

Each globular region can bind to a target. The final hexameric form of C1q has 18 globular domains (three in each "head") so it can bind to a target by up to 18 interactions. MBL has a similar structure, but it has only one type of polypeptide chain, which assembles in trimeric subunits. The polymerization of MBL is variable, however, and it forms mostly tetramers of subunits, although dimers, trimers, pentamers and hexamers also occur. Each MBL polypeptide has one globular domain (called a C-type lectin domain) through which it can bind one sugar (e.g. Mannose), in a Ca⁺⁺-dependent interaction. Each subunit therefore has three C-type lectin domains, and the fully assembled molecule has 12–18 lectin domains.

Each ficolin, similar to MBL, has only one type of polypeptide, and assembles mainly to form tetramers of subunits: so each ficolin molecule can bind to a target by 12 sites. The binding domain of ficolins is called a fibrinogen (fbg) domain. The fbg domains of H, L and M ficolins are homologous, but not identical, and each recognizes a different spectrum of targets [10, 16].

The alternative pathway does not have any recognition molecule of the type represented by C1q, MBL or ficolins. A hypothesis which is both old (1950s) and new (2007) suggests that another type of multimeric protein, properdin, may initiate alternative pathway activation [17]. Properdin binds to charge clusters. Properdin has a single type of polypeptide chain, about 50 kDa, which is made up of six similar domains (called TSRs, or thrombospondin domains) [18]. These chains form variable oligomers, from dimers to tetramers. The tetramers may have four charge-cluster binding sites, or may have a multiple of four, since it is not known whether more than one of the TSRs in each chain can participate in binding. Once properdin binds to a target, C3b, formed either from classical or lectin pathway activation, or from another low rate spontaneous activation process, binds to the properdin. Factor B then binds to the C3b, and is cleaved by the protease Factor D to form C3bBb. This is homologous to the classical pathway C3cleaving protease, C4b2a, and it activates more C3b, mediating the same C3, C5 turnover and MAC assembly as for the classical pathway (Fig. 1). The alternative pathway C3-activating enzyme is C3bBb: it contains C3b, the activation product of C3. This is a huge amplification mechanism. The enzyme makes C3b, which then binds Factor B, and makes more enzyme, C3bBb. Whenever some C3b is made by the classical or lectin pathways, it will trigger alternative pathway activation, and amplify turnover of C3. However the alternative pathway can be activated independently of the other two pathways.

C3 turnover is controlled by Factor H, an important down-regulator of complement activation: Factor H binds to C3b and competes out the binding of Factor B, preventing formation of C3bBb. Once a C3b–FH complex has formed, factor I, a protease cleaves C3b to a form called iC3b, which does not participate in forming C3bBb.

3 Collectins

The collectins are a small family of proteins which are collagenous lectins [19, 20]. MBL, discussed above, is a collectin. However there are several other collectins which do not activate the complement system. In humans, the other important collectins are two proteins found mainly in lung, called surfactant protein A (SP-A) and surfactant protein D (SP-D). SP-A and SP-D have a multimeric structure similar to C1q and MBL (Fig. 2) and are present in lung surfactant, the thin aqueous and lipid layer which forms the interface between inhaled air and the cells of the lungs. When we inhale, we take in enormous numbers of particles, including inorganic and organic dust, viruses, bacteria, fungal spores, allergenic particles, etc. Most of these particles become trapped in mucus and are moved back up the respiratory tract by the movement of cilia in the trachea. Once they have been moved back up from the lungs, they can be spat out or swallowed. Very small particles however, penetrate to the alveoli, and there they can cause damage, or establish infection, unless they are destroyed by alveolar macrophage. Although SP-A and SP-D have many roles, a major role is to bind to invading particles and then to promote their binding to alveolar macrophages. Their main mode of binding to targets is to recognize vicinal diols on sugar residues on bacterial, viral, fungal surfaces. This is a calcium ion-dependent interaction, in which a Ca⁺⁺ ion, bound to the lectin domain of SP-A or SP-D, interacts with the diols. Once a particle has become coated with multiple SP-A or SP-D molecules, these will interact, via their collagenous regions, with receptors on alveolar macrophage.

Any small particle (including of course nanoparticles) can be inhaled, and so it is important to know whether these interact with the innate immune proteins of the lung.

4 Cells and their Receptors

The cells of the innate immune system include all of the white blood cell types (except most lymphocytes, which are part of the adaptive immune system), red blood cells, macrophages and dendritic cells in all the tissues, and several other groups of cells, such as mast cells. These cells have receptors through which they can recognize and bind many "foreign" organisms, such as bacteria, viruses and fungi. Interaction with these receptors may result in adhesion, phagocytosis and destruction of the foreign particle, or may signal to the cell to cause it to secrete cytokines or chemokines. Receptor types involved include TLRs, scavenger receptors, integrins, lectin-like receptors (which bind to sugars) such as mannose receptor or dectin. The cells also have receptors which allow them to recognize particles which already have complement proteins or antibodies bound to them (complement receptors or, for antibodies, Fc or immunoglobulin receptors).

When a particle has been recognized by the complement system, it will activate complement and will have molecules of C1q (or MBL or ficolins) and many molecules of C3b bound to it. Once C3b has bound, it is gradually broken down by proteases to forms called iC3b and C3d. Each of these interacts with cellular receptors. A C3b-coated particle in the blood will bind mainly to red blood cells, which have a receptor (complement receptor 1 (CR1) which binds C3b (see, e.g. [21]). As the particle circulates, bound to red blood cells, the C3b will gradually be converted to iC3b, which binds only weakly to CR1, but binds strongly to CR3 and CR4 (complement receptors 3 and 4) which are found on phagocytic cells. When the red blood cells pass through the liver and spleen, where there are many macrophages, the particles, now coated mainly with iC3b, will transfer to phagocytic cells and be ingested and destroyed. If the particle is in circulation for longer, iC3b will eventually be broken down to C3d, which binds to a receptor called CR2. CR2 is not present on phagocytic cells, but is most abundant on B lymphocytes.

Receptors also exist for C1q, MBL, the ficolins and the lung collectins, SP-A and SP-D, so that these proteins, when bound to a target, may also promote adhesion of the target to cells. Generally however, this effect would be weaker than for C3b or iC3b, because fewer molecules of C1q, MBL or ficolins are bound to targets. Adhesion requires interactions between hundreds of receptor-ligand pairs, so C3b or iC3b, which can be fixed to the target in clusters of hundreds of molecules [22], are more effective. A receptor which will bind all of these collagenous proteins, C1q, MBL, ficolins, SP-A and SP-D has been identified. It is calreticulin, bound to cell surfaces via CD91 [14, 15, 23, 24].

5 Interaction of CNTs with Plasma Proteins and Components of Innate Immunity

Plasma Proteins

If carbon nanotubes are to be considered as potential novel compatibile and non-toxic biomaterials, there is a need for more detailed investigation of the interaction between CNTs and the innate immune system. Contact with human blood or body fluids is inevitable in some steps of a drug delivery process, so a deeper understanding of the interactions between CNTs and blood proteins in general is also essential.

Among hundreds of proteins present in human plasma or serum, only a few bind spontaneously to unmodified ("pristine") CNTs and so the binding is highly selective. This is not unexpected, as most homogeneous wettable surfaces, such as metal catalysts, silica-based materials and various organic polymers show highly selective binding of plasma proteins. The very abundant human plasma proteins, such as human serum albumin, fibrinogen, and high-density lipoprotein (HDL,

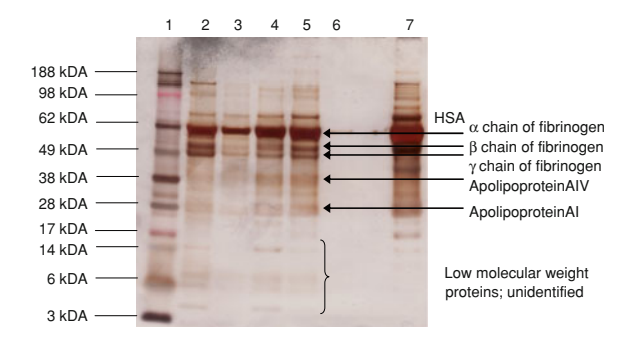


Fig. 3 Human plasma proteins bind selectively to DWCNTs. Samples of CNTs incubated with human plasma and washed were analyzed by SDS-PAGE in reduced conditions. *Lane 1* Molecular weight marker, *lane 2* human plasma proteins bound to oxidized DWCNTs, *lane 3* human plasma proteins bound to less oxidized DWCNTs, *lane 4* human plasma proteins bound to non-functionalized DWCNTs (1st batch), *lane 5* human plasma proteins bound to non-functionalized DWCNTs (2nd batch), *lane 6* control-human plasma proteins bound to Sepharose, used as a carrier for DWCNTs during incubation, *lane 7* human plasma. α chain of fibrinogen coruns with HSA. Protein bands were stained using a BioRad Silverstain Kit. The method used is similar to that in [3]

which contains lipid and apolipoproteins AIV, AI, CIII) bind to CNT to the greatest extent [2, 3]. Other very abundant proteins, such as IgG, IgM, alpha-2 macroglobulin, bind negligibly or not at all (Fig. 3).

In various experimental procedures, CNTs are often pre-coated with proteins such as bovine serum albumin (BSA) in order to form stable dispersions in biological buffers. When such BSA-coated CNTs are added to human serum or plasma, the BSA is gradually displaced by human proteins, with a half-life of about 0.5–1 h at 37°C (K.M. Pondman, unpublished data). There are several different modes of binding of proteins to pristine CNTs, and these have not yet been very extensively explored. Serum albumin (human or bovine), for example, bind independently of fibrinogen, so the two types of protein are not competing for the same type of binding site. Precoating of CNTs with either serum albumin or fibrinogen before exposure to human serum or plasma does not prevent the binding of the complement protein C1q, and subsequent complement activation, and so C1q is recognizing a third type of binding site on CNTs (K.M. Pondman, unpublished data).

Complement

Our studies show that non-functionalized single-walled and double-walled carbon nanotubes (SWCNTs and DWCNTs), when placed in contact with human serum, activate complement via the classical pathway, or to a lesser extent through the alternative pathway [3]. Studies with four types of covalently modified multi-

Table 1 Biological activators of complement, which act by binding C1q

Gram-negative bacteria via lipid A of lipopolysaccharides

Gram-positive bacteria via lipoteichoic acids

Viruses, including Moloney, vesicular stomatitis, HTLV-1, HIV-1, DNA polyoma Polyanions:

Heparin and chondroitin sulfate

Single- and double-stranded DNA and other polynucleotides

Anionic phospholipids in vesicles or on apoptotic cells

Other target-bound proteins:

Ligand-bound pentraxins (C-reactive protein and serum amyloid P-component)

Immunoglobulins: Fc portion of antigen-bound IgM, IgG Altered-host proteins: amyloids, fibrin clots, prion aggregates

walled carbon nanotubes (MWCNTs) [25] showed that the extent of complement activation can be increased or decreased by altering the surface properties of the CNTs [26]. For example, MWCNTs functionalized with alanine or ε-caprolactam showed >75 and >95% decrease in classical pathway activation when compared with pristine MWCNTs [26]. Surface alterations, which diminish classical pathway activation, however, do not necessarily diminish alternative pathway activation, so both pathways must be studied separately. For classical pathway activation, the extent of activation was proportional to C1q binding, whereas for the alternative pathway, extent of activation was inversely correlated with binding of factor H, a protein which downregulates activation [26].

Direct binding of C1q and factor H to CNTs has been shown. These proteins bind in much lower quantity than do serum albumin, fibrinogen or HDL. For biological targets, C1q binds generally by ionic interactions (Table 1) with rearrangement to stronger hydrophobic interaction [27]. C1q also binds to many synthetic materials (Table 2).

Chemical modifications of polymers and other types of nanoparticles (mainly liposomes) show that coating with heparin or high-density polyethylene oxide (PEO) or polystyrene sulphonic acid or polyethylene glycol (PEG) tends to diminish activation. This type of modification has not yet been tested extensively for CNTs, but Moghimi and colleagues have shown that PEGylated SWCNTs do still activate complement, not via C1q, but possibly by the binding of L-ficolin [28, 29].

Table 2 Synthetics and non-biologicals, which activate complement via C1q (a small selection from recent papers)

SiO₂

Polyvinylpyrrolidone-coated nanoparticles

Polyvinylchloride

Polymethylmethacrylates

Polystyrene nanoparticles

Polyacrylonitrile

Carbon nanotubes

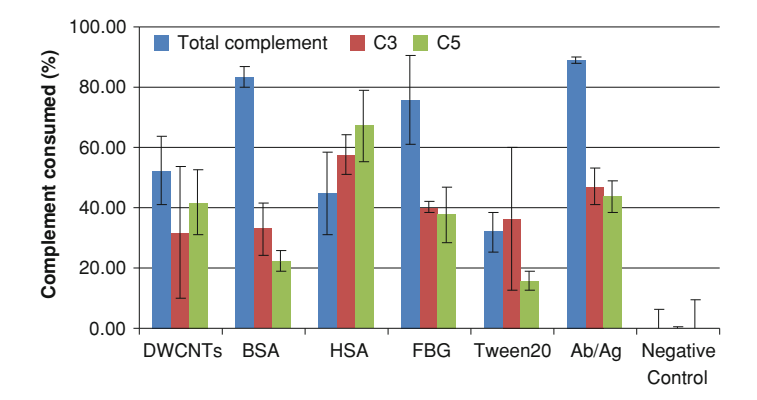


Fig. 4 Complement consumption by DWCNTs pre-coated with different proteins. Whole complement consumption and C3 and C5 consumption were determined in human serum incubated with CNTs. CNTs with no pre-coating (CNTs), and CNTs pre-coated with bovine serum albumin (BSA), human serum albumin (HSA), human fibrinogen (FBG), or the detergent Tween 20 were used. Ab/Ag is the positive control, representing complement activation by antibody-antigen complexes in the absence of CNTs. The negative control is serum incubated with no complement activator. The method used is similar to that in [3]

Clq binding alone does not guarantee that the whole complement system is activated, or that the nanotube becomes coated in C3b. Once C1q has bound, C1r and C1s are activated, followed by C4 and C2. For the next step, C4b2a has to be anchored to the surface of the nanotube. For biological targets which activate complement, the common mechanism for the binding of C4b (and also C3b) is covalent binding. This occurs by reaction of an internal thiolester in these proteins with surface OH, NH₂ or SH groups on the target. A much less common mechanism is hydrophobic adsorption. Pristine CNTs have no such reactive groups, but in serum, they adsorb other proteins, which could provide the necessary binding sites. Preliminary experiments (K.M. Pondman, unpublished) confirm that C4b and C3b do become bound to CNTs during complement activation, but there was no evidence that they bind covalently to other proteins, and so the binding is likely to be mostly by direct hydrophobic binding to the CNT surface. This is not entirely consistent with the finding mentioned above, that pre-coating CNTs with albumin or fibringen does not greatly alter total complement system activation (Fig. 4), but it does alter C3 and C5 consumption to a greater extent.

By whichever pathway CNTs activate complement, the MAC is the final product of the enzymatic and non-enzymatic protein cascade for each pathway. A significant rise in MAC levels after interaction between PEGylated SWCNT and undiluted human serum has been reported, indicating that complement activation proceeds through the whole complement cascade [28].

Nucleic acid wrapping or coating of the surface with surfactants, or other polymers can have a considerable impact on CNT interaction with human blood proteins, including complement. As shown in Fig. 4, pre-coating with Tween 20 diminishes overall complement activation. Ideally, the coating of CNT should be

stable in contact with blood or body fluids. Although it is very important to make CNT suspensions stable in conditions similar to physiological and make them more biocompatible by changing their surface properties, the non-covalent binding of proteins to DWCNTs is not stable over time and the proteins dissociate from the CNT surface to be replaced by other plasma proteins. Chemical modification of CNTs, either covalent or non-covalent, can significantly change the extent or perhaps the mechanisms by which CNTs interact with the innate immune system. Impurities present on the surface of CNTs, such as traces of Mo, Co or Fe, etc., may also influence the interaction of CNTs with blood proteins and lead to biological reactions, including reactive oxygen species (ROS) generation.

The chemical composition of CNT surface, size and the presence of catalytic impurities can affect the way complement is activated and in consequence cause possible harmful effect for cells or cell tissues. Activation of complement by both unmodified and chemically modified DWCNTs leads to the generation of peptides, C3a, C4a and C5a which can cause inflammation, which is strongly undesirable if the CNTs are to be used as biomaterials in the human body.

Regarding interaction between carbon nanotubes and complement in vivo, very little has been reported so far. To name one example, Hamad and co-workers have reported that PEGylated nanotubes can induce complement activation in rats, which is C4 dependent [28].

Although in vitro complement activation assays, including hemolytic assays and direct protein binding studies, are very valuable methods to determine whether CNTs interact with complement and in consequence cause complement activation in human serum or plasma, further investigation is needed to show whether the binding of complement proteins (mainly C3b, iC3b) does really influence the fate of CNT products placed in contact with the blood or other body fluids or influence the cellular internalization of CNTs by phagocytes and their cellular accumulation Further in vivo studies could provide more information about the interactions of CNTs with complement and the potential outcomes that may arise.

Collectins

Inhaled carbon nanotubes can be treated as 'foreign' material entering the lungs and therefore show potential pulmonary toxicity. The interaction of DWCNTs with collectins was recently investigated for the first time [30]. The lung proteins SP-A and SP-D selectively bind to DWCNTs and transmission electron microscopy revealed that the binding occurs through their heads [30]. This binding, unlike that of C1q or of serum albumin, fibrinogen or HDL, was found to be Ca⁺⁺-ion dependent. [30]. With biological targets, SP-A and SP-D bind to surface sugars by a Ca⁺⁺-dependent coordination of vicinal diols (adjacent hydroxyl groups). It was shown that SP-A and SP-D bind to oxidized CNT, and hypothesized that some binding to CNT which have not been deliberately oxidized is due to inadvertent oxidation during synthesis and purification. The presence of oxygen-containing

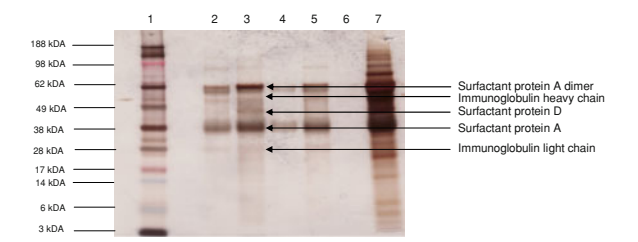


Fig. 5 Selective binding of BALF proteins to different DWCNTs. BALF (bronchoalveolar lavage fluid) was passed through Sepharose and Sepharose-CNT columns as in [26]. After exhaustive washing in the running buffer, samples were analyzed by SDS-PAGE in reduced conditions. *Lane 1* molecular weight marker, *lane 2* BALF proteins bound to less oxidized DWCNTs, *lane 3* BALF proteins bound to oxidized DWCNTs, *lane 4* BALF proteins bound to non-functionalized DWCNTs (1st batch), *lane 5* BALF proteins bound to non-functionalized DWCNTs (2nd batch), *lane 6* Control–BALF proteins bound to Sepharose, used as a carrier for DWCNTs during incubation, *lane 7*. BALF. Protein bands were stained using a BioRad Silverstain Kit

functional groups on the carbon nanotube surface is an important factor in this [31]. Figure 5 represents the selective binding of lung surfactant proteins to different chemically modified CNTs.

SP-A and especially SP-D are present in very low quantities, even in the lung, which is their major site of localization. If a relatively large quantity of well-dispersed CNT was inhaled, a proportion of these might escape entrapment in mucus, and reach the lower airways and alveoli. Here they might sequester a large proportion of the available SP-A and SP-D, leaving the lungs temporarily susceptible to infection. Chronic exposure to lower quantities of airborne CNTs would have similar effects. These events are relatively unlikely, but point to the need for good control of airborne particulates where CNTs are manufactured on industrial scale. Binding of these proteins to CNTs would be expected to promote their adhesion to alveolar macrophages, and their ingestion, if they are not too long or too large (aggregated). CNTs which cannot be ingested may cluster macrophages around them, with possible eventual formation of granuloma [30].

SP-A and SP-D have functions other than promoting adhesion to macrophage, and binding of these proteins may contribute to lung inflammation by other routes. C. Salvador-Morales (unpublished work) has shown that SP-A coated MWCNTs induced an inflammatory response in IFN γ -primed RAW cells (a mouse macrophage cell line), as assessed by MWCNT uptake and measurement of the generation of nitric oxide.

Cells and Cellular Receptors

There have not yet been any direct studies of the interaction of CNTs with the types of innate immune system receptors discussed above. However, in general

terms, using CNTs as potentially efficient drug or protein vehicles involves understanding of interaction between CNTs and cells and cell surfaces. The reported fates of CNTs in cells and their localization in cellular organelles varies widely. Determining their potential cytotoxicity and route of safe excretion from the cells is important. Drug-targeting involves the design of CNTs with specific ligand molecules present on the CNT surface which can be recognized by cellular receptors. Uptake of CNTs into cells is critically dependent on their length and degree of bundling (aggregation). Many studies of CNT uptake into cells do not give any information on the size distribution of the particles used in the experiments, and quite major differences in findings can often be attributed to the lack of characterization of the length distribution and dispersion of the CNTs. The uptake of DNA-wrapped SWCNTs, for example, is size and length dependent and endocytosis rate depends on tube bundle diameter [32].

CNTs can be taken up by many cells (primary and established lines), among them human monocyte derived macrophage (HMM) cells, which play a significant role in the body's immune response [33], T cells (Jurkat), Chinese hamster ovary cells (CHO), 3T3 fibroblasts [34], HeLa cells [35], H596, H446 and Calu-1 lung tumor cells [36], bacterial, fungal and yeast cells [37]. Unmodified CNTs can be toxic for many cell lines, including HEK 293 cells [38], Haca T cells [39] and alveolar macrophages [40] and induce cell death. SWCNTs reduce the amount of glial cells in both peripheral and central nervous system derived cultures [41], but the interaction of CNTs with the nervous system remains poorly understood. No uptake of SWCNTs was reported in A549 cells, BEAS-2B and RAW 264.7 (a mouse peritoneal macrophage cell line) [42]. CNTs, in contrast to graphite, can be highly adhesive to human osteoblast-like cells (Saos2) [43].

Certain functionalizations of CNT surfaces can not only reduce their toxicity, but also eliminate non-specific uptake by the cells and promote their prolonged circulation in the blood. PEG is frequently used for such surface modifications. The coating of SWCNTs by PEG adsorbed to their surface blocked their uptake by the ovarian cancer cell line SKOV-3 [44]. SWCNTs functionalized by PEG can be additionally functionalized for interaction with cell receptors. SWCNTs were functionalized by folate and EGF specifically to target FR α and EGFR receptors expressed on cancer cells [44]. Similar results were obtained with the ovarian cancer cell line OVCA 433 [44]. SWCNTs non-covalently functionalized with chitosan, linked with folate and fluorescently labeled were taken up by Hep G2 cells via a folate receptor-mediated pathway that is concentration-dependent [45]. When the folate receptors on the surface of the Hep G2 cell membrane were blocked, no internalization of the SWCNT was observed [45].

Modification of the surface chemistry of CNTs can change the interaction of CNTs with lipid bilayers and thereby influence the uptake into the cell. The compatibility of the CNT surface with biological components or proteins situated on the cell surface can play a key role in cell–CNT interactions. The CNT surface is intrinsically hydrophobic and this can lead to non-specific adsorption to the cell surface. To avoid this, the surface modification of CNTs can be considered as an effective method of eliminating unwanted non-specific cell adsorption. Mucins are

present on the surface of many cell lines and present epitopes for receptor-mediated cell-cell recognition. Glycosylated polymers on the CNT surface can mimic mucins. A coating which introduces α -GalNac residues onto the CNT surface, can be recognized by a specific receptor present on the cells [46].

SWCNTs have the ability to penetrate mammalian cells and serve as transporters for many different proteins. Among those which have been tested are streptavidin, protein A, bovine serum albumin and cytochrome c [47, 48]. Endocytosis was confirmed as the internalization mechanism for fluorescein-labeled proteins attached to SWCNTs. The SWCNT-protein conjugates were colocalized with endocytosis markers for endosomes, lysosomes and cytoplasm [48]. The mechanism of uptake of CNT can be either energy-dependent or energy-independent. In the majority of cases endocytosis is involved, but uptake is also possible under endocytosis-inhibiting conditions [37] or by incomplete phagocytosis [49]. After being internalized by cells, CNT can be located in different cellular organelles, such as cytoplasm, endosomes, lysosomes, Golgi apparatus or mitochondria. TEM studies by Kang et al. [45] revealed that functionalized SWCNTs are bound to the cellular membrane and then transfer to endosomes and lysosomes. The SWCNTs caused lysosomal damage and a concentration-dependent apoptosis. Generally CNTs are not localized in the nucleus, but functionalized SWCNT can be found in the perinuclear region [33, 37].

Macrophages play a central role in clearing particles from the alveolae of the lung. Currently little is known about the fate of MWCNTs in macrophages and the likelihood of being cleared from the lung via macrophages [49]. It might be expected that a proportion of CNTs ingested by lung macrophage will be moved up the airways by ciliary transport and then spat out or swallowed. Gold-labeled SWCNTs in the lungs can escape phagocytosis and migrate into the alveolar septae [42].

The interaction of CNTs with cells is very complex and dependent on many factors, such as the chemical composition of CNTs, their surface charge, length, dispersion, diameter, type of cells and the presence of cell receptors. Tip and side wall functionalization of CNTs may be important in cell or tissue engineering [50, 51]. Magnetically drivable CNTs can be used as efficient drug delivery vehicles. These magnetic CNTs can enter cells and tissues in the presence of an appropriately oriented magnetic field [52].

Being aware of the cellular uptake of CNTs can be very useful in designing new drug carriers. Additional information, like cytotoxicity, efficacy, cellular localization and the fate of CNTs inside the cell are also valuable.

6 Potential Toxicity and Immunotoxicity of CNT

In Sect. 5 the interaction of various CNTs with the complement system was described. Such interactions may or may not be desirable, depending on the intended function or targeting of the CNTs. Activation of complement may have

potential harmful effects (inflammation) on human tissues. Complement activation is not the only criterion in preclinical safety assessment of biocompatibility. Interaction of a potential drug candidate with blood cells, platelets and the coagulation system must also be considered [53]. For example, PEGylated liposomes were reported by Dobrovolskaia et al. [53] to activate complement, but were approved as a drug called 'Doxil', which can still be used in treatment of metastatic ovarian cancer. It is an aspiration that nanotechnology-based drugs will have an advantage over conventional drugs, as they can be designed to cause fewer adverse reactions [53]. However, supposedly CNTs can cause endothelial dysfunction, have effects on blood clotting and suppress immune responses and this may result in pathophysiological responses, like stroke, thrombosis, autoimmunity or artherogenesis. Nonetheless, the experimental evidence to support these potential side effects is still unsatisfactory [54].

Airborne CNTs can be simply inhaled into the lung and this organ is likely the most important target for potential CNT toxicity. Lungs are composed of more than 40 different cell types and therefore their interactions with CNTs can be quite complex. In vitro studies on triple cell cultures consisting of A549 human epithelial lung cells, human monocyte-derived macrophages and monocyte-derived dendritic cells were carried out by Müller et al. [55] and potential for oxidation stress and inflammation were observed. As shown by Simon et al. [56], MWCNTs were cytotoxic for A549, HepG2 and NRK-52E cell lines being models for lung, liver and kidney cells, respectively.

There are already many reviews discussing toxicity, safety concerns and potential dangers of CNT exposure to human lungs and other organs [57–62]. The impact of various types of CNTs on the lung has attracted substantial attention, but still relatively little is known about the potential toxicity of CNTs to other organs of the human body. Although CNTs can have asbestos-like structure and therefore be involved in lung toxicity, they probably do not exist in the air in the fibrous asbestos-like form [63].

When inhaled, non-aggregated CNTs can penetrate the aveoli and interact with lung surfactant proteins. As presented in Sect. 5, CNTs can bind SP-A and SP-D. Pulmonary surfactant proteins, SP-A and SP-D, are the main protein constituents of lung surfactant and are involved in innate immunity [19, 20]. The absence of SP-A and SP-D in knockout mice caused infection and emphysema in their lungs. SP-A and SP-D do not activate the complement system in contrast to mannan-binding lectin (MBL), another collectin involved in immune defence. SP-A can modify the inflammatory response in vivo by enhancing macrophage phagocytosis and clearance of bacteria. Clearance of apoptotic cells in lung inflammation is a principal role of SP-A and especially of SP-D [19, 20].

Interactions of CNT with collectins can affect the physiological functions of these proteins and could potentially lead to bronchial inflammation or increased susceptibility to lung infection or allergy, therefore it is necessary to understand the mechanism involved in the interactions. As shown by Salvador-Morales et al. [30, 31], no binding of SP-A and SP-D from BALF to DWCNTs occurred in the presence of EDTA, a commonly used divalent cation chelator. The binding of

SP-A and SP-D to CNTs was dependent on the presence of ketone, aldehyde, ester or carboxylic acid functional groups on CNT surface.

In in vivo studies of aspiration of MWCNTs suspended in phosphate buffer into mouse lungs, increased secretion of mucous and of SP-D was observed, with indications of systemic oxidative stress. These MWCNTs were not oxidized so probably did not bind SP-D [64, 65].

In further in vivo studies, Mitchell et al. [66] showed that inhalation of MWCNTs by C57BL/6 male mice affected systemic immunity, but did not cause lung damage. Studies using a natural killer cell assay showed that the innate immune response was suppressed by inhalation of MWCNTs [66]. Increased expression of an indicator of oxidative stress, NQO1, and an indicator of altered immunity, IL-10 were not observed in lungs, but were seen in spleen. IL-10 is one of anti-inflammatory cytokines and plays an important role in maintaining homeostatic control of innate and immune responses mediated by cells. IL-10 is secreted by macrophages and T cells [66]. Its expression can suppress normal immune responses and increase receptiveness to infection. The immune function responses observed in the spleen have not been evaluated in other parts of the body like the lymph nodes or immune cells in the lungs. The immune response to inhaled MWCNTs was time- and dose-dependent and was consistently observed even in the presence of low concentrations of MWCNTs [66].

A mechanism by which inhaled MWCNTs induce systemic immune suppression was proposed by Mitchell et al. [67]. $TGF\beta$ secretion in the lung can be activated by MWCNTs and have an effect on prostaglandin production in spleen cells, leading to the immune suppression and affect the function of T cells [67].

CNTs can be internalized by macrophages and cleared by the lymphatic system if they are short and tangled [68]. However, typically they are long and their prolonged accumulation in the lung (months or even years) can arise from incomplete phagocytosis [68]. The internalization of SWCNTs in macrophages can be responsible for activation of various transcription factors such as nuclear factor κB (NF- κB) and activator protein 1 (AP-1) followed by induction of oxidative stress, release of pro-inflammatory cytokines, leukocytes, gene expression and activation of T cells [69]. This can cause innate and adaptive immune responses including chronic pulmonary inflammation and granuloma formation. Histopathological studies by Warheit [70] revealed that pulmonary exposure to SWCNTs produced multifocal granuloma. Poland et al. [71] showed that long MWCNTs caused inflammatory changes to mouse lungs, further developing granuloma. The uptake of SWCNTs into macrophages induces oxidative stress in mitochondria. A remarkable increase in SOD2 (superoxide dismutase) expression in SWCNT-treated macrophages was observed by Chou et al. [69]. SWCNTs induced the expression of protective and antiapoptotic genes [69].

As shown by Jacobsen et al. [72], apolipoprotein E knockout (Apo E^{-/-}) mice developed lung inflammation when exposed to SWCNTs. Studies carried out by Elgrabli et al. [73] showed that MWCNTs can be present in rat lungs even 6 months after intratracheal instillation and therefore may cause pathological changes in lungs. Studies on female C57BI mice revealed that exposure to

MWCNTs can be more toxic than to ozone, which is known to cause pulmonary toxicity [64]. Pathological changes in the lungs of mice exposed to aerosolized MWCNTs were reported by Li et al. [74]. Exposure to SWCNTs caused lung inflammation and granuloma formation in rats that was lethal for several animals, as shown by Warheit et al. [75]. SWCNTs caused interstitial inflammation in mice and granuloma in contrast to the lungs of mice treated with carbon black as reported by Lam et al. [76]. Suppressed immune function was observed for mice inhaling low concentrations of MWCNTs [77]. Carbon nanomaterials, among them MWCNTs suspended in saline containing SDS, can induce pathological changes in guinea pig lung tissues on intratracheal exposure, as reported by Huczko et al. [78].

As discussed above, many studies performed on rodent models revealed CNT lung immunotoxicity, but some researchers report CNTs to be non-toxic. As reported by Qu et al. [79], carboxylated MWCNTs, well-suspended in PBS containing Tween-80, did not cause pathological changes in mouse lungs and liver and are more easily eliminated from the body as they do not form as many aggregates as less dispersed MWCNTs. However, the same MWCNTs caused mouse heart injuries, but no histopathological changes were observed in the brain [79].

No acute toxicity was observed by Pulskamp et al. [80] on macrophages (NR8383) and human A549 lung cells after SWCNT and MWCNT exposure. Purified CNTs had no effect on the formation of intracellular reactive oxygen species or the MMP potential of A549 cells, but a loss of mitochondrial functionality was reported. CNTs also affected the MMP potential in mitochondria in NR8383 cells [80].

As noted above, NF- κ B and AP-1 are activated by the uptake of SWCNTs by macrophages [69]. This can cause oxidative stress and release of proinflammatory cytokines. NADPH oxidase activation in macrophages can cause oxidative stress as a result of superoxide anion radical O_2^- and hydrogen peroxide H_2O_2 generation. In the presence of transition metals the most reactive hydroxyl radical HO can be produced from O_2^- [54].

Generation of HO· from H_2O_2 is common in physiological conditions, for instance during phagocytosis of particles by alveolar macrophages. It was reported by Fenoglio et al. [81] that purified MWCNTs in aqueous suspensions did not generate HO· and carbon-centred radicals, like CO_2^- . It was found by Shvedova et al. [82] that SWCNTs did not generate O_2^- or the nitric oxide radical NO· in RAW 264.7 macrophages. No O_2^- generation was reported when high purity SWCNTs (significantly reduced metal content) were exposed to human alveolar epithelial A549 cells, but unpurified SWCNT caused peroxynitrate ONOO $^-$ and O_2^- production [83]. No significant changes in the level of O_2^- generation were noted after treatment of peripheral blood mononuclear cells with CNTs [84]. ROS can be generated during phagocytosis of foreign particles by the activation of the NADPH oxidase system, which catalyses the conversion of O_2 to O_2^- . CNTs can stimulate the release of TNF- α and ROS in in vitro conditions. After treatment of monocytic cells by CNTs 'frustrated phagocytosis' as a negative response to CNT was observed [84].

NADPH oxidase-derived ROS play a role in determining the route of the pulmonary response to SWCNTs [85]. Exposure of SWCNTs to NADPH oxidase-deficient C57BL/6 mice resulted in significantly higher levels of pro-inflammatory cytokines: TNF- α , IL-6 and MCP-1 compared to non-deficient control animals. The level the anti-inflammatory cytokine, TGF- β , was also shown to be significantly higher [85].

It appears that CNTs may not generate ROS if there are no catalyst impurities present. Purified MWCNTs have the ability to effectively scavenge HO, generated by both Fenton reaction and photolysis of hydrogen peroxide H_2O_2 . Superoxide anion O_2^- can be generated by either physiological or pathophysiological processes. In the presence of MWCNTs the formation of O_2^- was shown to decrease when detected spectrophotometrically by reduction of cytochrome c generated in reaction catalyzed by xanthine oxidase. Although the scavenging properties of CNTs have been observed, this is still poorly understood [81].

Regarding the toxicity of CNTs, currently relatively little is known about other organs, as most researchers carry out studies on lungs. Murray et al. used engineered skin murine epidermal cells (JB6 P+) exposed to unpurified SWCNTs containing 30% iron and this caused HO· formation and activation of AP-1, in contrast to SWCNTs containing much less iron (0.23%). Unpurified SWCNTs caused oxidative stress to immune-competent hairless SKH-1 mice [86]. Inflammatory cytokines IL-6, IL-10, TNF- α or IL-12p70, etc., production and collagen accumulation were also observed for the dermally exposed mice [86].

Observed discrepancies in reports of toxicity caused by CNTs can be a function of many factors, such as their physicochemical properties, including size, length, presence of metallic impurities on the surface, hydrophobicity or hydrophilicity of the surface, its smoothness and the degree of oxidation. Other factors along with the ability of CNTs to form long fibrous particles (like asbestos) and their surface reactivity leading to the potential generation of ROS, can considerably influence CNT toxicity. Slow clearance of long and rigid CNT in the respiratory tract and their aggregation due to van der Waals forces are potentially dangerous for the body.

The presence of structural defects on CNT surfaces can have an important impact on their observed toxicity in vitro and in vivo. There are many surface defects that can be present in nanotubes, among them topological [pentagons instead of hexagons, pentagon–heptagon (5/7) pairs in the hexagonal structure of CNTs], rehybridization (between sp^2 and sp^3 hybridization) or defects caused by incomplete bonding (vacancies) [87, 88]. The defects can change CNTs' electronic properties [89, 90]. It was reported by Muller et al. [91] that the presence of structural defects of CNTs plays an important role in MWCNT toxicity in in vivo studies.

Toxic responses have been attributed to metal contamination, CNT length, oxidation or hydrophilicity. To see how some of these properties relate to toxicity, Muller et al. [91] and Fenoglio et al. [92] took a preparation of MWCNTs and modified it by (a) grinding (introducing structural defects) and subsequently heating in a vacuum at 600°C (to reduce oxygenated carbon adducts and metallic

oxides) or in an inert gas at 2,400°C (causing elimination of metals and annealing of defects) or (b) by heating at 2,400°C in an inert gas and subsequently grinding (introducing defects in a metal-depleted carbon framework). Unlike some toxic materials, CNTs may quench oxygenated free radicals, not generate them. The capacity of the MWCNTs to scavenge hydroxyl radicals was evaluated by spin trapping. The original ground material exhibited a scavenging activity toward hydroxyl radicals, which was eliminated by heating but restored by grinding. The scavenging activity appeared to correlate with both defects and genotoxic and inflammatory activity of the MWCNTs.

7 Modification of Surface Properties to Enhance Biocompatibility

The exceptional physicochemical properties of nanoparticles make them of great interest for biomedical applications. Different classes of nanoparticles including liposomes, polymers, metallic nanoparticles, quantum dots, carbon nanomaterials, their potential toxicity, and their pharmacological applications have been reviewed by Medina et al. [93].

However, the same physicochemical properties which make nanoparticles so unique, sometimes can cause their failure in biomedical applications. The interaction of various nanoparticles, liposomes, micelles and CNTs with biological systems depends on particle size, surface properties, and surface charge. Additionally, the presence of defects on their surfaces, length, hydrophobicity and surface roughness can significantly diminish their utility in biomedical applications. Non-functionalized SWCNTs (>90% purity) and MWCNTs (>95% purity) were shown by Schrand et al. [94] to be less biocompatible than nanodiamonds in studies carried out on neuroblastoma and alveolar macrophage cell lines. Different degrees of hydrophobicity of various latex nanoparticles was shown to have an impact on the amount of protein adsorbed on their surface [95]. Lück et al. showed in vitro plasma protein adsorption was dependent on the surface properties of polymeric nanoparticles with and without covalently bound charged functional groups [e.g. NR₃⁺ or C(NH₂)₂⁺]. Such modified latex had different particle sizes, surface charge densities, electrophoretic mobilities and hydrophobicities. Different amounts of proteins adsorbed to latex with various functional groups on their surface [96]. Purification of CNTs plays an essential role in CNT biocompatibility. Chłopek et al. [97] reported good cellular biocompatibility of high purity MWCNTs on the level observed for polysulfone currently in medical use. The interaction of the MWCNTs with osteoblast cell cultures did not cause release of pro-inflammatory cytokine, IL-6, and did not initiate ROS formation.

There are many limitations for nanoparticles being used as biomedical devices or drug vehicles. Functionalization of CNTs can significantly improve their utility as long as the functionalization is not harmful for tissues by itself. Modification of nanoparticle surface properties can make them more valuable in potential

biomedical applications. Proteins, including antibodies and enzymes can be attached to the surface of CNTs and carbon nanofibres (CNF). Naguib et al. [98] reported that CNFs could be coated with monoclonal anti-CD3 antibodies. Poly (L-lysine) (PLL) enhanced the binding of proteins to CNTs. The more hydrophilic the surface of CNFs, the more protein could bind to them. Biocompatibility aspects of CNT interactions with neuronal cells, osteoblasts, fibroblasts, ion channels, cellular membranes, mono- and polyclonal antibodies and the immune system were reviewed by Smart et al. [99]. The impact of various chemical functionalizations of CNTs, including covalent modifications (1, 3-dipolar cycloaddition) and PEGylation on their biocompatibility has been reviewed [100]. Covalent binding of various biologically active molecules, including streptavidin and siRNA to different types of functionalized or non-functionalized CNTs was presented. Encapsulation of small molecules and DNA, RNA and fluorescently labeled tags was also discussed [100]. Yang et al. [101] showed that positively charged SWCNTs could be utilized to carry siRNA. These siRNA-SWCNT complexes could be used to modify of functions of dendritic cells.

As discussed above, chemical modification of CNTs can considerably alter the level of complement activation. Salvador-Morales et al. [3] showed that unmodified SWCNTs and DWCNTs activated complement via both classical and alternative pathways, which may initiate inflammation or granuloma formation. The same researchers showed that covalent modification of MWCNTs can considerably change their biochemical properties and therefore increase their biocompatibility in human blood plasma. Complement activation by classical and alternative pathways was tested on four chemically modified MWCNTs [26]. ε-Caprolactammodified MWCNTs and L-alanine-modified MWCNTs showed significant reduction in activation of complement by the classical pathway in contrast to unmodified MWCNTs.

Studies carried out by Mooney et al. on COOH-functionalized SWCNTs and OH-functionalized MWCNTs showed that the COOH-functionalized SWCNTs were less toxic to human mesenchymal stem cells (hMSC). The localization of these SWCNTs in various cell compartments was also elucidated [102]. Biocompatibility tests were performed on fibroblast L929 mouse cells by Lobo et al. [103] for MWCNTs on titanium and silicon surfaces. Carrero-Sánchez [104] showed that MWCNTs doped with nitrogen were more tolerated by mice than pure MWCNTs.

Modification of CNTs with hydrophilic agents can influence CNT compatibility in vivo and in vitro. Coating of CNTs can modify their interaction with blood proteins and cells. Hemocompatibility studies of PEGylated alcohol/polysorbate nanoparticles (PEG-E78 NPs) and non-pegylated (E78 NPs) were performed by Koziara et al. [105]. Both types of nanoparticles had potential blood compatibility, did not activate platelets, did not cause blood cell lysis and did not have an effect on whole blood clotting time in the concentration range 0–250 μg/mL [105].

Kam et al. showed that SWCNTs functionalized by folic acid were internalized by folate receptor-overexpressing (FR⁺) cells. The same SWCNTs were not internalized by normal cells without folate receptors. SWCNTs functionalized

with Cy3-labeled DNA were shown to transport DNA inside of HeLa cells. Such modified SWCNTs can potentially be used in selective targeting of cancer cells [106].

Nanoparticles can be considered as effective drug vehicles if they can deliver the drug to the site of action without causing harm to human tissues and organs. Improvement of delivery of drugs to tumors by increasing drug bioavailability and abrogating drug resistance are major purposes in targeted drug delivery. Polymer micelles with cross-linked ionic cores consist of hydrophilic nanospheres and porous ionic cores. Block ionomer complexes of poly(ethylene oxide)-b-poly(methacrylic acid) (PEO-b-PMA) copolymer and Ca²⁺ cations were templates for these cross-linked polymeric micelles. The core of these cross-linked polymeric micelles is hydrophobic and consist of many functional groups which can be covalently attached to hydrophobic drugs, like cisplatin [107, 108]. Poly(ethylene oxide)-b-poly(methacrylic acid) (PEO-b-PMA) [109], Pluronic P85-b-poly(acrylic acid) [110], F87/poly(acrylic acid) [111] and poly(ethylene oxide)-block-poly(βbenzyl-L-asparate) [112] block copolymers were studied as potential delivery systems for cationic drugs, like doxorubicin. Effective encapsulation of potential drugs in cores of micelles can protect them from premature release in the human body. Additionally, hydrophilic PEO chains can provide increased solubility and prevent interactions of plasma components with the drug encapsulated into the core of the micelles. Paclitaxel, camptothecin and other anticancer agents can be carried by micelles, polymer conjugates and liposomes and a few of them are currently in medical use. Different clinical stages of anticancer agent-incorporating micelles in oncology were reviewed by Matsumura et al. [113, 114].

The main limitation of nanoparticles in drug delivery is their rapid uptake by the mononuclear phagocyte system (MPS). The presence of PEG chains on the surface of nanoparticles can significantly change their interactions with blood proteins. Extensive studies on these aspects of biocompatibility have been carried out on nanoparticles other than CNTs, but the findings from this work are likely to be applicable to CNTs. Studies on various nanoparticles consisiting of poly(lactic acid) (PLA), poly(lactic-co-glycolic acid) (PLGA) and poly(ε-caprolactone) (PCL) core and PEG coronas were carried out by Gref et al. [115] and showed the differences in uptake of these modified nanoparticles by polymorphonuclear cells (PMN), changes in plasma protein adsorption and zeta potentials.

The biological activity of pluronic block copolymers consisting of PEO and poly(propylene oxide) (PPO) blocks and pluronic micelles used in drug delivery was broadly reviewed by Batrakova et al. [116]. Vittaz et al. [117] showed very low complement consumption caused by poly(ethylene oxide)-poly(lactic acid) diblock copolymer (PLA-PEO) compared to poly(lactic acid) stabilized by pluronic F68 (PLA-F68). PLA-PEO phagocytosis was significantly reduced compared to PLA-F68.

Physicochemical properties of liposomes, especially their charge, can significantly influence their interactions with blood proteins and protein adsorption patterns. Gel filtration was used by Diederichs et al. [118] for the separation of liposomes from plasma to examine bound proteins. Chonn et al. [119] showed that

liposome surface charge can determine the pathway by which complement is activated. Positively and negatively charged liposomes activated the alternative and classical pathways, respectively. Liposomes with no charge on their surface were shown not to activate the complement system in vitro.

A review by LaVan et al. [120] presents different types of nanoparticles among them liposomes, as having potential in vivo drug delivery. The authors present techniques that are useful to improve biocompatibility of potential nanoscale drug vehicles.

Prolonged circulation of nanoparticles in the bloodstream is crucial for drug delivery purposes (i.e. particles should not be cleared by the liver and spleen before reaching their target). Moghimi et al. [121] reviewed protein-binding processes to stealth nanoparticles, including the influence of surface PEGylation on complement activation and the fate of these particles.

Salvador-Morales et al. showed differences in complement activation by various surface modified lipid-polymer hybrid nanoparticles (NPs). The NPs with methoxyl surface groups and amine surface groups induced the lowest and highest, respectively, complement activation via the alternative pathway. The modification of surface properties of NPs results in different protein binding patterns. NPs consisting of a lipid monolayer between a hydrophilic polymeric shell and a hydrophobic polymeric core can be utilized as drug delivery vehicles or novel adjuvants for vaccination [122].

The modification of surface of a variety of types of nanoparticles can change their reactivity and therefore make them more biologically active. This can considerably enhance their chances to be used in pharmacology and biomedical fields.

References

- 1. Kishore, U. (ed.): Target Pattern Recognition in Innate Immunity. Springer, Landes Bioscience, Austin (2009)
- Salvador-Morales, C., Green, M.L.H., Sim, R.B.: Interaction between carbon nanotubes and biomolecules. In: Basiuk, V.A., Basiuk, E.V. (eds.) Chemistry of Carbon Nanotubes. American Scientific Publishers, Valencia (2008)
- Salvador-Morales, C., Flahaut, E., Sim, E., et al.: Complement activation and protein adsorption by carbon nanotubes. Mol. Immunol. 43, 193–201 (2006)
- Kang, Y.H., Tan, L.A., Carroll, M.V., et al.: Target pattern recognition by complement proteins of the classical and alternative pathways. Adv. Exp. Med. Biol. 653, 117–128 (2009)
- 5. Mayilyan, K.R., Weinberger, D.R., Sim, R.B.: The complement system in schizophrenia. Drug News Perspect. **21**, 200–210 (2008)
- Mayilyan, K.R., Kang, Y.H., Dodds, A.W.: The complement system in innate immunity. In: Heine, H., et al. (eds.) Innate Immunity of Plants, Animals and Humans. Springer, Heidelberg (2008)
- 7. Sim, R.B., Tsiftsoglou, S.A.: Proteases of the complement system. Biochem. Soc. T 32, 21–27 (2004)
- 8. Gál, P., Dobó, J., Závodszky, P., et al.: Early complement proteases: C1r, C1s and MASPs. A structural insight into activation and functions. Mol. Immunol. **46**, 2745–2752 (2009)

- Wallis, R., Krarup, A., Girija, U.V.: The structure and function of ficolins, MBLs and MASPs. In: Reid, K.B.M., Sim, R.B. (eds.) Molecular Aspects of Innate and Adaptive Immunity. Royal Society of Chemistry, Cambridge (2008)
- Krarup, A., Mitchell, D.A., Sim, R.B.: Recognition of acetylated oligosaccharides by human L-ficolin. Immunol. Lett. 118, 152–156 (2008)
- 11. Carroll, M.V., Lack, N., Sim, E., et al.: Multiple routes of complement activation by *Mycobacterium bovis* BCG. Mol. Immunol. **46**, 3367–3378 (2009)
- 12. Cestari, I.D., Krarup, A., Sim, R.B., et al.: Role of early lectin pathway activation in the complement-mediated killing of Trypanosoma cruzi. Mol. Immunol. 47, 426–437 (2009)
- 13. Phillips, A.E., Toth, J., Dodds, A.W., et al.: Analogous interactions in initiating complexes of the classical and lectin pathways of complement. J. Immunol. **182**, 7708–7717 (2009)
- 14. Ghai, R., Waters, P., Roumenina, L.T., et al.: C1q and its growing family. Immunobiology 212, 253–266 (2007)
- 15. Kishore, U., Gaboriaud, C., Waters, P., et al.: C1q and tumor necrosis factor superfamily: modularity and versatility. Trends Immunol. **25**, 551–561 (2004)
- Matsushita, M.: Ficolins: complement-activating lectins involved in innate immunity.
 J. Innate Immun. 2, 24–32 (2010)
- Xu, W., Berger, S.P., Trouw, L.A., et al.: Properdin binds to late apoptotic and necrotic cells independently of C3b and regulates alternative pathway complement activation. J. Immunol. 180, 7613–7621 (2008)
- 18. Nolan, K.F., Kaluz, S., Higgins, J.M.G., et al.: Characterization of the human properdin gene. Biochem. J. 287, 291–297 (1992)
- 19. Sim, R.B., Clark, H., Hajela, K., et al.: Collectins and host defence. Novartis Found. Symp. 279, 170–181 (2006)
- Hickling, T.P., Clark, H., Malhotra, R., et al.: Collectins and their role in lung immunity.
 J. Leukocyte Biol. 75, 27–33 (2004)
- Carlisle, R.C., Di, Y., Cerny, A.M., et al.: Human erythrocytes bind and inactivate type 5 adenovirus by presenting Coxsackie virus-adenovirus receptor and complement receptor 1. Blood 113, 1909–1918 (2009)
- 22. Sim, R.B., Twose, T.M., Paterson, D.S., et al.: The covalent-binding reaction of complement component C3. Biochem. J. 193, 115–127 (1981)
- 23. Vandivier, R.W., Ogden, C.A., Fadok, V.A., et al.: Role of surfactant proteins A, D, and C1q in the clearance of apoptotic cells in vivo and in vitro: calreticulin and CD91 as a common collectin receptor complex. J. Immunol. **169**, 3978–3986 (2002)
- Sim, R.B., Moestrup, S.K., Stuart, G.R., et al.: Interaction of Clq and the collectins with the potential receptors calreticulin (cC1qR/collectin receptor) and megalin. Immunobiology 199, 208–224 (1998)
- 25. Basiuk, V.A., Salvador-Morales, C., Basiuk, E.V., et al.: 'Green' derivatization of carbon nanotubes with Nylon 6 and L-alanine. J. Mater. Chem. 16, 4420–4426 (2006)
- Salvador-Morales, C., Basiuk, E.V., Basiuk, V.A., et al.: Effects of covalent functionalization on the biocompatibility characteristics of multi-walled carbon nanotubes. J. Nanosci. Nanotechnol. 8, 2347–2356 (2008)
- Roumenina, L., Bureeva, S., Kantardjiev, A., et al.: Complement C1q-target proteins recognition is inhibited by electric moment effectors. J. Mol. Recogn. 20, 405–415 (2007)
- Hamad, I., Hunter, A.C., Rutt, K.J., et al.: Complement activation by PEGylated singlewalled carbon nanotubes is independent of C1q and alternative pathway turnover. Mol. Immunol. 45, 3797–3803 (2008)
- Hamad, I., Hunter, A.C., Szebeni, J., et al.: Poly(ethylene glycol)s generate complement activation products in human serum through increased alternative pathway turnover and a MASP-2-dependent process. Mol. Immunol. 46, 225–232 (2008)
- Salvador-Morales, C., Townsend, P., Flahaut, E., et al.: Binding of pulmonary surfactant proteins to carbon nanotubes; potential for damage to lung immune defense mechanisms. Carbon 45, 607–617 (2007)

- 31. Salvador-Morales, C: Study of the interaction between immune system proteins and carbon nanotubes. PhD Thesis. University of Oxford, Oxford, UK (2006)
- 32. Jin, H., Heller, D.A., Sharma, R., et al.: Size-dependent cellular uptake and expulsion of single-walled carbon nanotubes: single particle tracking and a generic uptake model for nanoparticles. ACS Nano 3, 149–158 (2009)
- Porter, A.E., Gass, M., Bendall, J.S., et al.: Uptake of noncytotoxic acid-treated singlewalled carbon nanotubes into the cytoplasm of human macrophage cells. ACS Nano 3, 1485–1492 (2009)
- 34. Kam, N.W.S., Jessop, T.C., Wender, P.A., et al.: Nanotube molecular transporters: internalization of carbon nanotube-protein conjugates into mammalian cells. J. Am. Chem. Soc. **126**, 6850–6851 (2004)
- 35. Yehia, H., Draper, R.K., Mikoryak, C.: Single-walled carbon nanotube interactions with HeLa cells. J. Nanobiotechnol. (2007). doi:10.1186/1477-3155-5-8
- 36. Magrez, A., Kasas, S., Salicio, V., et al.: Cellular toxicity of carbon-based nanomaterials. Nano Lett. 6, 1121–1125 (2006)
- Kostarelos, K., Lacerda, L., Pastorin, G., et al.: Cellular uptake of functionalized carbon nanotubes is independent of functional group and cell type. Nat. Nanotechnol. 2, 108–113 (2007)
- 38. Cui, D.X., Tian, F.R., Ozkan, C.S., et al.: Effect of single wall carbon nanotubes on human HEK293 cells. Toxicol. Lett. **155**, 73–85 (2005)
- Shvedova, A.A., Castranova, V., Kisin, E.R., et al.: Exposure to carbon nanotube material: assessment of nanotube cytotoxicity using human keratinocyte cells. J. Toxicol. Envrion. Heal A 66, 1909–1926 (2003)
- Jia, G., Wang, H.F., Yan, L., et al.: Cytotoxicity of carbon nanomaterials: single-wall nanotube, multi-wall nanotube, and fullerene. Environ. Sci. Technol. 39, 1378–1383 (2005)
- 41. Belyanskaya, L., Weigel, S., Hirsch, C., et al.: Effects of carbon nanotubes on primary neurons and glial cells. Neurotoxicology **30**, 702–711 (2009)
- 42. Shvedova, A.A., Kisin, E.R., Porter, D., et al.: Mechanisms of pulmonary toxicity and medical applications of carbon nanotubes: two faces of Janus? Pharmacol. Therapeut. 121, 192–204 (2009)
- Watari, F., Takashi, N., Yokoyama, A., et al.: Material nanosizing effect on living organisms: non-specific, biointeractive, physical size effects. J. Roy. Soc. Interface 6, S371– S388 (2009)
- 44. Zeineldin, R., Al-Haik, M., Hudson, L.G.: Role of polyethylene glycol integrity in specific receptor targeting of carbon nanotubes to cancer cells. Nano Lett. 9, 751–757 (2009)
- 45. Kang, B., Yu, D., Chang, S.: Intracellular uptake, trafficking and subcellular distribution of folate conjugated single walled carbon nanotubes within living cells. Nanotechnology (2008). doi: 10.1088/0957-4484/19/37/375103
- 46. Chen, X., Lee, G.S., Zettl, A., et al.: Biomimetic engineering of carbon nanotubes by using cell surface mucin mimics. Angew Chem. Int. Edit. 43, 6111–6116 (2004)
- 47. Konduru, N.V., Tyurina, Y.Y., Weihong, F.: Phosphatidylserine targets single-walled carbon nanotubes to professional phagocytes in vitro and in vivo. PLos One (2009). doi: 10.1371/journal.pone.0004398
- 48. Kam, N.W.S., Dai, H.J.: Carbon nanotubes as intracellular protein transporters: generality and biological functionality. J. Am. Chem. Soc. 127, 6021–6026 (2005)
- 49. Cheng, C., Muller, K.H., Koziol, K.K.K., et al.: Toxicity and imaging of multi-walled carbon nanotubes in human macrophage cells. Biomaterials **30**, 4152–4160 (2009)
- Kim, J.Y., Khang, D., Lee, J.E.: Decreased macrophage density on carbon nanotube patterns on polycarbonate urethane. Wiley InterScience, New York (2007). doi:10.1002/jbm.a.31799
- 51. Harrison, B.S., Atala, A.: Carbon nanotube applications for tissue engineering. Biomaterials **28**, 344–353 (2007)
- Cai, D., Blair, D., Dufort, F.J., et al.: Interaction between carbon nanotubes and mammalian cells: characterization by flow cytometry and application. Nanotechnology 19, 1–10 (2008)

- 53. Dobrovolskaia, M.A., McNeil, S.E.: Immunological properties of engineered nanomaterials. Nat. Nanotechnol. **2**, 469–478 (2007)
- 54. Yu, Y.M., Zhang, Q., Mu, Q.X., et al.: Exploring the immunotoxicity of carbon nanotubes. Nanoscale Res. Lett. 3, 271–277 (2008)
- 55. Müller, L., Riediker, M., Wick, P., et al.: Oxidative stress and inflammation response after nanoparticle exposure: differences between human lung cell monocultures and an advanced three-dimensional model of the human epithelial airways. J. Roy. Soc. Interface (2009). doi: 10.1098/rsif.2009.0161.focus
- Simon, A., Reynaud, C., Mayne, M., et al.: Cytotoxicity of Metal Oxide Nanoparticles and Multiwalled Carbon Nanotubes to Lung, Kidney and Liver Cells. John Libbey Eurotext, France (2008)
- Stern, S.T., McNeil, S.E.: Nanotechnology safety concerns revisited. Toxicol. Sci. 101, 4–21 (2008)
- 58. Donaldson, K., Aitken, R., Tran, L., et al.: Carbon nanotubes: a review of their properties in relation to pulmonary toxicology and workplace safety. Toxicol. Sci. **92**, 5–22 (2006)
- Helland, A., Wick, P., Koehler, A., et al.: Reviewing the environmental and human health knowledge base of carbon nanotubes. Environ. Health Perspect. 115, 1125–1131 (2007)
- De Jong, W.H., Borm, P.J.A.: Drug delivery and nanoparticles: applications and hazards. Int. J. Nanomed. 3, 133–149 (2008)
- Yang, W., Peters, J.I., Williams, R.O.: Inhaled nanoparticles—a current review. Int. J. Pharm. 356, 239–247 (2008)
- 62. Card, J.W., Zeldin, D.C., Bonner, J.C., et al.: Pulmonary applications and toxicity of engineered nanoparticles. Am. J. Physiol. Lung C 295, L400–L411 (2008)
- Royal Society (2004) Nanoscience and nanotechnologies: opportunities and uncertainties. Nanosci. Nanotechnol. http://www.nanotec.org.uk/report/Nano%20report%202004%20fin.pdf (accessed 29 July 2004)
- 64. Han, S.G., Andrews, R., Gairola, C.G.: Acute pulmonary effects of combined exposure to carbon nanotubes and ozone in mice. Inhal. Toxicol. **20**, 391–398 (2008)
- 65. Han, S.G., Andrews, R., Gairola, C.G.: Acute pulmonary response of mice to multi-wall carbon nanotubes. Inhal. Toxicol. **22**, 340–347 (2010)
- 66. Mitchell, L.A., Gao, J., Wal, R.V., et al.: Pulmonary and systemic immune response to inhaled multiwalled carbon nanotubes. Toxicol. Sci. **100**, 203–214 (2007)
- 67. Mitchell, L.A., Lauer, F.T., Burchiel, S.W., et al.: Mechanisms for how inhaled multiwalled carbon nanotubes suppress systemic immune function in mice. Nat. Nanotechnol. 4, 451–456 (2009)
- 68. Kostarelos, K.: The long and short of carbon nanotube toxicity. Nat. Biotechnol. 26, 774–776 (2008)
- 69. Chou, C.C., Hsiao, H.Y., Hong, Q.S., et al.: Single-walled carbon nanotubes can induce pulmonary injury in mouse model. Nano Lett. **8**, 437–445 (2008)
- 70. Warheit, D.B.: What is currently known about the health risks related to carbon nanotube exposures? Carbon 44, 1064–1069 (2006)
- 71. Poland, C.A., Duffin, R., Kinloch, I., et al.: Carbon nanotubes introduced into the abdominal cavity of mice show asbestos-like pathogenicity in a pilot study. Nat. Nanotechnol. 3, 423–428 (2008)
- 72. Jacobsen, N.R., Moller, P., Jensen, K.A, et al.: Lung inflammation and genotoxicity following pulmonary exposure to nanoparticles in ApoE(-/-) mice. Part Fibre Toxicol. (2009). doi:10.1186/1743-8977-6-2
- 73. Elgrabli, D., Floriani, M., Abella-Gallart, S, et al.: Biodistribution and clearance of instilled carbon nanotubes in rat lung. Part Fibre Toxicol. (2008). doi:10.1186/1743-8977-5-20
- Li, J.G., Li, W.X., Xu, J.Y., et al.: Comparative study of pathological lesions induced by multiwalled carbon nanotubes in lungs of mice by intratracheal instillation and inhalation. Environ. Toxicol. 22, 415–421 (2007)
- 75. Warheit, D.B., Laurence, B.R., Reed, K.L., et al.: Comparative pulmonary toxicity assessment of single-wall carbon nanotubes in rats. Toxicol. Sci. 77, 117–125 (2004)

- Lam, C.W., James, J.T., McCluskey, R., et al.: Pulmonary toxicity of single-wall carbon nanotubes in mice 7 and 90 days after intratracheal instillation. Toxicol. Sci. 77, 126–134 (2004)
- 77. Elder, A.: How do nanotubes suppress T cells? Nat. Nanotechnol. 4, 409–410 (2009)
- 78. Huczko, A., Lange, H., Bystrzejewski, M., et al.: Pulmonary toxicity of 1-D nanocarbon materials. Fullerenes Nanotubes Carbon Nanostruct. 13, 141–145 (2005)
- Qu, G.B., Bai, Y.H., Zhang, Y., et al.: The effect of multiwalled carbon nanotube agglomeration on their accumulation in and damage to organs in mice. Carbon 47, 2060–2069 (2009)
- Pulskamp, K., Diabate, S., Krug, H.F.: Carbon nanotubes show no sign of acute toxicity but induce intracellular reactive oxygen species in dependence on contaminants. Toxicol. Lett. 168, 58–74 (2007)
- 81. Fenoglio, I., Tomatis, M., Lison, D., et al.: Reactivity of carbon nanotubes: free radical generation or scavenging activity? Free Radic. Biol. Med. 40, 1227–1233 (2006)
- Shvedova, A.A., Kisin, E.R., Mercer, R., et al.: Unusual inflammatory and fibrogenic pulmonary responses to single-walled carbon nanotubes in mice. Am. J. Physiol. Lung C 289. L698–L708 (2005)
- Pulskamp, K., Worle-Knirsch, J.M., Hennrich, F., et al.: Human lung epithelial cells show biphasic oxidative burst after single-walled carbon nanotube contact. Carbon 45, 2241–2249 (2007)
- 84. Brown, D.M., Kinloch, I.A., Bangert, U., et al.: An in vitro study of the potential of carbon nanotubes and nanofibres to induce inflammatory mediators and frustrated phagocytosis. Carbon 45, 1743–1756 (2007)
- 85. Shvedova, A.A., Kisin, E.R., Murray, A.R., et al.: Increased accumulation of neutrophils and decreased fibrosis in the lung of NADPH oxidase-deficient C57BL/6 mice exposed to carbon nanotubes. Toxicol. Appl. Pharm. **231**, 235–240 (2008)
- 86. Murray, A.R., Kisin, E., Leonard, S.S., et al.: Oxidative stress and inflammatory response in dermal toxicity of single-walled carbon nanotubes. Toxicology **257**, 161–171 (2009)
- 87. Charlier, J.C., Ebbesen, T.W., Lambin, P.: Structural and electronic properties of pentagon-heptagon pair defects in carbon nanotubes. Phys. Rev. B 53, 11108–11113 (1996)
- 88. Charlier, J.C.: Defects in carbon nanotubes. Acc. Chem. Res. 35, 1063–1069 (2002)
- 89. Lambin, P.H., Lucas, A.A., Charlier, J.C., et al.: Electronic properties of carbon nanotubes containing defects. J. Phys. Chem. Sol. **58**, 1833–1837 (1997)
- 90. Charlier, J.C., Terrones, M., Terrones, H, et al.: Defects and coalescence in carbon nanotubes. AIP Conf. Proc. (2001). doi:10.1063/1.1426900
- Muller, J., Huaux, F., Fonseca, A., et al.: Structural defects play a major role in the acute lung toxicity of multiwall carbon nanotubes: toxicological aspects. Chem. Res. Toxicol. 21, 1698–1705 (2008)
- 92. Fenoglio, I., Greco, G., Tornatis, M., et al.: Structural defects play a major role in the acute lung toxicity of multiwall carbon nanotubes: physicochemical aspects. Chem. Res. Toxicol. **21**, 1690–1697 (2008)
- 93. Medina, C., Santos-Martinez, M.J., Radomski, A., et al.: Nanoparticles: pharmacological and toxicological significance. Br. J. Pharmacol. **150**, 552–558 (2007)
- 94. Schrand, A.M., Dai, L., Schlager, J.J., et al.: Differential biocompatibility of carbon nanotubes and nanodiamonds. Diam. Relat. Mater. 16, 2118–2123 (2007)
- 95. Gessner, A., Waicz, R., Lieske, A., et al.: Nanoparticles with decreasing surface hydrophobicities: influence on plasma protein adsorption. Int. J. Pharm. **196**, 245–249 (2000)
- Lück, M., Paulke, B.R., Schröder, W., et al.: Analysis of plasma protein adsorption on polymeric nanoparticles with different surface characteristics. J. Biomed. Mater. Res. 39, 478–485 (1998)
- 97. Chłopek, J., Czajkowska, B., Szaraniec, B., et al.: In vitro studies of carbon nanotubes biocompatibility. Carbon 44, 1106–1111 (2006)

- 98. Naguib, N.N., Mueller, Y.M., Bojczuk, P.M., et al.: Effect of carbon nanofibre structure on the binding of antibodies. Nanotechnology **16**, 567–571 (2005)
- 99. Smart, S.K., Cassady, A.I., Lu, G.Q., et al.: The biocompatibility of carbon nanotubes. Carbon 44, 1034–1047 (2006)
- Foldvari, M., Bagonluri, M.: Carbon nanotubes as functional excipients for nanomedicines:
 II. Drug delivery and biocompatibility issues. Nanomed. Nanotechnol. 4, 183–200 (2008)
- 101. Yang, R., Yang, X., Zhang, Z., et al.: Single-walled carbon nanotubes-mediated in vivo and in vitro delivery of siRNA into antigen-presenting cells. Gene Ther. 13, 1714–1723 (2006)
- 102. Mooney, E., Dockery, P., Greiser, U., et al.: Carbon nanotubes and mesenchymal stem cells: biocompatibility, proliferation and differentiation. Nano Lett. **8**, 2137–2143 (2008)
- 103. Lobo, A.O., Antunes, E.F., Palma, M.B.S., et al.: Biocompatibility of multi-walled carbon nanotubes grown on titanium and silicon surfaces. Mat. Sci. Eng. C Biol. S 28, 532–538 (2008)
- 104. Carrero-Sanchez, J.C., Elias, A.L., Mancilla, R., et al.: Biocompatibility and toxicological studies of carbon nanotubes doped with nitrogen. Nano Lett. 6, 1609–1616 (2006)
- Koziara, J.M., Oh, J.J., Akers, W.S., et al.: Blood compatibility of cetyl alcohol/polysorbatebased nanoparticles. Pharm. Res. 22, 1821–1828 (2005)
- 106. Kam, N.W.S., O'Connell, M., Wisdom, J.A., et al.: Carbon nanotubes as multifunctional biological transporters and near-infrared agents for selective cancer cell destruction. PNAS 102, 11600–11605 (2005)
- Bronich, T.K., Keifer, P.A., Shlyakhtenko, L.S., et al.: Polymer micelle with cross-linked ionic core. J. Am. Chem. Soc. 127, 8236–8237 (2005)
- 108. Bontha, S., Kabanov, A.V., Bronich, T.K.: Polymer micelles with cross-linked ionic cores for delivery of anticancer drugs. J. Control Release 114, 163–174 (2006)
- Kim, J.O., Kabanov, A.V., Bronich, T.K.: Polymer micelles with cross-linked polyanion core for delivery of a cationic drug doxorubicin. J. Control Release 138, 197–204 (2009)
- Tian, Y., Bromberg, L., Lin, S.N., et al.: Complexation and release of doxorubicin from its complexes with pluronic P85-b-poly(acrylic acid) block copolymers. J. Control Release 121, 137–145 (2007)
- 111. Tian, Y., Ravi, P., Bromberg, L., et al.: Synthesis and aggregation behavior of Pluronic F87/ poly(acrylic acid) block copolymer in the presence of doxorubicin. Langmuir 23, 2638–2646 (2007)
- 112. Kwon, G., Naito, M., Yokoyama, M., et al.: Block copolymer micelles for drug delivery: loading and release of doxorubicin. J. Control Release 48, 195–201 (1997)
- 113. Matsumura, Y., Kataoka, K.: Preclinical and clinical studies of anticancer agent-incorporating polymer micelles. Cancer Sci. 100, 572–579 (2009)
- Matsumura, Y.: Polymeric micellar delivery systems in oncology. Jpn. J. Clin. Oncol. 38, 793–802 (2008)
- 115. Gref, R., Luck, M., Quellec, P., et al.: 'Stealth' corona-core nanoparticles surface modified by polyethylene glycol (PEG): influences of the corona (PEG chain length and surface density) and of the core composition on phagocytic uptake and plasma protein adsorption. Coll. Surf. B 18, 301–313 (2000)
- Batrakova, E.V., Kabanov, A.V.: Pluronic block copolymers: evolution of drug delivery concept from inert nanocarriers to biological response modifiers. J. Control Release 130, 98–106 (2008)
- 117. Vittaz, M., Bazile, D., Spenlehauer, G., et al.: Effect of PEOsurface density on long-circulating PLA-PEO nanoparticles which are very low complement activators. Biomaterials 17, 1575–1581 (1996)
- 118. Diederichs, J.E.: Plasma protein adsorption patterns on liposomes: establishment of analytical procedure. Electrophoresis 17, 607–611 (1996)
- 119. Chonn, A., Cullis, P.R., Devine, D.V.: The role of surface-charge in the activation of the classical and alternative pathways of complement by liposomes. J. Immunol. 146, 4234–4241 (1991)

- 120. LaVan, D.A., McGuire, T., Langer, R.: Small-scale systems for in vivo drug delivery. Nat. Biotechnol. 21, 1184–1191 (2003)
- 121. Moghimi, S.M., Szebeni, J.: Stealth liposomes and long circulating nanoparticles: critical issues in pharmacokinetics, opsonization and protein-binding properties. Prog. Lipid Res. **42**, 463–478 (2003)
- 122. Salvador-Morales, C., Zhang, L.F., Langer, R., et al.: Immunocompatibility properties of lipid-polymer hybrid nanoparticles with heterogeneous surface functional groups. Biomaterials **30**, 2231–2240 (2009)

Toxicity and Environmental Impact of Carbon Nanotubes

E. Flahaut

Abstract As the number of applications of carbon nanotubes (CNT) in the field of nanomedicine is growing quickly (imaging, drug delivery, scaffolds for tissue engineering), questions are raised about their potential toxicity. Because their annual production is now reaching hundreds of tons per year, their application in composite materials is becoming a reality. Dissemination in the environment could also happen during different steps of their life cycle, from their production to their processing, use and finally during disposal or recycling. We will review in this paper the state of the art in the field of toxicity and ecotoxicity of carbon nanotubes and try to highlight some recommendations.

1 Introduction

As the number of industrial applications of CNT increases constantly with the production capacity at the worldwide level estimated to be a few hundreds of tons in 2007, it is reasonable to ask the question of their potential impact on both human health and the environment. It is important to consider that the number of different kinds of CNT (SWNT, DWNT, MWNT) and different synthesis routes [arc-discharge, laser ablation, (catalytic) chemical vapour deposition (C)CVD] make the investigation of the toxicity of CNT more complex, and comparison of the results already published almost impossible. CNT are most of the time not found as individual objects but in the form of bundles, or more likely as large

E. Flahaut (⊠)

E. Flahaut

micrometric aggregates. All samples contain different levels of residual catalyst(s), depending on the synthesis route and purification steps that they may have undergone. Usual purification treatments involve the combination of acids and oxidising agents, which lead to at least partial functionalisation of the outer wall, making the treated samples more hydrophilic. SWNT and DWNT usually form long and flexible bundles (typically hundreds of micrometers) while MWNT are generally shorter (tens of micrometers) and more rigid. MWNT also have more surface defects, which enhances their chemical reactivity. The specific surface area (m² g⁻¹) can range from a few tens of square metres per gram in the case of densely packed MWNT to just below 1,000 m² g⁻¹ in the case of SWNT and DWNT [1] (the theoretical limit being 1,300 m² g⁻¹ in the case of individual closed SWNT) [2].

Toxicity is generally defined as the degree to which a substance can harm. It can be acute or chronic. Acute toxicity involves harmful effects in an organism through a single or short-term exposure. Chronic toxicity is the ability of a substance or mixture of substances to cause harmful effects over an extended period, usually upon repeated or continuous exposure. Genotoxicity refers to alterations of the cell genetic material (DNA). Its effects are usually not visible in the short-term range and it is thus an indicator of potential long-term effects (mutagenesis, carcinogenesis).

The main exposure routes (Fig. 1) for dry CNT are first inhalation and then dermal contact (the latter being also possible in the case of suspensions of CNT). Ingestion is generally not considered likely to be accidental, although it is in fact

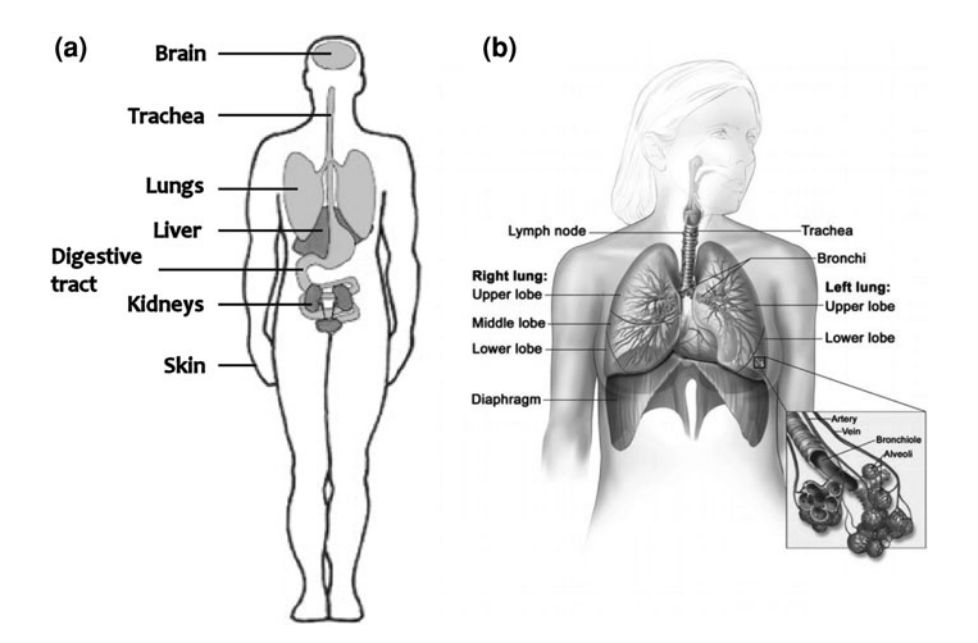


Fig. 1 a Main target organs, b details of lung anatomy

more or less related to inhalation because part of inhaled particles generally leave the respiratory system and reach the stomach from the upper airways (via the mucociliary escalator). Injection in the bloodstream is envisaged, but would not be accidental (biological applications such as imaging, targeted cell delivery, hyperthermia, etc.).

After entry in the body, and depending on the route, migration to other organs could be possible. This would be especially true if the nanoparticles are able to reach the blood circulation. Typical target organs would then be the liver and the kidneys, as well as the cardiovascular system in general. It has also been reported that nanoparticles could reach the brain via the olfactory nerve [3], although there is currently no evidence in the case of CNT.

2 Main Characteristics of CNT in Terms of Toxicity Investigation

Real CNT are usually not perfect cylindrical tubes made of pure sp² carbon. Their shape can vary from short and straight (typical for arc-discharge MWNT) to long and flexible (SWNT, DWNT). Their diameter can range from a nanometer (SWNT, DWNT) to ca. 100 nm (large MWNT). They can be individual (rare) or gathered into bundles. The diameter of the bundles can vary from a few nanometres to hundreds of nanometres. Interconnexions between the bundles are very often observed (web-like material). The size and shape are very important because they will determine the mobility of the nanoparticles within the body and their ability to be cleared or not (biopersistence): it is well known (and rather intuitive) that fibres are less mobile than spherical particles. In terms of length, macrophage will not manage to eliminate particles longer than them (about a few tens of micrometers for humans, depending on the organ where they are located). We have already mentioned that CNT can be more or less aggregated and this will also play a role in terms of biological interaction.

The chemical composition of CNT samples can vary strongly depending on their purity. Whatever the synthesis technique (arc-discharge, laser ablation, (catalytic) chemical vapour deposition), they usually still contain some catalyst (typically transition metals such as Fe, Co or Ni, as well as other additives including Y, Mo, S, etc.). The amount of residual catalyst can vary from a few tens of wt% in as-prepared samples to a few ppm in highly purified CNT. In purified samples, it is generally assumed that the residual catalyst is encapsulated in graphitised shells or within the CNT and cannot directly interact with the environment [4]. The presence of such metals can favour the production of free radicals such as reactive oxygen species (ROS) which can themselves modulate different biological functions.

Other parameters such as the specific surface area and the surface chemistry are also very important. Functionalisation of CNT can be deliberate (for example in the case of targeted delivery, or to stabilise a suspension by addition of surfactants)

214 E. Flahaut

or not (when it occurs during purification) and will control the interface with biological environments because of the resulting surface charge or modification of wettability for example.

The interactions of the CNT with their local environment may vary with time and will affect subtly the interaction with the target sites (Fig. 2).

In the case of the toxicity of nanoparticles, the relevant unit to quantify the exposure is probably the number of particles, and not the weight or even not the specific surface area. A simple comparison between MWNT and SWNT shows that the same weight of material can correspond to very different amounts of individual particles.

3 Models

Toxicity can be assessed both by in vitro and in vivo experiments. In the case of in vitro assays, cell cultures (usually immortalised cancer cells, but also primary cultures or even stem cells) are exposed to suspensions of CNT. The way the suspension is prepared (with or without addition of a surfactant, dispersion by sonication with a bath or a tip, etc.) and exposed to the cells are both very important. In the case of in vivo assays, the animals (mice, rats, worms, amphibians, fishes, etc.) are exposed either to aerosols (inhalation) or mainly to suspensions of CNT which will be administrated according to different protocols depending on the study (intra-tracheal instillation, injection, contact with the skin, etc.). It must be noted that transposition of toxicity results from animals (or even worse from cells) to humans is very uncertain but the data are however very useful

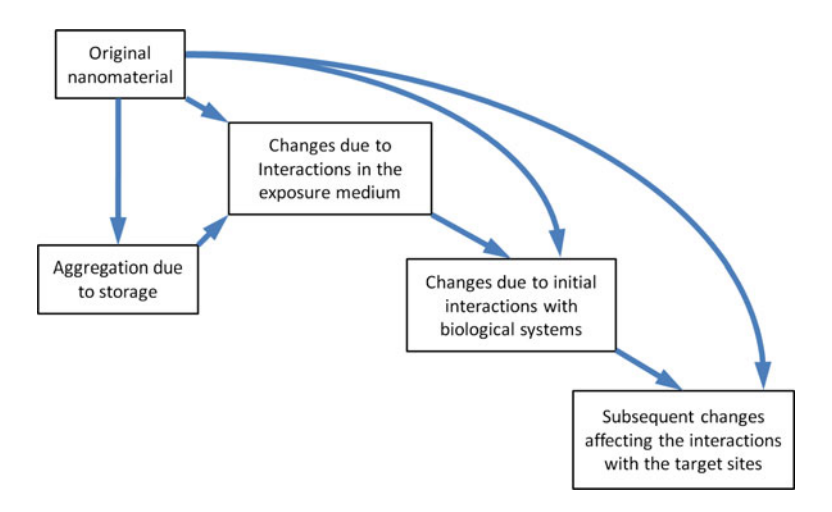


Fig. 2 Potential modifications of particles due to their environment (adapted from [5])

for the sake of comparison in a given system and with given experimental conditions.

In the case of the use of suspensions, the main issue concerns their stability. This question has been widely studied worldwide and the general approach is the addition of a surfactant in order to stabilise the CNT in the liquid. The main problem is that all commonly used surfactants are toxic to a certain extent and thus cannot be used in the presence of living cells or animals for in vitro or in vivo investigations, or must be used at such low concentrations that they no longer play anymore the role there are supposed to play. Although a few natural surfactants such as proteins [6], starch [7], Gum Arabic [8] or sugar derivatives [9] have been investigated, the stability of the suspensions in the presence of living organisms is often very different (fast destabilisation leading to flocculation).

4 Inhalation

Among respiratory tract cells, the lung (alveolar) ones are the most studied (nothing has currently been published about nasal cells for example). The target respiratory cells in the lungs are the epithelial cells and the macrophages. In particular, epithelial cells provide a selective and permeable interface between the lumen and the underlying tissue, for exchange of gases and other molecules. The intra-tracheal instillation of mice with suspensions of SWNT (purified or not) [10] led to an inflammatory response in the alveolar area. Granuloma (spheroidal accumulation of immune cells trying to destroy a foreign body) were observed after 90 days of exposure due to frustrated phagocytosis (impossibility for the macrophages to destroy or remove the CNT). Similar observations were reported in the case of other SWNT samples, but the granuloma vanished after 3 months [11]. The influence of the length of the CNT was investigated and it was shown, in the case of MWNT, that shorter nanotubes were much better dispersed in the lungs [12]. Recent studies have compared CNT and asbestos because of the well-known "fibre paradigm" in pulmonary toxicology: long thin fibres (longer than the cells of the lung that usually gets rid of fibres and other dusts—that is longer than about 15 μm and thin enough to enter the lungs—less than about 5 μm) tend to be biopersistent in the lungs and are likely to lead to mesothelioma. Poland et al. [13] have used peritoneal injection to compare the effect of different kinds of MWNT (different diameters, different lengths) with amosite, a known pathogenic form of asbestos. The results suggest that long and straight MWNT may be pathogenic in the same manner as amosite but both the small number of animals used in this study [13] and the unrealistic exposure conditions must moderate the validity of the conclusions. In another study involving mesothelial cell cultures, it was also shown that non-purified SWNT induced the activation of molecular pathways associated with oxidative stress [14], similarly to asbestos. In this case, it can clearly be questioned whether the oxidative stress came from the CNT themselves or from residual catalyst [15].

E. Flahaut

5 Contamination Through the Skin

It is generally admitted that nanoparticles do not cross a healthy dermis and may only accumulate in the upper layers of the epidermis, although they may reach the dermis along hair follicles (TiO₂) [16]. Only a few examples of skin penetration have been reported (in the case of Ag nanoparticles [17]), but none in the case of CNT. In vitro cytotoxicity of CNT versus keratinocytes was however shown [18]. Oxidative stress, alterations of cellular membrane, internalisation and production of pro-inflammatory cytokines were also described after in vitro exposure of human epidermal keratinocytes to MWNT [19].

6 Translocation

After the CNT have entered in the body, they could travel following different routes depending on the entry point (movements from one organ to another are called translocation) but also mainly on their physico-chemical characteristics. Objects recognised as non-self by the immune system usually end up in the liver or the kidneys if they can be transported there, and could possibly be excreted (eliminated) from the body. In the general case, CNT will just accumulate (biopersistence).

7 Mechanisms of Protection and Elimination

Foreign particles are usually intercepted by macrophages (cells present in all tissues the role of which is to phagocytose (engulf and then digest) cellular debris and pathogens as well as to stimulate lymphocytes and other immune cells to respond to the pathogens). Taking into account the small size of macrophages as compared to that of CNT aggregates, bundles or even individual CNT, the latter usually do not manage to eliminate the CNT by phagocytosis. However, they try to do so and thus release reactive oxygen species (ROS), enzymes, cytokines [interferons (IFN)], etc. and aggregate around them to isolate them from the body. Proteins present in the blood and most biological fluids (complement systeminnate immunity) will play a similar role by "labelling" of the CNT [20] (opsonisation) and possibly generating some inflammation reactions. The complement system strongly interacts with the leukocytes. These natural phenomena have deleterious consequences on the surrounding tissues: inflammation in a first instance, formation of granuloma (commonly observed in the lungs after exposure to CNT). Each target organ has its own phagocytic cells (Kupffer cells in the liver, Langerhans cells in the skin, etc.).

As soon as CNT are in contact with a biological fluid, their surface chemistry is likely to be modified very quickly by adsorption of proteins (complement system

[20], surfactants [21], etc.); this adsorption can be very specific [20, 21] and is likely to be dynamic and influenced by the affinity of the molecules for the surface of the CNT (pristine or functionalised). It is thus obvious that the surface chemistry of the CNT will play a very important role.

8 Genotoxicity

Genotoxicity deals with gene alterations and mutations and corresponds to the "hidden risk" during classical toxicity investigations because the consequences (mutagenic, carcinogenic effects) only appear after a long period of time and are thus not observed during the assay. Genotoxicity was only scarcely investigated in the case of human studies. A few papers by Muller et al. [22] however suggest a potential genotoxicity of MWNT and report chromosomal alterations in human epithelial cells or the observation of micronuclei after exposure of rat liver epithelial cells (immortalised) [23]. In the latter case, it was shown that the chemical purity of the MWNT samples played an important role. Recent publications also confirm the potential genotoxicity of CNT [24].

9 Environmental Impact of CNT

The potential use of CNT in commercial products (sports equipment such as tennis rackets, baseball bats or bikes are for example already available, flat-screen displays are expected to be soon available, use as additives in tyres and automobile industry under study, etc.) begs the question of their fate at the end of their lifecycle. If the impact of CNT on human health has been under investigation already for a few years now, it is noteworthy that the environmental impact has hardly been investigated. Only a few publications are currently available. A few studies on different aquatic organisms exposed to CNTs are available: aquatic worms exposed to SWNT [25], estuarine copepods exposed to SWNT [26], freshwater crustaceans (Daphnia magna) exposed to functionalized SWNT [27], cladocerans and amphipods exposed to raw and oxidized MWNT [28], zebrafish embryos (Danio rerio) exposed to SWNT and DWNT [29], trout exposed to dispersed SWNT in the presence of a surfactant [30] and amphibian larvae (Ambystoma mexicanum, Xenopus laevis) exposed to DWNT [31, 32]. In the last case, no genotoxic effects could be observed. All of these studies indicated that exposure to CNT leads to biological disorders at different levels, usually from or above 10 mg L⁻¹, which is much higher than what could be reasonably found in the environment (or this could only be very localised). Due to the potentially very high specific surface area of CNT, they could act as vectors for pollutants adsorbed on their surface [PAH, (polycyclic aromatic hydrocarbons) for example, ions, etc.], even if they themselves do not show any significant sign of toxicity.

218 E. Flahaut

10 Conclusions

There is currently no consensus about the toxicity of CNT, although ca. 600 papers have already been published on this topic within only the last 6 years. Despite the worldwide effort devoted to this field of research, the huge variety of CNT types, shapes, composition, etc. will make it very difficult to answer this simple question: "are CNT toxic?" The "principle of precaution" should not stop all research in this area but only draw the attention to a more responsible attitude for people working on their synthesis or manipulating them, and industrials willing to include them in consumer products. As well as adhering to local rules and safety practices, sensible precautions should be adopted at all times when handling CNTs in order to minimise exposure. Gloves should be worn at any time as well as an adapted (FFP3 type) disposable dust mask. Wearing a lab coat is recommended to limit contamination of clothes. CNT wastes should always be burnt.

References

- 1. Flahaut, E., Bacsa, R., Peigney, A., et al.: Gram-scale CCVD synthesis of double-walled carbon nanotubes. Chem. Commun. 12, 1442–1443 (2003)
- Peigney, A., Laurent, C., Flahaut, E., et al.: Specific surface area of carbon nanotubes and bundles of carbon nanotubes. Carbon 39, 507–514 (2001)
- 3. Oberdorster, G., Sharp, Z., Atudorei, V., et al.: TITRE. Inhal. Toxicol. 16, 437-445 (2004)
- Flahaut, E., Agnoli, F., Sloan, J., et al.: CCVD synthesis and characterization of cobaltencapsulated nanoparticles. Chem. Mater. 14, 2553–2558 (2002)
- 5. Risk assessment of products of nanotechnologies Technical report, SCENIHR, (2009)
- Zorbas, V., Ortiz-Acevedo, A., Dalton, A., et al.: Preparation and characterization of individual peptide-wrapped single-walled carbon nanotubes. J. Am. Chem. Soc. 126, 7222– 7227 (2004)
- 7. Star, A., Steuerman, D., Heath, J., et al.: Starched carbon nanotubes. Angew Chem. Int. Ed. 41, 2508–2512 (2002)
- 8. Bandyopadhyaya, R., Nativ-Roth, E., Regev, O., et al.: Stabilization of individual carbon nanotubes in aqueous solutions. Nano Lett. **2**, 25–28 (2002)
- 9. Datsyuk, V., Landois, P., Fitremann, J., et al.: Double-walled carbon nanotube dispersion via surfactant substitution. J. Mater. Chem. 19, 2729–2736 (2009)
- 10. Lam, C., James, J., McCluskey, R., et al.: Pulmonary toxicity of single-wall carbon nanotubes in mice 7 and 90 days after intra-tracheal instillation. Toxicol. Sci. 77, 126–134 (2004)
- 11. Warheit, D., Laurence, B., Reed, K., et al.: Comparative pulmonary toxicity assessment of single-wall carbon nanotubes in rats. Toxicol. Sci. 77, 117–125 (2004)
- 12. Muller, J., Huaux, F., Moreau, N., et al.: Respiratory toxicity of multi-wall carbon nanotubes. Toxicol. Appl. Pharmacol. **207**, 221–231 (2005)
- Poland, C., Duffin, R., Kinloch, I., et al.: Carbon nanotubes introduced into the abdominal cavity of mice show asbestos-like pathogenicity in a pilot study. Nat. Nanotechnol. 3, 423–428 (2008)
- 14. Pacurari, M., Yin, X., Zhao, J., et al.: Raw single-wall carbon nanotubes induce oxidative stress and activate MAPKs, AP-1, NF-B, and Akt in normal and malignant human mesothelial cells. Environ. Health Perspect. 116, 1211–1217 (2008)

- Kagan, V., Tyurina, Y., Tyurin, V., et al.: Direct and indirect effects of single walled carbon nanotubes on RAW 264.7 macrophages: role of iron. Toxicol. Lett. 165, 88–100 (2006)
- Lademann, J., Weigmann, H., Rickmeyer, C., Barthelmes, H., Schaefer, H., Mueller, G., Sterry, W.: Skin Pharmacol. Appl. Skin Physiol. 12, 247–256 (1999)
- 17. Larese, F., D'Agostin, F., Crosera, M., et al.: Human skin penetration of silver nanoparticles through intact and damaged skin. Toxicology **255**, 33–37 (2009)
- 18. Murray, A., Kisin, E., Leonard, S., et al.: Oxidative stress and inflammatory response in dermal toxicity of single-walled carbon nanotubes. Toxicology **257**, 161–171 (2009)
- 19. Monteiro-Riviere, N., Nemanich, R., Inman, A., et al.: Multi-walled carbon nanotube interactions with human epidermal keratinocytes. Toxicol. Lett. **155**, 377–384 (2005)
- 20. Salvador-Morales, C., Flahaut, E., Sim, E., et al.: Complement activation and protein adsorption by carbon nanotubes. Mol. Immunol. 43, 193–201 (2006)
- Salvador-Morales, C., Townsend, P., Flahaut, E., et al.: Binding of pulmonary surfactant proteins to carbon nanotubes; potential for damage to lung immune defence mechanisms. Carbon 45, 607–617 (2007)
- 22. Muller, J., Decordier, I., Hoet, P., et al.: Clastogenic and aneugenic effects of multi-wall carbon nanotubes in epithelial cells. Carcinogenesis **29**, 427–433 (2008)
- Muller, J., Huaux, F., Fonseca, A., et al.: Structural defects play a major role in the acute lung toxicity of multiwall carbon nanotubes: toxicological aspects. Chem. Res. Toxicol. 21, 1698– 1705 (2008)
- Lindberg, H., Falck, G., Suhonen, S., et al.: Genotoxicity of nanomaterials: DNA damage and micronuclei induced by carbon nanotubes and graphite nanofibres in human bronchial epithelial cells in vitro. Toxicol. Lett. 186, 166–173 (2009)
- 25. Petersen, E., Huang, Q., Weber, W.: Ecological uptake and depuration of carbon nanotubes by *Lumbriculus variegatus*. Environ. Health. Perspect. **116**, 496–500 (2008)
- Templeton, R., Ferguson, P., Washburn, K., et al.: Life-cycle effects of single-walled carbon nanotubes (SWNTs) on an estuarine meiobenthic copepod. Environ. Sci. Technol. 40, 7387– 7393 (2006)
- 27. Roberts, A., Mount, A., Seda, B., et al.: In vivo biomodification of lipid-coated carbon nanotubes by *Daphnia magna*. Environ. Sci. Technol. **41**, 3025–3029 (2007)
- Kennedy, A., Hull, M., Steevens, J., et al.: Factors influencing the partitioning and toxicity of nanotubes in the aquatic environment. Environ. Toxicol. Chem. 27, 1932–1941 (2008)
- 29. Cheng, J., Flahaut, E., Cheng, S.: Effect of carbon nanotubes on developing zebrafish (*Danio rerio*) embryos. Environ. Toxicol. Chem. **26**, 708–716 (2007)
- 30. Smith, C., Shaw, B., Handy, R.: Toxicity of single walled carbon nanotubes to rainbow trout, (*Oncorhynchus mykiss*): respiratory toxicity, organ pathologies, and other physiological effects. Aquat. Toxicol. **82**, 94–109 (2007)
- Mouchet, F., Landois, P., Flahaut, E., et al.: Assessment of the potential in vivo ecotoxicity of double-walled carbon nanotubes (DWNTs) in water, using the amphibian *Ambystoma* mexicanum. Nanotoxicology 1, 149–156 (2007)
- 32. Mouchet, F., Landois, P., Sarremejean, E., et al.: Characterisation and in vivo ectoxicity evaluation of double-wall carbon nanotubes in larvae of the amphibian *Xenopus laevis*. Aquat. Toxicol. **87**, 127–137 (2008)

Part IV Towards Targeted Chemotherapy and Gene Delivery

Carbon Nanotubes Loaded with Anticancer Drugs: A Platform for Multimodal Cancer Treatment

Elena Heister, Vera Neves, S. Ravi P. Silva, Johnjoe McFadden and Helen M. Coley

Abstract Approximately every fourth person in the world currently dies of cancer. Although many efficient anticancer drugs have been developed over the last 60 years or more, most therapeutic approaches still lack specificity for their intended site of action in the body, resulting in reduced effectiveness and severe side effects. The emerging field of nanomedicine provides a whole range of materials and techniques to develop customizable drug delivery vehicles that assist the targeting of therapeutic agents to the desired site of action. Amongst these, carbon nanotubes have emerged as promising candidates, being capable of penetrating mammalian cell membranes and allowing for the attachment of high loads of drugs and targeting agents on their surface or the inner cavity. This chapter will discuss the principles of targeted, anticancer chemotherapies and introduce carbon nanotubes as novel tools for vector-based, targeted drug delivery.

1 Introduction

Medicine in the twentieth century has mainly been driven by the quest for new active pharmaceutical agents. Drug companies started to synthesize constantly expanding collections of compounds by means of organic chemistry with subsequent screening for pharmacological activity. However, at the onset of the twenty-first century, an increasing part of pharmaceutical research focuses on the

E. Heister (☒), V. Neves, J. McFadden and H. M. Coley Faculty of Health and Medical Sciences, University of Surrey, Guildford, UK e-mail: e.heister@surrey.ac.uk

E. Heister, V. Neves and S. R. P. Silva Advanced Institute of Technology, University of Surrey, Guildford, UK

optimization of therapies already successfully used in the clinic, additionally to the discovery of new drugs. This comprises compound optimization, as well as optimization of administration, distribution, and selectivity of drugs, since interactions of materials with the human body not only depend on their effect on the molecular level, but also on physicochemical characteristics, such as particle size, shape, aggregation state, and surface properties. In this respect, nano-sized materials are becoming increasingly important. Their unique properties can enhance the performance of medicines by improving solubility and bioavailability, increasing in vivo stability, and minimizing side effects by acting as a targeting platform to guide therapeutic agents to the desired site of action.

Targeted, selective therapies are of particular importance in the field of oncology, since so many molecular features are shared by cancerous cells and healthy cells alike. Many different types of nano- or microscaled drug delivery systems are currently being developed, including quantum dots, silica nanoparticles, dendrimers, micelles, and liposomes. Amongst these, the carbon nanotube has emerged as a novel tool for the delivery of therapeutic molecules into cells. Carbon nanotubes are possibly one of the most striking discoveries in the quest for new materials in recent years, as they possess unique physical properties, such as tremendous strength, an extreme aspect ratio, and excellent thermal and electrical conductivity. Furthermore, their nanoscale dimensions enable them to bypass biological barriers, such as cell membranes, and their high surface area allows for the attachment of a whole spectrum of chemical and biological entities. The combination of these outstanding properties makes them promising candidates as a platform for the delivery of drugs.

This chapter will discuss the use of functionalised carbon nanotubes as a targeted drug delivery system in the setting of oncology.

2 A Brief Insight into Cancer: Pathophysiology and Problems of Conventional Cancer Therapies

Cancer is among the top three killers in modern society, next to heart disease and stroke. In 2009, more than 1,500 Americans died from cancer every day. Although much progress has been made in reducing mortality rates, stabilizing incidence rates, and improving survival, cancer still accounts for more deaths than heart disease in people under 85 years [1].

Cancer Pathophysiology

Cancer is the result of a process caused by multiple factors, which begins when one cell of an organ or tissue gets damaged or altered in a way that causes it to break free from its regulatory controls, resulting in uncontrolled growth, invasion of the surrounding tissue and metastasis (Fig. 1). This abnormal behaviour is the result of a series of mutations in key regulatory genes. The cells become progressively more abnormal, as more genes become damaged. Genetic abnormalities found in cancer typically affect two classes of genes: cancer promoting "oncogenes" and "tumor suppressor genes". The activation of oncogenes and/or the loss of tumor suppressor activity introduce malignant properties to healthy cells, e.g. limitless replicative potential, invasive growth and metastasis, insensitivity to antigrowth signals, self-sufficiency in growth signals and inhibited apoptosis. In case of solid tumors, the supply with oxygen and nutrients must be ensured. In order to expand, tumors encourage blood vessel growth, a process called "angiogenesis", which allows the tumor to grow beyond the limitations of passive nutrient diffusion and become connected to the bloodstream. Angiogenesis is induced by specific signals sent out by tumors, which cause nearby blood vessels to form new extensions to the tumor, delivering nutrients and oxygen. Importantly, the blood vessels also serve as a passageway for the movement of tumor cells to other parts of the body, thus preparing the ground for metastasis.

The exact causes of such mutations are still the subject of intense investigation. Several substances have been identified as "mutagens" (substances that cause DNA mutations) and "carcinogens" (mutagens that cause cancer) over the last 300 years. Prominent examples are tobacco smoke, which contains over 50 known carcinogens [2], or asbestos, a naturally occurring fibrous silicate mineral that has been widely used in a variety of building and household products, until it was found to cause an almost 100% lethal type of cancer called mesothelioma [3]. Apart from chemical carcinogens, a variety of other causes can be responsible for

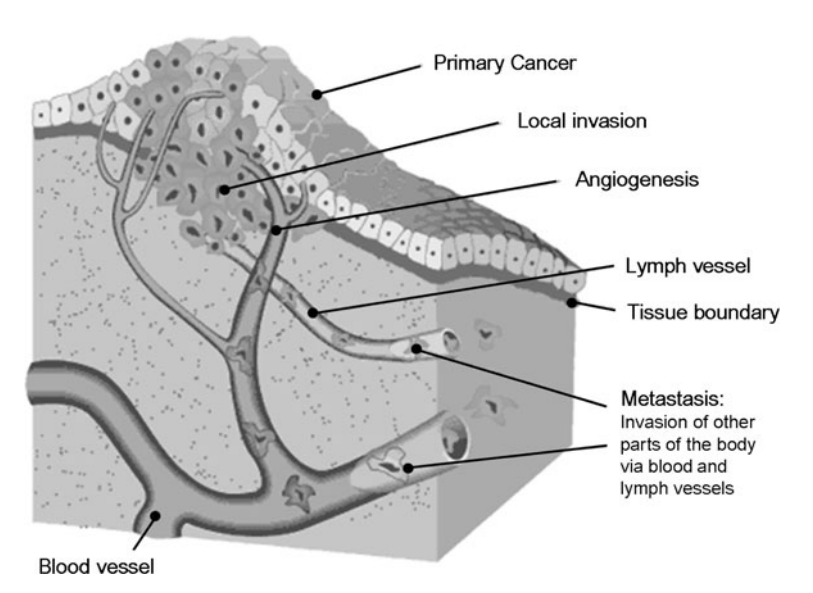


Fig. 1 Development and spread of cancer (adapted from the website of the Cancer Council New South Wales)

the induction of DNA damage, for example prolonged exposure to ultraviolet radiation from the sun or artificial sources [4], or viral and bacterial infections [5]. Furthermore, gene mutations may be passed down from a parent to a child and result in an increased cancer risk, which is known as "hereditary cancer syndrome" [6]. However, DNA damage and mutations may also occur without any known external cause.

Problems of Conventional Cancer Therapies

The major therapeutic approaches for the treatment of cancer are surgery, chemotherapy, radiation therapy, hormone therapy, and immune therapy. This rather wide range of treatment modalities already indicates that cancer is not a "simple" disease. In fact, cancer can be regarded as a multitude of independent disorders resulting in malignant cell growth. Even though all cancers have to overcome the same spectrum of regulatory controls in order to develop, the involved cell types and affected genes may differ, which results in a vast heterogeneity of more than a hundred different types. In the light of this overwhelming complexity, it becomes apparent why the development of a single cure or a so-called "magic bullet" has so far proven elusive.

In many cases, chemotherapeutic drugs exert their destructive effect on cells by damaging DNA, impairing mitosis or inhibiting some aspect of DNA synthesis. Although many available anticancer drugs have distinct mechanisms of actions, they lack specificity for cancerous cells. In fact, most of them simply "target" rapidly dividing cells, as cancer cells have largely been associated with unrestrained growth. However, fast-dividing cells can also be found in hair follicles, the bone marrow, the stomach, or the bowel lining, which explains some of the most common side effects of chemotherapies. Furthermore, this therapeutic approach is only effective for tumors with reasonably high growth fractions, such as some types of leukemia and aggressive lymphomas, and can induce resistance over time. For this reason, cancer chemotherapy may often comprise the use of drug combinations to increase effectiveness, for example of drugs targeting DNA in combination with drugs targeting microtubules.

3 A Brief Overview of "Classic" Anticancer Drugs

Anticancer drugs can be categorised according to their mechanism of action. Most of them affect cell division or DNA synthesis and function in some way, for example by damaging the DNA of the affected cancer cells (genotoxic drugs), by inhibiting the synthesis of new DNA strands to stop the cell from replicating (antimetabolites), or by inhibiting mitosis (spindle inhibitors). The first drug ever used for chemotherapy was originally developed for an entirely different purpose, namely as a chemical warfare agent during World War I. Since people exposed to

mustard gas were found to have very low white blood cell counts, it was reasoned that a similar effect might be achievable for cancerous cells, particularly those of the lymphocyte population, such as the high levels seen in lymphoma patients. Follow-up medical studies rapidly confirmed this assumption and soon, the nitrogen mustards became the prototype for a whole class of chemotherapeutic drugs: the alkylating agents.

Alkylating agents belong to the class of genotoxic drugs, which stop tumor growth by cross-linking guanine bases of DNA strands, thus preventing the strands to uncoil and separate in the process of cell division. Commonly used alkylating agents are nitrogen mustard derivatives (cyclophosphamide, chlorambucil), and platinum-based drugs (cisplatin, carboplatin, and oxaliplatin). Another type of genotoxic drugs inhibit key enzymes—the topoisomerases—which are involved in DNA replication by cutting and reconnecting DNA strands. Drugs like irinotecan or etoposide inhibit either class I or II of the topoisomerases and thus cause DNA damage. Antimetabolites, another class of chemotherapeutic agents, also interfere with DNA synthesis, but in a different way. Molecules belonging to this group possess similar structures to the building blocks of DNA—adenine, guanine, thymine, and cytosine—but are yet different enough to prevent their incorporation into DNA strands. As a result, the treated cells are unable to synthesize new DNA strands and are hence unable to divide and grow. Examples for antimetabolite chemotherapeutic drugs are 6-mercaptopurine, 5-fluorouracil, and gemcitabin. An entirely different mechanism of action to prevent cells from dividing is observed for the so-called spindle poisons. Mitotic spindles are part of the cytoskeleton in eukaryotic cells and help to separate the chromosomes into the daughter cells during cell division. Spindle poisons, such as the vinca alkaloids (vincristine, vinblastine) and the taxanes (paclitaxel, docetaxel) disrupt the formation of these spindles by interacting with their subunits—the microtubules—and therefore interrupt cell division.

Apart from these three main groups, many other chemotherapeutic agents exist, whose mechanisms of action do not neatly fit into one of these categories. The "anthracyclines", which are among the most important antitumor drugs available, are one such example. Their exact mechanism of action is complex: they are known to interact with DNA by intercalation and inhibition of topoisomerase II and further cause free-radical generation, chromosome damage, mitochondrial effects and membrane effects [7]. A prominent representative of this category is doxorubicin, which is widely used for the treatment of several solid tumors, and daunorubicin and idarubicin, which are used exclusively for the treatment of leukemia.

A characteristic attribute of all mentioned chemotherapeutic drugs mentioned is their inherent toxicity, leading to common side effects, such as nausea, bone marrow toxicity, hair loss, loss of appetite, and tiredness. However, some drugs can also cause much more severe side effects in some individuals, such as cardiotoxicity (doxorubicin), nephrotoxicity (platinum-based drugs), ototoxicity (platinum-based drugs, vincristine), or hepatotoxicity (cyclophosphamide, methotrexate, 6-mercaptopurine). Thus, the challenge for oncology in the twenty-first

century is to design targeted therapies, which aim at delivering the drugs directly to the target location and thereby not only allow for the application of smaller drug doses by increasing therapeutic effectiveness, but also minimise the damage to non-cancerous cells and its associated side effects.

4 Drug Targeting: As Crucial as the Drug Itself

As discussed in the previous sections, most cancer treatments suffer from a lack of effectiveness due to insufficient selectivity for their target. In this context, different types of targeting strategies are currently under investigation. Principally, oncological targeting strategies can be divided into three categories (Fig. 2): molecular targeting, active targeting, and passive targeting. The following subsections will discuss these three categories with a particular focus on drug delivery systems. This will set the stage for the final subsection, which will present carbon nanotubes as a platform for targeted drug delivery.

Molecular Targeting Strategies

Molecular targeting strategies comprise drugs and other therapeutic agents, which block the growth and spread of cancer by interfering with specific molecules or proximal events in signaling transduction cascades involved in tumor growth and progression [7]. This includes drugs interfering with cell growth signaling (signal transduction inhibitors), tumor blood vessel development (angiogenesis inhibitors), promoting the specific death of cancer cells (apoptosis inducers), or stimulating the immune system to destroy cancer cells (immune system modulators). Examples for FDA approved molecular targeted drugs are the so-called "tyrosine kinase inhibitors", which interfere with tyrosine kinase-dependent cellular signaling pathways involved in tumor development and progression, such as imatinib (Gleevec®) or dasatinib (Sprycel®). The first therapeutic monoclonal antibody that gained FDA approval for human use is trastuzumab (Herceptin®). It binds to the human epidermal growth factor receptor 2 (HER-2), which is expressed at high levels in some breast cancers, and possibly prevents it from sending growth-promoting signals.

Although molecular targeting can be extremely effective in individual patients (namely those who possess the target for the drug in question), and furthermore causes relatively low toxicity, response rates in the general patient population for a particular cancer are often as low as 10–20% due to the high complexity of the disease and genetic variation. In comparison, conventional, "old-style" anticancer drugs, which often target the downstream consequences of activated signaling pathways, exhibit a rather broad efficacy, but are highly toxic due to their lack of specificity [8].

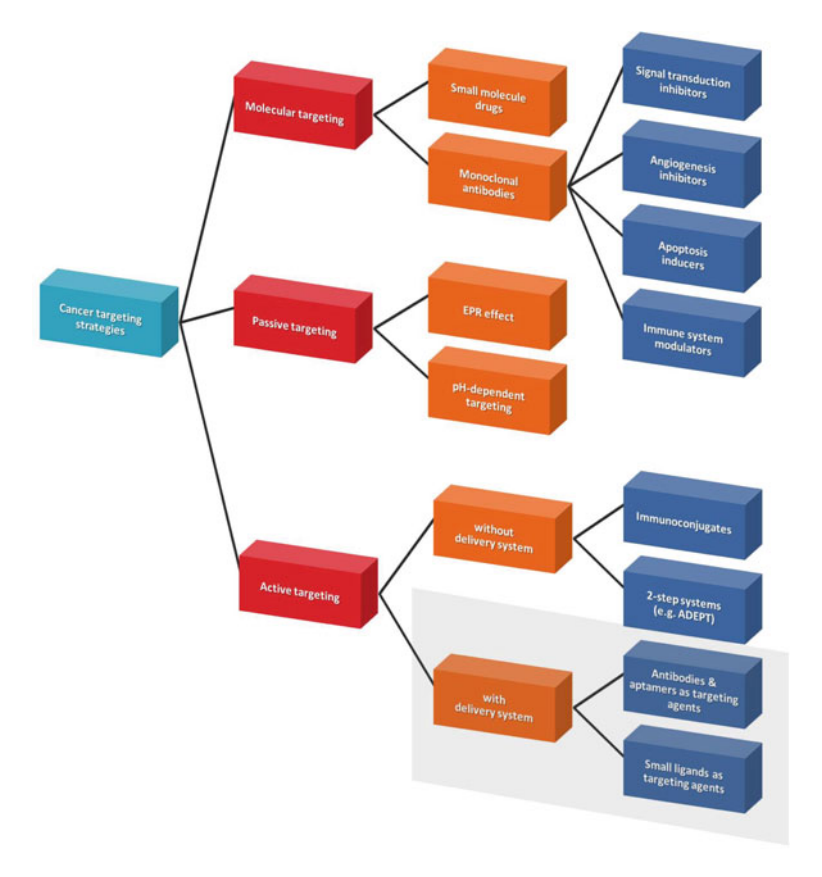


Fig. 2 Schematic overview of cancer targeting strategies

Active Targeting Strategies

Active targeting strategies usually involve the conjugation of a therapeutic agent to a recognition moiety. This may increase the effective drug concentration at the target area [9], which allows for lowering the dose of the drug and hence may prevent associated toxicities, especially in chronic treatments. Targeting agents can either be conjugated directly to anti-cancer drugs, rendering the so-called "immunoconjugates", or by attaching both entities to a nanocarrier.

5 Types of Targeting Agents

The characteristics of the targeting moiety are very important for circulation time, cell uptake, and elimination. The most intensively studied targeting agents, at least from a historical perspective, are monoclonal antibodies and Fab fragments

(protein structures containing only the variable region of an antibody). Both recognize specific surface structures, so called "antigens", which are overexpressed on tumors or cancerous cells. Ideally, antigenic targets for monoclonal antibodies should be expressed on malignant cells only, be present in abundance on the cell surface, and should not be shed into the blood circulation or the surrounding interstitium. Examples for tissue-specific cell surface markers are the proteins CD20, CD33, CD52 and other representatives of this class, which are found on B cells, leukemic blasts, and T- and B-lymphocytes and are already used in FDAapproved drug- and radioimmunoconjugates, as described in the last section. Furthermore, growth factor receptors, such as HER2/neu and the epidermal growth factor receptor have emerged as good targets for antibody-targeted therapies. Another example for an antigen of clinical importance is carcinoembryonic antigen (CEA), a peripheral membrane protein overexpressed by colorectal carcinomas and also a number of lung, breast, ovary, and pancreas carcinomas [12, 13]. As it is often released into the circulation by these tumours to cause elevated serum concentrations, it has gained great importance as a diagnostic tumor marker, although this fact is rather disadvantageous for the use of CEA as a therapeutical target.

Overall, monoclonal antibodies are quite effective targeting agents—however, they are associated with several innate problems, such as insufficient tumour penetration, circulating free antigen, binding to non-specific Fc receptors changes in the antigen over time, and interaction with the immune system [10, 11]. Besides, the conjugation method has a great influence on antibody affinity: when carried out in a random way, for example by creating stable amide bonds between carboxylic acid groups of the nanocarrier or drug and primary amine groups of the antibody or Fab fragment, the binding site of the antibody can become blocked [12]. It is thus advantageous to employ a conjugation method, which allows for attaching the antibody in a correctly oriented manner—for example by the use of Protein A, which binds to the Fc fragment of antibodies.

To overcome these bottlenecks of antibody-targeting, many researchers started to investigate other active targeting strategies. A rather novel approach is the use of aptamers, which are synthetic, single-stranded nucleic acid molecules able to fold up into unique 3D structures, which gives them molecular recognition properties similar to antibodies. Aptamers offer the advantage to be readily produced by chemical synthesis and eliciting little or no immunogenicity in therapeutic applications. Furthermore, they can be produced for a variety of targets, ranging from small molecules over amino acids and peptides to proteins, and usually retain their binding properties even after immobilization on a carrier material [13]. However, RNA-based aptamers are particularly prone to hydrolytic breakdown by cytoplasmic nucleases and are generally rapidly eliminated from the human body by renal clearance [14]. These problems may be overcome by modifications of the molecules, such as methylation of the bases, end cap modifications, or conjugation of PEG or cholesterol as anchor groups [15, 16]. Nevertheless, the use of aptamers as targeting agents is still at an early stage and their future role in drug delivery applications remains to be seen.

Another type of active targeting is based on ligand-receptor interactions. An example from the anti-angiogenetic area is the targeting of integrins $\alpha_v \beta_3$, which are endothelial cell receptors for extracellular matrix proteins possessing the RGD sequence (arginine-glycine-aspartic acid) and are highly expressed on neovascular endothelial cells [17, 18]. Conjugation of RGD peptides to nanovectors can lead to higher levels of cellular internalization and furthermore affect vascular endothelial growth factor receptor-2 (VEGFR-2) signaling due to an intrinsic association with this signaling pathway [19], leading to downregulation of the receptor and finally to reduced angiogenesis. Another example for active targeting based on ligandreceptor interactions relevant to the area of cancer therapeutics is the interaction of folate with its receptor [20, 21]. Folic acid is a vitamin and necessary for the synthesis of nucleotides, the DNA building blocks. Its counterpart, the folate receptor, is significantly upregulated by a broad spectrum of human cancers, in some cases by two orders of magnitude, facilitating cellular internalization of folate-conjugated nanovectors by receptor-mediated endocytosis [22, 23]. Normal cells, however, will only transport folate via this receptor, but not folate conjugates of any type [10], which adds an extra level of specificity. The folate targeting approach has been widely employed in the last decade using various types of vectors, and remains very promising for future applications. Especially for chemotherapy, folate-conjugated nanovectors loaded with anticancer drugs have shown huge potential in overcoming the problem of multi-drug resistance by evading P-glycoprotein-mediated efflux, which is considered to be a common problem in cancer drug administration [24, 25].

6 Immunoconjugates

Immunoconjugates are antibodies conjugated to a second molecule, which can be a toxin, radioisotope or label. In 2000, the first antibody-drug immunoconjugate (Mylotarg®) was approved by the FDA for the treatment of some patients with acute myeloic leukemia. It consists of the monoclonal antibody gemtuzumab, which is targeted at the cell surface protein CD33 present on the surface of leukemic blast cells, and the drug ozogamicin, which prevents DNA synthesis. Once the complex binds to CD33, the receptor-antibody conjugate is internalized and the drug released by hydrolysis. So far, Mylotarg® remains the only FDA approved antibody-drug immunoconjugate—however, two radiolabeled antibodies targeting the CD20 cell surface protein overexpressed by certain types of B-cell non-Hodgkin lymphoma, Bexxar® and Zevalin®, have also made their way into the market.

Besides conventional immunoconjugates, so-called "pretargeting strategies" are currently the focus of intense investigation. In this approach, antibody-based targeting and delivery/generation of the toxic agent is separated into two steps [26]. The most prominent example is ADEPT, or "antibody-directed enzyme prodrug therapy", in which target selectivity is achieved by an antibody in an

antibody-enzyme conjugate binding to antigens preferentially expressed on the surface of tumor cells or the tumor interstitium. In the first step, this complex is administered and accumulates at the target site. In the second step, a non-toxic prodrug is injected, which is converted into a cytotoxic drug in situ by the enzyme in the conjugate at the tumor [27]. A major advantage of ADEPT is the amplification effect, as one molecule of enzyme catalyses the conversion of many prodrugs into their cytotoxic form. This leads to higher drug concentrations at the tumor site compared to direct injection of the drug alone. Furthermore, a broad array of prodrugs can be used for site-specific activation, especially those exhibiting high toxicity.

Overall, therapies employing immunoconjugates have evolved a great deal over the past few years. Although several challenges still lie ahead, advances in protein engineering are likely to permit a greater control of antibody-based targeting, clearance and pharmacokinetics for the next generation of immunoconjugates, which will result in significantly improved delivery to tumors [26].

7 Drug Delivery Systems Featuring Active Targeting Agents

Another option for improving the clinical efficacy of active targeted drugs lies in the use of a drug delivery system. Many nano-sized carriers have been developed for this purpose in the last decades, as their small size enables them to pass through narrow capillaries and endothelial spaces. Furthermore, they possess high adaptability, allowing for the loading of various types of therapeutic agents and targeting moieties. Typically, a nanocarrier designed for targeted drug delivery consists of a core constituent material, a therapeutic payload, and a targeting agent [28]. This multifunctional concept allows for the delivery of large amounts of therapeutic agents per targeted site of action, which is a major clinical improvement over simple immuno-targeted drugs. So far, a plethora of materials has been investigated as vectors for drug delivery applications, including nanoparticles, nanocapsules, nanotubes, dendrimers, liposomes, and many more. Figure 3 shows an example for a drug delivery system, which was developed in our own lab. Therein, carbon nanotubes serve as a delivery platform, anti-CEA antibodies as targeting agents, and doxorubicin as an anticancer drug.

Passive Targeting Strategies

Besides active targeting, drug delivery systems also allow for passive targeting strategies, which often relying on mechanisms based on the size and physical properties of the nanocarriers or involve cleavable bonds. These are mostly based on the so-called "enhanced permeation and retention (EPR) effect", which originates from the leaky vasculature of tumor-associated, newly created blood

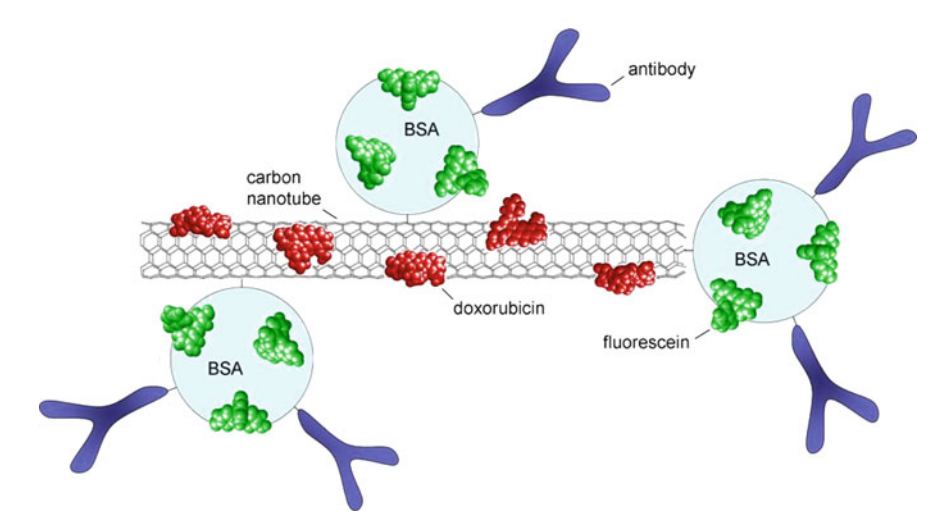


Fig. 3 Example for a vector-based drug delivery system developed in our own lab, featuring a carbon nanotube as the delivery vector, doxorubicin as therapeutic agent and monoclonal anti-CEA antibodies as targeting moiety. Adapted from [29]

vessels, and the lack of effective lymphatic drainage in tumor tissues [30]. Both effects contribute to tumor interstitial drug accumulation, and are widely exploited by vector-based drug delivery systems. The earliest one was approved by the FDA over 10 years ago for the treatment of Kaposi's sarcoma and comprises a liposome-encapsulated, pegylated formulation of the anthracycline anticancer drug doxorubicin (Doxil®/Caelyx®) [31]. Since then, three more products have reached the market: a pegylated, liposomal formulation of daunorubicin (DaunoXome[®]), a non-pegylated, liposomal preparation of doxorubicin (Myocet®) and a product featuring the anticancer drug paclitaxel bound to albumin nanoparticles (Abraxane®). The latter is a major improvement compared to traditional paclitaxel formulations in terms of toxicity: since paclitaxel is very hydrophobic and hence poorly bioavailable, it has usually been formulated with the pharmaceutic excipient Cremophor-EL, which is known to cause severe hypersensitivity reactions and toxic tissue side effects. Albumin, however, is the major protein in human blood and hence much more biocompatible than Cremophor-EL, thus allowing for the delivery of higher drug doses at lower toxicity.

Another passive targeting approach applied by vector-based drug delivery systems exploits distinctive features of the tumor microenvironment to achieve drug accumulation at the target site. For example, solid tumors often exhibit a lower extracellular pH than the surrounding tissues due to lactic acid produced by hypoxic cells [32], whereas the intracellular pH is essentially identical or slightly more basic in tumors than in normal tissue. As a consequence, the cellular pH gradient is substantially reduced or reversed in these tissues; a fact that has been exploited by various studies for drug delivery applications. One such example is the work of Ko et al. [33], who developed pH-responsive and biodegradable

polymeric micelles loaded with doxorubicin as a tumor-targeting drug delivery system, showing noticeable pH-dependent micellization—demicellization behaviour with rapid release of the drug doxorubicin from the micelles in weakly acidic environments, but very slow release under physiological conditions.

In summary, the greatest gain in therapeutic selectivity is most likely to be achieved by synergistic combinations of active and passive targeting strategies. In this respect, vector-based targeting strategies offer a great advantage, being capable of combining the EPR effect as a passive targeting strategy with active targeting by means of conjugated targeting agents. The next section will discuss drug delivery systems employing carbon nanotubes as delivery vectors and give an overview of the literature to date.

8 Carbon Nanotubes as a Platform for Targeted Drug Delivery

In the last 5 years, carbon nanotubes have emerged as a new type of targeted drug delivery system, especially in the field of oncology. Both their surface and their inner cavity allow for loading with drugs and other therapeutic and diagnostic entities, such as targeting or imaging agents. Furthermore, carbon nanotubes are capable of penetrating mammalian cell membranes and have been demonstrated to shuttle a broad spectrum of molecules into mammalian cells, including peptides [34], proteins [35], genes [36, 37], and drugs [37, 38]. Interestingly, the uptake mechanism of carbon nanotubes and carbon nanotube conjugates is still under discussion and seems to depend on the physicochemical properties of the nanotubes, as well as on the type of functionalization. Some researchers have described the internalization process as passive and endocytosis-independent, suggesting a mechanism in which the nanotubes act as "needles" with a piercing mode of entry through the cell membrane [34], whereas other groups have reported a clathrindependent, endocytotic uptake pathway [38]. For a more complete discussion on the uptake mechanism and intracellular distribution of carbon nanotubes, please refer to Chap. 9.

Functionalisation of Carbon Nanotubes with Anticancer Agents

In terms of functionalization, many different methods have been developed, according to the therapeutic requirements. Surface functionalisation techniques of carbon nanotubes can be divided into covalent and non-covalent methods; each of them possessing advantages and drawbacks. Covalent conjugation methods, for example, guarantee strong and stable chemical bonds. This is useful when the bound molecule is supposed to stay attached to the vector in all

conditions; molecules that are to be released at a later stage, however, need to be conjugated via a bond that is cleavable at the target site. One such example is the disulfide bond, which is readily cleaved into sulfhydryl groups by the reductive environment in the cytoplasm, as has been demonstrated by Chen et al. and Kam et al. for the attachment of a taxane anticancer drug [39] and siRNA [40] to carbon nanotubes. Another option are hydrazone bonds, which are cleavable in mildly acidic conditions, such as the interior of lysosomes. This method has been employed by Lai et al. to attach the anticancer drug doxorubicin to PAMAM dendrimers [47] and by Prabaharan et al. to attach the same drug to polymer-coated gold nanoparticles [41], both in the scope of drug delivery.

Non-covalent conjugation methods, on the other hand, result in less stable bonds that are mostly based on electrostatic interactions, van der Waals forces or π -stacking interactions between molecules. The bonds are susceptible to environmental factors, such as pH and salt concentration, which can be disadvantageous for in vivo applications, bearing in mind the different conditions an intravenously applied vector-based drug delivery system has to encounter before reaching its target location. On the other hand, it can be advantageous for the release of the drug at the target location; a fact that has been utilized by various groups, including ours, for the delivery of the anticancer drug doxorubicin [28, 43, 44]. Doxorubicin binds to the surface of carbon nanotubes via π - π interactions in a pH-dependent manner. At a high pH, the amino group in the sugar moiety of the molecule is deprotonated/uncharged, promoting strong hydrophobic interactions with the nanotubes' sidewalls and poor aqueous solubility. At a lower pH, however, the amino groups become protonated and charged, which increases the molecule's hydrophilicity and solubility in water. This property can be applied for vector-based drug delivery systems that are taken up by cells via an endocytotic pathway: the slightly acidic pH inside lysosomes will trigger the release of the drug from the nanotubes according to the mechanism described above.

A different approach to the functionalisation of carbon nanotubes with drugs is the filling of the inner cavity, which allows for the protection of unstable drugs and controlled drug release at the desired site of action in dependence of the tube diameter. However, although carbon nanotubes have already been filled successfully with a variety of molecules, including fullerenes, metals, DNA/RNA or polymeric nanoparticles [42, 45], filling of nanotubes with therapeutic agents is an approach still in its infancy. Hilder and co-workers have carried out a great deal of theoretical work on the filling of carbon nanotubes with drugs. In their first article on this subject, they looked at the suction behaviour of cisplatin, a widely-used, platinum-based anticancer drug, and concluded that a carbon nanotube should have a diameter of about 1 nm to entrap cisplatin and take advantage of the maximum suction energy [46]. In another publication, they investigated the encapsulation of paclitaxel and doxorubicin, two anticancer drugs with more complicated molecular structures [47]. In these cases, the highest probability of achieving both encapsulation and maximum uptake (or suction energy) occurs in the diameter range of about 1.83-2.54 nm for paclitaxel and 1.77-2.10 nm for doxorubicin.

Drug Delivery Studies

This subsection will present a review of all studies to date that have employed carbon nanotubes as a vector for targeted drug delivery; starting from early, non-targeted in vitro approaches to targeted in vivo studies with a special focus on the applied targeting strategy.

In Vitro Studies

The first study on in vitro drug delivery with carbon nanotubes was carried out by Wu et al. [48]. They conjugated the antibiotic drug amphoteric B to multi-walled carbon nanotubes; a drug considered problematic due to its poor aqueous solubility and narrow therapeutic index. These problems could be resolved by delivering the drug via a carbon nanotube vector, which lead to reduced toxicity towards cells, whilst preserving the drug's antifungal activity [48]. One year later, the same group reported the delivery of the first anticancer drug to human T lymphocytes. The drug, methotrexate, is widely used in chemotherapies, but suffers from poor cellular uptake and induction of drug resistance in cancer cells. Its internalization could be facilitated through conjugation to multi-walled carbon nanotubes, although its antitumor activity was not evaluated. In both studies, the drugs were attached covalently to the nanotubes. One of the first studies employing noncovalent attachment was carried out by Ali-Boucetta and co-workers, who attached the anticancer drug doxorubicin to multi-walled carbon nanotubes via π - π -interactions, as described in the last subsection. A simplified viability assay with human breast cancer cells demonstrated that doxorubicin-nanotube conjugates exhibited significantly enhanced cytotoxicity compared to the drug alone, indicating that nanotubes are a feasible option for mediating the delivery of drugs into cells and enhancing their therapeutic efficiency [49].

These studies have provided a solid foundation for future drug delivery studies—however, the aspect of targeting had not been considered, yet. The first step in this direction was undertaken by Feazell and co-workers, who conjugated a platinum(IV) prodrug to single-walled carbon nanotubes via a cleavable disulfide bond [50]. The use of a prodrug allows avoidance of many pathways in the body that are known to deactivate platinum(II)-based anticancer drugs. In a cytotoxicity test, a testicular carcinoma cell line was treated with the free platinum(IV) prodrug and the nanotube-conjugate to compare therapeutic effectiveness. Whilst the platinum(IV) prodrug did not have a significant effect on cell viability, the prodrugnanotube conjugate showed a substantial increase in cytotoxicity and surpassed that of cisplatin alone, a widely used platinum(II) anticancer drug, when compared on a per platinum basis.

Compared to the passive and simple targeting approach in that study, a subsequent study by Liu et al. [51] applied a much more advanced targeting approach.

They dispersed pristine, single-walled carbon nanotubes via an amine-terminated, phospholipid-PEG-based surfactant and loaded them with doxorubicin in the same way as described before. Next, they attached a cyclic RGD peptide to the amine groups of the surfactant as a ligand to integrin $\alpha_v \beta_3$ receptors, which are upregulated in a wide range of solid tumours. Cell viability testing using integrin $\alpha_{\rm v}\beta_{\rm 3}$ -positive U87MG human glioblastoma cancer cells revealed that free doxorubicin exerted the highest cytotoxicity with an IC₅₀ of about 2 µM, followed by the targeted nanotube-drug conjugates with an IC₅₀ of about 3 μM doxorubicin and finally the untargeted nanotube-drug conjugates with an IC₅₀ of about 8 µM (Fig. 4). This demonstrated that targeting of integrin receptors via an RGD peptide is a valid and promising method in an in vitro setting. Although the free drug was more effective than the conjugates, this is a result to be expected in in vitro assays, as there are no real barriers for membrane-permeable drugs. In an in vivo setup, however, drugs are subjected to many different environments and influences before reaching their target, and in this scenario, their attachment and delivery by a vector might be of significant advantage.

Another active targeting approach has been pursued by Chen and co-workers, who conjugated a taxane prodrug to single-walled carbon nanotubes via a cleavable disulfide linker, which releases the drug upon internalization and converts it into its activated form [39]. Additionally, they attached the vitamin biotin to serve as a targeting agent. This idea is based on a study of Russell-Jones et al. [23], who reported that biotin receptors are overexpressed on a wide range of tumor types and could thus serve as a new tumor-specific target, in a manner similar to the widely recognized folate receptors. An MTT cytotoxicity assay revealed that the targeted nanotube-drug conjugates were superior in cytotoxicity than the drug itself in L1210 leukemia cells. Another study by Dhar et al. [50] followed up the work of Feazell et al. [50], which was published a year earlier and described the

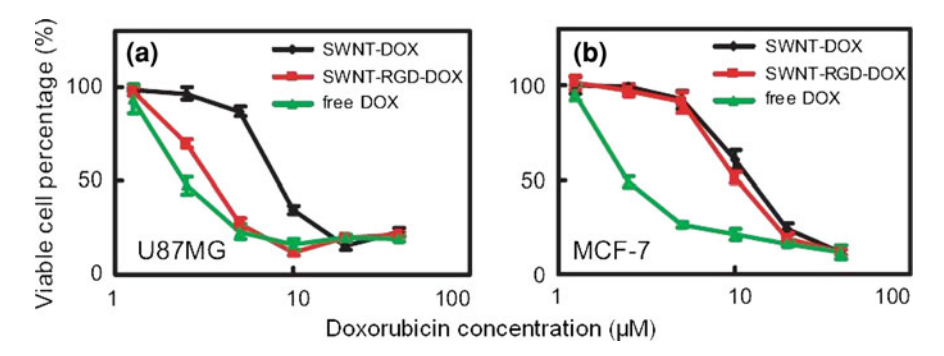


Fig. 4 Concentration-dependent survival curves of U87MG integrin $\alpha_v \beta_3$ positive cells (**a**) and MCF-7 integrin $\alpha_v \beta_3$ negative cells (**b**) treated with the various samples as indicated. The drugnanotube conjugates had a lower toxic effect than the free drug on both types of cells, while the targeted nanotube-drug conjugates exhibited increased toxicity to U87MG cells but not to MCF-7 cells, showing that RGD peptides selectively enhance doxorubicin delivery by SWNTs and toxicity to integrin $\alpha_v \beta_3$ positive cells. Adapted from [51]

delivery of a platinum(IV) prodrug by carbon nanotubes, albeit without a targeting strategy. Their next study, however, included the conjugation of folic acid to the nanotube-drug complexes as a targeting ligand for folate receptors [52]. As described earlier in this chapter, this targeting strategy is based on the fact that folate receptors are significantly upregulated by a broad spectrum of human cancers, thus facilitating cellular internalization of folate-conjugated nanovectors by receptor-mediated endocytosis. Indeed, the cytotoxicity of the targeted nanotube-drug conjugates was enhanced by a factor of 6.8 compared to complexes consisting of the drug and the targeting agent only.

Three more in vitro studies will be discussed in the framework of this subsection, before moving on to the more significant in vivo studies that have been carried out with carbon nanotube-based drug delivery systems so far. The first one carried out by Hampel et al. [53] has embarked on a very different strategy in terms of drug loading. Therein, the anticancer drug carboplatin was filled into multi-walled carbon nanotubes by a wet chemical approach (Fig. 5) [53]. In vitro studies revealed that the carboplatin-filled nanotubes exerted a concentration-dependent cytotoxic effect on human bladder cancer cells, whereas unfilled nanotubes did not affect cell viability in a significant manner.

The second study published by Ou et al. [54] focuses on the targeting aspect without delivering a drug. The applied targeting approach is again based on integrin $\alpha_{\rm v}\beta_3$ receptors—however, the researchers argue that RGD peptides, although commonly used as targeting ligands for integrin receptors, have a relatively low specificity due to their universal targeting ability to other integrins. Furthermore, they state that some RGD peptides are prone to degrade rapidly in vivo and have therefore decided to use a monoclonal antibody to integrin $\alpha_{\rm v}\beta_3$ receptors instead. The antibody was attached to carbon nanotubes via protein A. This is an elegant approach, since it ensures site-specific binding of the antibody, in contrast to random conjugation via EDC/NHS chemistry. Protein A (found in

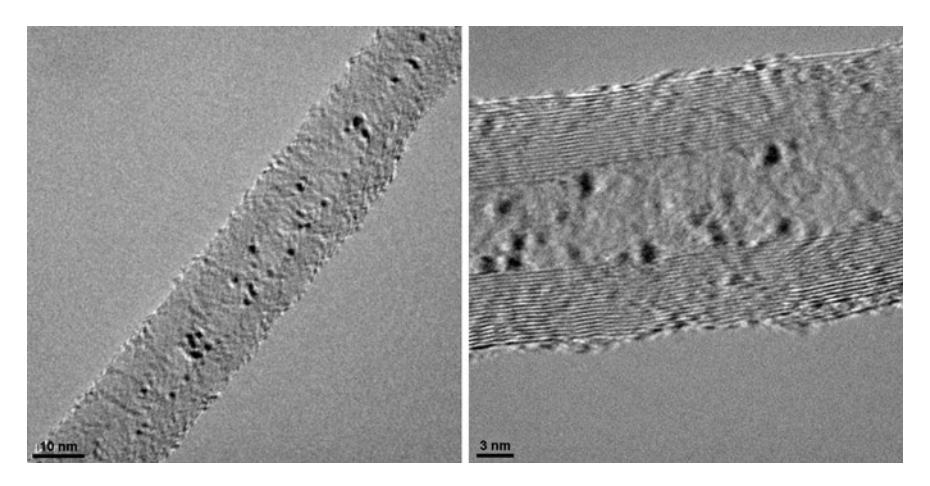


Fig. 5 Multi-walled carbon nanotube filled with carboplatin clusters. Courtesy of IFW Dresden

the cell wall of bacteria, and able to bind to the Fc region of immunoglobulins) was used as a linker between the nanotubes and the antibody ensuring correct orientation without blocking its binding site.

The last study to be discussed in this subsection is by Zhang and co-workers [55]. It has not only included a viable targeting option in the form of the folate system, but also taken a step forward towards controlled drug release. Two polysaccharides were chosen to wrap the surface of oxidised, single-walled carbon nanotubes: the cationic chitosan and the anionic alginate. Using them either on their own or in combination for nanotube functionalization allowed for manipulating the surface potential of the modified nanotubes, which not only controls efficient loading of the tubes with the selected, positively charged anticancer drug doxorubicin, but also the release rate of the associated drug inside cells. In fact, the drug delivery system displayed excellent stability under physiological conditions whilst efficiently releasing the drug at reduced pH (typical of the tumour environment or intracellular lysosomes) and inducing cell death.

In Vivo Studies

Following up the promising achievements of the in vitro studies discussed in the last subsection, researchers have more recently focused on in vivo settings. So far, five notable in vivo studies have been carried out using carbon nanotubes as a delivery vector for therapeutic agents; thereof four anticancer drugs and one radionuclide.

In the first study, McDevitt et al. [56] designed a SWNT-CD20 antibody construct to deliver a radionuclide to mice bearing lymphoma xenografts. Apart from the targeting aspect and quantification of tumor uptake, this study was one of the first to yield results about blood clearance and the distribution of the nanotube complexes to key organs. The anti-CD20 antibody employed, also known as "rituximab", has obtained FDA approval in 1997 as a therapeutic antibody for the treatment of B-cell non-Hodgkin lymphoma resistant to other chemotherapy regimens [57]. The study showed that covalent attachment of antibodies to the nanotube-radionuclide conjugates dramatically altered biodistribution and pharmacokinetics when comparing tumor-bearing and non-tumor-bearing mice, indicating that the targeting effect was antibody-mediated and not a result of the CNT portion of the construct.

In 2008, Liu and co-workers conducted the first successful study that demonstrated efficient in vivo tumor treatment in mice using carbon nanotubes as drug delivery vectors [58]. The microtubule binding anticancer drug paclitaxel was conjugated to branched polyethylene glycol chains on single-walled carbon nanotubes via a cleavable ester bond. These conjugates afforded much longer blood circulation times than paclitaxel alone or PEGylated paclitaxel and lead to a 10-fold higher tumor uptake, most likely mediated through the EPR effect. Additionally, they afforded similar therapeutic efficacy to paclitaxel alone in in

vitro experiments and a higher efficacy in suppressing tumor growth in the murine 4T1 breast cancer model. Future work is planned to enhance treatment efficacy by conjugating targeting ligands to their complexes, which would combine a passive and an active targeting strategy in a synergistic fashion.

In the same year, Villa et al. [59] designed a construct of single-walled carbon nanotubes functionalized with single-stranded oligonucleotides, radiotracing moieties and an RGD peptide as targeting moiety—although not for drug targeting purposes, but as a prototype for targetable nanotube platforms capable of hybridizing cDNA addresses. Nevertheless, their in vivo experiments rendered useful information in terms of the biodistribution behaviour of the complexes, showing that the radiolabeled SWNT-oligonucleotides were rapidly cleared from the blood circulation with significant retention in kidney, liver, and spleen only.

Shortly afterwards, Bhirde and colleagues published the first study demonstrating in vivo drug delivery by an active targeting approach [58]. They functionalized SWNTs with the first-line anticancer drug cisplatin, epidermal growth factor (EGF) as a targeting agent, and quantum dots for imaging purposes by covalent coupling chemistry (Fig. 6). The targeting approach was designed for head and neck squamous carcinoma and is based on the fact that many squamous cancer cells overexpress the EGFR (epidermal growth factor receptor). Preliminary in vitro studies showed that SWNT-cisplatin-EGF dispersions with 1.3 μM cisplatin were more cytotoxic than 10 μM free cisplatin. In the follow-up in vivo study, nude mice bearing tumour xenografts were injected with the nanotube-bioconjugates and tumour growth was monitored for 2 weeks. Mice treated with a non-targeted nanotube-cisplatin conjugate did not show tumor regression, whereas mice treated with the targeted conjugates showed a rapid decrease in tumor size.

One of the most recent studies published on in vivo drug delivery with carbon nanotubes was reported by Wu et al. [61]. They attached the anticancer agent 10-hydroxycamptothecin (HCPT) to multi-walled carbon nanotubes via the linker

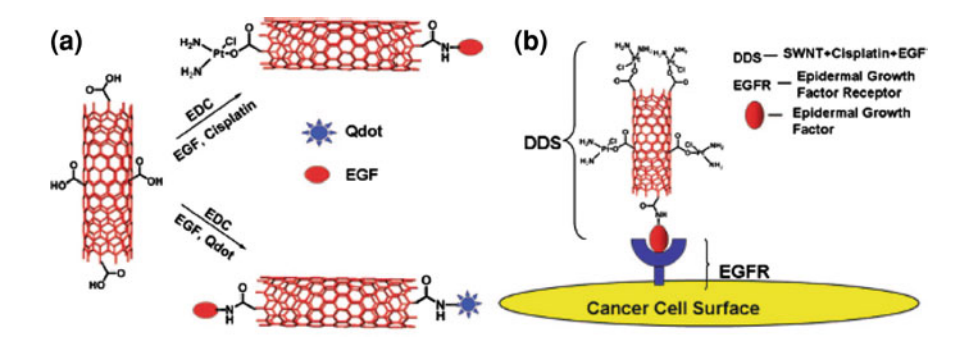
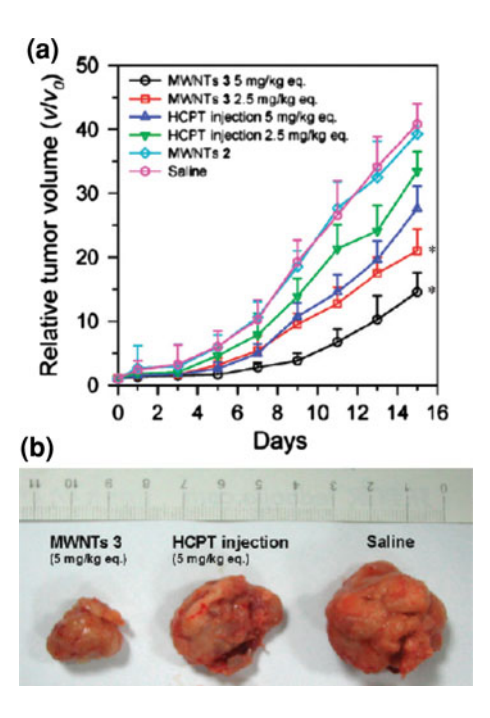


Fig. 6 Drug delivery system by Bhirde et al. **a** Illustration of chemical reactions used to attach EGF, cisplatin, and quantum dots to carboxylated SWNTs (*red*) using EDC as the coupling agent. **b** Schematic showing SWNT bundles bioconjugated with EGF and cisplatin targeting the cell surface receptor EGFR on a single head and neck squamous carcinoma cell. Adapted from [60]

Fig. 7 a In vivo drug delivery study by Wu et al [61]. The antitumor effect of the anticancer drug HCPT and HCTPcarbon nanotube conjugates (MWNTs 3), expressed as the average values of the relative tumor volume v/v0 (where v denotes the tumor volume at test time points and v_0 denotes the corresponding initial tumor volume at the beginning of treatment). *P < 0.05 (vs. HCPT injection group at the equivalent dose from the 5th day). MWNTs 2 represent amino-functionalized MWNTs, serving as a control. **b** Typical photographs of excised sarcomas from mice on the 16th day after treatments with MWNTs 3 (5 mg/ kg equiv), HCPT injection (5 mg/kg equiv), and saline



diaminotriethylene glycol, which is basically a bifunctional PEG molecule with an extremely short chain length of 3. The approach is based on the fact that even though PEGylation is viewed as a useful method to avoid uptake by the reticuloendothelial system and prolong blood circulation, it has been reported to block the interactions between nanotubes and cells [62]. Hence, the group compromised on these drawbacks by choosing a PEG spacer with a very low molecular weight, which was attached to the tubes via a biocleavable ester linkage. The treatment of mice bearing hepatic H22 tumors revealed that the nanotube-drug complexes inhibited tumor growth much more efficiently than HCPT injection alone (Fig. 7). This is due to enhancement of the drug's bioavailability, prolonged blood circulation owing to the use of carbon nanotube vectors, enhanced cellular uptake, and concentrated drug action due to multivalent presentation of the drug molecules on a single nanotube. Note that this study did not include a targeting strategy.

9 Conclusion

The promising results of the in vivo studies presented in the last subsection represent a milestone in the development of carbon nanotubes as therapeutic agents in the clinical setting. Carbon nanotubes offer several advantages over other nanovectors: their high surface area enables higher drug loading on the surface

compared to conventional, spherically shaped vectors, thus reducing the amount of excipient needed for therapeutic formulations. Furthermore, carbon nanotubes that are taken up by cells via a passive, endocytosis-independent mechanism allow for cytoplasmic delivery of drugs whilst avoiding the degradative lysosomal pathway. Finally, the possibility of incorporating drugs into the inner cavity of the carbon nanotube provides a protective environment for drugs of poor stability and affords diameter-dependent, controlled drug release.

On the other hand, carbon nanotubes are non-biodegradable and hence, their elimination from the body after i.v. or intratumoral application needs to be well understood and controlled. This could for example be achieved by carrying out rigorous toxicological assessments alongside pharmacokinetic and in vivo therapeutic studies. Nevertheless, drug delivery is clearly one of the most promising bioapplications of carbon nanotubes and the coming years will reveal the suitability of this rather novel material in comparison to more established drug delivery systems, such as liposomes.

References

- Jemal, A., Siegel, R., Ward, E., et al.: Cancer statistics 2009. CA Cancer J. Clin. 59, 225–249 (2009)
- Kuper, H., Adami, H.O., Boffetta, P.: Tobacco use, cancer causation and public health impact. J. Intern. Med. 251(6), 455–466 (2002)
- 3. Bourdes, V., Boffetta, P., Pisani, P.: Environmental exposure to asbestos and risk of pleural mesothelioma: review and meta-analysis—Environmental exposure to asbestos and mesothelioma. Eur. J. Epidemiol. **16**(5), 411–417 (2000)
- Rigel, D.S.: Cutaneous ultraviolet exposure and its relationship to the development of skin cancer. J. Am. Acad. Dermatol. 58(2), S129–S132 (2008)
- 5. zur Hausen, H.: Viruses in human cancers. Science **254**(5035), 1167–1173 (1991)
- 6. Frank, T.S.: Hereditary cancer syndromes. Arch. Pathol. Lab. Med. 125(1), 85–90 (2001)
- 7. Targeted Cancer Therapies. National Cancer Institute Fact Sheet 749 (2009)
- 8. Hait, W.N.: Targeted cancer therapeutics. Cancer Res. 69(4), 1263–1267 (2009)
- 9. McCarron, P.A., Olwill, S.A., Marouf, W.M.Y., et al.: Antibody conjugates and therapeutic strategies. Mol. Interv. 5(6), 368–380 (2005)
- Byrne, J.D., Betancourt, T., Brannon-Peppas, L.: Active targeting schemes for nanoparticle systems in cancer therapeutics. Adv. Drug Del. Rev. 60(15), 1615–1626 (2008)
- 11. Kirpotin, D.B., Drummond, D.C., Shao, Y., et al.: Antibody targeting of long-circulating lipidic nanoparticles does not increase tumor localization but does increase internalization in animal models. Cancer Res. **66**(13), 6732–6740 (2006)
- 12. Lee, L.S., Conover, C., Shi, C., et al.: Prolonged circulating lives of single-chain Fv proteins conjugated with polyethylene glycol: A comparison of conjugation chemistries and compounds. Bioconjug. Chem. **10**(6), 973–981 (1999)
- 13. Farokhzad, O.C., Cheng, J.J., Teply, B.A., et al.: Targeted nanoparticle-aptamer bioconjugates for cancer chemotherapy in vivo. Proc. Natl. Acad. Sci. USA **103**(16), 6315–6320 (2006)
- 14. Proske, D., Blank, M., Buhmann, R., et al.: Aptamers—basic research, drug development, and clinical applications. Appl. Microbiol. Biotechnol. **69**(4), 367–374 (2005)
- 15. Rusconi, C.P., Roberts, J.D., Pitoc, G.A., et al.: Antidote-mediated control of an anticoagulant aptamer in vivo. Nat. Biotechnol. **22**(11), 1423–1428 (2004)

- 16. Burmeister, P.E., Lewis, S.D., Silva, R.F., et al.: Direct in vitro selection of a 2'-O-methyl aptamer to VEGF. Chem. Biol. 12(1), 25–33 (2005)
- Garanger, E., Boturyn, D., Dumy, P.: Tumor targeting with RGD peptide ligands-design of new molecular conjugates for imaging and therapy of cancers. Anticancer Agents Med. Chem. 7(5), 552–558 (2007)
- Meyer, A., Auernheimer, J., Modlinger, A., et al.: Targeting RGD recognizing integrins: drug development, biomaterial research, tumor imaging and targeting. Curr. Pharm. Des. 12(22), 2723–2747 (2006)
- 19. Ruoslahti, E.: Specialization of tumour vasculature. Nat. Rev. Cancer 2(2), 83-90 (2002)
- 20. Sudimack, J., Lee, R.J.: Targeted drug delivery via the folate receptor. Adv. Drug Del. Rev. **41**(2), 147–162 (2000)
- 21. Zhao, X., Li, H., Lee, R.J.: Targeted drug delivery via folate receptors. Expert Opin. Drug Deliv. 5(3), 309–319 (2008)
- 22. Lu, Y., Sega, E., Leamon, C.P., et al.: Folate receptor-targeted immunotherapy of cancer: mechanism and therapeutic potential. Adv. Drug Deliv. Rev. **56**(8), 1161–1176 (2004)
- Russell-Jones, G., McTavish, K., McEwan, J., et al.: Vitamin-mediated targeting as a
 potential mechanism to increase drug uptake by tumours. J. Inorg. Biochem. 98(10), 1625

 1633 (2004)
- Shmeeda, H., Mak, L., Tzemach, D., et al.: Intracellular uptake and intracavitary targeting of folate-conjugated liposomes in a mouse lymphoma model with up-regulated folate receptors. Mol. Cancer Ther. 5(4), 818–824 (2006)
- Wu, J., Liu, Q., Lee, R.J.: A folate receptor-targeted liposomal formulation for paclitaxel. Int. J. Pharm. 316(1–2), 148–153 (2006)
- Wu, A.M., Senter, P.D.: Arming antibodies: prospects and challenges for immunoconjugates. Nat. Biotechnol. 23(9), 1137–1146 (2005)
- 27. Niculescu-Duvaz, I., Springer, C.J.: Antibody-directed enzyme prodrug therapy (ADEPT): a review. Adv. Drug Del. Rev. **26**(2–3), 151–172 (1997)
- 28. Ferrari, M.: Cancer nanotechnology: opportunities and challenges. Nat. Rev. Cancer 5(3), 161–171 (2005)
- Heister, E., Neves, V., Tîlmaciu, C., et al.: Triple functionalisation of single-walled carbon nanotubes with doxorubicin, a monoclonal antibody, and a fluorescent marker for targeted cancer therapy. Carbon 47(9), 2152–2160 (2009)
- 30. Iyer, A.K., Khaled, G., Fang, J., et al.: Exploiting the enhanced permeability and retention effect for tumor targeting. Drug Discov. Today 11(17–18), 812–818 (2006)
- 31. Gottlieb, J.J., Washenik, K., Chachoua, A., et al.: Treatment of classic Kaposi's sarcoma with liposomal encapsulated doxorubicin. Lancet **350**(9088), 1363–1364 (1997)
- 32. Tannock, I.F., Rotin, D.: Acid pH in tumors and its potential for therapeutic exploitation. Cancer Res. **49**(16), 4373–4384 (1989)
- 33. Ko, J., Park, K., Kim, Y.S., et al.: Tumoral acidic extracellular pH targeting of pH-responsive MPEG-poly (beta-amino ester) block copolymer micelles for cancer therapy. J Control. Release **123**(2), 109–115 (2007)
- 34. Pantarotto, D., Briand, J.P., Prato, M., et al.: Translocation of bioactive peptides across cell membranes by carbon nanotubes. Chem. Commun. (1), 16–17 (2004)
- 35. Kam, N.W.S., Jessop, T.C., Wender, P.A., et al.: Nanotube molecular transporters: internalization of carbon nanotube-protein conjugates into mammalian cells. J. Am. Chem. Soc. **126**(22), 6850–6851 (2004)
- 36. Pantarotto, D., Singh, R., McCarthy, D., et al.: Functionalized carbon nanotubes for plasmid DNA gene delivery. Angew. Chem. Int. Edn. **43**(39), 5242–5246 (2004)
- 37. Gao, L.Z., Nie, L., Wang, T.H., et al.: Carbon nanotube delivery of the GFP gene into mammalian cells. ChemBioChem 7(2), 239–242 (2006)
- 38. Kam, N.W.S., Liu, Z.A., Dai, H.J.: Carbon nanotubes as intracellular transporters for proteins and DNA: an investigation of the uptake mechanism and pathway. Angew. Chem. Int. Edn. **45**(4), 577–581 (2006)

 Chen, J., Chen, S., Zhao, X., et al.: Functionalized single-walled carbon nanotubes as rationally designed vehicles for tumor-targeted drug delivery. J. Am. Chem. Soc. 130(49), 16778–16785 (2008)

- Kam, N.W.S., Liu, Z., Dai, H.J.: Functionalization of carbon nanotubes via cleavable disulfide bonds for efficient intracellular delivery of siRNA and potent gene silencing. J. Am. Chem. Soc. 127(36), 12492–12493 (2005)
- 41. Prabaharan, M., Grailer, J.J., Pilla, S., et al.: Gold nanoparticles with a monolayer of doxorubicin-conjugated amphiphilic block copolymer for tumor-targeted drug delivery. Biomaterials **30**(30), 6065–6075 (2009)
- 42. Yudasaka, M., Ajima, K., Suenaga, K., et al.: Nano-extraction and nano-condensation for C-60 incorporation into single-wall carbon nanotubes in liquid phases. Chem. Phys. Lett. **380**(1–2), 42–46 (2003)
- 43. Leonhardt, A., Hampel, S., Muller, C., et al.: Synthesis, properties, and applications of ferromagnetic-filled carbon nanotubes. Chem. Vap. Deposition 12(6), 380–387 (2006)
- 44. Gao, H.J., Kong, Y., Cui, D.X., et al.: Spontaneous insertion of DNA oligonucleotides into carbon nanotubes. Nano Lett. **3**(4), 471–473 (2003)
- 45. Kim, B.M., Qian, S., Bau, H.H.: Filling carbon nanotubes with particles. Nano Lett. 5(5), 873–878 (2005)
- Hilder, T.A., Hill, J.M.: Carbon nanotubes as drug delivery nanocapsules. Curr. Appl. Phys. 8(3–4), 258–261 (2008)
- 47. Hilder, T.A., Hill, J.M.: Probability of encapsulation of paclitaxel and doxorubicin into carbon nanotubes. Micro Nano Lett. **3**(2), 41–49 (2008)
- 48. Wu, W., Wieckowski, S., Pastorin, G., et al.: Targeted delivery of amphotericin B to cells by using functionalized carbon nanotubes. Angew. Chem. Int. Ed. **44**(39), 6358–6362 (2005)
- Ali-Boucetta, H., Al-Jamal, K.T., McCarthy, D., et al.: Multiwalled carbon nanotubedoxorubicin supramolecular complexes for cancer therapeutics. Chem. Commun. (4), 459–461 (2008)
- Feazell, R.P., Nakayama-Ratchford, N., Dai, H., et al.: Soluble single-walled carbon nanotubes as longboat delivery systems for Platinum(IV) anticancer drug design. J. Am. Chem. Soc. 129(27), 8438–8439 (2007)
- 51. Liu, Z., Sun, X.M., Nakayama-Ratchford, N., et al.: Supramolecular chemistry on water-soluble carbon nanotubes for drug loading and delivery. ACS Nano 1(1), 50–56 (2007)
- 52. Dhar, S., Liu, Z., Thomale, J., et al.: Targeted single-wall carbon nanotube-mediated Pt(IV) prodrug delivery using folate as a homing device. J. Am. Chem. Soc. **130**(34), 11467–11476 (2008)
- 53. Hampel, S., Kunze, D., Haase, D., et al.: Carbon nanotubes filled with a chemotherapeutic agent: a nanocarrier mediates inhibition of tumor cell growth. Nanomedicine 3(2), 175–182 (2008)
- Ou, Z.M., Wu, B.Y., Xing, D., et al.: Functional single-walled carbon nanotubes based on an integrin alpha(v)beta(3) monoclonal antibody for highly efficient cancer cell targeting. Nanotechnology 20(10), 105102 (2009)
- 55. Zhang, X.K., Meng, L.J., Lu, Q.G., et al.: Targeted delivery and controlled release of doxorubicin to cancer cells using modified single wall carbon nanotubes. Biomaterials **30**(30), 6041–6047 (2009)
- McDevitt, M.R., Chattopadhyay, D., Kappel, B.J., et al.: Tumor targeting with antibodyfunctionalized, radiolabeled carbon nanotubes. J. Nucl. Med. 48(7), 1180–1189 (2007)
- 57. Scott, S.D.: Rituximab: a new therapeutic monoclonal antibody for non-Hodgkin's lymphoma. Cancer Pract. 6(3), 195–197 (1998)
- 58. Liu, Z., Chen, K., Davis, C., et al.: Drug delivery with carbon nanotubes for in vivo cancer treatment. Cancer Res. **68**(16), 6652–6660 (2008)
- Villa, C.H., McDevitt, M.R., Escorcia, F.E., et al.: Synthesis and biodistribution of oligonucleotide-functionalized, tumor-targetable carbon nanotubes. Nano Lett. 8(12), 4221– 4228 (2008)

- 60. Bhirde, A.A., Patel, V., Gavard, J., et al.: Targeted killing of cancer cells in vivo and in vitro with EGF-directed carbon nanotube-based drug delivery. ACS Nano 3(2), 307–316 (2009)
- 61. Wu, W., Li, R.T., Bian, X.C., et al.: Covalently combining carbon nanotubes with anticancer agent: preparation and antitumor activity. ACS Nano 3(9):2740–2750 (2009)
- 62. Zeineldin, R., Al-Haik, M., Hudson, L.G.: Role of polyethylene glycol integrity in specific receptor targeting of carbon nanotubes to cancer cells. Nano Lett. 9(2), 751–757 (2009)

Carbon Nanotubes Filled with Carboplatin: Towards Carbon **Nanotube-Supported Delivery** of Chemotherapeutic Agents

- D. Haase, S. Hampel, K. Kraemer, D. Kunze, A. Taylor, M. Arlt,
- J. Thomas, S. Oswald, M. Ritschel, R. Klingeler, A. Leonhardt and
- B. Büchner

Abstract Thanks to their capillary-like structure CNTs provide a well-characterized container material for hosting miscellaneous fillings. Here we present basic studies on the use of CNTs for drug delivery. By introducing carboplatin, an anticancer drug, into the CNTs via a wet chemical approach, drug-filled nanotubes have been produced. The maintenance of the structure of carboplatin was proven using electron energy loss spectroscopy and X-ray photoelectron spectroscopy. It was shown that the drug is released into cell culture medium leading to cell death. Cell viability assays performed with bladder cancer cells EJ28 demonstrated the cytotoxicity of CNTs filled with carboplatin. For comparison a reference of unfilled, open ended CNTs did not affect the cell viability. These results point out the general capabilities of CNTs as nanocarriers for drug delivery.

1 Introduction

In the recent past CNTs have grown to a highly attractive subject in biomedical research. The considerable stability of this carbon allotrope in combination with a

D. Haase (S), S. Hampel, A. Taylor, J.Thomas, S. Oswald, M. Ritschel, R. Klingeler,

A. Leonhardt and B. Büchner

Leibniz Institute for Solid State and Materials Research (IFW), Dresden, Germany e-mail: d.haase@ifw-dresden.de

K. Kraemer, D. Kunze, A. Taylor and M. Arlt

Department of Urology, Dresden University of Technology (TU Dresden), Dresden, Germany

R. Klingeler

Kirchhoff Institute for Physics, University of Heidelberg, Heidelberg, Germany

great potential for chemical and physical modifications opens a wide window for the development of novel biomedical sensing or delivery systems. It has been extensively discussed in the literature that CNTs can be modified exohedrally by diverse methods [4, 12, 13, 17, 19]. The Π-system of the outer shells and the defect sites especially at the end caps or at the sidewalls offer various options for altering the structure of the tubes. They may be opened [9, 22], cut [16, 21], functionalized with different functional groups [8, 13, 18, 19] or simply decorated by non-covalent attachment of long chain molecules wrapping themselves around the tubes [14].

Besides these modifications based on the reactivity of the C-network of the shells there is another beneficial way to change the properties of CNTs. Since they consist of tubular cylinders an easy consideration may be to fill the hollow inner space. Thus CNTs may act as a smart and safe casing for a chosen filling material in order to transport it within a system well shielded from the environment by the carbon shell to the desired location. So far, lots of work has been done regarding the filling of single-walled (SWCNT) as well as multi-walled CNTs (MWCNT). Various metals or metal compounds such as ferromagnets [11, 15], several halides [5, 6] and others have been introduced into the tubes successfully. Fewer efforts have been published dealing with the filling of CNTs with drugs. In using CNTs for biomedical applications the most common way is to attach active substances to the outer shells. However some work by Ajima et al. [1–3] describe the filling of single-walled carbon nanohorns with cisplatin [cisdiaminedichloroplatinum(II)].

Here, we present a particular drug delivery system based on MWCNT. Since these tubes exhibit larger inner diameters, they provide more space for filling as compared to SWCNT or nanohorns. Carboplatin [cis-diammine(cyclobutane-1,1-dicarboxylato)platinum(II)] a second generation cytostatic drug, which is more water soluble and has less adverse effects than its parent agent cisplatin (not nephrotoxic, less neuro- and ototoxic [10]), has been incorporated into MWCNT. The feasibility of use of these carboplatin-loaded nanocarriers was investigated and their effect on human bladder cancer cells was demonstrated in vitro.

2 Experimental Details

Compared with SWCNT it is more convenient to work with MWCNT since they exhibit several advantages. Due to the smaller diameter and higher surface energy SWCNT tend to accumulate in bundles. MWCNT are available rather individually and are thus much easier to disperse than SWCNT. Besides, MWCNT are simply more stable against chemical interventions since they consist of several graphene layers offering a stronger shield for internalized fillings against external interventions. Of course, MWCNT offer a bigger inner diameter than SWCNT thus providing more space for the potential filler.

Synthesis of MWCNT

The MWCNT to be filled with carboplatin were synthesized via solid-source chemical vapor deposition (ssCVD) with ferrocene as the precursor as described by Ritschel et al. [20]. The resulting CNTs consist of 20–30 walls with inner diameters of 10–20 nm according to transmission electron microscopic (TEM) data. The length varies from 10 to 30 μm .

Purification Process

The MWCNT grown by ssCVD are found along with amorphous carbon and free catalyst particles as is common for most CVD methods. Hence, a purification process has to be conducted prior to filling. A washing step in hydrochloric acid (6 M) was used to remove magnesium oxide which acts as supporting material for the catalyst for the synthesis. For further purification the raw MWCNT were treated in air at 450°C for 1 h in order to remove amorphous carbon and to oxidize carbon shells covering free catalyst particles which are then removed subsequently by allowing the CNTs to stand in hydrochloric acid (6 M) overnight. Afterwards, CNTs were stirred in nitric acid (7.2 M) at 80°C under reflux. In this final step the acid attacks the CNTs themselves. This leads to open ends and removal of catalyst particles enclosed by CNTs. After each washing step with acid CNTs were neutralized by washing with distilled water.

This treatment leads to open ended MWCNT applicable for filling but also enables a better dispersion since the oxidation also attacks defect sites of the CNTs apart from the end caps. These opened CNTs are in the following paragraphs referred to as empty CNTs (e-CNT) since they provide the unfilled starting material for the filling procedure with carboplatin.

Incorporation of Carboplatin

For filling experiments e-CNT were firstly dispersed in an aqueous carboplatin solution (infusion solution: 10 mg/ml, Mayne Pharma, UK) by sonication for 10 min and stirred for 24 h at 90°C afterwards (thermal decomposition starting at 200°C). After the process the water was allowed to evaporate at 22°C while stirring. The dry material obtained was redispersed in distilled water by ultrasonication. The CNTs were recovered by filtration and washed with distilled water several times and rinsed with ethanol. Finally, CNTs were dried at 105°C overnight.

D. Haase et al.

Characterization

The samples obtained were investigated in detail. Images were taken using a high resolution transmission electron microscope (TEM/STEM/Tecnai F30/FEI Company operated at 300 kV, Hillsboro, OR, USA). The chemical composition of the material was investigated using energy-dispersive X-ray analysis (EDX/EDAM-III, Edax, Mahwah, NJ, USA), electron energy loss spectroscopy (EELS/Tecnai F30, FEI Company) and X-ray photoelectron spectroscopy (XPS/PHI 5600-CI, Physical Electronics, Chanhassen, MN, USA).

Toxicity Studies

The cytotoxicity of the empty and the carboplatin-filled CNTs (CNT-CP) was probed by means of tests of cell viability, cell proliferation, apoptosis rate and cell cycle distribution. A prostate cancer cell line (PC-3, American Type Culture Collection CRL-1435, Manassas, VA, USA) and human fibroblasts (harvested from foreskin, Department of Pediatrics, Dresden University of Technology, Dresden, Germany) were used for toxicity studies with e-CNT and human bladder cancer cells (lineage EJ28, University of Frankfurt, Germany) for toxicity studies with drug-filled CNT-CP, respectively. The cells were cultured under standard conditions (37°C, humidified atmosphere containing 5% CO₂) in DMEM (Dulbecco's Modified Eagle Medium; 4.5 g/l glucose) with 10% fetal calf serum, 1% minimum essential medium (MEM), 1% 2-(4-(2-hydroxyethyl)-1-piperazine)ethanesulfonic acid (HEPES) and 1% of a stock penicillin-streptomycin solution (all from Invitrogen, Karlsruhe, Germany). After seeding in 96- or 24-well plates and adherence for 24 h CNTs dispersed in cell culture medium or carboplatin solution were added to the culture wells. To achieve well dispersed CNTs all solutions were treated with a probe tip sonicator for 30 s with a power of 40% (UW2070 Bandelin, Berlin, Germany) immediately before adding to the cells. After incubation for 4 h, wells were washed two times with pure physiological phosphate buffered saline (PBS, PAA, Cölbe, Germany) and after that incubated with media for further 24, 48, and 72 h. For control experiments, PBS was added instead of the CNTs dispersions.

Cell viability was evaluated by the widely established water soluble tetrazolium (WST)-1 assay by adding 10 μ l of cell proliferation agent WST-1 (4-[3-(4-iodophenyl)-2-(4-nitrophenyl)-2*H*-5-tetrazolio]-1,3-benzene disulfonate; Roche, Mannheim, Germany) to cells incubated in 100 μ l of media. The assay was performed 24, 48 and 72 h after incubation of PC-3 and fibroblasts, 48 and 72 h after incubation of EJ28, respectively.

Cell proliferation was investigated by automatic cell counting (Z2 Analyzer, Beckman-Coulter, Krefeld, Germany) of harvested cells in a cell counting diluent. Apoptosis was assessed by flow cytometry 48 and 72 h after treatment. Cells

were incubated with Annexin V and Propidium Iodide (PI) for labeling the early

and late apoptotic cells (Annexin V-FITC Apoptosis Detection Kit I; FACScan, BD Biosciences, Heidelberg, Germany). The Annexin V-FITC-PI plots were examined by quadrant analysis using the software WinMDI2.8 (http://facs.scripps.edu/software.html). PI counterstaining allows the quantification of early (Annexin V-positive, PI-negative) and late apoptotic cells (double positive). The CycleTest Plus DNA Reagent Kit (BD Biosciences) was used for cell cycle analysis according to the provider's instructions. Representative data of cell viability are shown for the toxicity studies performed on fibroblasts and PC-3 with e-CNT, data from two independent experimental series with similar results for determination of cell viability, cell count and apoptosis on EJ28 with CNT-CP.

3 Results and Discussion

Characterization of Filled MWCNT

The solution-phase method that was applied for filling the CNTs is both facile and highly suitable in the case of carboplatin. The driving force of this approach is the capillarity force. CNTs exhibit diameters in the range of several nm thereby acting like tiny capillaries into which liquids of certain surface tensions are drawn in quite easily. According to Ebbesen [7] there is a cut off value for surface tensions 100-200 mN/m below which liquid substances are well suited fillings for nanotubes. As water exhibits a low surface tension of 72 mN/m its wetting behavior towards the CNTs is positive and thus it might act as a carrier for carboplatin. Additionally, the hydrophilicity of the MWCNT is enhanced due to the oxidation that occurred by the purification and opening procedure beforehand. The interaction between the CNTs and the carboplatin solution is moreover intensified by increasing the temperature since heating lowers the surface tension of water. The optimum temperature for the filling process was found out to be 90°C resulting in an adequate filling yield. The filling yield is quantified by means of atomic absorption spectroscopy (AAS) by measuring the platinum content. In Fig. 1 platinum contents of samples filled applying different temperatures are shown with respect to the total mass of samples. It is displayed that the samples produced at 90°C contain the highest amount of Pt.

TEM images of CNT-CP are displayed in Fig. 2. There is clear indication that the carboplatin is located inside the CNTs. Interestingly, it forms spherical agglomerates of 1–5 nm in diameter. As depicted in Fig. 2, these clusters are aligned to the inner walls of the tubes which points out clearly that they are situated inside the hollow core of the CNTs.

To ascertain the maintenance of the original structure of the complex carboplatin (structure shown in Fig. 3a) detailed elemental analyses were performed. By EDX only platinum was detected aside from the high amount of carbon deriving from the CNTs (see Fig. 3a). Nitrogen and hydrogen have not been observed in the D. Haase et al.

Fig. 1 Platinum content of CNTs filled with carboplatin: dependence on the filling temperature

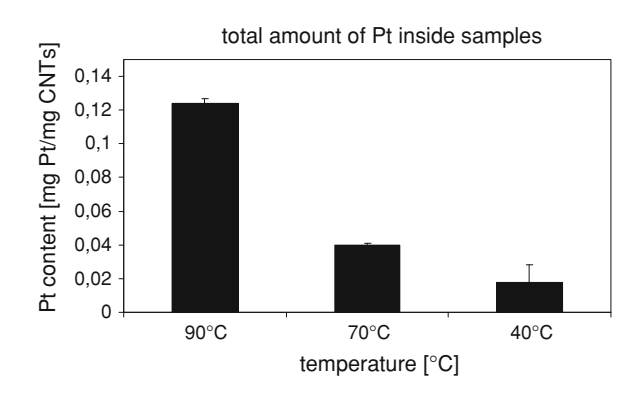
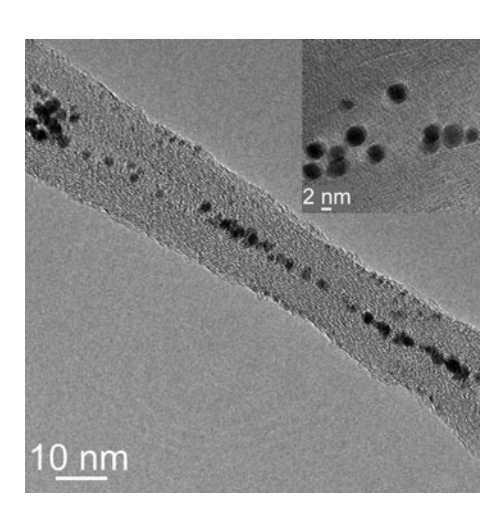


Fig. 2 TEM image of carboplatin clusters enclosed by a MWCNT



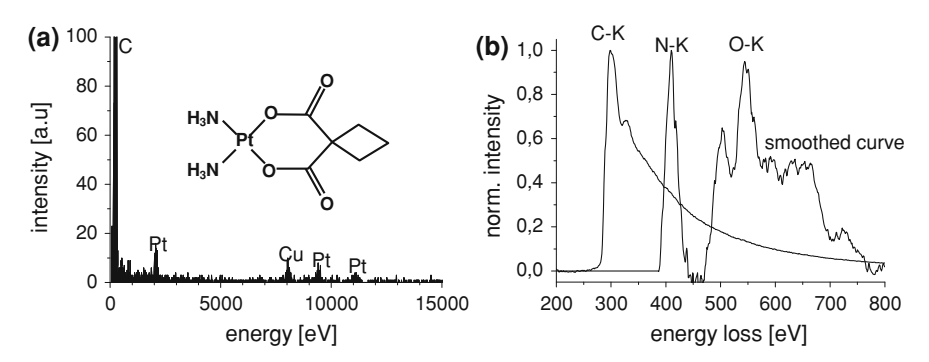


Fig. 3 a EDX spectrum of carboplatin-filled CNTs. Structure of carboplatin (*inset*). b EEL-Spectrum of a carboplatin accumulation inside a MWCNT

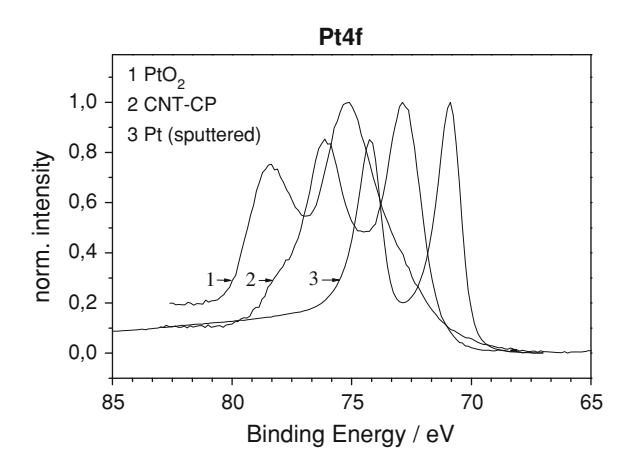
spectrum due to the low atomic weight of these elements which makes them unverifiable for the EDX analysis. EELS on a carboplatin accumulation enclosed in a CNTs revealed oxygen and nitrogen that correspond to the ammonium and cyclobutane-1,1-dicarboxylligands of the carboplatin complex. These EELS results, however, do not clearly verify that the oxygen derived from incorporated carboplatin only since e-CNT also showed the characteristic energy loss of oxygen. This fact might be due to some carboxylic groups which can be introduced by HNO₃ treatment since it was used as the oxidizing agent for the opening procedure.

Proof for the constitution of the complex was finally achieved by XPS measurements. XP-spectra of CNT-CP were compared with those of pure platinum (Goodfellow, Bad Nauheim, Germany) and platinum(IV)-oxide (Johnson Matthey, London, UK). In CNT-CP the XPS data revealed carbon, oxygen, nitrogen and platinum, respectively. By comparison of the Pt4f-spectrum of this sample with the ones of the two reference samples the binding energy of the central atom was found to be situated between the values of metallic platinum (Pt⁰) and platinum oxide (Pt⁴⁺) (Fig. 4).

This result reveals that neither an auto-reduction of the central atom to metallic platinum nor an oxidation to Pt⁴⁺ took place during the filling process. In particular, the original planar carboplatin complex still exists. In accordance to the EELS measurements XPS revealed the presence of oxygen, too, which might correspond to carboxyl groups from functionalized outer shells of the CNTs. Hence, the data clearly imply that nitrogen found in the CNT-CP exclusively originates from the carboplatin itself since no nitrogen was found in e-CNT via XPS. Oxygen arises from carboplatin and the carboxyl groups at the outer carbon shells.

A preliminary release experiment with filled CNTs was performed by incubation of CNT-CP in cell culture medium for several time points (0.5–24 h) and subsequent analysis by TEM. Although individual nanotubes varied in filling yield after incubation for 0.5 h the filling yield was relatively high. We noted, however, that most of the carboplatin clusters were situated at the end of the tubes. A

Fig. 4 Pt4f-spectra of platinum oxide, carboplatin-filled CNTs and platinum, respectively



D. Haase et al.

decrease of carboplatin clusters within the CNT-CP was recognized after an incubation period of 24 h as only a few clusters could be detected inside the tubes then (Fig. 5b). However, for an accurate quantification of the carboplatin release from CNT-CP into the culture medium and its content in cells further studies are required.

Toxicity of Empty MWCNT

In order to evaluate the feasibility of CNTs as potential drug carrier systems the cytotoxicity of unfilled and filled CNTs was investigated by means of cell viability, cell proliferation, apoptosis rate and cell cycle distribution.

For estimation of the toxicity of unfilled CNTs towards cells PC-3 cells and fibroblasts were incubated with different concentrations of e-CNT. Viability was measured at 24, 48 and 72 h after incubation. Results are depicted in Fig. 6. After 24 h fibroblasts exhibit no significant changes in viability. After 48 h a

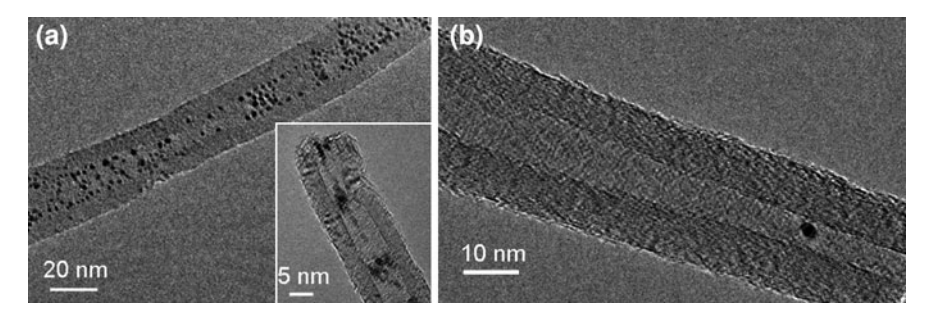


Fig. 5 HRTEM images of carboplatin-filled CNTs after release experiments. **a** CNT-CP incubated in cell culture medium for 0.5 h. Carboplatin clusters located at the end of a CNTs (*inset*). **b** CNT-CP incubated in cell culture medium for 24 h

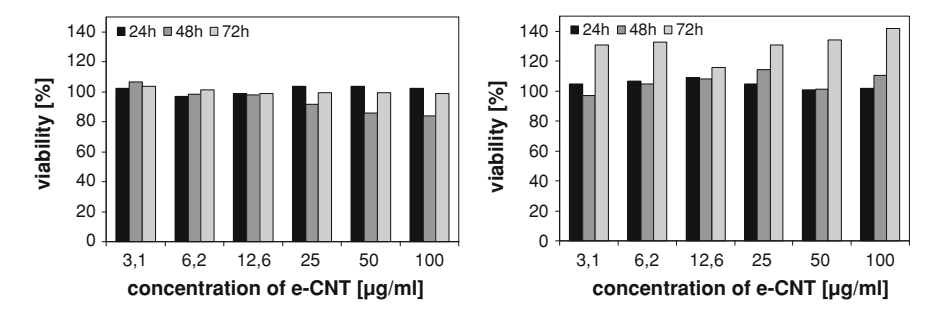


Fig. 6 Cell viability of fibroblasts (*left*) and PC3-cells (*right*) measured by cell viability test WST-1 after 24, 48 and 72 h, respectively. Values are normalized to control conditions without e-CNT

small decrease was observable for fibroblasts at higher concentrations of e-CNT (25, 50, 100 μ g/ml). But viability at those concentrations was recovered after 72 h and no significant differences remained in comparison to the control. For the PC-3 cells no relevant changes were found except after 72 h, where viability increased for cells incubated with concentrations of 3.1, 6.3, 25 and 100 μ g/ml of e-CNT.

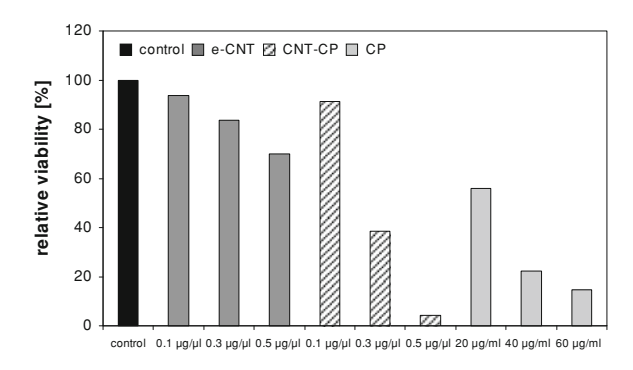
Proliferation of PC-3 cells and fibroblasts was not constricted by e-CNT. An exponential growth with cell numbers comparable to the control conditions was observable for both lineages.

Toxicity of Carboplatin-Filled MWCNT

The medical virtue of CNT-CP was studied using human bladder cancer cells of the cell line EJ28 that were incubated with different concentrations of both types of nanotubes, CNT-CP and e-CNT, simultaneously. The results of the cell viability assay using WST-1 in Fig. 7 reveal that e-CNT cause no $(0.1 \ \mu g/\mu l)$ or only minor $(0.3 \ and \ 0.5 \ \mu g/\mu l)$ cell viability reduction 72 h after treatment (Fig. 7). Thus, e-CNT are not toxic towards bladder cancer cells in the conditions tested. However, the long-term effect of CNTs on cells should be investigated in future studies.

Another basic requirement—besides the lack of toxicity of e-CNT—is the cytotoxicity of free carboplatin to EJ28 cells, which was shown in a concentration-dependent way (Fig. 7). 20 µg/ml of carboplatin decreased the viability of the cells to almost 50%. Similar to free carboplatin, CNT-CP caused a concentration-dependent cytotoxic effect. 0.1 µg/µl of CNT-CP reduced the viability of EJ28 cells only slightly whereas 0.3 and 0.5 µg/µl of CNT-CP produced a strong inhibition of viability (Fig. 7). Since we currently have no quantitative data on the release of carboplatin from CNT-CP a direct comparison of the effects of the free drug with those of CNT-CP is not possible. However, the data confirm that the MWCNT used could be promising candidates to deliver cytotoxic drugs. It is also important to note that the total number of nanotubes is lower in CNT-CP samples than in samples containing e-CNT since their mass is increased by the incorporated drug.

Fig. 7 Cell viability of EJ28-cells treated with different concentrations of empty CNTs (e-CNT) and filled CNTs (CNT-CP) and free carboplatin (CP) measured by cell viability test WST-1 72 h after start of the treatment. Values are normalized to control conditions without e-CNT



D. Haase et al.

Fig. 8 Cell count of EJ28 cells 72 h after treatment with a CNTs-concentration of 0.3 μg/μl or free carboplatin. Values are normalized to control conditions without e-CNT (*e-CNT* empty CNTs, *CNT-CP* carboplatin-filled CNTs, *CP* carboplatin)

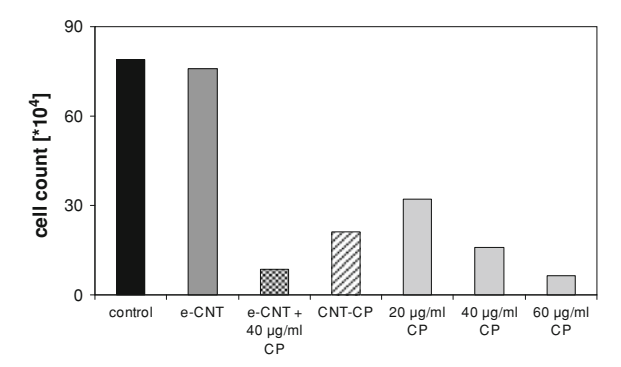
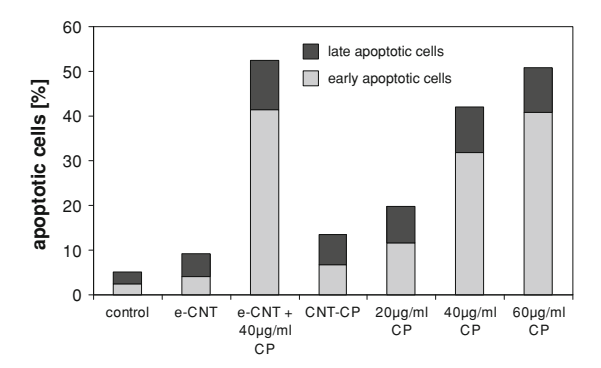


Fig. 9 Apoptosis rate of EJ28 cells 72 h after treatment with a CNTs-concentration of 0.3 μg/μl or free carboplatin. Values are normalized to control conditions without e-CNT (*e-CNT* empty CNTs, *CNT-CP* carboplatin-filled CNTs, *CP* carboplatin)



In the case of EJ28, treatment with e-CNT (0.3 $\mu g/\mu l$) did not cause alterations in cell count, apoptosis rate and cell cycle distribution (data not shown) compared with untreated cells 72 h after incubation start. Treatment with free carboplatin alone resulted in a concentration-dependent decrease of cell number which is shown in Fig. 8, increase of apoptosis rate (Fig. 9) and changes of the cell cycle distribution in favor of a G2/M arrest (not shown). The treatment with e-CNT + 40 $\mu g/m l$ free carboplatin clearly enhances the cellular effects induced by monotreatment with 40 $\mu g/m l$ carboplatin. Yet, it is not clear in which way the treatment with e-CNT additional to carboplatin causes a synergistic effect. A possible explanation might be the altered integrity of the cellular membrane caused by internalization of CNTs, which could lead to increased uptake of carboplatin as a positive side-effect. Treatment with 0.3 $\mu g/\mu l$ CNT-CP also reduced cell count, slightly induced apoptosis and a cell cycle arrest in the G2/M phase (data not shown).

4 Conclusions

MWCNT are shown to be promising templates for the development of nano carrier systems for drug delivery. Carboplatin-filled CNTs have been produced

successfully by applying a wet-chemical approach. Evidence for carboplatin clusters inside the CNTs was given by HRTEM studies. Detailed elemental analyses using EDX, EELS and XPS confirmed the maintenance of the drug during the filling procedure. As EDX analysis detected only carbon and platinum, the presence of nitrogen and oxygen was confirmed by EELS and XPS measurements. Additionally, the original oxidation state was confirmed by comparing the XPS spectra of our sample with those spectra of pure platinum and platinum oxide in a higher oxidation state.

In vitro studies were performed in order to test the CNTs for their toxicity towards cells. It was demonstrated that our CNTs neither influenced the viability of malignant (prostate cancer cell line PC-3) nor of non-malignant (fibroblast) cells. Viability tests also approved the effectiveness of the carboplatin-filled CNTs in destroying cancer cells of the cell line EJ28. An increase of the concentration of CNT-CP induced a strong inhibition of cell viability. Furthermore, a decrease of cell number, an increase of apoptosis rate and a G2/M arrest in cell cycle was observed. Combining the treatment of empty CNTs with carboplatin solution clearly enhanced the toxic effects of carboplatin.

In conclusion we have demonstrated that CNTs are well suited matrices for the development of nanosized drug carrier systems and a promising material for the design of future therapies working on the cellular level.

Acknowledgments The authors would like to thank G. Kreutzer and S. Pichl for the SEM/TEM-investigations. This work was supported by the Leibniz Association within the "Pakt für Forschung und Innovation". Further financial support was given by the European Community through the Marie Curie Research Training Network CARBIO under contract No. MRTN-CT-2006-035616.

References

- Ajima, K., Yudasaka, M., Murakami, T., Maigné, A., Shiba, K., Iijima, S.: Mol. Pharm. 2, 475–480 (2005)
- 2. Ajima, K., Yudasaka, M., Maigné, A., Iijima, S.: J. Phys. Chem. B 110, 19097–19099 (2006)
- Ajima, K., Yudasaka, M., Maigné, A., Miyawaki, J., Iijima, S.: J. Phys. Chem. B 110, 5773–5778 (2006)
- 4. Balasubramanian, K., Burghard, M.: Small 1, 180-192 (2005)
- 5. Chen, G., Qiu, J., Qiu, H.: Scripta Mater. 58, 457-480 (2008)
- 6. Chikkannanavar, S.B., Taubert, A., Luzzi, D.E.: J. Nanosci. Nanotechnol. 3, 159–163 (2003)
- 7. Ebbesen, T.W.: J. Phys. Chem. Sol. **57**, 951–955 (1996)
- 8. Gabriel, G., Sauthier, G., Fraxedas, J., Moreno-Mañas, M., Martínez, M.T., Miravitlles, C., Casábo, J.: Carbon 44, 1891–1897 (2006)
- Geng, H.Z., Zhang, X.B., Mao, S.H., Kleinhammes, A., Shimoda, H., Wu, Y., Zhou, O.: Chem. Phys. Lett. 399, 109–113 (2004)
- 10. Gott, I., Gust, R.: Pharm. Unserer Zeit 2, 124-129 (2006)
- 11. Hampel, S., Leonhardt, A., Selbmann, D., Biedermann, K., Elefant, D., Mueller, C., Gemming, T., Buechner, B.: Carbon 44, 2316–2322 (2006)
- 12. Hsin, Y.L., Lai, J.Y., Hwang, K.C., Lo, S.C., Chen, F.R., Kai, J.J.: Carbon 44, 3328–3335 (2006)

D. Haase et al.

13. Klumpp, C., Kostarelos, K., Prato, M., Bianco, A.: Biochim. Biophys. Acta 1758, 404–412 (2006)

- Kum, M.C., Joshi, K.A., Chen, W., Myung, N.V., Mulchandani. A.: Talanta. 74, 370–375 (2007)
- Leonhardt, A., Moench, I., Meye, A., Hampel, S., Buechner, B.: Adv. Sci. Technol. 49, 74–78 (2006)
- 16. Li, J., Zhang, Y.: Appl. Surf. Sci. 252, 2944–2948 (2006)
- 17. Marshall, M.W., Popa-Nita, S., Shapter, J.G.: Carbon 44, 1137–1141 (2006)
- 18. Montesa, I., Muñoz, E., Benito, A.M., Maser, W.K., Martinez, M.T.: J. Nanosci. Nanotechnol. 7, 3473–3476 (2007)
- 19. Pastorin, G., Wu, W., Wieckowski, S., Briand, J.P., Kostarelos, K., Prato, M., Bianco, A.: Chem. Commun. 1182–1184 (2006)
- Ritschel, M., Leonhardt, A., Elefant, D., Oswald, S., Buechner, B.: J. Phys. Chem. C 111, 8414–8417 (2007)
- Tran, M.Q., Tridech, C., Alfrey, A., Bismarck, A., Shaffer, M.S.P.: Carbon 45, 2341–2350 (2007)
- 22. Tsang, S.C., Chen, Y.K., Harris, P.J.F., Green, M.L.H.: Nature 372, 159–162 (1994)

Functionalized Carbon Nanotubes for Gene Biodelivery

V. Sanz-Beltrán, Ravi Silva, Helen Coley and Johnjoe McFadden

Abstract The principles of non-covalent functionalization of carbon nanotubes will be described. The abilities of these biomolecules to solubilize carbon nanotubes and bind DNA will be also compared. Approaches for using functionalized carbon nanotubes to deliver genes to target cells and associated problems will be described. Evidence pertaining to the mechanism of entry of nucleic acid-loaded carbon nanotubes into mammalian cells will be also presented.

1 Non-Covalent Functionalization of Carbon Nanotubes

One of the most important problems when using carbon nanotubes for applications in the biomedical field is the inherent difficulty in handling [1]. Carbon nanotubes tend to aggregate in bundles through strong attractive interactions which are very difficult to disrupt [2]. The development of methods to disperse carbon nanotubes from the bundles they form and obtain stable suspensions (a process often called "solubilization") in water is crucial for the progress of the nanotechnology field. In recent years, new functionalization methods have been developed to disperse carbon nanotubes in water which allows their applications in physiological environments [3]. However, the current production methods generate carbon nanotubes

V. Sanz-Beltrán (⋈), H. Coley and J. McFadden Faculty of Health and Medical Sciences, University of Surrey, Guildford, GU2 7XH, UK e-mail: vasanz@unizar.es

V. Sanz-Beltrán and R. Silva Nanoelectronics Centre, Advanced Technology Institute, University of Surrey, Guildford, GU2 7XH, UK

V. Sanz-Beltrán et al.

with impurities such as amorphous carbon and metal catalysts [4]. The application of carbon nanotubes in the biomedical field requires both purification and functionalization. Functionalization of carbon nanotubes has been performed by covalent [5] and non-covalent [6] approaches. The non-covalent functionalization has many advantages over covalent ones. Non-covalent methods preserve the structural and electrical properties of carbon nanotubes which may be advantageous for carbon nanotube taking up and processing in the cell. Furthermore, these procedures are usually quite simple and quick, involving steps such as ultrasonication, centrifugation and filtration. In addition, most of the surfactants that are commonly used in these methods are easily available and low-cost. Although surfactants are efficient in the dispersion of carbon nanotubes, they are known to permeabilize plasma membranes being cytotoxic on their own which could limit the possible biomedical applications of such surfactant-functionalized carbon nanotubes. However, the new functionalization methods involving the conjugation of carbon nanotubes with biological species such as proteins, carbohydrates and nucleic acids open new alternatives in the bioapplications of carbon nanotubes. In the following sections we will describe the different methodologies that have been developed for the non-covalent functionalization of carbon nanotubes.

Implications of Carbon Nanotube Structure on Non-Covalent Functionalization

Non-covalent functionalization is based on the binding to the graphene sheet of carbon nanotubes through hydrophobic, van der Waals, electrostatic and π -stacking interactions [7]. An amphiphilic surfactant is commonly used which binds to the carbon nanotube wall through its hydrophobic part, leaving the hydrophilic part exposed to the solvent, usually water, rendering the complex dispersible in that medium.

Given that the non-covalent approach implies the interaction of the surfactant with the nanotube wall some considerations regarding carbon nanotube structure have to be taken into account. Carbon nanotubes are hollow cylindrical tubes made of one or more concentric sheets of ${\rm sp}^2$ carbons whose diameter, curvature and electronic properties are defined by the way hexagonal rings constituting the nanotube sidewall are joined together. Given that the carbon atoms in a nanotube are pyramidalized due to the curvature of its sidewall, the character of the C–C bond in nanotubes differs from that of graphite. The pyramidalization gives the π -orbitals of C-atoms some σ character and distorts the π -orbitals to be larger and softer on the exterior of the nanotube. This effect gives nanotubes an intrinsic π -type semiconducting behaviour. Furthermore, curvature in the nanotube makes the π -orbitals within the graphene sheet not to be pointed towards the central axis of the nanotube. As the nanotube diameter increases, both the pyramidalization angle and π -orbital misalignment angle decrease, lowering the chemical reactivity of the C–C bonds.

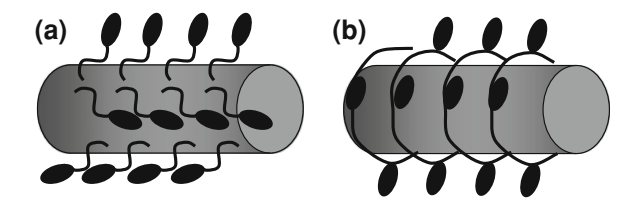


Fig. 1 Different structures that surfactants can adopt on the carbon nanotube surface: **a** micelle structure and **b** polymer wrapping around nanotube. Hydrophilic groups are represented by *ellipsoids* and hydrophobic groups by *black lines*

Theoretical modeling has shown that the interior of a nanotube is more inert than the exterior [a]. Given that π -orbital misalignment is inversely proportional to diameter, wider nanotubes tend to have a greater binding energy for aromatic rings, due to a better geometric match with planar benzene and a decrease in π -orbital misalignment. Therefore, the dispersive interactions for surfactants depend on the nanotube curvature and π -orbital orientation and can be different on the inside and outside of the nanotube. When van der Waals interactions are dominant, the ratio of van der Waals diameter of the molecule to carbon nanotube diameter is the main factor defining the favorable location of the molecule.

The structures that the surfactant molecule adopts when it is attached to the carbon nanotube wall are diverse (Fig. 1). In the case of charged surfactants, the dispersion of nanotubes is stabilized by electrostatic repulsion between the micelles; and in the case of charge-neutral surfactants by the large solvation shell created by hydrophilic moieties of surfactants assembled around the nanotube. The length and the shape of alkyl chains determines the efficiency of the dispersion. Longer and more branched alkyl groups are better than linear and straight ones. Surfactant molecules containing aromatic groups generally form more specific and directional π - π stacking interactions with the nanotube wall. Molecules containing groups such as pyrene, anthracene, porphyrins, phthalocyanins have been reported to give good interactions with carbon nanotubes. Polymers are better at stabilizing nanotube dispersions than small molecular weight surfactants. Polymers reduce the entropic penalty of micelle formation and have higher energy of interaction with nanotubes. The main problem for polymers is that interactions with mechanically rigid nanotubes may force them into energetically unfavorable conformation, although to minimize strain in their conformations some polymers can wrap around nanotubes in a helical fashion. The interactions of hydrophobic parts of surfactants can alter the properties of nanotubes.

Non-Covalent Functionalization of Carbon Nanotubes

As was stated above, an amphiphilic molecule may be used to disperse carbon nanotube in aqueous media. The dispersion yields that are usually achieved with

these methods are in the range of 0.1-1 mg mL⁻¹ which is acceptable for biological use [8]. Furthermore, the thermodynamic characteristics of the dispersed complexes have implications in their biomedical applications. The strength of the surfactant-nanotube interaction determines the non-specific adsorption of biological species that can replace the surfactant on the nanotube surface. The detachment of the surfactant can also have cytotoxic implications. The non-covalent approach has been used not only for functionalization purposes but also for other kind of applications. For example, the non-specific adsorption of a wide range of molecules on nanotubes can be avoided by the coating of the nanotubes with polymers such as polyethylene oxide chains [9]. In addition, some functionalization methods show preferential reactivity toward metallic nanotubes over the semiconducting single-walled carbon nanotubes [10]. Such interactions include the selective adsorption of bromine, amines and DNA. Different classes of molecules have been used for carbon nanotube dispersion, mainly polymers and biopolymers. In the following sections we will describe the different molecules that have been used to disperse carbon nanotubes by the non-covalent approach.

Polymers

Different nonionic and ionic polymers have been used to disperse carbon nanotubes. Carbon nanotubes were found to be dispersed by polymers such as Nafion [11] sodium dodecyl sulfate (SDS) [8], sodium dodecylbenzene sulfonate (SDBS) [8], Triton X-100 [8], Tween 20 [12], polyethyleneglycol (PEG) [13], poly-(m-phenylenevinylene) [14], stilbenoid polymers [15], polyvinyl pyrrolidone [2] and polystyrene sulfonate [2]. The molecular weight of the polymer and the percentage of hydrophilic and hydrophobic parts in the polymer has been shown to have an important effect on the dispersion yield, as was demonstrated with dispersion studies with the nonionic polymer Pluronic (poly(ethylene oxide)-poly(propylene oxide)-poly(ethylene oxide) [16]. Another strategy to prepare polymer-dispersed carbon nanotubes is based on the synthesis of cross-linked polymeric micelles [17]. In this approach, the hydrophilic outer shell of the polymer-nanotube micelle, which contains poly(acrylic acid) groups, is cross-linked by a diamine linker.

Another method of functionalization of carbon nanotubes is based on the use of pyrene-carrying succinimide groups [18]. In this approach, the pyrene group attaches to the nanotube surface via π - π stacking interaction and the succinimide groups remain available to couple to a variety of molecules via amide bounds. Similarly, pyrene-carrying ammonium ions were used to help disperse carbon nanotubes in water [19] (Fig. 2).

Nanotube–polymer complexes which form stable suspensions in aqueous media can be prepared by in situ polymerization of phenylacetylene [20]. Short rigid conjugated polymers, such as poly(arylene ethynylene)s [21], have also been used as dispersing agents. Activated Tween 20 with 1,1-carbonyldiimidazole (CDI) was used to functionalized carbon nanotubes for the further covalent binding of aminecontaining molecules [22].

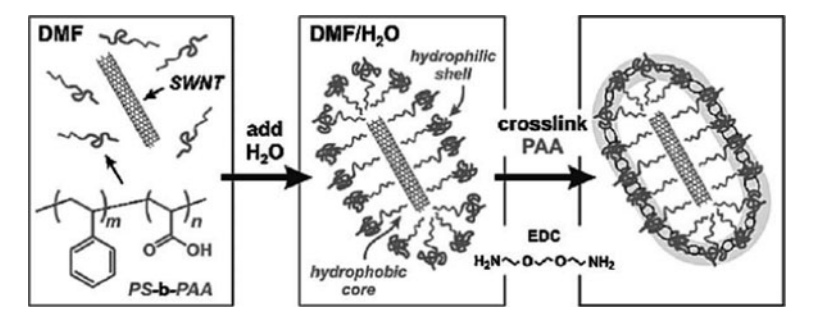


Fig. 2 The preparation of micelle-encapsulated single-walled carbon nanotubes (Ref. [17])

Fig. 3 γ -Cyclodextrin used for the functionalization of carbon nanotubes

Carbohydrates

Single-walled carbon nanotubes have been functionalized with monosaccharides to disperse them in water [25]. The nanotube-carbohydrate complexes have been studied for immunological purposes, such as direct binding to pathogenic cells via specific adhesin-receptor interactions [25]. Starch, composed of linear amylose and branched amylopeptin, has also been reported to wrap single-walled carbon nanotubes in an helical fashion [26]. Carbohydrates have also been bound covalently to carbon nanotubes with synthetic amino-carbohydrates [27]. Furthermore, synthetic carbohydrates, such as Gum Arabic [23] and cyclodextrins [24] (see Fig. 3) can also disperse carbon nanotubes by non-covalent interactions.

Nucleic Acids

It has been reported that a variety of single-stranded DNAs, short double-stranded DNAs, and RNAs can disperse single-walled carbon nanotubes [28]. The interaction between the nanotube and the nucleic acid is based on π -stacking through the nucleic acid base, with the hydrophilic sugar-phosphate backbone pointing to

the exterior interacting with the solvent. The use of poly(A) and poly(C) strands, which strongly self-stack in solution, exhibit much lower dispersion compared to poly(T), which supports the base-stacking mechanism and is also consistent with the fact that the interaction with single-stranded DNAs are more favorable than with double-stranded ones [29]. Non-specific DNA insertion into the opened cavity of MWNTs has also been reported [30]. Furthermore, RNA can be used to purify single-walled carbon nanotubes by a two-step method consisting of RNA-wrapping and treatment with RNAse [31].

Proteins

Functionalization with proteins may have several advantages over nucleic acids, such as modified immune response, ease of adding further functionalities (e.g. adding additional groups such as fluorescent dyes via amine and sulfide groups). Different procedures for the attachment of proteins to CNTs have been already described. Covalent methods use, for example, the diimide-activated amidation of nanotubes carrying carboxylic groups after acid treatment, or the reaction of protein amine groups with a succinimidyl derivative of pyrene adsorbed onto the sidewall of single walled carbon nanotubes by π -stacking [19]. Proteins can also be attached to CNTs by means of the biotin-streptavidin system [32]. Many proteins, such as streptavidin, HupR and cytochrome c, can be spontaneously adsorbed onto the carbon nanotube surface [33]. However, non-specific protein adsorption can be prevented by the coating of the nanotube with some polymers, such as PEG. Immobilization of proteins in a more controllable fashion on carbon nanotubes can also be achieved. Several studies have been performed on the adsorption of proteins and designed peptides onto carbon nanotubes [34, 35]. The characterization of the properties of carbon nanotube-protein complexes is important in the development of nanoelectronic devices and nanosensors [36].

2 Carbon Nanotubes for Gene Delivery

The design of new strategies for the delivery of drugs and molecular probes into cells is necessitated by the poor cellular penetration of many small molecules and macromolecules, including proteins and nucleic acids being used as drugs [3, 37, 38]. Strategies in which a poorly permeating drug or probe molecule is covalently attached to a transporter to produce a cell-penetrating conjugate offer a solution to this problem. Several classes of transporters have been investigated including lipids, PEGs, and more recently peptides [39]. The use of non-viral vectors as delivery systems in gene therapy has been extensively studied recently owing to their advantages over viral vectors [40]. Although viral vectors are characterized by their higher transfection efficiency they have several disadvantages such as

possible immunogenic reactions, possible oncogenic effects, lower stability, and expensive production, making non-viral vectors an attractive alternative [41]. Nonviral vectors offer various alternatives regarding the size and type of vectors. They are chemically controllable, and display a reduced immunogenicity. The use of carbon nanotubes as gene carriers has received considerable interest recently because of their nano proportions, biocompatibility, low cytotoxicity and their ability to cross the cell membrane [42–45]. Encouragingly, SWCNTs are reported to localize in tumours in mice, probably because of increased vascularisation inherent in tumours, making tumour targeting a feasible approach [46]. However, the dynamics of SWCNT encapsulation by the cell and the subsequent effects on gene expression has not been fully explored.

Functionalization of Carbon Nanotubes for Binding Genetic Material

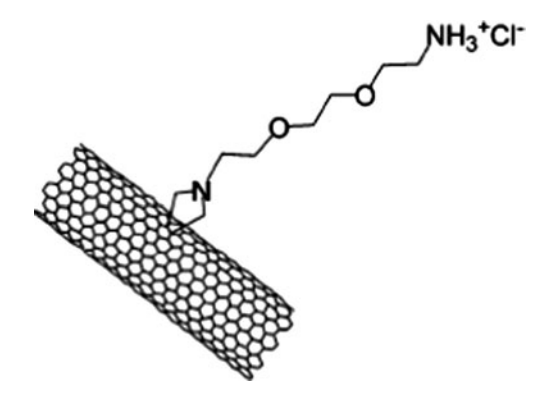
The use of carbon nanotubes as gene delivery vectors requires functionalization to disperse the nanotubes in aqueous media but also to render them able to effectively bind to the genetic material. Functionalization of carbon nanotubes for genetic material binding has been performed by covalent and non-covalent approaches. DNA molecules have been attached to carbon nanotubes by covalent linkages [47]. These methods consist of covalently linking thiol-terminated oligonucleotides to single-walled carbon nanotubes pre-functionalized with diamines by using a succinimide-maleimide linker, commonly used for thiol-amino coupling. Other covalent approaches involve the chemical modification of the carbon nanotube surface to introduce positively charged groups to bind the nucleic acid. In the non-covalent approaches, cationic surfactants are attached to carbon nanotubes, with the negatively charged nucleic acid bound to the functionalized carbon nanotubes by ionic interactions. The main disadvantage of non-covalent functionalization when used for gene delivery is that subsequent DNA binding to the nanotubes may be unstable [48].

Different methodologies have been developed for the binding of DNA to carbon nanotubes based on non-covalent functionalization. In general, these methodologies are based on the non-covalent wrapping of positively charged groups to bind negatively charged nucleic acids. On the other hand, positive groups have also been introduced on the nanotube wall by covalent modifications. For example, single-walled carbon nanotubes have been functionalized with ammonium and lysine groups introduced by chemical modification of the nanotube surface for DNA binding (see Fig. 4) [49]. Furthermore, multi-walled carbon nanotubes have been grafted with polyethylenimine, a positively charged polymer known for its excellent binding properties for DNA [50].

Other methods for DNA condensation on or in carbon nanotubes, such as the DNA insertion and transport in the opened cavity of multi-walled carbon nanotubes, have also been reported and could be another means of preparation of gene

V. Sanz-Beltrán et al.

Fig. 4 Ammoniumfunctionalized single-walled carbon nanotubes for plasmid DNA binding (Ref. 49)



delivery systems [30]. RNA-wrapped carbon nanotubes are an attractive method of solubilising carbon nanotubes because RNA gives high solubilisation yields and is non-cytotoxic [31]. However, RNA-wrapping confers negative charges on to the carbon nanotubes which makes them unsuitable for DNA binding.

Different methods have been used to characterize and optimize the binding of DNA to carbon nanotubes [49]. For example, the affinity between DNA and carbon nanotubes has been measured by SPR (Surface Plasmon Resonance). In this study, the functionalized carbon nanotubes were bound to the gold surface of a chip by an amide bond between the amine groups on the nanotubes and carboxylic groups on the gold surface. The sensorgram response was used to study the association and dissociation of DNA on the nanotubes. The PicoGreen dye exclusion assay was be used to evaluate the degree of DNA compaction by the nanotubes. The PicoGreen fluorescence increases when intercalated between the dsDNA base pairs. When DNA is condensed, the dye is unable to intercalate decreasing the fluorescence. For this assay it is necessary to correct the background fluorescence from carbon nanotubes on their own. Agarose gel electrophoresis can also be used to quantify the amount of DNA that can be attached to the functionalized carbon nanotubes. In this assay, a fixed amount of plasmid DNA is incubated with decreasing concentrations of functionalized carbon nanotubes. Only free plasmid is able to run in the gel whereas nanotube-plasmid complexes remain in the well. The maximum amount of plasmid DNA that can be attached to the carbon nanotubes is given by the lane with the highest carbon nanotube dilution at which there is not free plasmid band.

Biological Barriers in Gene Transfection with Carbon Nanotubes

The transfection efficiencies reached with viral vectors are still much greater than those obtained with non-viral vectors, such as carbon nanotubes, and therefore further optimization has to be carried out. Most of these problems are related to the

different barriers at systemic, tissue and cellular levels that the vector has to be able to overcome in order to reach its target [51, 52]. The intracellular trafficking of the internalized vector plays an important role in obtaining efficient gene expression [53-55]. The most important intracellular barriers are: cellular internalization pathways, DNA degradative processes and nuclear translocation of DNA. Although it has not been fully elucidated, carbon nanotubes seem to be internalized by endocytosis and end up encapsulated in lysosomes. Being able to escape from these degradative cellular compartiments is crucial in getting a suitable transfection efficiency for therapeutical purposes [56]. When carbon nanotubes enter by endocytosis [57, 58] they are brought into an endosome, in which there is no nuclease activity. When the endosome fuses with a lysosome nuclease activity (DNAse 1) is present. Several strategies have been developed to overcome the intracellular DNA degradative barrier based on the destabilization of endosomal and lysosomal membranes [59]. For example, the use of the proton sponge effect [60] of cationic polymers that causes a swelling and rupture of the organelles by sequestering protons and their counterions and creates an osmotic imbalance. Another alternative is the use of fusogenic peptides [61] which become protonated upon acidification on the endosomes. These hydrophobic fusion peptide domains interact with the endosomal membrane causing its destabilization. The addition of lysosomotropic compounds in the cultured media has been reported as a way to promote lysosomal escape [62]. Lysosomotropic agents are hydrophobic weak bases that enter the lysosome and become protonated inside the organelle as a result of the low pH, are then unable to cross the membrane and so being accumulate in the organelle. Subsequent swelling of the lysosome by the osmotic pressure causes the destabilization of the lysosomal membrane releases the genetic material and its carrier. Among the biological barriers, the translocation of DNA through the nuclear membrane seems to be the limiting step. In order to overcome this barrier a protein with a nuclear localization signal (NLS) can be used [63]. These proteins bind to cytosolic receptors known as importings enabling the complex to be translocated to the nucleus. For example, protamine is a small peptide with NLS and very basic due to its high arginine content which strongly binds DNA.

Methods developed for the Use of CNTs as Gene Delivery Systems

As explained in the previous section, the development of a new vector for therapeutic gene transfer requires protection of DNA from degradation and good nuclear membrane translocation. Plasmid DNA expressing β -galactosidase was condensed on ammonium-functionalized carbon nanotubes by ionic interactions and the levels of gene expression on CHO cells was found to be 5 to 10 times higher than plasmid on its own [64]. However, the transfection efficiency with carbon nanotubes was improved by the use of carbon nanotubes functionalized

V. Sanz-Beltrán et al.

with PEI, a polymer that has been reported to have a proton sponge effect which reduces the DNA degradation, enhancing the levels of gene expression [50]. Amino-functionalized multi-walled carbon nanotubes were also found to efficiently deliver plasmid DNA encoding green fluorescent protein gene into mammalian cells [65]. Small interfering RNA has also been delivered into cells by carbon nanotubes functionalized with ammonium groups bound to siRNA (telomerase reverse transcriptase siRNA) by ionic interactions [66]. In addition, covalent approaches based on binding nucleic acids directly to carbon nanotubes have also been tested. For example, siRNA for gene silencing was covalently bound to carbon nanotubes using a cleavable disulfide bond [67]. The enzymatic and acid conditions of the endosomal/lysosomal compartments after siRNAnanotube complexes entering allow the release of siRNA into the cytosol and efficient gene silencing. In a different approach, single-stranded DNA attached to single-walled carbon nanotubes was used to transport and deliver single stranded ssDNA [68]. In this method, the ssDNA is released after the ssDNA-nanotube complex enters the cells by endocytosis by applying a short burst of near-infrared radiation. Recently, an alternative physical method of gene delivery has been reported called nanotube spearing [69]. In this method, carbon nanotubes contain nickel particles on their tips allowing them to respond to a magnetic field. Cells like Bal 17, B-lymphoma and primary neurons were incubated with magnetic carbon nanotubes carrying DNA strain encoding green fluorescent protein. A static magnetic field pulled the tubes into the cells, which were then efficiently transfected.

Further advances in using carbon nanotubes as gene delivery vectors can be achieved exploiting the inherent properties of carbon nanotubes. Carbon nanotubes are versatile materials that can be exohedrically functionalized by attaching different groups or molecules to the external walls but also can be filled with different compounds [70–72]. Different functionalization methods have already been developed for the binding of plasmid DNA on carbon nanotubes for gene delivery based on attaching cationic functional groups on the outside wall. However, the development of methods for the efficient filling of carbon nanotubes is still an emerging field [73]. The main problems arise with the design of the nanotube to obtain a high capability of uptake of the compound in order to get maximum filling yield together with release of the compound inside the cells. As it was stated above, DNA can be inserted into carbon nanotubes in an aqueous environment and the encapsulated nanotube-DNA complex can be further exploited for applications as gene delivery systems.

Elucidation of the Mechanism of Entry of Carbon Nanotubes and Implications for Their use in Gene Biodelivery

One important issue to be addressed is the mechanism of entry that regulates the cellular internalization of carbon nanotubes. Some research groups suggest that

carbon nanotubes traverse the cellular membrane through endocytosis [58, 74] whereas other groups have suggested an energy independent nonendocytotic mechanism that involves insertion and diffusion of nanotubes through the lipid bilayer of the cell membrane [44, 75]. Endocytosis is an energy-dependent uptake that is inhibited when incubations are carried out at low temperature or in ATPdepleted media. Treatment with sodium azide is known to disturb the production of ATP in cells, thus inhibiting the endocytic pathway. There are different endocytic pathways, including phagocytosis, pinocytosis, clathrin-dependent receptor mediated and the caveolae or lipid-raft pathway. In clathrin-dependent endocytosis, the clathrin coat forms invaginations on the plasma membrane leading to the budding of clathrin-coated vesicles which trap the extracellular species and bring them inside the cells. On the other hand, caveolae are flask-shaped membrane invaginations on cell surfaces that are rich in cholesterol and sphingomyelin. Pretreatment of the cells with sucrose (hypertonic treatment) or a K+-depleted medium are known to disrupt the formation of clathrin-coated vesicles on the cell membrane. Pre-treatment of cells with the drugs filipin and nystatin, which are known to disrupt the cholesterol distribution within the cell membrane, is known to inhibit the lipid-rafts pathway. Using these pretreatments, it has been possible to elucidate the mechanism of entry of carbon nanotubes in cells [45, 58]. For example, it has been reported that single-walled carbon nanotubes with lengths of <1 µm and functionalized with proteins are internalized in mammalian cells by a clathrin pathway. However, bundles and aggregates of single-walled carbon nanotubes, microns in length and submicron in bundle diameter, functionalized with positively charged peptides have been reported to be internalized by an energy-independent non-endocytic mechanism. It has been also reported that unoxidized and therefore hydrophobic areas of the nanotubes could associate with hydrophobic regions of the cell surface and internalize by endocytosis. It has been shown that entry of carbon nanotubes into cells is enhanced when they are functionalized with positively charged groups compared to negatively charged ones possibly due to the repulsion from the negatively charged cell membrane.

References

- Tasis, D., Tagmatarchis, N., Georgakilas, V., Prato, M.: Soluble carbon nanotubes. Chem. Eur. J. 9(17), 4000–4008 (2003)
- O'Connell, M.J., Boul, P., Ericson, L.M., Huffman, C.B., Wang, Y.H., Haroz, E., Kuper, C., Tour, J.M., Ausman, K.D., Smalley, R.E.: Reversible water-solubilization of single-walled carbon nanotubes by polymer wrapping. Chem. Phys. Lett. 342(3–4), 265–271 (2001)
- 3. Lin, Y., Taylor, S., Li, H., Fernando, K.A.S., Qu, L., Wang, W., Gu, L., Zhou, B., Sun, Y.P.: Advances toward bioapplications of carbon nanotubes. J. Mater. Chem. 14, 527–541 (2004)
- Liu, J., Rinzler, A.G., Dai, H., Hafner, J.H., Bradley, R.K., Boul, P.J., Lu, A., Iverson, T., Shelimov, K., Huffman, C.B., Rodriguez-Macías, F., Shon, Y.S., Lee, T.R., Colbert, D.T., Smalley, R.E.: Fullerene pipes. Science 280, 1253–1256 (1998)
- Dyke, C.A., Tour, J.M.: Covalent functionalization of single-walled carbon nanotubes for materials applications. J. Phys. Chem. A 108(51), 11151–11159 (2004)

270 V. Sanz-Beltrán et al.

6. Fu, K., Sun, Y.P.: Dispersion and solubilization of carbon nanotubes. J. Nanosci. Nanotechol. **3**(5), 351–364 (2003)

- 7. Britz, D.A., Khlobystov, A.N.: Noncovalent interactions of molecules with single walled carbon nanotubes. Chem. Soc. Rev. **35**, 637–659 (2006)
- 8. Islam, M.F., Rojas, E., Bergey, D.M., Johnson, A.T., Yodh, A.G.: High weight fraction surfactant solubilization of single-wall carbon nanotubes in water. Nano Lett. 3, 269–273 (2003)
- 9. Yang, W., Thordarson, P., Gooding, J.J., Ringer, S.P., Braet, F.: Carbon nanotubes for biological and biomedical applications. Nanotechnology (2007)
- Zheng, M., Jagota, A., Semke, E.D., Diner, B.A., McLean, R.S., Lustig, S.R., Richardson, R.E., Tassi, N.G.: DNA-assisted dispersion and separation of carbon nanotubes. Nat. Mater. 2, 338–342 (2003)
- 11. Wang, J., Musameh, M., Lin, Y.H.: Solubilization of carbon nanotubes by nafion toward the preparation of amperometric biosensors. J. Am. Chem. Soc. 125, 2408–2409 (2003)
- Chen, R.J., Bangsaruntip, S., Drouvalakis, K.A., Kim, N.W.S., Shim, M., Li, Y., Kim, W., Utz, P.J., Dai, H.: Noncovalent functionalization of carbon nanotubes for highly specific electronic biosensors. Proc. Natl. Acad. Sci. USA 100, 4984

 –4989 (2003)
- Shim, M., Kam, N.W.S., Chen, R.J., Li, Y.M., Dai, H.J.: Functionalization of carbon nanotubes for biocompatibility and biomolecular recognition. Nano Lett. 2, 285–288 (2002)
- Star, A., Stoddart, J.F., Steuerman, D., Diehl, M., Boukai, A., Wong, E.W., Yang, X., Chung, S.W., Choi, H., Heath, J.R.: Angew. Chem. 2001(113), 1771–1775 (2001)
- Steuerman, D.W., Star, A., Narizzano, R., Choi, H., Ries, R.S., Nicolini, C., Stoddart, J.F., Heth, J.R.: Interactions between conjugated polymers and single-walled carbon nanotubes. J. Phys. Chem. B 106(12), 3124–3130 (2002)
- Moore, V.C., Strano, M.S., Haroz, E.H., Hauge, R.H., Smalley, R.E.: Individually suspended single-walled carbon nanotubes in various surfactants. Nano Lett. 3(10), 1379–1382 (2003)
- 17. Kang, Y., Taton, T.A.: Micelle-encapsulated carbon nanotubes: a route to nanotube composite. J. Am. Chem. Soc. 125(19), 5650–5651 (2003)
- Dai, H.: Carbon nanotubes: synthesis, integration and properties. Acc. Chem. Res. 35(12), 1035–1044 (2002)
- 19. Nakashima, N., Tomonari, Y., Murakami, H.: Water-soluble single-walled carbon nanotubes via noncovalent sidewall-functionalization with a pyrene-carrying ammonium ion. Chem. Lett. **31**, 638–639 (2002)
- 20. Tang, B.Z., Xu, H.: Preparation, alignment and optical properties of soluble poly(phenylacetylene)-wrapped carbon nanotubes. Macromolecules **32**(8), 2569–2576 (1999)
- Chen, J., Liu, H., Weiner, W.A., Halls, M.D., Waldeck, D.H., Walker, G.C.: Noncovalent engineering of carbon nanotube surfaces by rigid, functional conjugated polymers. J. Am. Chem. Soc. 124(31), 9034–9035 (2002)
- 22. Byon, H.R., Hong, B.J., Gho, Y.S., Park, J.W., Choi, H.C.: Pseudo 3D single-walled carbon nanotube film for BSA-free protein chips. Chem. Bio. Chem. 6, 1331–1334 (2005)
- Bandyopadhyaya, R., Nativ-Roth, E., Regev, O., Yerushalmi-Rozen, R.: Stabilization of individual carbon nanotubes in aqueous solutions. Nano Lett. 2(1), 25–28 (2002)
- 24. Chen, J., Dyerand, M.J., Yu, M.F.: Cyclodextrin-mediated soft cutting of single-walled carbon nanotubes. J. Am. Chem. Soc. 123(25), 6201–6202 (2001)
- Sudibya, H.G., Ma, J., Dong, X., Ng, S., Li, L.J., Liu, X.W., Chen, P.: Interfacing glycosylated carbon nanotubes-network devices with living cells to detect dynamic secretion of biomolecules. Angew. Chem. Int. Ed. Engl. 48, 2723–2726 (2009)
- Star, A., Steuerman, D.W., Hetah, J.R., Stoddart, J.F.: Starched carbon nanotubes. Angew. Chem. Int. Ed. 41, 2508–2512 (2002)
- 27. Pompeo, F., Resasco, D.E.: Water solubilization of single-walled carbon nanotubes by functionalization with glucosamine. Nano Lett. **2**(4), 369–373 (2002)
- Zheng, M., Jagota, A., Semke, E.D., Diner, B.A., McLean, R.S., Lustig, S.R., Richardson, R.E., Tassi, N.G.: DNA-assisted dispersion and separation of carbon nanotubes. Nat. Mater 2, 338–342 (2003)

- 29. Nakashima, N., Okuzono, S., Murakami, H., Nakai, T., Yoshikawa, K.: DNA dissolves single-walled carbon nanotubes in water. Chem. Lett. **32**(5), 456 (2003)
- 30. Gao, H., Kong, Y., Cui, D.: Spontaneous insertion of DNA oligonucleotides into carbon nanotubes. Nano Lett. **3**(4), 471–473 (2003)
- 31. Jeynes, J.C.G., Mendoza, E., Chow, D.C.S., Watts, P.C.P., McFadden, J.: Generation of chemically unmodified pure single-walled carbon nanotubes by solubilizing with RNA and treatment with ribonuclease A. Adv. Mater. 18, 1598–1602 (2007)
- 32. Star, A., Gabriel, J.C.P., Bradley, K., Gruner, G.: Electronic detection of specific protein binding using nanotube FET devices. Nano Lett. 3(4), 459–463 (2003)
- 33. Balavoine, F., Schultz, P., Richard, C., Mallouh, V., Ebbesen, T.W., Mioskowski, C.: Helical crystallization of proteins on carbon nanotubes: a first step towards the development of new biosensors. Angew. Chem. Int. Ed. 38, 1912–1915 (1999)
- Chen, R.J., Zhang, Y., Wang, D., Dai, H.: Noncovalent sidewall functionalization of singlewalled carbon nanotubes for protein immobilization. J. Am. Chem. Soc. 123(16), 3838–3839 (2001)
- 35. Shim, M., Kam, N.W.S., Chen, R.J., Li, Y., Dai, H.: Functionalization of carbon nanotubes for biocompatibility and biomolecular recognition. Nano Lett. **2**(4), 285–288 (2002)
- Chen, R.J., Bangsaruntip, S., Drouvalakis, K.A., Kam, N.W.S., Shim, M., Li, Y., Kim, W., Utz, P.J., Dai, H.: Noncovalent functionalization of carbon nanotubes for highly specific electronic biosensors. PNAS 100, 4984

 –4989 (2003)
- 37. Sinha, N., Yeow, J.T.W.: Carbon nanotubes for biomedical applications. IEEE Trans. Nanobiosci. 4, 180–195 (2005)
- Polizu, S., Savadogo, O., Poulin, P., Yahia, L.: Applications of carbon nanotubes-based biomaterials in biomedical nanotechnology. J. Nanosci. Nanotechnol. 6, 1883–1904 (2006)
- 39. Brown, M.D., Schätzlein, A.G., Uchegbu, L.F.: Gene delivery with synthetic (non viral) carriers. Int. J. Pharm. **229**(1–2), 1–21 (2001)
- 40. Davis, M.E.: Non-viral gene delivery systems. Curr. Opin. Biotechnol. 13(2), 128–131 (2002)
- 41. Hatefi, A., Canine, B.F.: Perspective in vector development for systemic cancer gene therapy. Gene Ther. Mol. Biol. **13**, 15–19 (2009)
- 42. Bianco, A., Kostarelos, K., Prato, M.: Applications of carbon nanotubes in drug delivery. Curr. Opin. Chem. Biol. 9(6), 674–679 (2005)
- Dumortier, H., Lacotte, S., Pastorin, G., Marega, R., Wu, W., Bonifazi, D., Briand, J.P., Prato, M., Muller, S., Bianco, A.: Functionalized carbon nanotubes are non-cytotoxic and preserve the functionality of primary immune cells. Nano Lett. 6(7), 1522–1528 (2006)
- 44. Pantarotto, D., Briand, J., Prato, M., Bianco, A.: Translocation of bioactive peptides across cell membranes by carbon nanotubes. Chem. Commun. 1, 16 (2004)
- 45. Kam, N.W.S., Jessop, T.C., Wender, P.A., Dai, H.: Nanotube molecular transporters: internalization of carbon nanotube–protein conjugates into mammalian cells. J. Am. Chem. Soc. **126**(22), 6850–6851 (2004)
- 46. Liu, Z., Cai, W.B., He, L.N., Nakayama, N., Chen, K., Sun, X., Chen, X., Dai, H.: In vivo biodistribution and highly efficient tumour targeting of carbon nanotubes in mice. Nat. Nanotechol. **2**, 47–52 (2006)
- 47. Baker, S.E., Cai, W., Lasseter, T.L., Weidkamp, K.P., Hammers, R.J.: Covalently bonded adducts of desoxyribonucleic acid (DNA) oligonucleotides with single-wall carbon nanotubes: synthesis and hybridization. Nano Lett. 2(12), 1413–1417 (2002)
- 48. Kostarelos, K., Lacerda, L., Pastorin, G., Wu, W., Wieckowski, S., Luangsivilay, J., et al.: Cellular uptake of functionalized carbon nanotubes is independent of functional group and cell type. Nature 2, 108–113 (2007)
- Singh, R., Pantarotto, D., McCarthy, D., Chaloin, O., Hoebeke, J., Partidos, C.D., Briand, J.P., Prato, M., Bianco, A., Kostarelos, K.: Binding and condensation of plasmid DNA onto functionalized carbon nanotubes: toward the construction of nanotube-based gene delivery vectors. JACS 127(12), 4388–4396 (2005)

50. Liu, Y., Wu, D.C., Zhang, W.D., Jiang, X., He, C.B., Chung, T.S., Goh, S.H., Leong, K.W.: Polyethylenimine-grafted multiwalled carbon nanotubes for secure noncovalent immobilization and efficient delivery of DNA. Angew. Int. Ed. **44**, 4782–4785 (2005)

- Smrekar, B., Wightman, L., Wolschek, M.F., Lichtenberger, C., Ruzicka, R., Ogris, M., Rödl, W., Kursa, M., Wagner, E., Kircheis, R.: Tissue-dependent factors affect gene delivery to tumors in vivo. Gene Ther. 10, 1079–1088 (2003)
- 52. Wiethoff, C.M., Middaugh, C.R.: Barriers to nonviral gene delivery. J. Pharm. Sci. 92(2), 203–217 (2002)
- 53. Khalil, I.A., Kogure, K., Akita, H., Harashima, H.: Uptake pathways and subsequent intracellular trafficking in nonviral gene delivery. Pharm. Rev. 58, 32–45 (2006)
- 54. Lechardeur, D., Lukacs, G.L.: Intracellular barriers to non-viral gene transfer. Curr. Gene Ther. **2**, 183–194 (2002)
- Gratton, S.E.A., Ropp, P.A., Pohlhaus, P.D., Luft, J.C., Madden, V.J., Napier, M.E., DeSimone, J.M.: The effect of particle design on cellular internalization pathways. PNAS 105, 11613–11618 (2008)
- 56. Lechardeur, D., Verkman, A.S., Lukacs, G.L.: Intracellular routing of plasmid DNA during non-viral gene transfer. Adv. Drug Deliv. Rev. 57(5), 755–767 (2005)
- 57. Kam, N.W.S., Jessopm, T.C., Wender, P.A., Dai, H.: Nanotube molecular transporters: internalization of carbon nanotube–protein conjugates into mammalian cells. JACS **126**(22), 6850–6851 (2004)
- 58. Kam, N.W.W., Liu, Z., Dai, H.: Cover picture: expanding the genetic code. Angew. Int. Ed. 44, 1–3 (2005)
- Wattiaux, R., Laurent, N., Wattiaux-De Coninck, S., Jadot, M.: Endosomes, lysosomes: their implication in gene transfer. Adv. Drug Deliv. Rev. 41(2), 201–208 (2000)
- 60. Valladier, P.B., Behr, J.P.: Cytotechnology 35, 1573 (2001)
- Wagner, E., Plank, C., Zatloukal, K., Cotton, M., Birnstiel, M.L.: Influenza virus hemagglutinin HA-2 N-terminal fusogenic peptides augment gene transfer by transferringpolylysine–DNA complexes: toward a synthetic virus-like gene-transfer vehicle. PNAS 89, 7934–7938 (1992)
- 62. Ciftci, K., Levy, R.J.: Enhanced plasmid DNA transfection with lysosomotropic agents in cultured fibroblasts. Int. J. Pharm. 218, 81–92 (2001)
- 63. Sorgi, F.L., Bhattacharya, S., Huang, L.: Protamine sulfate enhances lipid-mediated gene transfer. Gene Ther. **4**, 961–976 (1997)
- Pantarotto, D., Singh, R., McCarthy, D., Erhard, M., Briand, J.P., Prato, M., Kostarelos, K., Bianco, A.: Functionalized carbon nanotubes for plasmid DNA gene delivery. Angew. Chem. Int. Ed. 43, 5242–5246 (2004)
- 65. Gao, L., Nie, L., Wang, T., Qin, Y., Guo, Z., Yang, D., Yan, X.: Carbon nanotubes delivery of the GFP gene into mammalian cells. Chem. Biochem. **7**, 239–242 (2005)
- 66. Shang, Z., Yang, X., Zhang, Y., Zeng, B., Wang, S., Zhu, T., Roden, R.B.S., Chen, Y., Yang, R.: Delivery of telomerase reverse transcriptase small interfering RNA in complex with positively charged single-walled carbon nanotubes suppresses tumor growth. Clin. Cancer Res. 12, 4933–4939 (2006)
- Kam, N.W.S., Liu, Z., Dai, H.: Functionalization of carbon nanotubes via cleavable disulfide bonds for efficient intracellular delivery of siRNA and potent gene silencing. JACS 127, 12492–12493 (2005)
- Kam, N.W.S., O'Connell, M., Wisdom, J.A., Dai, H.: Carbon nanotubes as multifunctional biological transporters and near-infrared agents for selective cancer cell destruction. PNAS 102, 11600–11605 (2005)
- Cai, D., Huang, Z., Carnahan, D., Mataraza, J.M., Chiles, T.C., Qin, Z.H., Huang, J., Kempa, K., Ren, Z.: Highly efficient molecular delivery into mammalian cells using carbon nanotube spearing. Nat. Methods 2, 449–454 (2005)
- Hirsch, A.: Functionalization of single-walled carbon nanotubes. Angew. Chem. Int. Ed. 41, 1853–1859 (2002)

- Borowiak-Palen, E., Mendoza, E., Bachmatiuk, A., Rummeli, M.H., Gemming, T., Nogues, J., Skumryev, V., kalenczuk, R.J., Pichler, T., Silva, S.R.P.: Iron filled single-wall carbon nanotubes—a novel ferromagnetic medium. Chem. Phys. Lett. 421, 129–133 (2006)
- 72. Hilder, T.A., Hill, J.M.: Gold nanoparticles bound on microgel particles and their application as an enzyme support. Nanotechnology **18**, 275704 (2007)
- 73. Hilder, T.A., Hill, J.M.: Carbon nanotubes as drug delivery nanocapsules. Curr. Appl. Phys. **8**, 258–261 (2008)
- 74. Kam, N.W.S., Dai, H.J.: Single walled carbon nanotubes for transport, delivery of biological cargos. Phys. Stat. Sol. B **243**, 3561–3566 (2006)
- 75. Pantarotto, D., Briand, J.P., Prato, M., Bianco, A.: Translocation of bioactive peptides across cell membranes by carbon nanotubes. Chem. Comm, pp. 16–17 (2004)

A	Bladder cancer cells, 238
Acid oxidation, 158	Bovine serum albumin (BSA), 156, 190
Activators of complement, 191	
Active targeting, 229	
Adaptive immunity, 184	C
ADEPT, 231	Cancer Therapies, 75, 224
AFM: Dynamic force microscopy	Capillarity, 45
imaging, 155	Carbohydrates, 263
AFM: Topographical	Carboplatin, 227, 238, 247, 251
imaging, 154	Catalyst particles, 16, 100, 105–109,
AgCl nanowires, 46	111–112, 200
Albumin, 233	Cell manipulation, 17
Alkylating agents, 227	Cell Patterning, 11
Alternative pathway, 187, 190	Cell proliferation, 250
Alveolar macrophages, 199, 194	Cell transfection, 32
Angiogenesis, 170, 225	Cell viability, 250, 254
Antenna Properties, 22	Cells, 160
Antennas, 4	Cells and their Receptors, 188
Antibodies, 239	Cells of the innate immune system, 188
Anticancer drug, 223, 247	Cellular internalization, 268
Aqueous suspension, 262	Cellular organelles, 196
Atomic force microscopy (AFM), 153	Cellular Receptors, 195
Avidin, 159	Chemical vapor deposition, 68, 249
α-Fe, 100, 104	Chemotherapeutic Agents, 247
α-Fe nanowires, 46	Chemotherapies, 223
	Cisplatin, 75, 227, 235
	Classical pathway, 185, 190
В	Clathrin dependent pathway, 269
B cell receptors, 184	Clq, 191, 186
Bacteria, 184, 188	CNT release, 174
Binding of lung surfactant, 194	CNT Spearing, 16
Biocompatibility, 34, 201, 203	CNT uptake, 161, 164, 174
Biodistribution, 19, 35, 170, 176	Coercive field, 107
Biodistribution behaviour, 240	Collections, 184, 188, 193, 198
Biological barriers, 170	Complement, 185, 190, 202
Biosensors, 7	Complement activation, 204
Biotin functionalized CNTs, 159	Complement consumption, 192

C (cont.)	Filling CNT in Solution, 41, 45, 47, 72,
Complement in vivo, 193	238, 249
Complement receptor 1 (CR1), 189	Filling Rate, 54
Complement receptors 3 and 4, 189	Fullerenes, 141
Complement system, 183, 184, 216	Fungi, 184
Confinement in a nanotube, 57	
Contrast agent, 34, 140, 141	
Contrastivity, 120	G
Covalent functionalisation, 55, 234	Gadolinium, 36
Covalent functionalisation	Gadonanotube, 142
of CNTs, 157	Gene Biodelivery, 268
Critical diameter, 102	Gene Delivery, 264
Cytotoxicity, 216, 237, 250	Gene silencing, 268
Cytotoxicity, 210, 257, 250	Gene Transfection, 266
	Genotoxicity, 212, 217
D	
D	Glioblastoma, 237
Dendritic cells, 188	Granuloma, 198, 199, 202
Diamagnetic CNT, 106	
Diffusion order spectroscopy, 127	
Distribution of nanotubes inside	Н
the cells, 175	Hall Magnetometry, 100, 101, 105
DNA, 202, 265	Hall sensor, 100
DOSY, 159	HeLa cells, 162
Double-walled CNT, 42, 156, 212	High-density lipoprotein (HDL), 190
Doxorubicin, 227, 233, 235, 239	High-resolution magic angle
Drug delivery, 31, 204, 233, 247	spinning, 126, 138
Drug-delivery system, 31, 232	Human bladder cancer cell, 250
Drug Targeting, 288	Human serum albumin, 190
DSPE-PEG2000-NH ₂ , 156	Hyperthermia, 76, 98
Σ,	Hysteresis loop, 101
	,
E	
Ecotoxicity, 211, 217	Ī
ECV cells, 162	Imaging, 34
Electrical properties, 5	Immune system, 184
Electro Poration, 12	Immunoconjugates, 231
Electrostatic interactions, 260	Immunotoxicity, 197
Embryonic stem cells, 31	In Vitro Studies, 236
•	
Endocytic pathway, 269	In Vivo Studies, 239
Endocytosis, 171, 196, 268, 269	Infectious microorganisms, 184
Enhanced permeability and retention	Inflammation, 193, 216
(EPR), 170	Inhalation, 212, 214
Exocytosis, 174	Inhaled carbon nanotubes, 193
Extracellular pH, 233	Innate Immune System, 183, 184
EPR effect, 232	Innate immunity, 184
	Integrins, 184
	Internalisation (endocytosis), 174
F	Internalization process, 234
Factor H, 187	Intoxicity, 227
Fibroblasts, 250, 254	Intracellular Localization, 169
Ficolin, 186, 187	Intracellular pH, 233
Field emission, 12	Iron filled CNT, 105
Filling, 235	Iron nanowire, 74, 100, 101,
Filling CNT from the melt, 41, 52, 72	103, 104
	100, 107

K	Nanothermometer, 120
Korringa relaxation, 136	Nanotube spearing, 268
	Nanowires, 100
	Near infrared (NIR) fluorescence
L	microscopy, 34
Lectin-like receptors, 189	Near-IR fluorescence, 19
Lectins, 184	Neural Systems, 10
Lipid-raft pathway, 269	Neuron, 10
Liposome, 204	Neutrophils, 184
Lung inflammation, 199	NIR, 18
Lung macrophage, 196	NIR Heaters, 21
Lungs, 188	NIR Imaging, 18
Lymphocytes, 184	NIR radiation, 22
	NMR, 125
	¹³ C NMR Spectroscopy, 130
M	¹ H NMR Spectroscopy, 127
MAC, 192	2D Correlation NMR Spectroscopy, 129
Macrophages, 184, 188, 196	2D Correlation Spectroscopy, 127
Magnetic force microscopy, 103	NMR Imaging, 140
Magnetic functionalisation, 100	Non-covalent functionalisation, 234, 259
Magnetic heating, 98	Non-covalent functionalisation of CNTs, 156
Magnetic nanoparticles, 98	n-situ filling of CNT, 69
Magnetic properties, 15	Nuclear magnetic resonance, 118
Magnetic resonance thermometry, 118	Nuclear Membrane, 160
Magnetic switching, 101	Nucleic acid, 263
Magnetisation, 100, 106, 107	
Magnetism of CNT ensembles, 105	
Magneto-crystalline anisotropy, 100	0
Mannose-binding lectin, 186	Oncogencs, 225
MBL, 187	Optical absorption, 35
Mechanical properties, 28	Optical Properties, 18
Membrane attack complex (MAC), 185	Optical Slimutation, 21
MFM, 104	Oxaliplatin, 227
Micelle structure, 261	Oxidative stress, 198, 199, 215
Microwave, 22	Oxidized CNT, 194
Microwave radiation, 13	π -Orbitals, 260
Molecular targeting, 288	n-Orbitals, 200
Monoclonal antibodies, 230, 233, 283	
MRI, 18, 36, 120, 125	P
	Passive targeting, 232
MRI contrast agents, 143	
Multi walled carbon nanotubes, 42, 68, 236	PC ₃ Cells, 254
Multifunctional nanocarrier, 76, 100, 232	Peapods, 43 Permandilization, 12
MWCNT, 27, 248	Permeabilization, 12
	Phagocytosis, 171, 184, 196, 199, 269
NT	Photoacoustic (PA) imaging, 35
N Name comics 256	Photoacoustic stimulation, 33
Nano carrier, 256 Nano medicine, 4	Photothermal Therapy, 21 Pinocytosis, 269
	•
Nano Scaffolds, 28	Plasma proteins, 189, 190, 203 Ploymers, 262
Nano transducers, 4	•
Nano wires, 56	Ploystyrene sulponic acid, 191 Polyethylene glycol (PEG), 191
Nanocomposites, 28, 30	
Nanocontainer, 120	Polyethylens oxide(PEO), 191
Nanomedicine, 223	Polymerwrapping, 261

P (cont.)	ss-DNA, 268
Potential cytotoxicity, 195	Streptavidin, 159
Pristine CNT, 100, 106, 107, 254	Structural defects, 200
Properdin, 187	Surface plasmon Resonance, 266
Proteins, 194, 264	Surfactant, 260
p-stacking interactions, 260	Surfactant protein A (SP-A), 188
Purification, 60, 249	Surfactant protein D (SP-D), 188
	SWCNT, 27
	Switching fields, 104
R	SWNT, 5
Radial breathing modes, 173	Systemic clearance, 178
Raman, 35	
Raman G' band, 173	The state of the s
Raman G-band, 173	T
Raman mapping, 174	T cell receptors, 184
Raman Microscopy, 35	Targeted drug delivery, 76, 203, 234
Reactive oxygen species (ROS), 193	Targeting, 159, 203
Red blood cells, 188	Temperature accuracy, 120
Regenerative medicine, 31	The Complement system, 185
Relaxivity, 36	The EPR effect, 239
Release rate of, 239 Resonance enhanced Person bands, 173	Therapeutics, 31
Resonance-enhanced Raman bands, 173	Thermonatry on the collular level 118
Respiratory tract, 188 Reversal process, 101	Thermometry on the cellular level, 118 Tissue engineering, 9, 27
RNA, 156, 202	TLRs, 184, 188
KIVA, 130, 202	Toxicity, 197, 200, 201, 211, 218
	Toxicity Studies, 250
S	Translocation, 216
Scavenger receptors, 184	Tumor suppressor genes, 225
Scavenger recptors, 188	Tween, 192
Shape anisotropy, 100	1 1 1 2 2
Shielding, 118	
Sidewall funtionalization, 32	U
Single-domain particle, 101	Ultra short SWCNT, 30
Singlewalled, 68	Uptake machanism, 269
Single-walled CNT, 42, 68, 107, 142, 162,	Uptake of CNT, 169
212, 200	
si-RNA, 268	
Solid State NMR, 132	\mathbf{V}
Solution-State NMR, 127	Van der Waals interactions, 261
SP-A, 193, 197	Viruses, 184, 188
SP-D, 193, 197	
Spin-lattice relation time, 120, 140, 141	
Spin-spin relaxation, 140	\mathbf{W}
Spin-spin relaxation time, 128	Wetting, 43
SPIO particles, 140	White blood cells, 188
SQUID, 106	